CELLULAR AND PROTEOMIC STUDIES OF THE MITOCHONDRIAL ABAD/Aβ COMPLEX: INVESTIGATING ITS ROLE IN ALZHEIMER'S DISEASE

Margaret Taylor

A Thesis Submitted for the Degree of PhD
at the
University of St Andrews

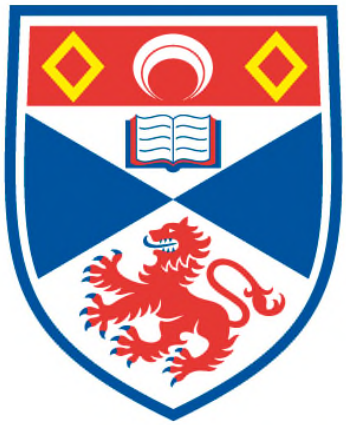

2012

Cellular and proteomic studies of the mitochondrial ABAD/Aβ complex

Investigating its role in Alzheimer's disease

Margaret Taylor

A thesis submitted for the degree of

Doctor of Philosophy

University of St Andrews March 2012

University of StAndrews March 2012

Declaration

1. Candidate's declarations:

I, MARGARET TAYLOR, hereby certify that this thesis, which is approximately 64,000 words in length, has been written by me, that it is the record of work carried out by me and that it has not been submitted in any previous application for a higher degree.

I was admitted as a research student in SEPT 2001 and as a candidate for the degree of PhD in [month, year]; the higher study for which this is a record was carried out in the University of St Andrews between 2001 and 2009.

Date 30 August 2012 signature of candidate .....

2. Supervisor's declaration:

I hereby certify that the candidate has fulfilled the conditions of the Resolution and Regulations appropriate for the degree of PhD in the University of St Andrews and that the candidate is qualified to submit this thesis in application for that degree.

Date 30 August 2012 signature of supervisor .....

3. Permission for electronic publication: (to *be signed by both candidate and supervisor)*

In submitting this thesis to the University of St Andrews I understand that I am giving permission for it to be made available for use in accordance with the regulations of the University Library for the time being in force, subject to any copyright vested in the work not being affected thereby. I also understand that the title and the abstract will be published, and that a copy of the work may be made and supplied to any bona fide library or research worker, that my thesis will be electronically accessible for personal or research use unless exempt by award of an embargo as requested below, and that the library has the right to migrate my thesis into new electronic forms as required to ensure continued access to the thesis. I have obtained any third-party copyright permissions that may be required in order to allow such access and migration, or have requested the appropriate embargo below.

The following is an agreed request by candidate and supervisor regarding the electronic publication of this thesis: acccess to all of printed copy but embargo of all of electronic publication of thesis for a period of 2 years on the following ground: publication would preclude future publication.

Date 30 August 2012 signature of candidate ...

signature of supervisor ...

Abstract

The focus of this thesis is to investigate the intracellular protein-peptide complex 3-hydroxyacyl-CoA dehydrogenase (HADH), also known as ABAD (amyloid-binding alcohol dehydrogenase) and amyloid-beta peptide (Aβ). This complex has been identified in the development of Alzheimer's disease (AD), and this study tries to identify if ABAD is a useful biomarker for genetic risk profiling strategies for the early diagnosis of Alzheimer's disease, or a suitable target for disease-modifying drug development. The major aim of this project is to explore the biochemical and cellular processes activated as a result of the interaction of ABAD and Aβ. Understanding the cellular responses to these interactions could help identify important biomarkers and/or drug targets for the diagnosis or treatment of Alzheimer's disease. This study assesses the cytotoxic effects of Aβ in tissue culture and in animal models overexpressing ABAD.

An *in vitro* cell system using SK-N-SH cells was developed for investigating the effects of ABAD expression in cells when incubated with synthetic Aβ peptide. *In vitro* studies confirmed ABAD to be a mitochondrial protein. There were problems with the efficiency of the synthetic Aβ peptide used, which was found to aggregate excessively. Trial of a soluble oligomeric Aβ peptide proved to be more efficient.

A cell system was also developed, culturing neurospheres from murine stem cells. This proved to be a reliable system for culturing primary cells and keeping them

in culture for up to 8 weeks. Cells were grown from a wild type strain and then differentiated and stained for endogenous expression of proteins.

Proteomic studies were carried out with novel transgenic mouse models for AD. Seven proteins were identified with changed expression in the 2x Tg mouse model. Further immunocytochemistry of human AD brain tissue confirmed the upregulation of peroxiredoxin II and endophilin I. Both proteins could be returned to normal expression in the mouse models by peritoneal injection for two weeks of a novel peptide inhibitor to ABAD, confirming the involvement of the ABAD/Aβ complex in the increased expression of these proteins.

Finally ABAD/Aβ was investigated as a possible target for AD therapy by screening with a small molecule fragment library. Only an initial screen was carried out, but several small molecule compounds were found to bind to ABAD. Further screening may produce lead compounds for a synthetic drug to inhibit the enhanced Aβ toxicity associated with the ABAD/Aβ complex

Acknowledgements

I would like to thank my supervisor Dr Frank Gunn-Moore for giving me the opportunity to work on this project and submit it as a PhD thesis. He has been very generous in support and encouragement and patient with my unconventional approach to research. I would also like to thank Dr Jim Aiton for his support. Other people who worked on Floor E in the Medical Bute building who need a mention are Tina Briscoe, Dr Michelle McRobbie and Dr Lindsey Gray who made life fun and interesting. Also thanks to Sarah Lynch, who started as a disgruntled project student and has become a friend. It has been exciting watching her progress to a PhD graduate and go on to develop her scientific career.

Thanks also to several people whose help along the way was invaluable: Tony Vaughan for help with fluorescent microscopy who helped me develop a passion for the technique; Huanting Liu, the most patient, helpful and knowledgable molecular biologist I know, Peter Coote for help with 2D gel proteomic analysis and Catherine Botting, Robin Antrobus and Alex Houston for their invaluable help with Mass Spec analysis data.

No PhD would be complete without visits to exotic places. For me, that included working in Prof. Shi Du Yan's laboratory in Columbia University, New York, where the Tg mouse brain samples were prepared, in Prof. Sandra D'Azzo's laboratory in St Jude Children's Research Hospital, Memphis where I learned much, including the Neurosphere culture and Prof. Sue Wonnacott's laboratory in Bath, UK. Thanks for all their help and advice.

I am grateful for all the funding that I have received for the project from SHERT (Scottish Hospital Endowment Research Trust) and the Cunningham Trust. Also thanks for travel grants from BRAIN (now 'guarantors of Brain') and the Minshull trust.

Finally to the present. Thanks to all who I work with in the Biomolecular Science building, especially the Taylor group lab 3.10 and everyone in the 2nd floor labs. Thanks especially to my current PI, Dr Rupert Russell who has encouraged me to write up my thesis and generously allowed me time to do this. Thanks to my colleagues Dr Phil Kerry and Dr Claudia Haas who have steered the ship while I have been writing. (Cupcakes on return please).

Thank you to my friends in USA, for encouragement, laughs and support: Allen and Mary in Memphis; Nancy, Bob, Paulette, Marie and Ron, Frank and Rob, Kathy, Alex et al in Salt Lake City. And many thanks to friends Tina, Annie and Nicola for much encouragement and lubrication to keep me going and Dr Milton Kiefel who provided a wonderful meal when Garry abandoned me to travel to Australia. And thanks to Nicola for initial reading of the thesis while simultaneously moving home. And of course thanks to Garry who has watched, listened and helped during the whole process. Many thanks for his patience at the end of the writing, which was more stressful for him than me, as he hates being late!

Abbreviations

17β-HSD10	17β-hydroxysteroid dehydrogenase type 10
4HNE	4-hydroxynonenal
ABAD	amyloid-binding alcohol dehydrogenase
Aβ	beta amyloid peptide
Aβ40	beta amyloid peptide
Aβ42	beta amyloid peptide
AD	Alzheimer's disease
ADAM10	a disintegrin and metalloprotease 10
ADP	adenosine diphosphate
AMPA	α-amino-3-hydroxy-5-methyl-4-isoxazolepropionic acid
ApoE	apolipoprotein E
ApoJ	apolipoprotein J
APP	amyloid precursor protein
APS	ammonium persulfate
ATP	adenosine triphosphate
BACE1	βeta site APP cleaving enzyme
BSA	bovine serum albumin
CAT	computerized axial tomography
CFP	cyan fluorescent protein
CK	creatine kinase
CNS	central nervous system
CSF	cerebrospinal fluid
CypD	cyclophilin D
DAB	diaminobenzidine
DAPI	4', 6'- diamidino-2-phenylindole
DMEM	Dulbecco's modified Eagle's medium
DMSO	dimethyl sulfoxide
DTT	dithiothreitol
dUTP	deoxyuridine triphosphate
ECE1	endothelin-converting enzyme

EDTA	ethylenediaminetetraacetic acid
EGCG	epigallocatechin gallate
EGF	epidermal growth factor
ELISA	enzyme-linked immunosorbent assay
ER	endoplasmic reticulum
ERAB	endoplasmic reticulum binding amyloid beta
FBS	fragment based screening
FCS	foetal calf serum
FITC	Fluorescein isothiocyanate
GAB2	GRB2-asscoiated binding protein 2
GAPDH	glyceraldehyde 3-phosphate dehydrogenase
GFAP	glial fibrillary acidic protein
GFP	green fluorescent protein
HADH	3-hydroxyacyl-CoA dehydrogenase
HBSS	Hanks buffered salt solution
4HNE	4 hydroxynonenal
HRP	horseradish-peroxidase
17βHSD10	17β hydroxysreroid dehydrogenase type 10
Hsp60	heat shock protein 60
HTS	high throughput screening
IDE	insulin degrading enzyme
IEF	isoelectric focusing
KPI	Kunitz protease inhibitor
LCHADD	long-chain hydroxyacyl-CoA dehydrogenase deficiency
MAP	microtubule associated protein
MALDI-TOF	matrix-assisted laser desorption/ionization time-of-flight
mAPP	mutant amyloid precursor protein
MARK	microtubule affinity regulating kinase
MCADD	medium-chain acyl dehydrogenase deficiency
MRI	magnetic resonance imaging
MTC	methylthioninium chloride

MTS	mitochondrial targeting sequence
MTT	3-(4,5-dimethylthiazol-2-yl)- 2,5 diphenyltetrazolium bromide
NEP	neprilysin
NMDA	N-methyl D-aspartate
NSAID	non-steroidal anti-inflammatory drugs
PAGE	polyacrylamide gel electrophoresis
PBS	phosphate buffered saline
PCR	polymerase chain reaction
PET	positron emission tomography
PFA	paraformaldehyde
PIB	Pittsburg compound B
Pin1	peptidyl prolyl *cis-trans* isomerise
PKA	protein kinase A
PKN	protein kinase
PICALM	phosphattidyllinositol-binding clathrin assembly lymphoid-myeloid leukaemia gene
PRB	plasma retinol binding protein
PrxI	peroxiredoxin I
PrxII	peroxiredoxin II
PS1	presenilin 1
PS2	presenilin 2
ROS	reactive oxygen species
R/T	room temperature
SCHAD	short chain L-3-hydroxyacyl-CoA dehydrogenase
SDH	succinate dehydrogenase
SDS	sodium dodecyl sulphate
SORL 1	sortilin-related receptor 1
SPR	surface plasmon resonance
TACE	TNFα converting enzyme
TEMED	tetramethylethylenediamine
Tg	transgenic
TNF	tumour necrosis factor

Tris	tris(hydroxymethyl)aminomethane
TUNEL	TdT-mediated dUTP nick-end labelling
UCH-L1	ubiquitin carboxy-terminal hydrolase L-1
WT	wild type

Contents

List of figures

List of tables

Chapter 1

Introduction

1.1 History and epidemiology of Alzheimer's disease

Alzheimer's disease (AD) is the most common form of dementia, accounting for approximately 65% of all dementia cases in the elderly (Henderson and Jorm, 1997; Luengo-Fernandez *et al.*, 2010). There is a lack of consistent data on the prevalence of AD around the world, but the percentage of all dementia in the elderly has increased since studies published in the 1990's. In 2009 it was estimated that there would be over 35 million cases of AD worldwide (2009 World Alzheimer Report; Alzheimer's Disease International), with numbers increasing especially in heavily populated regions e.g. Asia, Africa and South America. The disease affects all cultures worldwide, although there are three cited examples where AD is rare: in Japan, Kashmir and in Cree native American Indians (Graves *et al.*, 1996; Hendrie *et al.*, 1993; Raina *et al.*, 2009; Razdan *et al.*, 1994; White *et al.*, 1996). However, from the Honolulu-Asia Ageing Study, Japanese immigrants living in Hawaii and King County, Washington State USA, have the same incidence of AD as others in the USA or Europe (White *et al.*, 1996), adding evidence to there being an environmental influence on the disease, although no single factor has been identified. According to the 2009 World Alzheimer Report, predictions for 2010 show '57.7% of individuals with dementia worldwide live in low- and middle-income countries, but this percentage will rise to 70.5% by 2050'. Forecasted growth figures for East Asia are 117%, 107% for South Asia, 134% to 146% in parts of Latin America, and 125% in North Africa and the Middle East. The report also forecasts an increase of 40% in

the number of people with dementia in Europe, 63% in North America, 77% in southern Latin America, and 89% in the developed Asia Pacific countries.

A report in 2003 for the UK has shown that the incidence of AD is increasing worldwide, estimating an increase of 37% in developed countries over 10 years (Comas-Herrera *et al.*, 2003). This report, by Prof. Martin Knapp of the London School of Economics (LSE), estimates that there will be a 66% increase of cases in the UK from 1998 - 2031. This will create a serious financial burden to governments for the future care of Alzheimer patients. However the LSE report concludes that if there were a treatment available that could reduce the rate of cases of cognitive impairment by 1% per year, this would offset the long-term costs.

AD was first described as a medical condition in 1906 by the German medical researcher Alois Alzheimer (1864-1915) as 'an unusual disease of the cerebral cortex'. He had identified this in a woman, Auguste Deter, in her fifties with symptoms of 'memory loss, disorientation, hallucinations and an untimely death in 1906 aged 55yrs'. At post mortem he found 'abnormal clumps' (now called amyloid plaques) and 'tangled bundles of fibres' (neurofibrillary tangles of the tau protein). These are now recognised as the two classic hallmarks of AD seen at post mortem (Selkoe and Abraham, 1986). However this was an unusual case, as most AD is found in the elderly, the incidence doubling every 5 years over 65yr of age, with 20-25% affected over 80yrs age (Yesavage *et al.*, 2002). It is estimated that early onset AD, which occurs below 65 years of age, affects about 5% of the AD population (Campion *et al.*, 1999).

It is possible that symptoms of AD were first described in a non-professional, but accurate way, in 1726 by Jonathon Swift, in his novel Gulliver's Travels in his 'struldbrugs' (the people who never died). Ironically Swift probably suffered from the disease himself (Lewis, 1993). Early signs of AD are short-term memory loss that disrupts daily life, this progresses to an inability to recognise and use everyday objects and loss of verbal and communication skills such as forgetting words and problems with speaking and writing. As the disease develops, spreading to more areas within the brain, the AD sufferer becomes more withdrawn due to an inability to make decisions or join in with social situations as their mood and personality changes, becoming confused, suspicious, depressed or anxious. AD is a progressive neurodegenerative disorder with survival following the onset of symptoms being variable but shortened. The main predictor of life expectancy is the age of onset. The expected life span can be as long as 7 to 10 years for patients whose conditions are diagnosed when they are in their 60s and early 70s, to only about 3 years or less for patients whose conditions are diagnosed when they are in their 90s (Zanetti *et al*., 2009). AD is a complex disease and all the research indicates that it is probably caused by the interaction of more than one factor including genetic, environmental and life-style.

1.2 Neuropathology of AD

AD is a progressive neurodegenerative disease for which there is no cure. There is no absolute diagnosis except at post mortem when the two characteristic hallmarks are seen, extracellular amyloid plaques and intraneuronal fibrillary tangles (NFTs). Several types of neurons are involved: glutamatergic, cholinergic,

serotonergic and noradrenergic. The location and type of neuron involved will influence the symptoms (Perl, 2010).

The extracellular plaques consist mainly of beta amyloid peptide (Aβ). These plaques are also found in the cerebral cortex of non-demented elderly persons, so alone are not significant in AD. Neuroimaging, using ^{11}C Pittsburgh compound-B positron emission tomography (^{11}C-PiB PET) is able to discriminate between frontotemporal dementia and AD, showing significantly higher PiB retention in the grey matter of AD patients. PET scanning matches histopathological reports in aging and dementia, reflecting the true regional density of Aβ plaques in cortical areas. However there is no correlation with analyses of cognitive decline and cognition in AD, as ~30% of healthy older people, and ~60% with mild cognitive impairment, show cortical retention of ^{11}C-PiB retention, consistent with a high concentrations of plaques. Aβ plaques correlate with the rate of memory decline and episodic memory, suggesting that Aβ deposition is not a normal event in ageing. This supports the idea that Aβ deposition is an early event, occurring before the start of symptoms, possibly representing preclinical AD (Fodero-Tavoletti *et al*., 2009).

However the gradual accumulation of hyperphosphorylated tau protein within neurons correlates well with the progression of AD, as seen by worsening clinical symptoms. Levels of tau in cerebrospinal fluid (CSF), taken from patients with and without AD, show a very high correlation with the cognitive results from the Mini Mental State Examination (MMSE). Six stages of increasingly severe cortical destruction have been described (Braak and Braak, 1996). Stages I and II

are characterized by NFTs in the trans-entorhinal region, and stages III and IV are marked by severe involvement of both the entorhinal and transentorhinal regions. Isocortical destruction occurs during stages V and VI. NFTs alone are not diagnostic of AD as they are also found in frontotemporal dementia and other neurodegenerative diseases (Perl, 2000). Other pathological abnormalities seen in AD are a profound loss of neurons and synapses, reactive gliosis, microglial activation and inflammatory changes (Aisen, 2002).

1.2.1 Extracellular amyloid plaques and amyloid precursor protein (APP) processing

Extracellular amyloid plaques are solid insoluble lesions composed mainly of the beta amyloid peptide Aβ42, deposited in the brain. A proteomic analysis of over 2000 plaques from two AD post mortem brains identified 168 proteins in plaques that were not identified in non-plaque controls (Liao *et al*., 2004). From these, 26 proteins were identified as enriched by a minimum of 2-fold in the plaques, by quantitative comparison with surrounding non-plaque tissues. These included the classic components: Aβ42, α1-antichymotrypsin, α-synuclein, apolipoprotein E (ApoE), collagen type XXV, cystatin C, proteoglycans and clusterin. This study used laser capture microdissection (LCM) to collect the tissue samples, which allows cutting a microscopic region as small as 3-5 μm in diameter, followed by analysis using liquid chromatography combined with tandem mass spectrometry (LC-MS/MS). This study shows the complexity and diversity of cellular processes involved in Aβ plaque formation (Liao *et al*., 2004). The beta amyloid peptide Aβ42 is a product from the metabolism of the amyloid precursor protein

(APP), by proteolytic cleavage by β- and γ-secretases. Aβ42 is the toxic peptide and is found at the core of the amyloid plaques.

1.2.1.1 Aβ discovery and links with Down's syndrome

Aβ was first sequenced 20 years ago from meningeal blood vessels of AD patients and also individuals with Down's syndrome (Glenner and Wong, 1984). In 1985 Aβ was identified as the main component of senile neuritic plaques of AD brain tissue (Masters *et al.*, 1985). As the most common of the neurodegenerative diseases, these discoveries marked the beginning of extensive research into AD. Cloning of the APP gene and its localisation to chromosome 21, linked with the knowledge that individuals with Down's syndrome, which possess a trisomy of chromosome 21, invariably develop AD, led to the hypothesis that excessive Aβ accumulation in the brain was the primary event in the development of AD (Tanzi *et al.*, 1987).

1.2.1.2 APP processing

APP is a transmembrane glycoprotein with a 590-680 amino acid extracellular amino terminal domain, a single membrane-spanning region, and an approximately 55 amino acid cytoplasmic tail, which contains intracellular trafficking signals. Human APP contains a neural-specific promoter element, the physiological significance of which is still unclear (Collin and Martens, 2006). The APP gene is located on chromosome 21, spans 291 kilobases and contains at least 18 exons. APP can produce eight possible isoforms, three of which (the 695, 751 and 770 amino acid isoforms) predominate in the brain (Kang *et al.*, 1987).

The APP695 isoform is expressed mainly in neurons (Thakur and Mani, 2005). The APP751 and APP770 isoforms, which contain a Kunitz-protease inhibitor (KPI) domain, are found mostly in non-neuronal glial cells. All three isoforms share the same Aβ, transmembrane and intracellular domains and are thus all potentially amyloidogenic. APP has been found in the cytoplasm of rat brain cells and is present in most neurons but in different amounts depending on the neuron size, the larger the neuron, the greater amount of APP. This would indicate that APP may play a specific role in the function of several different classes of neurons (Ouimet *et al*., 2004). The complete function of APP is still unclear, although it has been demonstrated that APP localizes in the synapses of neurons where it may play a role in neurite growth and synaptic formation and repair (Priller *et al*., 2006). APP knock-out mice are viable with only minor effects in their phenotype, demonstrating evidence of memory loss and some impaired long-term potentiation but without general neuron loss (Phinney *et al*., 1999). However, APP expression in neurons increases with age in non-demented individuals, but APP expression in neuronal somata decreases in AD patients in direct correlation with the mature amyloid plaque aggregation (Barger *et al*., 2008). Interestingly ApoE expression correlates with the mature amyloid plaque aggregation and excess ApoE was detected in plaques. It is probable that *in vivo,* over expression of ApoE and APP are linked during cellular stress but this link is disrupted during AD pathogenesis.

1.2.1.3 Protein sequence of human APP770

The protein sequence for human APP 770 isoform is shown in Figure 1.1.

```
        10          20          30          40          50          60
MLPGLALLLL AAWTARALEV PTDGNAGLLA EPQIAMFCGR LNMHMNVQNG KWDSDPSGTK

        70          80          90          100         110         120
TCIDTKEGIL QYCQEVYPEL QITNVVEANQ PVTIQNWCKR GRKQCKTHPH FVIPYRCLVG

        130         140         150         160         170         180
EFVSDALLVP DKCKFLHQER MDVCETHLHW HTVAKETCSE KSTNLHDYGM LLPCGIDKFR

        190         200         210         220         230         240
GVEFVCCPLA EESDNVDSAD AEEDDSDVWW GGADTDYADG SEDKVVEVAE EEEVAEVEEE

        250         260         270         280         290         300
EADDDEDDED GDEVEEEAEE PYEEATERTT SIATTTTTTT ESVEEVVREV CSEQAETGPC

        310         320         330         340         350         360
RAMISRWYFD VTEGKCAPFF YGGCGGNRNN FDTEEYCMAV CGSAMSQSLL KTTQEPLARD

        370         380         390         400         410         420
PVKLPTTAAS TPDAVDKYLE TPGDENEHAH FQKAKERLEA KHRERMSQVM REWEEAERQA

        430         440         450         460         470         480
KNLPKADKKA VIQHFQEKVE SLEQEAANER QQLVETHMAR VEAMLNDRRR LALENYITAL

        490         500         510         520         530         540
QAVPPRPRHV FNMLKKYVRA EQKDRQHTLK HFEHVRMVDP KKAAQIRSQV MTHLRVIYER

        550         560         570         580         590         600
MNQSLSLLYN VPAVAEEIQD EVDELLQKEQ NYSDDVLANM ISEPRISYGN DALMPSLTET

        610         620         630         640         650         660
KTTVELLPVN GEFSLDDLQP WHSFGADSVP ANTENEVEPV DARPAADRGL TTRPGSGLTN

        670         680         690         700         710         720
IKTEEISEVK MDAEFRHDSG YEVHHQKLVF FAEDVGSNKG AIIGLMVGGV VIATVIVITL

        730         740         750         760         770
VMLKKKQYTS IHHGVVEVDA AVTPEERHLS KMQQNGYENP TYKFFEQMQN
```

Fig. 1.1 Amino acid sequence of human APP isoform 770 (UniprotKB P05067). The residues in red (672-713) show the sequence of Aβ42. The residues in green (1-35) show an ER targeting sequence. The residues in blue (40-51) show a mitochondrial targeting sequence (section 1.2.15) (Anandatheerthavarada *et al*., 2003).

APP is cleaved by three secretases in specific, successive sequences: α-secretase is member of the ADAM (A Disintegrin And Metalloprotease) family that are

expressed on the surface of cells, are zinc dependent and are anchored to the cell membrane. ADAM10, ADAM17, ADAM9 and tumour necrosis factor α (TNFα) or TNFα converting enzyme (TACE) show α-secretase activity (Postina, 2008). α-secretase cleaves within the Aβ domain initiating the non-amyloiogenic pathway. ß-secretase, also known as beta-site APP cleaving enzyme 1 (BACE1) is a transmembrane aspartic acid protease and cleaves at the N terminus of the Aβ domain, and this initiates the amyloidogenic pathway. γ-secretase is a protease complex of at least four proteins: presenilin, nicastrin, anterior pharynx-defective 1 (APH-1), and presenilin enhancer 2 (PEN-2), and cleaves residues in the intramembrane space, around the C terminus of the Aβ domain. The sequence of cleavages promotes proteolytic processing via two pathways: non-amyloidogenic and amyloidogenic (Figures 1.2 and 1.3).

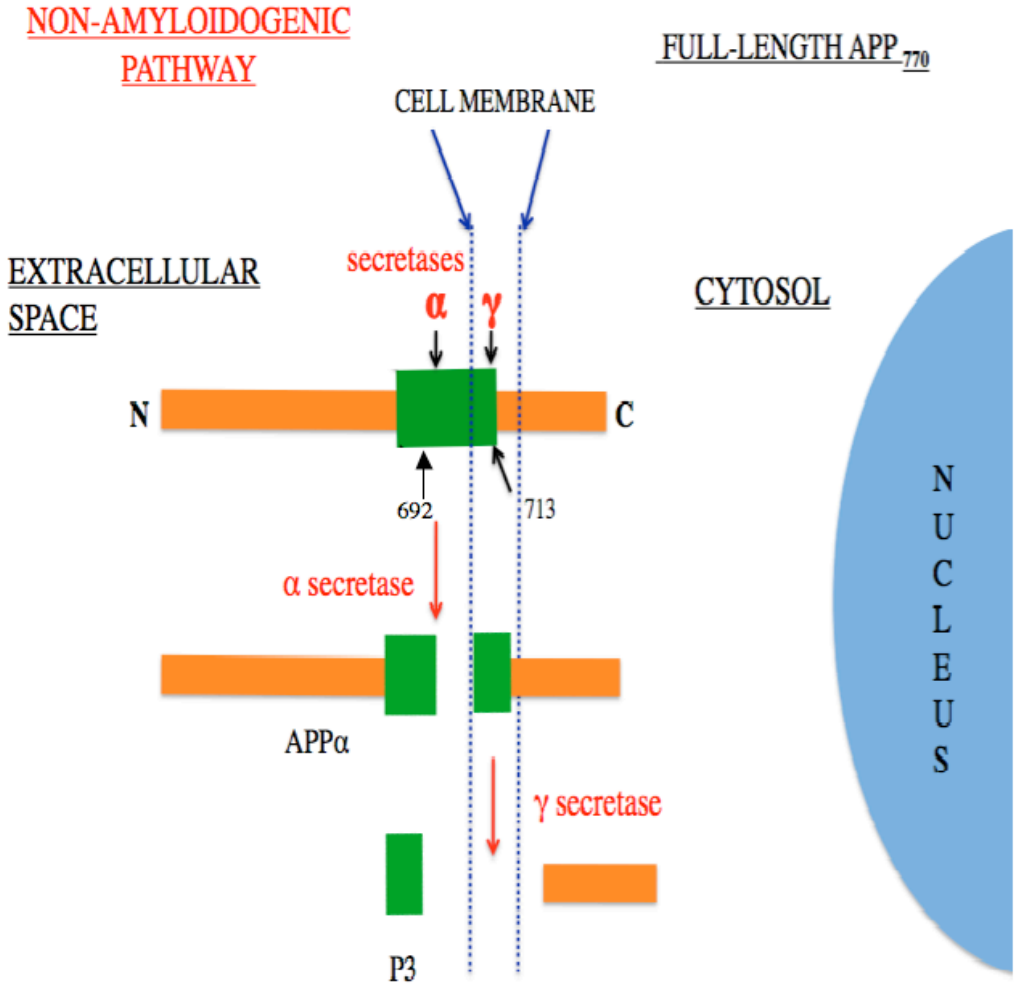

Fig. 1.2. APP processing of APP770 promoting the non amyloidogenic pathway. Cleavage by the α-secretase at amino acid 692(A), splitting the Aβ domain (green), creates a non-amyloidogenic soluble N-terminal fragment APPα. Further cleavage by γ-secretase at residue 713(A), in the intramembranous space, forms a non-toxic peptide P3 and non-amyloidogenic C-terminal fragment.

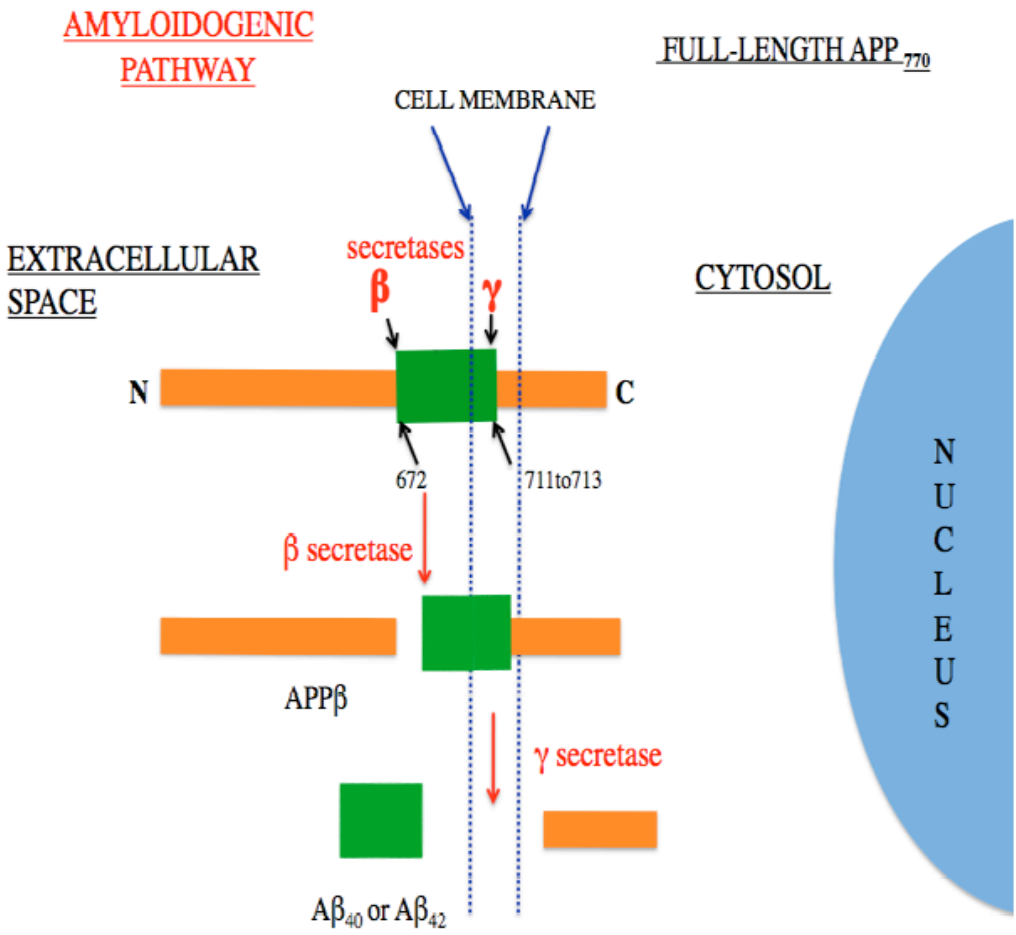

Fig. 1.3. APP processing of APP770 promoting the amyloidogenic pathway. The Aβ peptides are produced by proteolytic cleavage, first by the ß-secretase at the extracellular residue 672(D) which creates a shorter N-terminal soluble peptide APPβ. Further cleavage by the γ-secretase at residue 711 or 713, in the intramembranous space, forms the insoluble peptides Aβ40 or Aβ42.

1.2.1.4 Aβ42 the toxic peptide in AD

Aβ40 and Aβ42 are the two most common Aβ species containing 40 and 42 amino acids, respectively, but Aβ42 is the toxic peptide found in excess in the brains of AD patients, with Aβ40 being found mainly in blood vessels (Tekirian *et al*., 1996). Other smaller Aβ peptides (38 or 39 amino acids) can be formed if the

γ-secretase cuts before residue 711. Both α- and β-secretase cleave the extracellular domain of APP. The γ-secretase cleaves the transmembranous domain, and it is suggested that this may be why the Aβ peptides still retain their affinity for membrane binding (Williams and Serpell, 2011).

The two extra amino acids in Aβ42, isoleucine and alanine, are hydrophobic (Figure 1.4). This increases its affinity to bind to itself and aggregate in aqueous solutions, more than Aβ40. It is thought that this tendency to cluster is responsible for its toxicity. Evidence for this has been shown by substitution of the two residues with hydrophilic amino acids that results in a decrease in aggregation (Kim and Hecht, 2005).

Aβ40

```
672       680         690         700         710
  DAEFRHDSG YEVHHQKLVF FAEDVGSNKG AIIGLMVGGV V
            10          20          30          40
```

Aβ42

```
672       680         690         700         710
  DAEFRHDSG YEVHHQKLVF FAEDVGSNKG AIIGLMVGGV VIA
            10          20          30          40
```

Fig. 1.4. Amino acid sequences of Aβ40, residues 672-711 of APP and Aβ42, residues 672 to 713 of APP. The residue numbers of the peptides 1-40 and 1-42 are shown in blue. The two residues at the C terminus of the Aβ42, shown in red, are the hydrophobic residues isoleucine and alanine.

Certain other residues also play a key role in aggregation. Two hydrophobic regions of Aβ42 at residues 17–21(LVFFA) and 31–42 (IIGLMVGGVVIA) are

considered to be important for fibril structure (Luhrs *et al*., 2005). Substitution at residue 20 for the hydrophilic glutamic acid, F20E, in the Aβ sequence also reduces aggregation (Fraser *et al*., 1992). There is much research aimed at reducing the toxic effect of Aβ by inhibiting its expression and/or its aggregation thus reducing its direct interaction with neuronal cellular mechanisms.

Aβ can disrupt membrane integrity by direct or indirect effects. Aβ binds to phospholipid membranes with a high affinity and it is suggested that the head-group charge of the phospholipids contributes to the association between Aβ and the membrane via electrostatic interactions (Kremer and Murphy, 2003). Aβ interacts with several cell surface receptors inducing membrane permeation or cell death. The formation of stable pores and ion channels is a model proposed for amyloid-induced toxicity. The disruption of Ca^{2+} homeostasis has been recognized as a potential mechanism associated with AD, and was shown to be involved in the amyloid cascade hypothesis, where elevated Ca^{2+} was suggested to be a consequence of both tau phosphorylation and cell death (Hardy and Higgins, 1992).

There is considerable evidence of Aβ binding at neuronal surfaces and at synapses (Lambert *et al*., 1998). Interaction of Aβ42 with cell surface receptors triggers cell signal transduction leading to changes in intracellular protein expression with toxic effects (Irvine *et al*., 2008). Several examples of cell surface receptors have been postulated to be affected by Aβ42, including the insulin receptor, amylin receptor, receptor for glycation end products (RAGE) (Patel and Jhamandas,

2012), α7- nicotinic acetylcholine receptor (Parri *et al*., 2011), p75 neurotrophin receptor (p75NTR), NMDA glutamate receptors and monosialoganglioside (GM1). Aβ42 peptides compete with insulin for the insulin receptor and this may be the cause of impaired glucose metabolism in AD (Xie *et al*., 2002). A study using primary cultures of rat cholinergic forebrain neurons showed that an amylin receptor antagonist blocked Aβ induced neurotoxicity (Jhamandas and MacTavish, 2004). Inhibition of the RAGE-Aβ interaction suppresses accumulation of Aβ in the brain (Deane *et al*., 2003). The α7-nicotinic acetylcholine receptor mediates survival pathways via the PI3-AKT pathway leading to up-regulation of anti-apoptotic proteins BCL2 and BCL-X and initiates jak2/stat3 survival pathway. This receptor is highly expressed on cholinergic basal forebrain neurons (Patel and Jhamandas, 2012). Aβ binding to α7-nicotinic acetylcholine receptors triggers endocytosis of glutamate receptor subunits and the insulin receptor and alters trafficking of metabotropic glutamate receptors (Patel and Jhamandas, 2012).

Aβ binding to NMDA receptors causes abnormal Ca^{2+} mobilization and there is an overall reduction of NMDA receptors in the presence of Aβ causing a loss of memory and reduced learning capacity. RAGE controls the entry of Aβ into the blood–brain barrier (BBB), by binding soluble Aβ in a dose-dependent manner at nanomolar concentrations and mediating Aβ transcytosis across the BBB in a time- and temperature-dependent manner (Chen *et al*., 2007; Deane *et al*., 2003; Mackic *et al*., 2002). Aβ binding to GM1 enables Aβ to cross the blood-brain barrier. These interactions could all be useful as therapeutic targets for AD.

1.2.1.5 Aβ42 and mitochondrial dysfunction

Aβ has also been shown to insert into the cell membrane, with a short section associating with lysosomal membranes, causing lysosomal destabilization leading to toxic effects in the cell (Liu *et al*., 2010). There is now evidence that Aβ42 enters mitochondria, binding to mitochondrial proteins, causing mitochondrial dysfunction and eventually cell death. Evidence suggests that Aβ42 interferes with the mitochondria permeability transition pore, which disrupts normal protein functions, leading to cell homeostasis and cell death, reviewed in (Muirhead *et al*., 2010). Mitochondrial Aβ was first described in 2004 (Lustbader *et al*., 2004). This study showed, using immunoelectron microscopy, that Aβ binds to 3-hydroxyacetylCoAdehydrogenase (HADH2), also known as amyloid binding alcohol dehydrogenase (ABAD), an enzyme which is expressed in the matrix of mitochondria. This was shown to occur only in AD affected brains (Lustbader *et al*., 2004), and this was confirmed and also shown in a Tg mAPP mouse model (Caspersen *et al*., 2005). The Caspersen study showed that Aβ40 and Aβ42 colocalised with the mitochondrial matrix chaperone heat shock protein 60 (HSP60) but a protease-protection assay could not discriminate between the matrix compartment and the intermembrane space or the inner mitochondrial membrane. The ability of Aβ to enter the cell is a matter of debate. As shown in Figure 1.3, the Aβ peptides are assumed to be cleaved outside the cell. However studies have shown Aβ present within the mitochondrial membrane in mitochondrial preparations from non-demented brain biopsies (Hansson Petersen *et al*., 2008). Subsequent studies on a human neuroblastoma cell line revealed Aβ was imported, independent of the mitochondrial membrane potential, and

dependent on the outer mitochondrial membrane (TOM) translocase pathway, using TOM20, TOM40 and TOM70 (Hansson Petersen *et al*., 2008). Other studies have shown indirect import of Aβ into mitochodria can also occur by localised APP processing followed by Aβ synthesis. It is reported that APP has a chimeric N-terminal targeting sequence (Figure 1.1), causing the peptide to translocate to the ER and the mitochondria (Anandatheerthavarada *et al*., 2003). The APP is seen in a transmembrane arrested form, in an N- in C- out orientation, with a 73kDa C-terminal domain in the cytosol. Anandatheeravarada proposed that the acidic domains 220-290 of APP 695 hindered the transfer and the transmembrane arrested form is associated with mitochondrial dysfunction. Anandatheeravarada colocalised APP with mitochondrial translocase proteins TOM 40, TIM 23 and TIM44, indicating that APP translocating to the mitochondria is dependent on the translocase pathway. APP accumulates in the protein import channels of mitochondria in AD brains but not in age matched controls (Devi *et al*., 2006). Devi showed APP formed a 480kDa complex with TOM40 and a 620kDa complex both with TOM40 and the translocase of the inner mitochondrial membrane 23 (TIM23). This was shown to inhibit the import of cytochrome C oxidase subunits IV and Vb proteins, which was associated with decreased cytochrome C oxidase activity and increased H_2O_2 production. This mitochondrial APP was found to be concentrated in areas of the brain vulnerable to AD toxicity, such as the frontal cortex, hippocampus, and amygdala and the levels of APP correlated directly with mitochondrial dysfunction. It is still unclear whether Aβ accumulates in the mitochondria matrix or in the membrane

compartment of AD affected brain. But it has been shown that it is possible that the translocase system is a direct method of importing APP and Aβ into the cell.

1.2.2 Intracellular neurofibrillary tau tangles (NFTs)

Intracellular NFTs are formed from aggregates of the hyperphosphorylated tau protein that is deposited inside neurons. Tau is a very soluble microtubule-associated protein (MAPT) and is expressed in six isoforms ranging from 352 to 441 amino acid residues. It contains 3 or 4 binding domains at the C terminus, depending on the isoform. The tau gene is located on chromosome 17, locus 17q21 and contains 16 exons. In the cell, MAPT reacts with tubulin to stabilise microtubules in the cytoskeleton, and in humans MAPT stabilises the axons of neurons. Post-translational modification of MAPT is caused by glycation, glycosylation, phosphorylation, ubiquitination and proteolytic processing that may disrupt its normal function (Gong *et al.*, 2005). In AD the stability of microtubules may be disrupted by phosphorylation of MAPT, which is controlled by certain kinases e.g. protein kinase N (PKN), glycogen synthase kinase 3 (GSK3) and cyclin-dependent kinase 5 (cdk5) (Schneider *et al*., 1999). Phosphorylation by microtubule affinity regulating kinase (MARK) and protein kinase A (PKA) at sites that interfere with microtuble binding, interfere with tau tangle production (Schneider *et al.*, 1999). In AD, MAPT becomes hyperphosphorylated and aggregated when paired helical filaments join to become 'tau tangles', the hyperphosphorylated tau being insoluble. Recent studies have also identified the involvement of prolyl isomerase (PIN1) a protein that protects neurons (Butterfield *et al*., 2006). PIN1 acts on proteins after phosphorylation at certain sites, changing the structural conformation. This change in conformation

promotes cellular health in AD by untwisting APP and tau to return them to a functional state. Loss of PIN1 leads to over production of Aβ and accumulation of abnormal tau (Butterfield *et al*., 2006; Driver and Lu, 2010). There is still some debate as to whether NFTs appear before amyloid plaques in the progression of AD as the dementia symptoms correlate more with the production of NFTs in the brain than with amyloid plaque formation (Gomez-Isla *et al.*, 1997) and NFT formation follows a specific pattern of distribution in AD, starting in the entorhinal cortex which is not age related (Braak and Braak, 1991). However, it is more generally accepted that NFTs appear after Aβ production, as explained by the amyloid cascade hypothesis (Hardy and Higgins, 1992). Interestingly mutations in the MAPT gene do not result in AD but are related to frontotemporal dementia like Pick's disease also called frontotemporal dementia with Parkinsonism linked to chromosome 17 (FTDP-17), cortico-basal degeneration and progressive supranuclear palsy (Hutton *et al*., 1998; Spillantini and Goedert, 2000). These dementias do not have amyloid plaques indicating that tau aggregation is downstream from Aβ effects.

Similar to Aβ, it is now thought that MAPT may be present as a toxic, soluble, oligomeric, phosphorylated form, before aggregating into the insoluble tangles (Haass and Selkoe, 2007). The progression of soluble to insoluble tau is now most likely the important physiological/pathological change in AD. However there is little agreement as to whether tau is a good target for drug treatment for AD. Some pharmaceutical companies are looking at inhibiting the phosphorylation, while other research concentrates on preventing tau aggregation and expression

(Roberson *et al.*, 2007) and improving microtubule function (Schneider and Mandelkow, 2008).

1.3 Genetics of AD

Genetic studies have identified four genes associated with AD. Three are associated with early onset familial AD (FAD): APP, presenilin 1 (PS1) and presenilin 2 (PS2) and one with sporadic late onset AD (LOAD): ApoE.

(1) APP located on chromosome 21 which produces the Aβ peptides.

(2) PS1 located on chromosome 14 which interacts with the Aβ peptide.

(3) PS2 located on chromosome 1 which also interacts with the Aβ peptide.

(4) ApoE is located on chromosome 19 and binds lipoproteins and cholesterol.

FAD is rarer than sporadic AD and is caused by mis-sense mutations that account for less than 5% of all cases of AD (Campion *et al.*, 1999). Autosomal dominant mutations of APP, PS1 and PS2 genes increase the risk of early onset familial FAD, i.e. before 60yrs age.

1.3.1 Early onset AD

Research on Down's syndrome, a genetic abnormality where there are three copies of chromosome 21, found genetic mutations causing AD (Goate *et al.*, 1991). This was significant as the APP gene is located on chromosome 21 and therefore the protein is expressed in excess, giving rise to a higher probability of AD because of excess Aβ being produced.

1.3.1.1 APP point mutations

In the Goate study, two families with early onset AD and symptoms occurring before 60 years of age, were identified with a point mutation at residue 717 (V717I) in APP770. This APP mutation was found to produce Aβ deposits and was recognised as a marker for early onset familial AD (FAD). Prior to this, Aβ deposits had been found in individuals with a history of hereditary cerebral haemorrhage with amyloidosis–Dutch (HCHWA-D) (Levy *et al.*, 1990). A point mutation at codon 693 (E693Q) in APP770 was identified in these patients, and was named the Dutch mutation. Twenty five other APP point mutations have since been found (Hardy J 2010 Alzheimer Research Forum). The most well known disease associated with intra-Aβ mutations, include Flemish A692G, Italian E693K, Arctic E693G, Dutch E693Q, Iowa D694N, and London V717I. A double missense mutation in a Swedish family occurs at residues K670N/M671L (Figure 1.5 and Table 1.1).

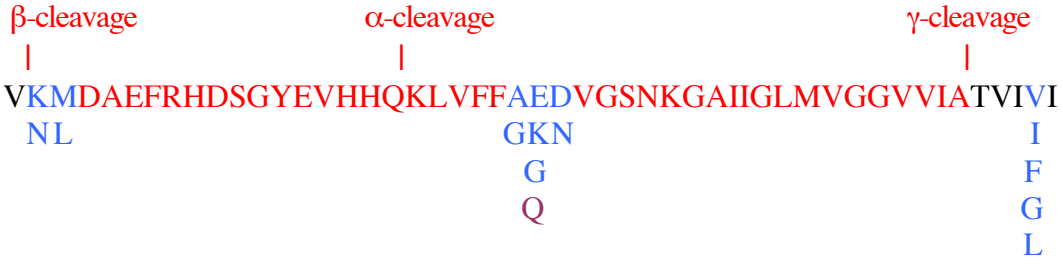

Fig. 1.5 Amino acid sequence 669-718 of human APP isoform 770, showing the secretase cleavage sites. The residues in red show the sequence of Aβ42. The residues in blue show the point mutations found in APP causing FAD and in purple the point mutation for HCHWA-D.

Most of the mutations are at, or very near, the sites within APP that are normally cleaved by the α-, β- and γ-secretases. APP mutations within the Aβ sequence increase the aggregation of Aβ into amyloid fibrils. Mutations at or near the γ-

secretase cleavage site appear to increase the Aβ42/Aβ40 ratio without altering the overall quantity of Aβ. This can only happen when the mutations exert an effect on γ-secretase (Bentahir *et al*., 2006; Citron *et al*., 1997). Mutations near the α-secretase cleavage site are thought to create more vascular amyloidosis or a mixed vascular/AD pathology (De Strooper and Annaert, 2000).

NAME	**CODON**	**MUTATION**	**CLOSE TO SECRETASE CLEAVAGE SITE**	**Aβ PRODUCTION**
ARCTIC	693	E-G	α-secretase	Decreased Aβ40 and Aβ42 production in plasma, but increased protofibril formation.
DUTCH	693	E-Q	α-secretase	HCHWA-D and increased Aβ and p3 production.
FLEMISH	692	A-G	α-secretase	HCHWA & increased Aβ and p3 production.
IOWA	694	D-N	α-secretase	
ITALIAN	693	E-K	α-secretase	
		V-G		
LONDON	717	V-I	β-secretase	increased Aβ42 production.
		V-L		
SWEDISH	670/671	K-N/M-L	γ-secretase	increased Aβ40 and Aβ42 production due to increased affinity for BACE for the cleavage site.

Table 1.1 Examples of well-known APP mutations showing the codon and mutation, common nomenclature and effect on Aβ peptide production.

All of the mutations in Table 1.1 (except the Flemish) alter the charge properties of Aβ, which probably increases the likelihood of Aβ aggregation. Recently it has been suggested that the Flemish mutation causes an increase in γ-secretase

cleavage by preventing an inhibitory influence by the middle region of Aβ on γ-secretase activity.

1.3.1.2 Presenilins in AD

Both presenilins are highly homologous at the DNA sequence, protein sequence and gene structure levels (Alzheimer's Collaborative Group 1995). The proteins are large multi-pass transmembrane proteins (PS1 contains 467 amino acid residues, and PS2 contains 448) and they each contain 6 or 8 transmembrane domains. Several studies indicated that the functions of PS1 and PS2 are the catalytic components of γ-secretase (De Strooper *et al*., 1999; Haass and De Strooper, 1999), γ secretase being a protein complex composed of at least four proteins: presenilin, nicastrin, anterior pharynx-defective 1(APH-1), and presenilin enhancer 2 (PEN-2). Presenilins are also involved with Notch signalling (Baumeister *et al*., 1997; Levitan *et al*., 1996) and presenilins have been found to play a key role in the modulation of intracellular Ca^{2+} involved in presynaptic neurotransmitter release and long-term potentiation induction (Zhang *et al*., 2006). More recently, presenilin has been identified in having a fundamental role in autophagy, the process by which cells dispose of unwanted proteins which is essential for neuronal survival (Nixon and Yang, 2011).

Mutations in PS1 or PS2 lead to amyloidogenic processing of APP with an increasing ratio of toxic Aβ42 to Aβ40. Their role in AD was noted after observations that presenilins lead to altered APP processing in the same way as APP717 mutations (Scheuner *et al*., 1996). Approximately 20 point-mutations have been identified in PS1 and over 10 in PS2. Most of the pathogenic mutations

are missense mutations in residues conserved in the two proteins. They are not randomly distributed, but cluster in exon 8 and along faces of the transmembrane alpha-helices (Crook *et al*., 1997; Perez-Tur *et al*., 1996). Most single and double transgenic mouse models for AD have been developed based on mutations in APP and presenilins. Some triple transgenic models have been developed recently including tau or a tau mutation (Oddo *et al*., 2003).

1.3.2 Late onset Alzheimer's disease (LOAD)

Most AD is sporadic, of uncertain cause and occurs in the elderly. Tau, located on chromosome 17, is thought to be activated later in the progression of both early onset and late onset disease. Apolipoprotein E allele 4 (ApoE4) located on chromosome 19 is associated with LOAD.

1.3.2.1 ApoE

The ApoE gene is associated with late onset AD and is known as the late onset susceptibility gene. The ApoE gene contains four variants (alleles). Allele 3 is the most common. Allele E2 reduces the risk of getting AD, but allele E4 increases the risk of getting the disease. It is suggested that ApoE4 promotes excess deposition of Aβ42 in a similar manner to the mutations of the other genes associated with AD (Esler *et al*., 2002; Golabek *et al*., 1996). Importantly, E3 and E4 bind to different lipoprotein particles. E3 and E2 bind preferentially to high-density lipoproteins (HDL). E4 preferentially binds very low lipoproteins (VLDL). There is an increased prevalence of ApoE E4 in late onset AD (Corder *et al*., 1998) but it is unclear how it perturbs the cellular activity; however, the ApoE E4 allele is without a cysteine that will affect its ability to crosslink with

other molecules by disulphide bridging. It is also suggested that E4 preferentially binds very low lipoproteins (VLDL) because its structure is different from E3 (Ruiz *et al*., 2005). The amino acid substitution R112C, causes a hidden arginine at position 61 to point outwards and this then forms a salt-bridge between with glutamic acid at position 255. This completely changes the conformation of the structure and causes this isoform to bind preferentially to VLDL instead of HDL. In addition the cysteine in apoE2 and apoE3 means that they form dimers (via a disulphide bond) whereas apoE4 does not. This affects lipid binding, the dimers reducing LDL binding. ApoE4 also has a greater tendency to form a molten globule state being more unstable. ApoE2 is most stable at the N-terminal region and this may contribute to its reported protective effect in AD.

1.3.2.2 Other genes associated with LOAD

Other genes have also recently been identified with LOAD: clusterin (CLU), also known as ApoJ (apolipoprotein J) and PICALM (phosphatidyl-inositol-binding clathrin assembly lymphoid-myeloid leukaemia gene) an intracellular signalling protein (Harold *et al*., 2009). ApoJ has previously been linked with expression of cholesterol (Gelissen *et al*., 1998) and ischaemic heart disease. ApoJ is known to be induced in myocarditis and numerous other inflammatory injuries (McLaughlin *et al*., 2000). Clusterin is now identified with Aβ clearance due to its action in removing cellular debris. Angiotensin-converting enzyme (ACE) has significantly increased levels in the AD brain (Miners *et al*., 2009b).

Other mutations and genes have also been identified with AD but they present a lower risk. These include on chromosome 12 (Scott *et al*., 2000), an

antichymotrypsin gene, serotonin transporter gene, butyryl cholinesterase E gene and various ApoE receptor genes. More recently two more genes associated with AD have been identified. Sortilin-related receptor (SORL 1) protein protects neurons but varients in the gene increase Aβ production (Lee *et al*., 2008). GRB2-associated binding protein 2 (GAB2) is a modifying factor of ApoE epsilon 4 allele (Williamson *et al*., 2009) but another group found no link with GAB2 when genotyping 1116 individuals (521 AD patients and 475 normal controls) from a national population in Spain (Ramirez-Lorca *et al*., 2009).

1.3.3 Risk factors for sporadic, late onset AD (LOAD)

AD is a complex disease and its pathogenesis is probably multifactorial but can be influenced by genetic factors. Studies consistently identify the main risk factors as increasing age, genetic susceptibility especially the presence of the apoE4 polymorphism, obesity and diabetes.

ApoE is the best established genetic risk factor for LOAD. The presence of the ApoE4 polymorphism increases the chance of developing sporadic AD. ApoE has 3 main polymorphisms, with E2 and E4 differing each from E3 by only one amino acid:

ApoE2 – C158 & C112

ApoE3 – R158 & C112

ApoE4 – R158 & R112

ApoE4 may be such a robust risk factor for AD for a number of reasons. One of these is that it is poorly lipidated. The E4 form, because of its constrained

structure, compared with other isoforms, is not able to bind HDL but binds VLDL instead. Lipidated ApoE3 is able to bind Aβ and thus to clear it from the brain. ApoE4, being less lapidated, binds to Aβ and fibrillises it rather than clears it. However all the polymorphisms are associated with NFTs and Aβ plaques in the brain. In the transgenic model of a cross of the knockout ApoE mouse with a mutant APP (mAPP) over-expressing mouse has shown reduced amyloid plaques without changing the total amount of Aβ produced. ApoE receptors mediate several intracellular signalling kinases including PI3K, CDK-5, JnK and MAPK, some of which are involved with phosphorylation of tau. ApoE receptor binding APP and Reelin also influence cell signalling. Reelin increases neurite outgrowth possibly by keeping APP at the cell surface and not allowing its endocytosis (Hoe and Rebeck, 2008).

In the search for environmental factors, diet has been investigated. In a three-centre study in France, between 1999 and 2004, the conclusion was that 'frequent consumption of fruits and vegetables, fish, and omega-3 rich oils may decrease the risk of dementia and AD, especially among ApoE4 non-carriers' (Barberger-Gateau *et al*., 2007). Antioxidants and certain naturally occurring dietary polyphenolic phytochemicals have all been investigated, in particular, curcumin from turmeric, resveratrol from grapes and wine, and green tea catechins, epigallocatechin gallate (EGCG) because of their anti-amyloidogenic, anti-oxidative, and anti-inflammatory properties (Kim *et al*., 2010). It is claimed that protection against Aβ-induced cytotoxicity can be shown for some antioxidants. In addition, increased activities of superoxide dismutase and catalase have been

shown to inhibit neuronal cell death induced by Aβ (Behl *et al*., 1994; Qin *et al*., 2002). Studies have also suggested a link between dietary intake of antioxidants and a reduced risk for AD (Gonzalez-Gross *et al*., 2001; McDaniel *et al*., 2003).

In the early stages of AD, aerobic exercise slows the progression, 'showing a positive effect on cognition, glucose metabolism, and hypothalamic-pituitary-adrenal axis and trophic activity', particularly in women (Baker *et al*., 2010).

1.4 The amyloid cascade hypothesis

It was first proposed that the neurodegeneration in AD may be caused by the accumulation of Aβ in *extracellular* plaques in brain tissue. This became known as 'the amyloid cascade hypothesis', showing that accumulation of extracellular Aβ in the brain is the primary event in the development of AD (Hardy and Higgins, 1992) (Figure 1.6).

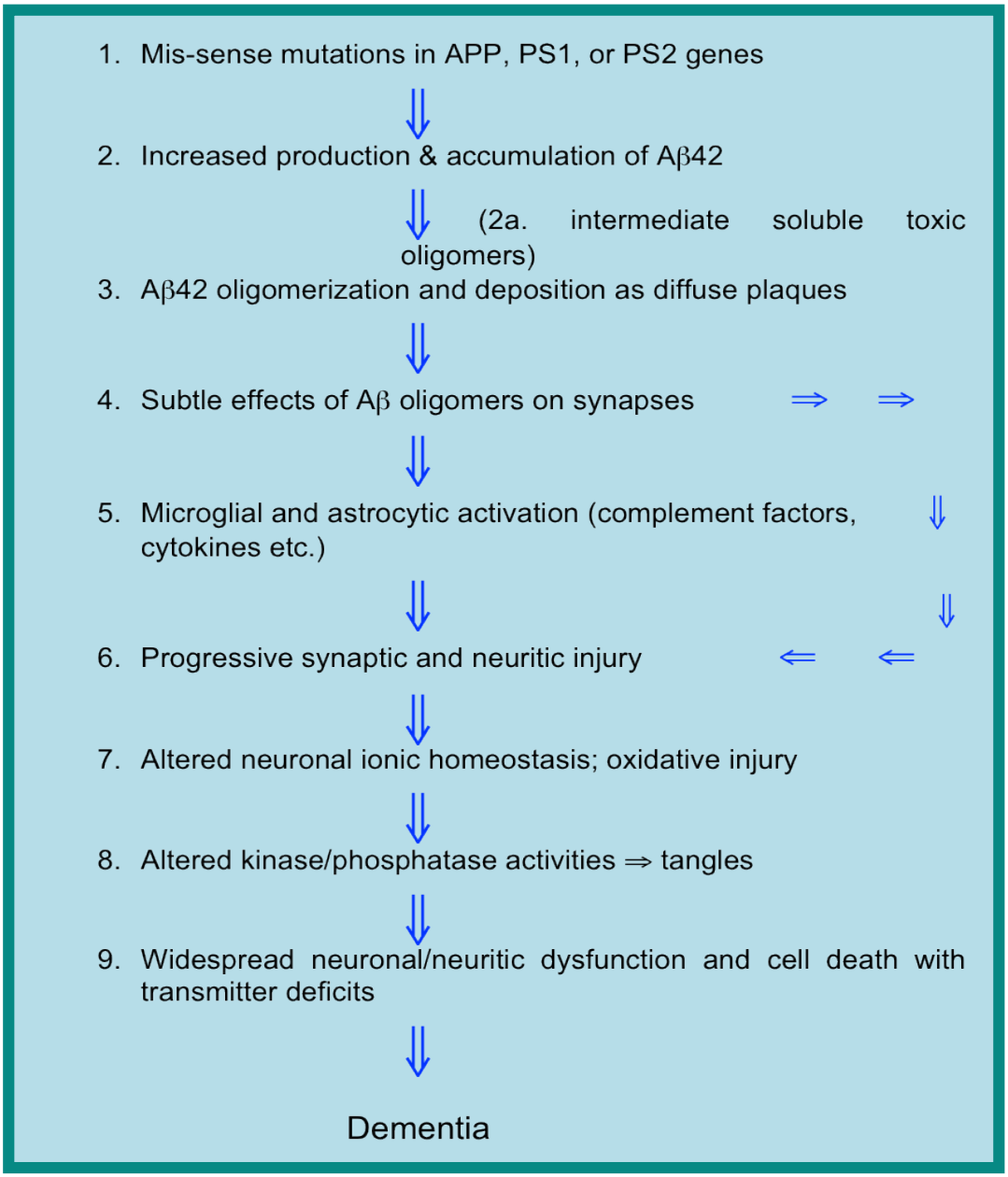

Fig. 1.6. The amyloid cascade hypothesis.

Other processes of the disease occur later, including formation of NFTs. NFTs are thought to result from an imbalance between Aβ production and clearance.

There has been recent evidence that *intracellular* soluble oligomeric Aβ accumulation is more likely the cause of a pathological cascade (Wirths *et al*., 2004), leading to the clinical signs of AD and the amyloid cascade hypothesis has subsequently been modified (Hardy, 2009; Wirths *et al*., 2004). The observation of intermediary toxic soluble oligomers of Aβ initiating AD (2a in Figure 1.6), would help explain why amyloid plaque deposits have also been found in cognitively normal elderly patients. There is evidence to support the effects of intracellular Aβ, for when Aβ42 fibrils were injected into the brains of P301I mutant tau transgenic mice, the intracellular Aβ was able to influence NFT formation (Gotz *et al*., 2010).

In AD, Aβ accumulates as a result of an imbalance between the production of Aβ and its removal from the brain, with increasing evidence that in the majority of sporadic forms of AD, the accumulation of Aβ is a result of defects in its removal (Miners *et al*., 2008). The secretases influence the production of Aβ. BACE1 is recognised as a rate-limiting enzyme affecting the production of the peptide from APP. A recent publication suggests regulation also occurs by ADAM10 suppressing the α-secretase cleavage, allowing the β-secretase to cleave preferentially, thereby increasing Aβ production (Kuhn *et al*., 2010). There are several enzymes identified in the degradation of Aβ, most of which are expressed

in neurons or glia, but some are found in the cerebral vasculature. These include including plasmin, insulin degrading enzyme (IDE), endothelin-converting enzymes (ECE1 and ECE2) and neprilysin (NEP) and angiotensin converting enzyme (ACE). NEP is a zinc metalloendopeptidase localised to the plasma membrane where it functions to degrade extracellular peptides. Findings suggest that reduction in NEP and IDE activity is not the primary cause of Aβ accumulation in AD but rather a late-stage phenomenon secondary to neurodegeneration (Miners *et al*., 2009a).

1.5 Proteomic analysis in AD

Proteomic studies of cerebrospinal fluid (CSF), blood and AD brain tissue have identified numerous proteins linked to the development of AD (Korolainen *et al*., 2010). However it is unusual for different proteins to be replicated in different studies. Korolainen's recent review noted only seven proteins showing similar changes in at least two studies performed by independent laboratories where the same brain regions were analysed. These seven proteins were: aldolase A in the frontal cortex, heart specific fatty acid binding protein (H-FABP) in the temporal cortex, peptidyl prolyl *cis-trans* isomerise (Pin1) and ubiquitin carboxy-terminal hydrolase L-1 (UCH-L1) in the frontal cortex as well as increased levels of α-enolase in hippocampus, glial fibrillary acidic protein (GFAP) in the frontal cortex, and glyceraldehyde 3-phosphate dehydrogenase (GAPDH) in hippocampus.

For this thesis, a proteomic approach was taken to identify proteins up-regulated in the brain tissue of two novel AD mouse models. The tissue was examined

from mice at 4 months and 8 months of age to imitate closely early and late stage AD pathology. All additional factors contributing to the onset and progression of the disease is of great importance in order to develop both preventive and therapeutic intervention.

1.6 Diagnosis of AD

Criteria for clinical diagnosis of AD relies on a diagnosis of dementia using the mini-mental state examination (MMSE) (Folstein *et al*., 1975) combined with deficits in two or more areas of cognition. Other systemic orders that could give rise to similar symptoms, such as a brain tumour, need to be excluded. Other forms of dementia also need to be excluded. The MMSE results need to be supported by progressive deterioration of memory, cognition and other neuropsychological aspects such as language (aphasia), motor skills (apraxia) or perception (agnosia) (McKhann *et al*., 1984).

At present there is no a simple biochemical diagnostic test for AD. Diagnostic tests include cerebrospinal fluid (CSF) analysis after an invasive spinal tap, showing concentrations of tau and phosphorylated tau proteins and a change in the ratio of Aβ40:Aβ42 over a period of time (De Meyer *et al*., 2010). This study examined CSF in 102 Alzheimer's patients, 200 people with mild cognitive impairment and 114 individuals with no cognitive impairment. They found low amyloid levels and high phosphorylated tau levels present in 90% of the AD patients, 72% with mild cognitive impairment (MCI) and 36% in individuals with no cognitive impairment. High phosphorylated-tau levels and low amyloid levels identified patients with MCI who progressed to Alzheimer's with 100% accuracy.

Brain imaging has become very useful in identifying markers early in the progression of the disease. Magnetic resonance imaging (MRI) and computerized axial tomography (CAT) scanning can show gross anatomical and structural changes in the brain. This is useful in differentiating AD from frontotemporal dementia. AD is usually characterized by global atrophy with prominent atrophy of the medial temporal lobe. MRI can help in establishing clinical progression by monitoring atrophy of the amygdala or hippocampus by measuring its size and shape. The amygdala, an area of the brain, anterior and superior to the hippocampus, atrophies in a comparable manner to the hippocampus. Amygdala atrophy is strongly related to MMSE results (Poulin *et al*., 2011). Brain imaging using radioisotope labelled compounds can show brain function and metabolism. A change in brain metabolism normally precedes any structural change (Scheltens, 2009). Positron emission tomography (PET), using 2-[^{18}F] fluoro-2-deoxy-D-glucose, (^{18}F-FDG PET) enables glucose metabolism in the brain to be assessed. The ^{18}F-FDG is located in the brain where there is the most glucose metabolism. The gamma radiation from ^{18}F is detected using a gamma camera, a series of photomultiplier tubes targeted onto a large flat crystal plate of sodium iodide that scintillates when hit by the gamma photons. Increased levels of metabolism are shown by a greater incidence of radiation. Studies have shown that individuals with normal cognitive functions, but who have a mother with late onset AD, show reduced glucose metabolism, similar to patients with AD (Mosconi *et al*., 2010) indicating a predisposition to AD later in life. It is possible to identify Aβ deposits in the brain with PET using ^{11}C Pittsburgh compound-B (^{11}C-PIB) in a similar way. PIB binds to extracellular fibrillar deposits and is a sensitive marker for cognitively normal, MCI and individuals with AD. PIB-PET

imaging confirms the early accumulation of Aβ in cognitively normal elderly patients, progressing to greater accumulation in AD. PIB-PET may help select suitable anti-amyloid treatment when used with clinical assessment (Rabinovici *et al*., 2010). However to date the only absolute confirmation of the disease is at post mortem.

1.7 Treatment for AD

1.7.1 Current drug treatment specific for AD

Drug treatments currently available are used to stabilise symptoms, but do not affect the pathological progression. These are cholinesterase inhibitors, galantamine, rivastigmine and donepezil, drugs which reduce the breakdown of the neurotransmitter acetylcholine at the synapses in the brain. Alzheimer patients have low levels of acetylcholine and these drugs are used in the early to mid stages of the disease. One other drug, memantine, is a glutamate receptor antagonist of AMPA/NMDA receptors, protecting neurons against excess of glutamate and inhibiting prolonged influx of Ca^{2+}. The receptor function is not disrupted and is still activated by high concentrations of glutamate released after presynaptic neuron depolarisation. Reviews have shown it has a small positive effect on cognition, mood, behaviour and the ability to perform daily activities in moderate to severe AD (Herrmann *et al*., 2011b). This is the first drug designed to act on the glutamergic system. In the UK memantine is licensed for use in moderate to severe cases of AD but is not routinely provided by the NHS.

1.7.2 Other drug treatments

Both oxidative damage and inflammation are elevated in AD. A reduced AD risk has been associated with a high intake of both non-steroidal anti-inflammatory drugs (NSAIDs) and antioxidants. Studies with transgenic APP mice with the Swedish mutations (TgAPPsw) (see Table 1.1.) showed ibuprofen reduces amyloid accumulation without suppressing many inflammatory markers (Cole *et al*., 2004). The anti-inflammatory omega-3 fatty acid docosahexaenoic acid (DHA) had a very significant impact on pathogenesis but did not significantly reduce inflammation, while surprisingly vitamin E was not effective in reducing oxidative damage or amyloid in the aged APPsw mouse (Amtul *et al*., 2011). In contrast, the NSAID/antioxidant curcumin lowered oxidative damage, cognitive deficits, synaptic marker loss, and amyloid deposition. Curcurmin (diferuloylmethane) is a polyphenol similar to green tea, epigallcatechin 3-gallate (EGCG). In a neuronal cell culture study, both curcumin and EGCG suppressed Aβ induced BACE-1 upregulation and both significantly reduced amyloid induced reactive oxygen species (ROS) production (Shimmyo *et al*., 2008). Other studies have shown that NSAID, taken for other medical reasons, afford some protection from AD (Gasparini *et al*., 2004). It has also been reported that taking statins, normally prescribed to reduce cholesterol levels have beneficial neuroprotective effects. Statins, which lower neuronal cholesterol, have been shown to decrease the amount of Aβ secreted by neurons (Ostrowski *et al*., 2007). One study shows that use of statins in cell cultures result in a large increase of secreted soluble APPα and ADAM 10 was responsible for the α-secretase activity (Kojro *et al*., 2001). However a recent report from the Cochrane Database Systematic Review, identified two trials with over 20,000 participants, which

concludes ‘There is good evidence that statins given in late life to individuals at risk of vascular disease have no effect in preventing AD or dementia’ (McGuinness *et al*., 2009).

A tumour necrosis factor (TNF) antagonist, Etanacept, developed as an anti-inflammatory for arthritis, has shown temporary cognitive reprieve with perispinal administration (Tobinick, 2009). This study reported a rapid improvement in verbal abilities, within 20 minutes of administration, in a patient with severe primary progressive aphasia. With repeated weekly dosing, sustained improvement at one month was documented. It is unclear how this works, but the study hypothesises that this may be related to TNF's role as a gliotransmitter and modulator of synaptic communication, although the rapidity of the change observed in cognition, mood, memory, motor function and attention suggest they are mediated by non-synaptic signalling mechanisms. The study states that there are populations of cells, including CSF-contacting neurons and modified ependymal cells, called tanycytes, which have receptive surfaces in direct contact with the CSF. Tobinick hypothesises that CSF-contacting cells may constitute a therapeutic target for a diverse group of brain, psychiatric and spinal disorders (Tobinick, 2009).

1.8 Current therapeutic and vaccine developments for AD

Development of more suitable drugs for AD is an urgent medical need. In recent years, several approaches aimed at inhibiting AD progression have advanced to clinical trials, with those targeting the production and clearance of Aβ being the

most advanced. Disease modifying drugs such as α-secretase activators (Kuhn *et al*., 2010), β- and γ-secretase inhibitors, inhibitors of Aβ aggregation and enhancers of Aβ degradation, are being developed. Some of these drugs are in phase III clinical trials and are expected to be available for clinical use in the near future (Tabira, 2010). Approaches aimed at modulating the abnormal aggregation of tau filaments and targeting neuronal metabolic dysfunction, are also being evaluated such as 'Rember' (methylthioninium chloride or MTC) that is in phase II clinical trials (Deiana *et al*., 2009).

1.8.1 Drugs involved with APP processing

- BACE1 inhibitors – e.g. CTS-21166 (CoMentis Inc.). Phase II studies were due to begin in 2008 but limited information has been released so far. Unfortunately, finding suitable BACE inhibitors has been slow (Panza *et al*., 2009).
- Modulating γ-secretase activity – e.g. (R)-flurbiprofen (Myriad Genetics Inc.). Phase III clinical trials, in 2008, showed no benefit when the R-racemate of flurbiprofen was used (Barrett *et al*., 2011; Green *et al*., 2009).
- γ-secretase inhibitors- e.g. Semagacestat LY45013 (Eli Lilly). In a multicentre Phase II trial, plasma Aβ40 decreased by 58-65% in 100-140 mg/day groups (Carlson *et al*., 2011). There are over forty endogenous substrates for γ-secretase inhibitors that play critical roles in the adult human, most notably Notch which is essential for differentiation of T and B lymphocytes. Phase III trials in 2010 showed a decline in cognitive

function compared to the placebo group but was associated with a greater risk of skin cancer. Eli Lilly has halted development and Bristol-Myers Squibb now have a competitor drug named BMS708163.

- Prevention of peptide accumulation – e.g. Alzhemed (tramiprosate, also called homotaurine) (Neurochem Inc.) is a small molecule designed to stop aggregation of Aβ (Aisen *et al.*, 2007). It is similar in structure to GABA. Alzhemed is safe and well tolerated, but a North American Phase III trial did not meet its 18-month endpoints. 1,052 mild-to-moderate Alzheimer's patients received a placebo, or a 100 or 150 mg dose of Alzhemed given along with conventional treatments.

  Although not significant, cognitive tests did improve with Alzhemed and data suggested an effect on CSF levels of Aβ and tau, and a difference in hippocampal volume approached statistical significance. However more than 50% of patients on placebo did not show cognitive decline, and some who were declining for many months, suddenly started to improve. The FDA is open to Neurochem Inc. adjusting its ongoing European Phase III trial to increase the likelihood of success based on knowledge gained in the North American trial.

1.8.2 Drugs used for preventing and reversing tau aggregation

- Methylene blue, methylthioninium chloride (MTC), tradename REMBER (TauRx Therapeutics). This compound was first used by Paul Ehrlich in 1890. The formulation used by TauRx is different from that commonly available and caution has been expressed about the presence of heavy metals. It is thought that methylene blue has an effect on tau aggregation

and probably aids clearance of tau aggregates. This is orally available and has been successful in Phase II clinical trials. It was given to patients with MMSE scores of 10 to 25 (top score = 30). Overall there was no effect because mild AD showed no decline of MMSE. Moderate AD patients did decline and MTC showed dose related improvement. There was no effect with 100mg, due to cross-linking of protein to the gelatin capsule. This is going to a Phase III trial at a cost of $80M. Using mouse models, SS295-390 mice (overexpressing tau fragment) that show Braak staging, perform badly in T-maze and Morris water maze experiments. However, this is reversed by MTC. Similarly in FTDP-tau mice (P301S/G335D).

- GSK3 inhibitors - NP031112 (Neuropharma), is a non-ATP GSK3 inhibitor, down-regulating the phosphorylation of tau and preventing tau phosphorylation (Luna-Medina *et al*., 2007). This compound has passed Phase I trials.
- Cdk5 inhibitors. - The cyclin-dependent kinase Cdk5 is implicated in the phosphorylation of tau. Kosik tested ~58,000 small molecules in a high-throughput screen of tau phosphorylation and discovered inhibitors that block Cdk5 phosphorylation of tau (Glicksman *et al*., 2007). Crystal structures of inhibitor-enzyme complexes show that two of the compounds occupy Cdk5's ATP pocket. More recently Kosik delivered a Cdk5 RNAi that reduced the phosphorylation of tau and decreased the number of neurofibrillary tangles in the hippocampi of 3XTg-AD mice.

1.8.3 Other treatments

- Nerve growth factor (NGF) maintains cholinergic neurons and prevents their death via the TrkA receptor. In a Phase I clinical trial in Alzheimer's patients, fibroblasts engineered to produce human NGF were implanted into the brain near the cholinergic nucleus. Improvements were seen in cognition and brain glucose utilization. Ceregene Inc. (San Diego) successfully carried out a Phase I study to assess adeno-associated virus (AAV) mediated delivery of NGF (CERE-110). CERE-110 is an AAV serotype 2-based vector producing human NGF administered by stereotactic injection to the nucleus basalis. A USA-based multicentre Phase II clinical trial has now begun recruiting patients for a randomized, controlled study in up to fifty subjects with mild to moderate Alzheimer's disease, with half of the patients due to undergo a placebo surgery with no medication injected (Mandel, 2010).

- Folic acid, DHA and increased exercise have been examined in trials or epidemiologically.

  Folic acid and folate (vitamin B9). Folic acid controls blood levels of the amino acid homocysteine, and elevated levels of homocysteine are linked to depression and AD. A few clinical trials with folic acid, e.g. 579 people aged ≥60 were followed for 7 years. Those who consumed ≥ 400 μg of folic acid had a 55% less risk of AD (Dangour *et al*., 2010).

  In a study of 815 people >65 years, eating fish gave a 60% reduction in the risk of developing AD. Docosahexaenoic acid (DHA) is an omega 3 fat (Oster and Pillot, 2010).

Exercise and mental activity. An exercise programme of 1hr, twice a week in 134 AD patients in 5 nursing homes showed reduced decline in activities of daily living after 1 year. >800 elderly patients in Chicago followed over four years showed that AD was more than double in lonely persons. This confirms behavioural studies that show enriched surroundings improve mental function. DHA on its own did not improve AD symptoms.

1.8.4 Vaccines

Active and passive forms of immunotherapy against Aβ have shown lowering of its cerebral levels and improved cognitive function in animal mouse models. An active, immunotherapeutic treatment was developed following positive results in transgenic mice (PDAPP V717F). The mice developed fewer plaques after immunisation with full length Aβ42 peptide both before and after onset of AD pathology (Vehmas *et al*., 2001). An Aβ vaccine, produced by Elan Corporation, reached phase II clinical trials in 2002 but had to be withdrawn when 6% of patients developed encephalitis. However some of the results from this trial demonstrated some cerebral clearance of Aβ and a moderate improvement in cognitive function (Schenk, 2002). Following this, there are at least seven passive Aβ immunotherapies in clinical trials in patients with mild to moderate symptoms. The Aβ42 peptide has been shortened. At least two examples use only the N terminal residues 1-6. Several active Aβ vaccines are also in clinical trials. From the pre-clinical data, these vaccines appear to be the most effective in slowing the disease when given at an early stage in the disease (Lemere and Masliah, 2010).

Passive vaccination injects antibodies directly into the patients, crossing the blood brain barrier and stimulating a microglial response, without involving T cells. Eli Lilly have a phase III clinical trial running, using Solanezumab. So far this has shown Aβ40 and Aβ42 serum levels increasing, indicating reduced levels in the brain. Other phase II trials are being run by Pfizer Inc., Elan Corp., and Johnson & Johnson with Bapineuzumab. Results have been mixed so far and the companies are having difficulties getting patients to volunteer for Phase III trials.

1.9 Mitochondrial dysfunction in AD

Mitochondrially-generated and age-dependent reactive oxygen species (ROS) are important factors responsible for cell death and disease progression, particularly in late-onset diseases, where genetic mutations are not causal factors (Reddy, 2009a, b). Mitochondrial dysfunction and oxidative stress have been proposed as important mechanisms in the development of AD. Important cellular functions of the mitochondria include ATP production by phosphorylation of ADP, generation of ROS, regulation of calcium homeostasis and initiation of the apoptotic pathway. The mitochondrial electron transport system is the major source of free oxygen radicals and hydrogen peroxide. ROS also cause damage to mitochondria (Polidori *et al*., 2007). The brain is particularly vulnerable to ROS damage due to lack of antioxidant enzymes compared to other organs. It is thought that impairment of mitochondrial function leads to reduction of ATP and an increase in free radicals leading to neurodegeneration in AD (Polidori *et al*., 2007). Positron emission tomography showed a decline in cerebral metabolic activity in parietal and temporal lobes in AD patients (Kessler *et al*., 1991). This indicated possible mitochondrial dysfunction.

Studies have shown that Aβ plaques do not significantly affect neuronal survival (Carpenter *et al*., 1993). But transient intraneuronal accumulation of Aβ, in the early to middle stages of AD, cause neuronal damage and death (Christensen *et al*., 2008a; Christensen *et al*., 2008b; LaFerla *et al*., 2007). Intracellular Aβ has been found to affect cellular function by disturbing mitochondrial respiration (Yan and Stern, 2005). There is growing evidence for the role of soluble intracellular Aβ in the progression of AD (Muirhead *et al*., 2010). Three proteins in the mitochondria have been identified as binding Aβ: ABAD, cyclophilin D (CypD) and heat shock protein 60 (Hsp60) (Caspersen *et al*., 2005; Du *et al*., 2008; Lustbader *et al*., 2004). The interactions of Aβ with these proteins interfere with their normal functions, resulting in damage and eventually death to the cell. Aβ binding to ABAD and CypD results in increased levels of ROS leading to neuronal death.

1.9.1 3-hydroxyacyl-CoA dehydrogenase (HADH2/ABAD)

There are two fatty-acid beta-oxidation systems in most eukaryotic cells, one located in the mitochondria and one in the peroxisomes (Birktoft *et al*., 1987). HADH2/ABAD is a member of the short-chain dehydrogenases/reductases (SDR) family and is a multifunctional mitochondrial enzyme acting as an oxidoreductase. The human HADH2 gene is mapped to the chromosome X, (Location: Xp11.2), coding for a 261-residue protein (Q99714- UniprotKB) with a molecular weight of 27kDa. HADH2 is expressed in all tissues and is also found to be over-expressed in neurons of patients with AD at post mortem (Yan *et al*., 1997a) suggesting a role in the neuronal dysfunction associated with this disease.

From a yeast two hybrid screen using a murine brain library, HADH2 was the only protein identified to bind Aβ (Yan *et al*., 1997a). From this observation HADH2 became known as amyloid-binding alcohol dehydrogenase (ABAD), and this name is now used when associated with AD. The first eleven amino acids at the N terminal are thought to be a mitochondrial targeting sequence, but HADH2 has also been identified in the endoplasmic reticulum (ER) (Yan *et al*., 1997a). Because of this link, in the literature HADH2 is also known as ERAB, Endoplasmic Reticulum binding Amyloid Beta. ABAD has since been identified within the mitochondria, but it is suggested that its distribution may be cell-line dependent (Frackowiak *et al*., 2001). Other names have also been allocated; SCHAD, Short Chain L-3Hydroxyacyl-CoA Dehydrogenase; and 17β-HSD10, 17β- Hydroxysteroid Dehydrogenase Type 10, as it also oxidises simple alcohols and hydroxysteroids, in particular 17β-estradiol. As an enzyme, ABAD catalyses a broad spectrum of substrates (Table 1.2).

Results are means±S.D.; -, not determined.

Substrate	Co-factor	Specific activity ($\mu mol \cdot min^{-1} \cdot mg^{-1}$)	V_{max} ($\mu mol \cdot min^{-1} \cdot mg^{-1}$)	K_m (μM)	k_{cat} (s^{-1})
S-Acetoacetyl-CoA	NADH	–	430±45	68±20	190
	NADH	–	–	89±5.4	37±1.6
	NADH	1.1	–	22.7	–
	NADH	–	–	53±9	11.1±0.7
17β-Oestradiol	NAD^+	–	23±3	14±6	10
	NAD^+	–	–	15±7	0.00088±0.0012
	NAD^+	0.0156±0.0008	–	43±2.1	0.011±0.0002
Dihydroandrosterone	NAD^+	0.130±0.0018	–	34±2.4	0.093±0.0028
Androsterone	NAD^+	0.0121±0.0009	–	45±9.3	0.011±0.0013
Ethanol	NAD^+	–	2.2±0.4	1210±260	1.0
1-Propanol	NAD^+	–	4.2±0.5	272000±62000	1.9
	NAD^+	–	–	83200±21100	0.0060±0.0005
2-Propanol	NAD^+	–	36±2	150000±17000	16
	NAD^+	–	–	156000±18000	0.0179±0.0008
	NAD^+	–	–	280000±33000	0.036±0.0023
β-Hydroxybutyryl-CoA	NAD^+	65.7	–	9.8	–
	NAD^+	–	26.3	134	–
L-β-Hydroxybutyrate	NAD^+	–	0.004	1600	–
D-β-Hydroxybutyrate	NAD^+	–	0.004	4500	–

Table 1.2. The substrates of ABAD, taken from (Muirhead *et al*., 2010).

1.9.2 ABAD/Aβ interaction

The first report of an interaction between ABAD and Aβ reported a K_d of 88nM (Yan *et al*., 1997a). Confirmation of ABAD binding Aβ has since been reported by a number of different techniques. Including X-ray crystallography (Lustbader *et al*., 2004), SPR (Yan *et al*., 2007b), ELISA based studies (Xie *et al*., 2006), co-immunoprecipitation (Frackowiak *et al*., 2001; Yan *et al*., 2007b) and immunocytochemistry followed by confocal microscopy (Lustbader *et al*., 2004). Aβ40 and Aβ42 both inhibit the activity of ABAD with K_i values of 1.2-1.6 μM for the reduction of acetoacetyl-CoA (Oppermann *et al*., 1999; Yan *et al*., 1999), 2.6 μM for the oxidation of octanol and 3.2 μM for the reduction of 17β-oestradiol (Yan *et al*., 1999). These concentrations are higher than the nanomolar binding constants of ABAD to Aβ. This implies that Aβ monomers are not enough to cause ABAD inhibition and that Aβ aggregation may be required to alter the ABAD structural conformation. The Opperman study showed that residues 13-22 of Aβ were critical for inhibiting ABAD activity. This region, residues 16-20, is also characterised by its fibril forming properties.

Recently, several studies have shown that Aβ is found in the mitochondria (Caspersen *et al*., 2005; Lustbader *et al*., 2004), which supports the hypothesis that the ABAD/Aβ complex is involved in the pathogenesis of AD. The Aβ peptide is generated in cells before extracellular amyloid plaques have formed, suggesting a possible early interaction with ABAD, possibly initiating neuronal dysfunction. There is still much interest in the exact mechanism of Aβ toxicity and the ABAD/Aβ complex is therefore of interest for its possible role in neuronal

damage during the early stages of AD. In neuronal cell culture studies, Aβ is independently cytotoxic, but the ABAD/Aβ complex enhances this toxicity, coincidentally generating the toxic aldehydes, malondialdehyde and 4-hydroxynonenal (4HNE), leading to oxidative stress (Yan *et al*., 1997a). The enzymatic activity of ABAD is essential for this toxicity, as mutations at the catalytic binding site have been shown to inhibit the cytotoxic effects (Yan *et al*., 1999).

1.9.3 The function of ABAD

The primary function of ABAD as a mitochondrial enzyme, is to catalyse the third stage of β fatty acid metabolism. It catalyses the oxidation of 3-hydroxyacyl-CoA to 3-ketoacyl-CoA by reduction of NAD^+ (Figure 1.7). As this is its main function, ABAD is involved in energy production and may be important in glucose-deficient environments, where other energy sources become more significant e.g. in situations of neuronal stress. An example is the increased ability of cells to use ketones as an energy source, when ABAD was overexpressed in COS cells (Yan 2000). Overexpression of ABAD can have a positive effect with regard to cellular stresses and probably plays a cytoprotective role during stress. For example, in mouse stroke models, following transient middle cerebral artery occlusion, ABAD expression was increased in both transgenic ABAD overexpressing and wild type mice. However the transgenic animals showed fewer effects of the stroke, and fewer neurological deficits (Yan *et al*., 2000b). Conversely, ABAD levels were shown to be decreased in the ventral midbrain of PD (Parkinson's disease) patients, and in the ventral midbrain of 1-methyl-4-phenyl-1,2,3,6,tetrahydrapyridine (MPTP) mice. MPTP-treated

mice overexpressing HADH2/ABAD were protected against apoptosis and the loss of dopaminergic neurons in this brain region (Tieu *et al*., 2004).

Other functions of HADH2/ABAD have been identified, such as oxidation of alcohols and hydroxysteroids eg. 17β-estradiol (He *et al*., 1998), and with the degradation of isoleucine (Ofman *et al*., 2003). Ofman identified the molecular basis for clinical cases of (2-methyl-3-hydroxybutyryl-CoA dehydrogenase) MHBD deficiency. Mass spectrometry identified the MHBD protein to be identical to HADH2. Sequence analysis of the HADH2 gene from patients with MHBD deficiency revealed two missense mutations (R130C and L122V) (see 1.9.11).

1.9.4 Fatty acids and β-fatty acid oxidation

Fatty acids are long hydrocarbon chains, typically 14 - 24 carbons, terminated with a carboxylate group. They have four major physiological roles:

1. They are building blocks of phospholipids and glycolipids.

2. They modify proteins by covalent attachment, which targets them to cell membranes.

3. They are an important source of energy and ATP for cells. They produce more energy than carbohydrates and are stored as triacylglycerols in adipose cells until required.

4. Fatty acid derivatives act as hormones or intracellular messengers. The triacylglcerols are degraded in the cells by lipases and released into the blood plasma as insoluble free fatty acids and glycerol. The fatty acids are bound by serum albumin and are transported to the tissue requiring fuel. They are released

by the serum albumin to cross the cell membrane into the cytosol. They are then activated on the outer mitochondrial membrane to produce Acyl CoA.

The Acyl CoA is transported across the outer mitochondrial membrane conjugated to carnitine, to produce Acyl carnitine, catalysed by carnitine-palmitoyl transferase1 (CPT-1) that is bound to the outer mitochondrial membrane. Acyl carnitine is further transferred across the inner mitochondrial membrane by a carnitine-acylcarnitine translocase. Once on the matrix side the acyl group is transferred back to CoA. Once in the mitochondrial matrix, Acyl CoA undergoes β-oxidation, which is a recurring sequence of a four-stage process: 1. oxidation by flavin adenine dinucleotide (FAD) to $FADH_2$, 2. hydration, 3. oxidation by NAD^+, and 4. thiolysis by CoA.

During the four stage process two carbon molecules are repeatedly cleaved from the Acyl-CoA. At the end of the process Acetyl-CoA is produced which enters the citric acid cycle which eventually produces ATP, the energy required by the cell (Figure 1.7).

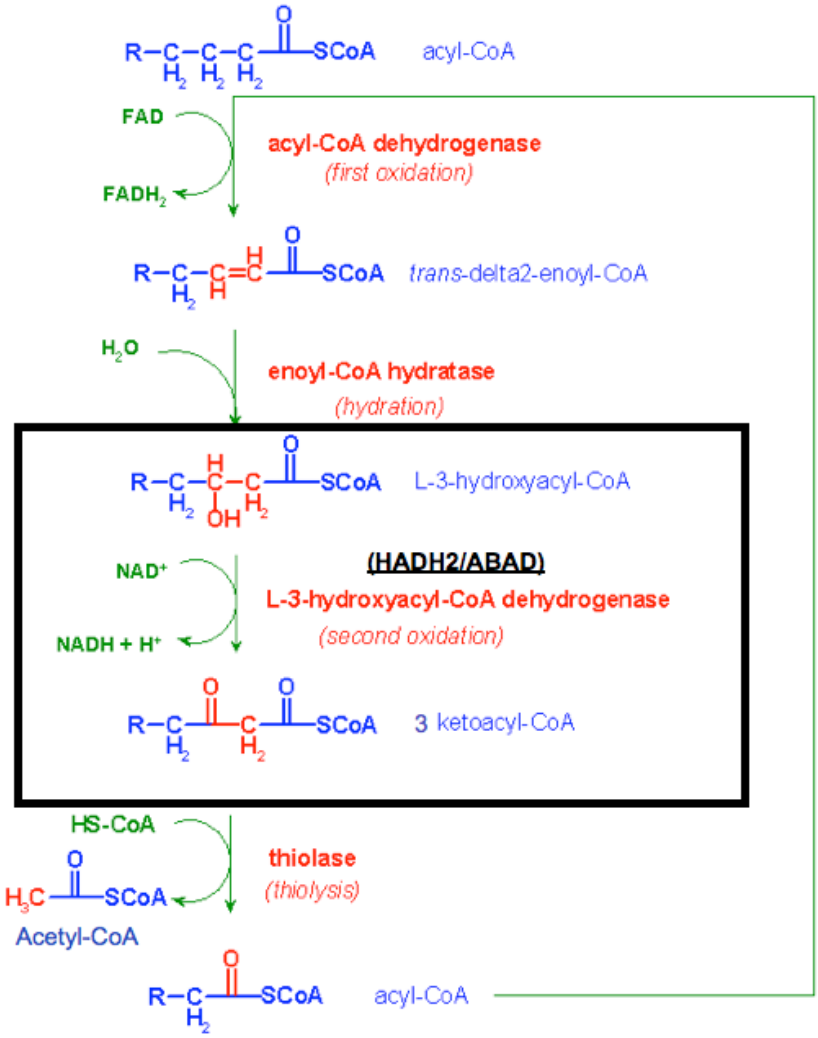

Fig. 1.7. Four step fatty-acid β-oxidation pathway. HADH2/ABAD is highlighted in the black box.

1.9.5 Crystal structures of ABAD

The 3D protein structures from rat and human ABAD have been determined by crystallography (Barycki *et al*., 2000; Birktoft *et al*., 1987; Engel *et al*., 1996; Lustbader *et al*., 2004; Powell *et al*., 2000) . These include a structure of ABAD with its cofactor NAD^+ (Birktoft *et al*., 1987; Powell *et al*., 2000), human ABAD binding Aβ (Lustbader *et al*., 2004), and human ABAD with a small molecule

inhibitor (Kissinger *et al*., 2004). All show it to exist as a tetramer and identify residues Ser155, Tyr168 and Lys172 as key conserved residues in the catalytic binding site (Figures 1.8, 1.9). Mutation at these residues to glycine, inactivate the enzyme activity (Yan *et al*., 1999). The crystal structure with Aβ was unable to see electron density for the Aβ but the active site and NAD^+ binding sites were distorted as evidence of its presence, with no co-factor present. SDS-PAGE of the crystal confirmed the ABAD/Aβ complex. Further studies of ABAD binding to Aβ using SPR confirmed binding at nanomolar concentrations (Yan *et al*., 2007a). Saturation-transfer difference NMR showed competitive binding of ABAD with Aβ inhibiting the binding of NAD^+ in a concentration dependent manner. Conversely the ability of Aβ to bind to ABAD was reduced in the presence of NAD^+ (Lustbader *et al*., 2004).

```
10          20          30          40          50          60
MAAACRSVKG LVAVITGGAS GLGLATAERL VGQGASAVLL DLPNSGGEAQ AKKLGNNCVF
        70          80          90         100         110         120
APADVTSEKD VQTALALAKG KFGRVDVAVN CAGIAVASKT YNLKKGQTHT LEDFQRVLDV
       130         140         150         160         170         180
NLMGTFNVIR LVAGEMGQNE PDQGGQRGVI INTASVAAFE GQVGQAAYSA SKGGIVGMTL
       190         200         210         220         230         240
PIARDLAPIG IRVMTIAPGL FGTPLLTSLP EKVCNFLASQ VPFPSRLGDP AEYAHLVQAI
       250         260
IENPFLNGEV IRLDGAIRMQ P
```

Fig. 1.8 Amino acid sequence of ABAD: highlighted in yellow are residues (S155, Y168, K172) which on mutation inactivate the enzyme activity. Underlined 93-116 (loop D) found in TAT-ABAD 24aa inhibitor (see Chapter 3). Highlighted in blue are the two mutations (L122V and R130C) seen in MHBD deficiency.

1.9.6 Structure of ABAD - mutations and activity

Structures of rat ABAD indicated the presence of an active site loop, from residues 200-220 in the rat ABAD and from the conformation indicated that Thr

208 of this loop would form a strong hydrogen bond with the substrate (Powell *et al*., 2000). The same study showed that binding with either 3-ketobutyrate or 17β-oestiadol as substrates bound in the same position within the active site. These structures showed the close proximity of the substrate-binding site to the catalytic site. Molecular modelling (Marques *et al*., 2008) suggests that without a substrate the loop is in an open conformation but closed in the presence of NAD^+. Rat and human ABAD have two significant insertions between 100-110 and 140-150 compared with other HAD type I short chain enzymes. A model of CoA binding in the active site has suggested that CoA linked substrates are more efficiently oxidised when bound to the positively charged residues in the 100-110 region and this would indicate that the sex steroids are not the main substrates for ABAD (Kissinger *et al*., 2004; Powell *et al*., 2000). The region comprising residues 100-110 was a disordered loop in the crystal structure of ABAD binding Aβ (Lustbader *et al*., 2004). Point mutations with alanine at residues within this loop region prevented the binding of Aβ to ABAD. Two groups of residues were highlighted as important: Ser98, Lys99, Thr100, Tyr101 and Thr108, His109, Thr110. This region is thought to be Aβ binding specific as similar bacterial enzymes 3β/17β dehydrogenase and HADH1 are unaffected by Aβ and do not contain this loop (Figure 1.9) (Lustbader *et al*., 2004). The lack of order in the Aβ component of the complex is either due to high levels of flexibility within the amino acid chain of Aβ or due to a disordered aggregation of the peptide, which would fit with the aggregation hypothesis. Figure 1.9 also shows the tetrameric structure of human ABAD in complex with NAD and a small molecule inhibitor.

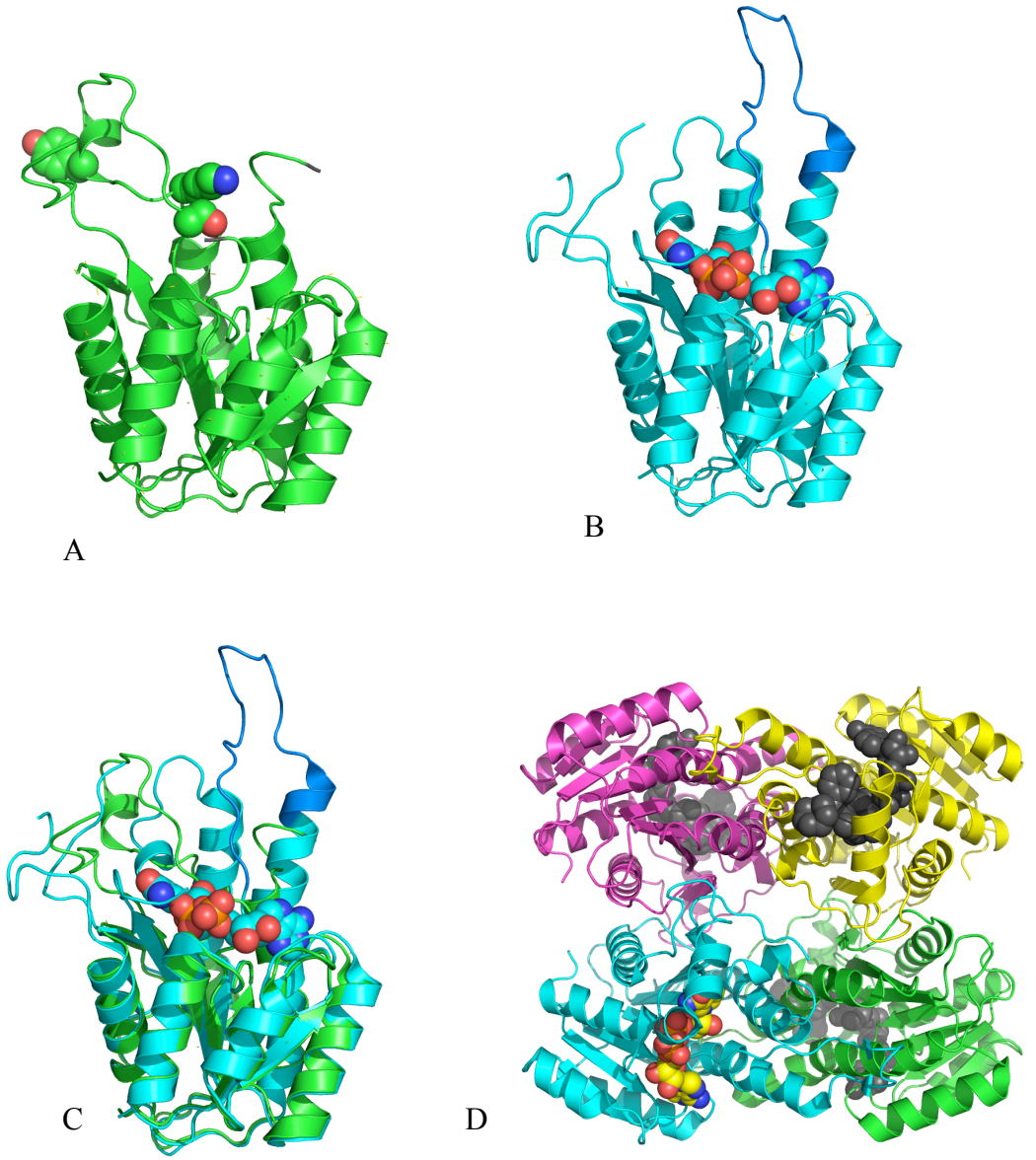

Fig. 1.9. 3D crystal structure of ABAD. (A) Monomer of rat ABAD in presence of Aβ showing active site residues S155, Y168 and K172 (Protein Data Bank (PDB) code 1so8). (B) Monomer of rat ABAD in complex with NADH (PDB code 1e3s). (C) Superposition of rat ABAD shown in A and B, with the loop (residues 94-114) that is disordered in the presence of Aβ highlighted in darker blue. (D) Tetrameric structure of human ABAD (PDB code 1u7t) with NAD in atom colours in one monomer, and the covalent complex formed between NAD and an inhibitor shown in grey in the other three monomers. All pictures drawn with PyMol (Schrödinger Inc.)

1.9.7 Aβ and ABAD expression

Aβ influences ABAD expression. Transgenic mAPP mice show increased ABAD expression in the hippocampus (Yan *et al*., 1997a). This increased expression has also been observed in neurons in the temporal lobes of AD brains. Overexpressing a catalytically inactive form of ABAD in the presence of Aβ does not enhance cytotoxicity in cell cultures compared with Aβ alone. Therefore cellular effects are not simply based on the inactivation of ABAD, but are due to other downstream effects mediated by the active enzyme once bound with Aβ. This is supported by the observed discrepancies in the binding constants of Aβ and ABAD (in the nanomolar range) and the Ki values determined for the inhibition of ABAD by Aβ (in the micromolar range).

1.9.8 Toxicity of ABAD plus Aβ

Aβ was found to increase DNA fragmentation and apoptosis in SK-N-SH cells and reduce cell viability as detected by MTT assay; 3-(4,5-Dimethylthiazol-2-yl)-2,5-diphenyltetrazolium bromide, a yellow tetrazole, that is reduced to purple formazan in living cells. These effects were reduced in the presence of anti-ABAD antibodies, indicating the interaction ABAD and Aβ was important for the toxicity (Yan *et al*., 1997a). Apoptosis and DNA fragmentation were also greatly enhanced in COS cells co-transfected with plasmids expressing Aβ and ABAD, or mAPP and ABAD, compared with those transfected with Aβ or ABAD alone (Yan *et al*., 1999). The toxicity was not seen in cells transfected with a mutant ABAD that made it inactive, in the presence of Aβ, despite Aβ having a similar binding affinity for the mutant and wild-type forms (Kd of 64.5 nM and 38.9 nM

respectively). This indicates that the toxicity is due to a combination of increased ABAD activity and Aβ expression (Yan *et al*., 1999).

Increase of toxic aldehydes HNE and MDA are found in AD (Delibas *et al*., 2002; Sayre *et al*., 1997). SH-SY5Y or HeLa cells transfected with ABAD and then treated with HNE for 24 hours have improved survival (Murakami *et al*., 2009). However cells overexpressing both ABAD and APP (either wild-type or mAPP forms) showed increased production of MDA and HNE, compared with those expressing ABAD or APPm alone. Transfection with mutant ABAD, that made it inactive and mAPP together did not produce this response (Yan *et al*., 1999). Although the ABAD/Aβ interaction induces the production of toxic aldehydes, it is possible that ABAD alone is able to remove them. This suggests that ABAD protects against toxic aldehydes such as HNE and MDA and it is proposed that a main function of ABAD may be to remove toxic aldehydes but that Aβ inhibits this function (Murakami *et al*., 2009).

The toxic effects of overexpressing ABAD, together with Aβ, has also been confirmed in an AD mouse model. E18 cortical neurons cultured from double transgenic mAPP and ABAD (2 x Tg mAPP/ABAD) mice produced higher levels of hydrogen peroxide, decreased mitochondrial function and increased cell death (Takuma *et al*., 2005b). Mitochondrial dysfunction was observed *in vivo* in 2 x Tg mAPP/ABAD mice, which had decreased glucose utilization and ATP production and deficits in spatial and temporal memory as early as 4–5 months (Takuma *et al*., 2005a). These results again emphasize that it is the combination of ABAD and Aβ that is necessary for effects to be seen and that these effects occur early in the disease.

1.9.9 Localisation of ABAD

Localization of ABAD has been reported to change in the presence of Aβ. The study reported ABAD redistribution from the ER and mitochondria to the inner surface of the plasma membrane in the presence of Aβ (applied externally or produced from a transfected APP plasmid) (Yan *et al*., 1997a).

1.9.10 *In vivo* ABAD/Aβ

The *in vitro* evidence does not necessarily mean that the enzyme will behave in the same way *in vivo*. But *in vivo* binding of ABAD and Aβ has been demonstrated by a variety of techniques. Immunoprecipitation of tissue samples of human cerebral cortex identified the ABAD/Aβ complex in AD brains. Similar results were seen in mitochondria isolated from the cerebral cortex of single transgenic Tg mAPP and double transgenic 2 x Tg mAPP/ABAD mice (Lustbader *et al*., 2004). Co-localisation of ABAD and Aβ was shown by immunocytochemistry in mitochondria both co-localised with voltage-dependent anion channel (VDAC) a mitochondrial membrane protein (Lustbader *et al*., 2004). Aβ influence on ABAD has been shown in Tg mAPP mice and a triple transgenic AD model (expressing mAPP, mPS1 and tau) where both showed increased ABAD expression in the hippocampus compared to non-transgenic litter mates (He *et al*., 2002; Yao *et al*., 2009). Increased ABAD expression in the neurons of the temporal lobe has also been seen in human AD brains compared with normal age-matched controls (Yan *et al*., 1997a). The binding of Aβ to ABAD inhibits ABAD activity. This was shown when Aβ was added to cells overexpressing a catalytically inactive ABAD. The cytotoxicity was not enhanced compared to the effects of Aβ alone. This indicated that the cytoxic

effects on cells was not due to ABAD activity alone but must induce some downstream effects. This is supported by the discrepancies in the binding constants of ABAD and Aβ, which are nanomolar and the k_i values determined for inhibition of ABAD by Aβ in the micromolar range (Yan *et al*., 1999).

1.9.11 ABAD deficiency

Deficiency of this enzyme has been identified and studied in drosophila and humans. In drosophila, deficiency of this enzyme known as Scully, produces numerous gross abnormalities and is a lethal phenotype (Torroja *et al*., 1998). In humans the deficiency is due to two missense mutations, R130C and L122V and symptoms in infancy are hyperinsulinaemia, hypoglycaemia and hyperammonia syndrome (Filling *et al*., 2008; Ofman *et al*., 2003) with a report of sudden infant death (Treacy *et al*., 2000). Other mutations in ABAD (HSD17B10) have been identified in males with mental retardation where an imbalance in neurosteroid and isoleucine metabolism could be the cause. (Yang *et al*., 2009). The evidence of neuronal involvement with ABAD provides evidence that ABAD may be involved in the neuronal damage in AD.

1.10 Mouse models in Alzheimer's disease

Mice have been used as animal models in research due to their genetic similarity to humans and the ease with which they can be kept in laboratory conditions. Transgenic mice were developed in the 1980's, allowing genetically altered animal models to be produced for research into specific diseases. Animal models of disease aim to reproduce the symptoms, the lesions and/or the cause of the disease (Duyckaerts *et al*., 2008). Due to their rapid rate of reproduction, effects

of specific diseases can be monitored over a lifetime of the animal.

Mice have a remarkable genetic similarity to humans, with approximately 85% similarity between human and mouse genes. However the proteins expressed can vary considerably in the two species due to post-translational modifications or alternative splicing (US Human Genome Project 2011; (Carver and Stubbs, 1997)). A study by Strand and colleagues examined if mouse models were a good representation for human CNS gene expression. They reported that expression patterns across comparable regions of human and mouse brains have mainly been conserved since divergence of the two lineages. This correlates with the general conservation of gross mammalian brain structure, and the conservation of cell types within comparable regions of the brain that have long been known from classical comparative neuroanatomy. The use of model organisms, or species, is also supported by the conserved patterns of gene expression in the mammalian brain. Finally, the three brain regions examined in mouse and human brain (cerebellum, motor cortex and striatum) are more alike between the two species than to different regions of the brain within a species (Strand *et al*., 2007).

Several genetically modified mice have been bred as models for AD using the genes or mutations of genes associated with the onset of the disease. These are APP, PS1, PS2, ApoE4 and Tau protein. Double transgenic (2xTg) mice available as models for investigating AD include: Tau + $PS1_{(M146L)}$, tau + $APP_{(swe),}$ $APP_{(V717)}$ + ApoE, APP + AlphaSynuclein (recently implicated in mitochondrial dysfunction in AD (Devi and Anandatheerthavarada, 2010). A novel triple transgenic mouse was developed in 2003, $APP_{(Swe)}$ + $PS1_{(M146V)}$ + $tau_{(P301L)}$ (Oddo *et*

al., 2003). This model exhibits Aβ plaques by 6 months of age as well as neurofibrillary tangles by 10-12 months of age, showing both AD phenotypes in one model and consistent with the amyloid cascade hypothesis.

Over expressing wild type APP alone does not cause Aβ plaques in most mouse lines. Double transgenic 2xTg APP/mPS1 develop lesions but much earlier than expected. The Tg APP mouse lines have provided information on the kinetics involved with cellular changes. But the relationships between behaviour, increase in Aβ and the lesions produced are still not completely in synchronisation with the human pathology (Duyckaerts *et al*., 2008). Other transgenic mice have been developed where BACE1 has been knocked out or overexpressed. Also mouse lines with altered expression of neprilysin, the main degrading enzyme of Aβ, have been bred.

This project has had access to two novel transgenic mice, Tg ABAD and 2 x Tg mAPP/ABAD, which overexpress either ABAD alone or mAPP and ABAD which produces an over-production of Aβ. These mice were specifically bred as models for AD for our collaborator, Professor Shi Du Yan at Columbia University, New York. The 2 x Tg mAPP/ABAD mice express high levels of ABAD and produce high concentrations of Aβ peptide (Lustbader *et al*., 2004) and their behaviour shows cognitive decline from 5 months but they do not develop the tau phenotype. Neurons from the double transgenic mice show evidence of free radical-induced stress. These models have been useful in analysing the Aβ toxicity in AD including showing evidence of mitochondrial

dysfunction by identifying ABAD and Aβ in the mitochondria (Lustbader *et al*., 2004).

1.11 Aims of this thesis

Chapter 3 describes *in vitro* experiments that were designed to identify the toxic effects of the ABAD/Aβ complex and further experiments were then designed to identify the type of toxicity induced in the cells. Fluorescent microscopy was used to identify the involvement of the mitochondria by studying the localisation of ABAD and Aβ in a neuroblastoma cell line, and MTT assays together with western blots were used to analyse the toxicity within the cells. These experiments were planned to evaluate the ABAD/Aβ model in the pathogenesis of AD. Another *in vitro* cell culture system was developed from murine neuronal stem cells to produce neurospheres, and this allowed primary cells to be cultured for a minimum of 8 weeks. Cells could be differentiated to neuronal cells by removal of the growth factors. Cell culture and differentiation of mouse brain stem cells was carried out and immunostaining of endogenous mitochondrial proteins showed this to be a useful model to develop further.

Chapter 4 describes a proteomic study that was undertaken to identify proteins upregulated in a novel AD mouse model. Proteomic studies are providing increasingly detailed information on cellular pathways activated during the pathogenesis in AD. For this thesis two novel transgenic mouse models for AD, expressing ABAD (Tg ABAD) or mAPP and ABAD (2 x Tg mAPP/ABAD) were used to explore pathways activated by the ABAD/Aβ complex, in particular to

identify cellular pathways activated early in AD. 2D gel proteomic analysis and MALDI-TOF mass spectrometry identified proteins upregulated in the 2x Tg or single Tg genotypes compared with non transgenic littermates. Further analysis by western blot was carried out on 4 month old mice to identify how early protein expression changes.

Chapter 5 describes the use of fragment based screening to identify compounds that bind to ABAD alone or ABAD in the presence of its NAD^+ co-factor. Several compounds were identified as potential small molecule binding partners to ABAD. This has been useful as a proof of concept experiment allowing for further compounds to be examined. Finding an inhibitor of the ABAD/Aβ complex without disrupting ABAD's normal function in the mitochondria could be another useful therapeutic approach in the treatment of AD.

Chapter 2

Materials and Methods

Most chemicals were supplied by Sigma Aldrich unless stated otherwise. Solutions were made with ultrapure distilled water (18 MΩ resistance). Most plastic tissue culture dishes and flasks were sourced from Nunc unless stated otherwise.

2.1 Mammalian cells and tissue culture

All work with mammalian cells was carried out under standard aseptic procedures in a class II safety cabinet. Cells were counted using a Beckman Coulter Z1 cell and particle counter.

2.1.1 Cell lines

Two cell lines were used in the work presented in this thesis: SK-N-SH, human neuroblastoma (ECACC 86012802); and PC12, rat pheochromocytoma. Cells were obtained from ECACC (The European Collection of Cell Cultures, United Kingdom).

2.1.2 Cell culture

Cell cultures were maintained in 75cm^2 vented tissue culture flasks in Dulbecco's modified Eagle's medium (DMEM) supplemented with 10% foetal calf serum (FCS) (Cambrex, United Kingdom), 2 mM L-glutamine, 100 units/ml of penicillin and 0.1 mg/ml streptomycin. Cells were incubated in a humidified incubator, at

37°C under 5% CO_2. Cells were routinely passaged when 80-90% confluent (8 x 10^6 cells). They were detached using 1ml trypsin-EDTA in either PBS (Phosphate Buffered Saline) or HBSS (Hanks Buffered Salt Solution). Immediately after the cells were detached, the trypsin was neutralised by the addition of 10% FCS in DMEM and cells were diluted and split 1:6. Flasks were reused for 4 passages.

2.1.3 Cryopreservation and resuscitation of SK-N-SH and PC12 cells

For cryopreservation, cells were detached with trypsin EDTA and neutralised as described in 2.1.2. The cells were collected into 15ml Falcon centrifuge tube and pelleted at 800g for 5min. The cells were resuspended gently in 4ml cryopreservation medium: DMEM, FCS, and 10% DMSO. 1ml cell suspension was aliquoted into 1.5ml cryotubes (Corning). The cells were frozen slowly by placing the cryotubes into an isopropanol freezing container (Nalgene) at room temperature. This container was then put into a -70°C freezer for a minimum of 5hrs. The gradual freezing of the isopropanol reduces the cell temperature by 1°C per hour. The slow freezing process is optimal for preservation of mammalian cells. The cryotubes were transferred to liquid nitrogen for long term storage.

For resuscitation, cells were thawed quickly. After removal from liquid nitrogen, the cells were heated by placing in a water bath at 37°C until thawed. The cell suspension was diluted slowly with 10ml pre-warmed DMEM with supplements. The cells were then placed in a 75cm^2 flask and incubated for 24hrs. The medium was then replaced with DMEM 10% FCS, to remove all DMSO, as this can inhibit cell growth. Cells were grown to 80% confluence and passaged twice before use in experiments.

2.2 Transfection of cells

2.2.1 Liposomal transfection of DNA into cells

Twenty four hours before transfection, cells were seeded onto tissue culture dishes, at a density of 1 x 10^4 cells/cm^2. If required for microscopy, the cells were seeded onto 22mm^2 glass coverslips. The cells were transfected when 50% confluent as a monolayer, using Lipofectamine Reagent (Invitrogen UK) at a ratio of 1μg DNA to 4μg Lipofectamine. Lipofectamine and DNA were mixed in serum free OptiMEM (Gibco) and incubated together at room temperature, light protected, for 30min. The cells to be transfected were washed and covered in serum free OptiMEM. The DNA Lipofectamine mix was added dropwise to the cells and then incubated for 5-8hrs. The medium was then replaced with DMEM 10% FCS plus supplements as required, and the cells incubated for a further 18-24hrs. For live imaging, Willco 35mm, glass bottom tissue culture dishes with lids were used.

2.2.2 Making stable expressing mammalian cell lines.

Stable cell lines were made by transfecting 75cm^2 vented tissue culture flasks, when 50% confluent, with 10μg of the relevant DNA (with G418 resistance) per flask, using the Lipofectamine protocol described above and in accordance with the manufacturer's instructions. Cells were grown for 48hrs after transfection in their normal growth medium. Medium was then supplemented with 1mg/ml G418-sulfate and the cells were maintained in this medium thereafter.

2.2.3 Cloning out stable cell lines expressing ABAD-EGFP.

Stable cell lines were cloned out by plating cells at low seeding densities (typically 10 to 50 cells) onto 60mm tissue culture plates. After 10-14 days, plates were imaged and plates with individual colonies were chosen. Selected colonies were enclosed and separated from the rest of the plate by placing a sterile stainless steel cloning ring around the colony. The individual colonies were trypsinised (as described above) and grown in individual wells in a 96 well tissue culture plate to 80-90 % confluency. Transfection was checked by immunofluorescent imaging for 95% cells expressing ABAD-EGFP and western blot for confirmation using anti ABAD antibody.

2.2.4 Culture of multipotent neurospheres and immunocytochemistry

(Carried out in the laboratory of Professor Alessandra D'Azzo, St Jude Children's Research Hospital, Memphis, USA.)

Cerebella and subependymal zones were isolated from brains of 3- to 6-day-old newborn mice and dissociated into a single-cell suspension by 5 min incubation in 0.25% trypsin-EDTA (GIBCO) and trituration with glass pipettes. Single-cell dissociates were resuspended in growth medium containing DMEM/F12 supplemented with N2 growth supplement (GIBCO), 5% FBS, 20ng ml^{-1} epidermal growth factor (EGF), and 10 ng ml^{-1} basic fibroblast growth factor (bFGF). The cells were then plated on ultra low attachment polystyrene 6-well dishes (Corning Costar) at a density of 100,000 cells ml^{-1}. Cultures were supplemented with fresh growth factors every other day. To analyze their cell composition, the neurospheres were transferred onto glass coverslips, coated sequentially with poly- L-ornithine (10 g ml^{-1}) and laminin (5 g ml^{-1}). The cells

quickly attached and began to differentiate. After an additional 48 hr, attached neurospheres were fixed in PBS containing 4% PFA, washed well, and processed for immunocytochemical analysis with polyclonal antibodies against the astrocyte-specific intermediate filament protein, glial fibrillary acid protein (GFAP), and the mAb against the neuronal marker β-III tubulin. Images were analyzed with the confocal laser scanning microscope (Leica, TCS-NTSP).

2.2.4.1 Differentiation of neurospheres

Wild-type neurospheres were trituration with glass pipettes to a single cell suspension and transferred onto Petri dishes coated sequentially with poly-L-ornithine (10g ml^{-1}) and laminin (5g ml^{-1}) and grown in DMEM/F12 supplemented with only N2; FBS or EGF was not added to promote neuronal differentiation. Cells were maintained for 2 days in serum-free DMEM and then fixed in PBS containing 4% PFA and processed for immunocytochemical analysis with polyclonal antibodies. Images were analyzed with the confocal laser scanning microscope (Leica, TCS-NTSP).

2.2.5 Fixing cells and mounting for microscopy

The media was removed from the cells. The cells were then washed 3 times with ice-cold PBS, incubating for 5mins for each wash. The PBS was removed and replaced with ice-cold 4% PFA (paraformaldehyde) to cover the cells. The cells were incubated for 20mins and the PFA removed and discarded in accordance with local rules for toxic waste. Next the cells were rinsed 4 times with ice-cold PBS, incubating for 5mins for each rinse. To mount coverslips, the PBS was

removed and the cells air-dried for 5mins. 10 - 20µl mounting fluid was pipetted onto a microscope slide and the coverslips were placed carefully onto the slide. Several mounting fluids were used including Vectashield (Vector Laboratories), and Mowiol (Calbiochem). Mowiol with added anti-fade was the most successful and provided a hard set. DAPI (4', 6'- diamidino-2-phenylindole), a DNA-binding fluorochrome, was added for nuclear staining, at a concentration of 0.5 µg/ml. Coverslips mounted with Vectashield were sealed at the edges with nail-varnish.

2.2.6 Preparation of Mowiol mounting medium

Mowiol is a high quality mounting medium with good anti-fade characteristics. It hardens and matches the refractive index of immersion oil and is particularly suited for immunofluorescent microscopy. Anti-fade DABCO is added to further retard photobleaching.

Preparation protocol: 2.4g Mowiol 4-88 (Calbiochem) was added to 6g glycerol and stirred briefly with a pipette. 12ml dH_2O was added and stirred at room temperature for 1-2 hrs. Then 12ml 0.2M Tris pH 8.5, was added and heated to 50°C for 1-2hr while stirring. When the Mowiol had dissolved, it was clarified by centrifugation at 55g for 15min. DABCO was added to 2.5% (0.72g). DAPI was added at 0.5ug/ml. Bubbles were removed by centrifugation. 1.5ml aliquots were stored up to 2 weeks at 4°C or frozen at -20°C for long-term storage.

2.2.7 Preparation of 4% PFA (paraformaldehyde)

4g PFA was added to 100ml PBS. In a fume hood, it was mixed and heated to approximately 60°C and then 6-7 drops of 10M NaOH was added until dissolved. It was left to cool and then the pH was adjusted to 7.4 with concentrated HCl. The solution was aliquoted and frozen at -20°C.

2.2.8 Permeabilising and immunostaining fixed cells

After fixing the cells, the PBS was discarded. 0.2%Triton X100 in PBS was added to each dish and incubated for 10min at R/T. Each dish was rinsed 4 times with PBS, incubating for 5 mins for each rinse.

The antibodies were diluted in 3% BSA in PBS. The coverslips were placed into a humidified 90mm tissue culture dish, containing a damp tissue and parafilm. The cells were incubated with the primary antibody, by pipetting 100µl onto the coverslip and incubating for 1hr at R/T. The cells were then rinsed 4 times with 5ml PBS, incubating for 5 mins for each rinse. Then the coverslip was returned to the humidified dish. The cells were incubated with the secondary immunofluorescent-antibody, by pipetting 100µl onto the coverslip and incubating for 1hr at R/T. Each dish was rinsed 4 times with PBS, incubating for 5 mins for each rinse. The coverslips were mounted onto slides as above.

2.2.9 Transfection of cells using the Chariot® protein delivery reagent

Chariot (Actif Motif) is provided as a lyophilized powder and reconstituted in sterile PBS at a concentration of 2mg ml^{-1}. Cells were seeded at 2.5-5.0 x 10^4 cells cm^2 and incubated at 37^0C with 5% CO_2 for 16hr until 40-50% confluent.

The Aβ peptide (4kDa) was diluted in PBS to achieve 100-500ng per transfection reaction and 200μl was needed per 60mm tissue culture dish giving a final concentration of ~ 1.0ng μl^{-1}). The Chariot was further diluted 1:10 in sterile H2O and 20μl was needed per 60mm tissue culture dish. The diluted Aβ peptide was added to the diluted Chariot and incubated at room temperature for 30min for the complex to form.

To transfect the cells, the medium was aspirated from cells and the cells were washed once with PBS. The Chariot-Aβ complex was added to the cells and the appropriate amount of serum-free medium added to the plate and rocked gently to ensure even delivery. The cells were incubated at 37^0C with 5% CO_2 for 60min. To prevent the cells deteriorating due to being in a serum starved environment, complete growth medium was added to the cells without removing the Chariot-Aβ complex. No more than 25% v/v of complete growth medium was added to the cells, as the presence of serum can interfere with the Chariot transfection efficiency. The cells were incubated for a further 30-60min. Cells were fixed and immunostained.

2.3 Protein analysis

2.3.1 Protein concentration microassay (1-10 μg).

The protein concentration was determined using Bradford's reagent. Samples to be assayed were diluted to a final volume of 500μl and added to 500μl of Bradford reagent. Absorbance was measured at λ595 nm with a

spectrophotometer, and the protein concentrations were calculated from a standard curve created using known concentrations of BSA, between 2 and 10μg.

2.3.2 SDS PAGE (sodium dodecyl sulphate polyacrylamide gel electrophoresis)

SDS-PAGE was performed using Invitrogen's NuPAGE polyacrylamide gel system as per the manufacturer's instructions. When necessary SDS-PAGE gels were also prepared manually as follows. The resolving gel was prepared (8-10% (v/v) acrylamide, 0.37M Tris-HCl pH 8.8, 0.1% w/v SDS) and polymerised by adding 20μl APS (ammonium persulfate 10% w/v) and 20μl (TEMED) NNN'N'-tetramethylethylenediamine. The acrylamide mixture was poured gently into a gel-casting rig and covered with water-saturated butanol. When the gel was set the butanol was removed and the gel rinsed with 20mM Tris pH 6.8. The stacking gel was prepared (acrylamide 4.7% (v/v), 0.121M Tris-HCl pH 6.8, 0.46% (v/v) SDS), and again polymerised with 10% w/v APS and 20μl TEMED. The polymerised mixture was poured gently onto the resolving gel, and a comb was placed into the stacking gel. The gel was allowed to set at room temperature.

Samples were prepared for equal loading, normally 20-40μg protein per lane, by adding NuPAGE LDS Sample Buffer (4X) and reducing agent with approximately 50mM dithiothreitol (DTT). Samples were heated at 70°C for 10mins then cooled on ice, or samples were reduced in a standard protein sample buffer: 0.001% (w/v) bromophenol blue, 4.3% (w/v) DTT, % (w/v) glycerol, 0.06M Tris-HCl pH 6.8, 2.2% (w/v) SDS and boiled at 100°C for 5 mins, then cooled on ice. Samples were loaded onto Invitrogen NuPAGE Novex 4-12%

gradient Bis-Tris gel, with one lane containing 5µl of Invitrogen SeeBlue Plus2 protein standards. The gel was run at a constant voltage (200V) for 40 min.

2.3.3 Coomassie blue staining of SDS-PAGE gels

For detection of protein expression, gels were stained using Coomassie blue stain solution (0.1% (w/v) Coomassie brilliant blue R-250, 45% (v/v) methanol, and 10% (v/v) glacial acetic acid for 5 to 10 mins at room temperature. The gels were then destained using multiple changes of destain solution: (10% (v/v) glacial acetic acid, 20% (v/v) methanol), until protein bands were clearly seen. Gels were imaged by scanning and photographed (Gel Doc 2000 UV transilluminator /photography system; Bio-Rad UK).

2.3.4 Western immunoblotting

For identification of individual protein expression, proteins were transferred to a nitrocellulose membrane for western immunoblotting. Proteins separated by SDS-PAGE were transferred to a nitrocellulose membrane using NuPAGE transfer buffer (Invitrogen), with added methanol (10%) and antioxidant in accordance with the manufacturer's instructions. Transfer was completed at 30V for 1hr (for proteins <100 kDa) or 25V for 1hr (proteins > 100 kDa). Transfer was verified by staining membranes with Ponceau S solution (Sigma 0.1 % Ponceau S (w/v), 5% acetic acid) for 1 min at room temperature. Excess Ponceau S was removed by washing with distilled water.

Protein binding sites on nitrocellulose membrane were blocked by incubating the membrane in 5% (w/v) fat free powdered milk in PBS-T (0.1% (v/v)

polyoxyethylenesorbitan monolaurate (Tween-20) in PBS), either at 4°C overnight or 1-2hrs at room temperature. Membranes were then washed with PBS-T and incubated for 1hr at room temperature, with the primary antibody diluted in 5% (w/v) fat-free powdered milk in PBS-T. The primary antibody was removed by washing the membrane 3 times, for 10 mins with PBS-T. Membranes were then were incubated for 1hr at room temperature, with horseradish peroxidase (HRP) conjugated secondary antibody, diluted with 5% (w/v) fat free powdered milk in PBS-T. The membrane was washed 3 times, for 10 minutes with PBS-T. Immunoreactive bands were visualised by enhanced chemiluminescence (Pierce west pico ECL), on Kodak X-Ray film, as per the manufacturers instructions. The antibodies used in proteomic studies for western blotting are shown in Table 2.1.

Antibody	**Host**	**Supplier**	**Conc'n used**	**epitope specificity**
endophilin-1	rabbit	Zymed	0.5 ug/ml	middle region human, mouse, rat endophilin 1
ATP synthase β monoclonal		Pierce	1.0 ug/ml	human, mouse, rat
Creatine Kinase polyclonal			0.5 ug/ml	mouse and rat
PrxII	rabbit	Alexis	0.5 ug/ml	human, mouse, rat, hamster. Does not cross react with PrxI
B Actin		Pierce	0.5 ug/ml	

Table 2.1. Antibodies used in the western blotting experiments in Chapter 4.

2.3.5 Stripping primary and secondary antibodies from a nitrocellulose membrane

The nitrocellulose membrane was washed 3 times for 10 min in 10ml of distilled water and then incubated for 45min in stripping buffer (0.2M glycine, 0.1% SDS, 1.0% Tween-20, pH 2.2) at room temperature. The membrane was then washed a further 3 times for 10min in 10 ml of distilled water and incubated with the primary and secondary antibodies as described above.

2.4 Cell viability assays

Cellular toxicity was induced using a number of known cytotoxic compounds including: glutamate, actinomycin D, staurosporin and Aβ peptide (Biosource).

Aβ peptide was solubilised to a concentration of 1mg/ml from lyophilised stock. This was incubated at 37°C for between 16 and 48hr to allow peptide folding to occur, since this seems necessary for the production of amyloid toxicity. However, even with this pre-incubation step, effects of Amyloid toxicity were difficult to reproduce. An oligomeric form of the peptide was kindly donated by Aynun Begum from UCLA, for further toxic studies. The dose response of this peptide was more reproducible.

2.4.1 The MTT Assay

Cell survival was measured using a colorimetric spectrophotometric assay, first described by Mossman et al 1983. The tetrazolium ring of MTT (3-(4,5-dimethylthiozyl-2-yl)-2,5-diphenyl tetrazolium bromide) is cleaved by active mitochondria, leaving a blue/purple formazan product, absorbing at a wavelength

of 570nm. The spectrophotometric reading is directly proportional to the number of living cells in each well.

Cells were seeded in a 96 well plate, at a seeding density of 1 x 10^4 cells (1 x 10^5 cells cm^{-2}) in 100µl medium per well, unless indicated otherwise, and incubated in DMEM 10%FCS for 18-24hr. The toxins were then added at various concentrations and cells were incubated for a further 24hrs. Cells of the negative control were 80-90% confluent at the time of assay. 25µl of 5mg/ml MTT was added to each well of the plate. (final concentration 1mg/ml). The plate was covered in foil to protect from light and incubated at 37°C, 5% CO_2, humidified for 4 hr. After 4hr the plates were centrifuged at 1500g for 5min. The medium and MTT were then discarded, leaving the formazan product in the wells. This was dissolved by the addition of 200µl DMSO followed by 50ul Sörensens buffer (0.1M glycine and 0.1M NaCl pH 10.5). The absorption at a wavelength of 570nm was measured on a 96 well plate reader, (MRX-ELISA – Dynex Technologies, Virginia) with a setting of 570nm test wavelength and 690nm reference wavelength.

2.4.2 Mitochondrial Fractionation (with the Actif Motif kit)

For fractionation of ~5 x 10^7 cells:

1. Cells were washed 1x with 10 ml ice-cold PBS.
2. 10 ml of ice-cold PBS was added and the cells were scraped off the dish using a cell scraper, and transferred to a pre-chilled 15 ml centrifuge tube and spun at 600 x g for 5 minutes at 4°C.
3. The supernatant was removed and the cell pellet washed 1x by gently resuspending it in 5 ml ice-cold PBS, and spun at 600 x g for 5 minutes at

4°C and the supernatant removed.

4. 1 ml of ice-cold cytosolic buffer was added and the cell pellet resuspended by pipetting up and down gently with a pipette, followed by incubation on ice for 15 minutes, then transferred to a pre-chilled pestle homogenizer.
5. On ice, the cells were homogenized using 30-50 strokes with the homogenizer, and the supernatant transferred to a pre-chilled microcentrifuge tube.
6. The lysate was spun at 800 x g (~3000 rpm) for 20 minutes at 4°C, and the resulting pellet was the nuclei, cellular debris and intact cells, whereas the supernatant contained the cytosol, including the mitochondria.
7. The supernatant was transferred to a fresh, pre-chilled microcentrifuge tube, and spun a second time at 800 x g (~3000 rpm) for 10 minutes at 4°C to remove any residual nuclei.
8. The supernatant was transferred to a fresh, pre-chilled microcentrifuge tube and spun at 10,000 x g (~11,000 rpm) for 20 minutes at 4°C to pellet the mitochondria. The supernatant was the cytosolic fraction, which was transferred to a fresh pre-chilled microcentrifuge tube.
9. The mitochondrial pellet was washed with 1x with 100 µl 1x cytosolic buffer and spun at 10,000 x g for 10 minutes at 4°C. The supernatant was discarded.
10. The mitochondrial pellet was lysed by adding 100 µl complete mitochondria buffer and incubated on ice for 15 minutes. After incubation, it was vortexed for 10 seconds to mix thoroughly. This was the mitochondrial fraction.
11. The cytosolic supernatant was centrifuged at 16,000 x g (~14,000 rpm) for

at least 20 minutes at 4°C to remove any residual mitochondria. The cytosolic supernatant was transferred to a fresh, pre-chilled microcentrifuge tube. This was the cytosolic fraction.

12. The protein concentration of each fraction was measured by Bradford assay.
13. Fractions were aliquoted and stored at -80°C.

2.5 Plasmid production and cloning procedures.

2.5.1 Polymerase chain reaction (PCR).

PCR was used to amplify cDNA. Forward and reverse primer sequences were designed with restriction sites specific to the cDNA fragment. Primers were supplied by Invitrogen UK. A 50µl PCR reaction mix was made up of 200ng/µl DNA template, 200 µM dNTPs (Promega), 0.5µM of each primer and 0.8µl pfuTURBO polymerase (Stratagene), in enzyme buffer diluted with nuclease free dH_2O. PCR was carried out in a Biometra Thermocycler. The PCR program conditions were: melting at 95°C for 45s, annealing at 55°C for 45s and extension at 72°C for 1min/kb. The PCR was set for 30 cycles with an initial melting step of 95°C for 2min and a final extension at 72°C for 10min.

2.5.2 Agarose gel electrophoresis

Amplified and linearised DNA, and DNA fragments from restriction digests, were analysed by gel electrophoresis in horizontal mini-gels. 1µg/ml ethidium bromide was added to gels made of 1% (w/v) agarose/TBE buffer, and these gels were run in TBE buffer (0.045 M Tris-borate, 0.001 M EDTA.). For analysis, 5µl DNA

samples were mixed with 1μl of 6x DNA loading buffer (Promega, United Kingdom), prior to electrophoresis. Samples were separated at 60V constant volts, until bands were clearly resolved, approximately 45min. Along with the samples, known DNA molecular weight markers were run (1kb ladder; Promega, United Kingdom.). Electrophoresed DNA was exposed to UV light (λ365nm) and photographed (Gel Doc 2000 UV transilluminator/photography system; Bio-Rad, United Kingdom).

2.5.3 Purification of DNA fragments from agarose gels

Following analysis of DNA by agarose gel electrophoresis, as described above, the DNA fragments of interest were subsequently purified by excision of resolved bands from the gel. The remaining samples were separated on a new gel and imaged by short wavelength UV light to prevent UV damage to DNA (λ320nm). The DNA bands were excised from the gel with a sterile scalpel blade. DNA excised from the gel was then recovered using the Promega Wizard SV Gel and PCR Clean-UP System kit as per the manufacturer's instructions. Typically, DNA was eluted in 50ml of nuclease free dH_2O. A fraction of the purified samples (usually 1/10 of the total volume of the eluate) was usually re-run on agarose gels, in order to check the purification of DNA.

2.5.4 Restriction enzyme digests

Restriction enzymes were used to digest 1 μg of plasmid DNA or PCR product for 1 hour at the recommended temperature. Restriction digest enzymes (Promega) were used according to the manufacturer's instruction using the buffers supplied. In general, 10 units of the restriction enzyme reactions were subsequently

terminated by heat inactivation (65°C incubation for 15 min). Restriction digested DNA that was to be used in further restriction digests or ligation reactions was eluted with nuclease free water, using the Promega Wizard SV Gel and PCR Clean-UP System kit as per the manufacturer's instructions.

2.5.5 Plasmid construct production

Purified DNA insert and the vector were ligated using T4 ligase (Promega) with supplied buffer, incubated at 4°C overnight. The final construct was checked by single and double restriction digest on agarose gel and finally by sequencing at DNA sequencing lab., University of Dundee.

2.5.6 Preparation of competent *E. coli* cells (DH5α) using calcium chloride

DH5α *E. coli* was cultured overnight in 5 ml of Luria Broth (LB) at 37°C. 50ml of pre-warmed LB was inoculated with 500 µl of overnight culture and grown in a 1.0 litre flask (37°C, 210 rpm) for approximately 2 hrs. When the absorbance of the bacterial culture reached 0.3 to 0.4 absorbance units at a wavelength of 600nm, the culture was transferred to a pre-chilled 50ml plastic centrifuge tube. The cells were centrifuged at 3500 g for 10 minutes at 4^0C. The supernatant was discarded and the pellet was resuspended in 20 ml of ice-cold filter sterile 100 mM $CaCl_2$ and incubated on ice for 30 minutes. Bacteria were pelleted at 1500g for 5min. and the pellet was resuspended in 1 ml of 100 mM $CaCl_2$. Bacteria were left on ice for a further 30 minutes and either used immediately or DMSO was added slowly, to a final concentration of 10%, and the cells stored at -70°C for up to 4 weeks.

2.5.7 Transformation of competent *E.coli* cells and clonal isolation

To replicate specific DNA, bacteria were transformed by adding either 0.5 μl of plasmid DNA or 10 μl of a ligation reaction mixture to 200 μl of calcium chloride competent cells (DH5α), and incubated on ice for 20 minutes. The bacteria were then heat shocked at 42°C for 45 seconds and immediately incubated on ice for a further 3 to 4 minutes. The bacterial culture was made up to 1 ml, with SOC medium (2% (w/v) tryptone, 0.5% (w/v) yeast extract 10mM NaCl, 10mM KCl, 5mM $MgSO_4$, 5mM $MgCl_2$ and 20mM glucose), and incubated at 37°C with vigorous shaking (210 rpm) for 1 hr. 100 μl of the culture medium was spread on to an agar plate containing the appropriate selection antibiotic(s) for the plasmid. The remaining bacteria were pelleted (13,000g for 10s) resuspended in approximately 100μl of culture medium and plated on a second agar plate. Agar plates were placed agar side up into a 37°C incubator overnight. The next day single colonies were isolated for inoculation into LB with antibiotics for further monoclonal culture.

2.5.8 Preparation of glycerol stocks of transformed *E. coli*

Glycerol stocks were prepared for all new plasmids. 600μl of overnight bacterial cultures was mixed with 400μl of sterile 50% glycerol (= 20% glycerol final concentration) and stored at -70°C.

2.5.9 Bacterial culture

Bacteria were cultured by adding a minute amount of the glycerol stock to 1-5ml LB and incubated at 30-37°C shaking for 12-16hr.

2.5.10 Preparation of plasmid DNA ('mini' and 'midi' preps)

Small-scale preparation of DNA (50µl at 0.2ug/ul) for cloning and transfecting was prepared from a 5ml overnight bacterial culture, using the Promega plasmid miniprep kit in accordance with the manufacturer's instruction. Large-scale preparation of DNA (500-800µl at 0.6ug/ul) for analysis, cloning, and transfection into mammalian cell lines was prepared from a 50-100ml overnight bacterial culture, using the Promega plasmid midikit, in accordance with the manufacturer's instructions.

2.6 Proteomics

2.6.1 2D gel electrophoresis

Protein samples were prepared and separated, first dimension by isoelectric focusing (IEF), separating by isoelectric point then second dimension by molecular weight (SDS PAGE). Amersham Biosciences equipment and chemicals used unless stated otherwise.

2.6.2 1st dimension IEF

400µl samples with load dye were placed in the channels of the Immobiline Drystrip Reswelling Tray. The IEF strips (Immobiline Drystrip pH 4-7, 18cm) were placed in the channels, gel side down, with '+' anode marks to the front. The sample was distributed evenly under strip avoiding trapping any air bubbles. The strips were covered with 2ml mineral oil (Drystrip Cover Fluid). The

samples were covered and left to rehydrate at room temperature overnight (10-20hr).

The IEF equipment was prepared by pouring oil onto the base and placing the glass base plate onto this and then the electrodes were attached. Oil was poured onto the base plate and the strip holder put onto this. The rehydrated IEF strips were removed from the holder and rinsed well with dH_2O. The strips were dried on filter paper (gel side up) and covered with clingfilm. The samples were placed in wells in the strip holder (gel side up) '+' ends to the anode (red). Two paper electrode strips were cut to 11cm and placed across both ends of IEF gel strips (touching the gels). These were fixed in place with electrode clips (red top right and black bottom left) and the strips were covered with oil.

The program was set on power pack: 1hr at150V; 1hr at 300V; 1.5hr at 1500V; and 20.5hr at 3000V. Total run time 24hr. This was left running for 24 hr with the equipment cooler set at 20°C. After 24hr the strips were removed and frozen at -20°C, individually placed into plastic 10ml pipettes.

2.6.3 2nd dimension SDS-PAGE

Enough acrylamide gel was prepared to make a gel for each IEF strip. For each 10% gel:- 37ml 30% bis-acrylamide; 27ml 1.5M Tris pH 8.8; 43ml dH_2O; 1.5ml 10% SDS; 1.5ml 10% APS and 200ul 10% TEMED. The gel rig was prepared with Perspex blocks and glass plates in the middle. Thin plastic spacers were placed between each block and plate. The acrylamide gel solution was poured into the rig through a tube in the base, until it reached approx. 5-10cm from the top of the glass plates. Displacing fluid (50ml 1.5M Tris HCl pH 8.8, 100ml 50% glycerol, 50ml dH_2O, 2mg bromophenol blue) was then poured into the tube until

the acrylamide was only 1cm from the top. The tube was then clipped. 2-3ml H_2O (or H_2O saturated butanol) was poured onto gels and left to polymerise (minimum 1hr). The top of the gels were rinsed thoroughly and covered with SDS electrophoresis buffer. The IEF strips were thawed and equilibrated in SDS equilibration fluid for 15mins before applying firmly to the top of the gels, between the plates. Molecular weight markers were pipetted onto filter paper and pushed into one end of each gel. The strips were sealed into place with an agarose sealing solution to prevent movement of the strip. The gels were placed in the vertical tank and submerged in the tank electrophoresis buffer. The electrophoresis conditions were selected at 30mA/gel for 1-2hr.

For visualisation the gels were either stained with Coomassie blue stain or silver stain for better sensitivity. For more detailed analysis of the spots, the gels were stained with SYPRO Ruby fluorescent protein stain (Invitrogen) and the gels were scanned with a laser scanner (Fujifilm FLA-5000). The images of the protein spots were then analysed.

Chapter 3

Investigation of Aβ toxicity on SK-N-SH cells transfected with ABAD

3.1 Background and aims

The binding of Aβ peptide to plasma membranes has been shown to cause direct cell toxicity, producing a local inflammatory response and Aβ fibrillar production (Yan *et al.*, 1997b). This suggests that specific interactions of Aβ with cell surface receptors may trigger signal transduction early in AD, before the production of tau tangles and amyloid plaques (Yan *et al.*, 1997a). It is also known that Aβ toxicity induces apoptosis in primary neuronal cells (Kadowaki *et al.*, 2005; Yankner, 1996), but whether or not Aβ toxicity causes apoptosis *in vitro* in immortal neuronal cell lines has remained to be disputed in different studies (Behl *et al.*, 1994; Cotman and Su, 1996; Gschwind and Huber, 1995). Intracellular accumulation of Aβ has been identified in different cell types (LaFerla *et al.*, 2007; Yamazaki *et al.*, 1996), and the most characterised intracellular protein that has been identified to bind Aβ, is ABAD (Du *et al.*, 2008; Yan *et al.*, 1997a). The ABAD/Aβ complex has been shown to mediate cell toxicity and to induce apoptosis in several cell lines (Yan *et al.*, 1999) (Oppermann *et al.*, 1999).

Confocal microscopy in the Yan study identified the protein distributed within the endoplasmic reticulum (ER) (Yan *et al.*, 1997a). Because of its reported cellular localisation, the protein was initially called 'ERAB' (Endoplasmic Reticulum

binding Amyloid Beta). In the protein sequence, amino acid residues 169 - 173 (YSASK) correspond to the highly conserved active site residues 153-157 (YGASK) from the NADH-binding enzyme 3α,20β-hydroxysteroid dehydrogenase of *Streptomyces hydrogenans* (Yan *et al.*, 1997a). This indicated that 'ERAB' had potential enzyme activity, with the YSASK region putatively being part of the active site. Both proteins also share NAD(H) binding domains. Yan also showed by site-directed mutagenesis experiments, at residues 168 and 172, that a mutation at or near the active site reduced the toxicity of the Aβ peptide, suggesting that this enzyme could have an effect in AD (Yan *et al.*, 1999).

The initial aim of this part of the project was to confirm and identify the cellular localisation of ABAD in a human neuroblastoma cell line, SK-N-SH cells, and to set up an *in vitro* model to investigate the effect of ABAD in these cells and thus help to define the role of ABAD in AD. Although animal models are critical for biomedical research and drug development in neurodegenerative diseases, no model perfectly mimics the human disease (Duyckaerts *et al.*, 2008). Animal experiments are time consuming and costly, therefore it is essential to have an effective and reliable *in vitro* model for neurotoxic and neuroprotective effects within the laboratory.

To establish a cell line as an AD model, SK-N-SH cells were transfected with a plasmid referred to as ABAD-EGFP that included enhanced green fluorescent protein (EGFP) as a reporter of expression that was C-terminally tagged to ABAD. Fluorescent microscope imaging was performed and cytotoxic assays

were designed to investigate the effect of ABAD overexpressed in these transfected cells. Toxicity was induced using a synthetic Aβ42 peptide. MTT cell viability assays and live cell imaging were used to monitor viability and potential toxic effects on the cells. Further experiments were carried out to establish if cell death was due to apoptosis. The initial experiments consisted of western blot analysis of subcellular fractionated cells to identify cytochrome C release from mitochondria into the cytosol. Further MTT assays were carried out to identify inhibition of Aβ42 toxicity by a pan-caspase inhibitor, BocD-fmk and also by a novel peptide inhibitor, TAT-ABAD, a peptide which was developed based on the amino acid protein sequence of ABAD that is thought to bind Aβ. There were several problems encountered during these experiments that are discussed. However, it led to the search for different appropriate cell lines and forms of the Aβ42 peptide to try and develop an improved *in vitro* model for the future. Some initial experiments were carried out to investigate the use of neuronal stem cells as a useful cell line closer in phenotype to primary cells in cultivation. Murine cortical neuronal cells were also cultured and a system to produce neurospheres from murine stem cells was established.

3.2 Cellular localisation of ABAD in SK-N-SH, a human neuroblastoma cell line

The cellular localisation and naming of this protein has been a contentious issue. It has been reported to be present in both the endoplasmic reticulum (ER) and mitochondria (Yan *et al.*, 1997a), but other studies have it solely expressed in the mitochondria (He *et al.*, 1999a). It has been suggested that its cellular localisation is cell-line dependent (Frackowiak *et al.*, 2001). ABAD was identified as being

localised in the ER of SK-N-SH cells (Yan *et al.*, 1997a), and its function would be dependent on its activity in its particular cellular localisation.

3.2.1 Previous studies on the cellular location of ABAD

Previous studies of ABAD have indicated that there are targeting sequences either for the lumen of ER and lysosomes (Sambamurti and Lahiri, 1998), or for mitochondria (Filling *et al.*, 2001; He *et al.*, 2001).

Sambamurti and Lahiri detected a putative signal peptide, by computer analysis of the ABAD sequence, that could potentially direct the protein into the ER-Golgi secretory pathway. The peroxisome signal sequence, AHL is found near the C terminus of the protein. This signal sequence was found in human, rodent, and bovine isoforms of ABAD suggesting that it was a type II integral membrane protein in vertebrates (Sambamurti and Lahiri, 1998). Peroxisomes can be derived from the ER (Hoepfner *et al.*, 2005), but as this sequence was predicted by computer analysis it was recognised that this may not be a true localisation of the protein in the cell.

He *et al*. had previously constructed an expression plasmid encoding a fusion protein consisting of the first eleven residues of ABAD: MAAACRSVKGL, highlighted in Figure 3.1, fused to GFP. By fluorescent microscopy, they noted the GFP fusion protein expressed in organelles co-localised with a fluorescent stained mitochondrial marker, cytochrome oxidase, confirming this sequence to be a mitochondrial targeting sequence (He *et al.*, 2001).

MAAACRSVKG LVAVITGGAS GLGLATAERL VGQGASAVLL DLPNSGGEAQ AKKLGNNCVF **60**

APADVTSEKD VQTALALAKG KFGRVDVAVN CAGIAVASKT YNLKKGQTHT LEDFQRVLD **120**

NLMGTFNVIR LVAGEMGQNE PDQGGQRGVI INTASVAAFE GQVGQAAYSA SKGGIVGMTL **180**

PIARDLAPIG IRVMTIAPGL FGTPLLTSLP EKVCNFLASQ VPFPSRLGDP AEYAHLVQAI **240**

IENPFLNGEV IRLDGAIRMQ P **261**

Fig. 3.1. The human ABAD protein sequence. The first eleven amino acid residues are highlighted in red as a potential mitochondrial targeting sequence (He *et al.*, 2001). Amino acid residues 168 to 172 are also highlighted to identify the conserved sequence in NADH binding enzymes and suggested active site for the enzyme ERAB/ABAD. The residues highlighted in blue are those predicted by computer analysis as a putative peroxisomal signal sequence.

3.2.2 Cellular localisation of ABAD by fluorescent microscopy in SK-N-SH cells

As the overall aim of this chapter was to establish a reliable cellular model in which to study ABAD, it was necessary to choose an appropriate cellular background and to clearly establish the exact subcellular localisation of ABAD within the selected cell line. Given the previous body of work, and to expand on the previous experiments (Yan *et al.*, 1997a; Yan *et al.*, 1999) (section 3.1), SK-N-SH cells were selected for use in this study and an ABAD-EGFP fusion protein was used to visualise the ABAD localisation.

The SK-N-SH cell line is derived from a human neuroblastoma and they are routinely and extensively used for cytotoxic assessments (Biedler *et al.*, 1973). The cells are grown as an adherent monolayer with a long doubling time of 44hr. The growth remains constant and they can be trypsinised and passaged to 70-80% confluence more than 20 times. It is possible to differentiate up to 50% of the

cells into a neuronal phenotype, characterized by extensive neurite outgrowth, thick neurite bundles, and large cellular aggregates by the addition of retinoic acid (Preis *et al.*, 1988).

3.2.3 Transient transfection of SK-N-SH cell line with ABAD-EGFP

To confirm the cellular localisation of ABAD in SK-N-SH cells, the cells were transiently transfected with a plasmid coding for an ABAD-EGFP fusion protein, hereinafter called ABAD-EGFP. This plasmid had been cloned previously in the laboratory, using the full-length cDNA human ABAD clone and cloning into pEGFP-N3 vector (Clontech) by PCR, using Taq polymerase (Figure 3.2).

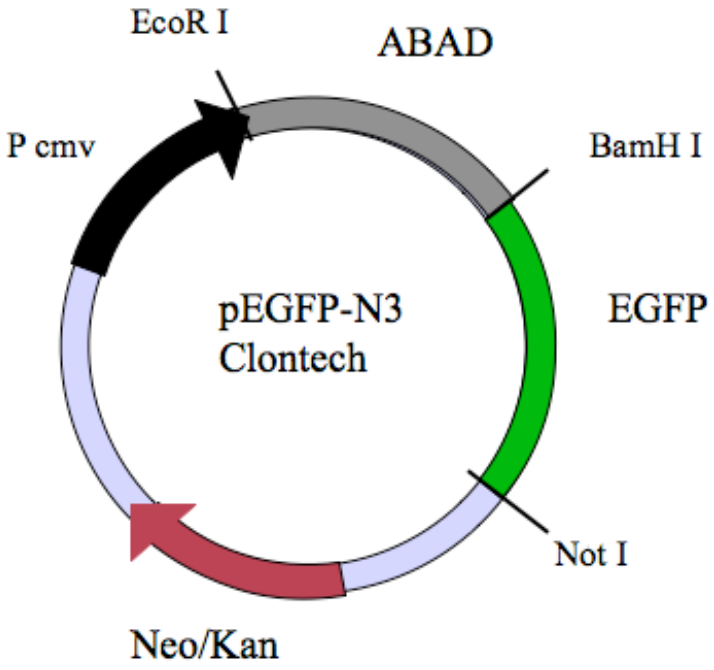

Fig. 3.2. The ABAD-EGFP plasmid showing restriction sites EcoRI and BamHI for ABAD (grey) and BamH I and Not I for EGFP (green). The vector and plasmid contain a kanamycin resistance gene (red).

The SK-N-SH cells were grown on glass cover slips and grown in DMEM growth media with glutamine, penicillin/streptomycin and 10% FCS (Section 2.2.1). After 24 hr, when 80% confluent, the cells were transfected with 1μg of the ABAD-EGFP plasmid, using Lipofectamine (Invitrogen), a lipid based transfection reagent. The transfected cells were incubated for a further 18hr to allow for protein expression and then were fixed with 4% paraformaldehyde, rinsed, mounted and then imaged by fluorescent microscopy (Figure 3.3).

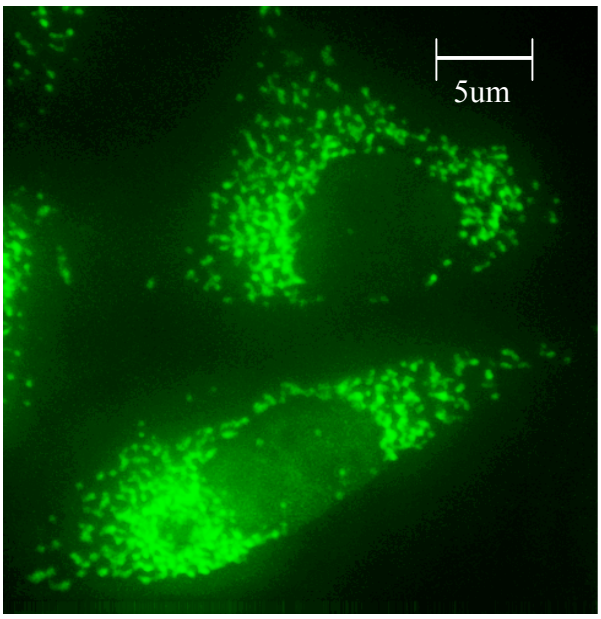

Fig. 3.3. A fluorescent microscope image of paraformaldehyde fixed SK-N-SH cells after transient transfection with ABAD-EGFP (imaged on Zeiss Axioscope fluorescence microscope). This shows ABAD-EGFP protein was expressed in discreet spots surrounding the nucleus, which potentially were organelles. However in the bottom cell there appeared to be diffuse green staining throughout the cell.

Diffuse green staining was seen throughout some the cells, and at first it was unclear why this might be the case but may have been suggestive of mis-targeting of the ABAD-EGFP protein. To overcome this, two methods were developed later to improve the targeting and expression of ABAD in the cells.

3.2.4 Further subcellular localisation by fluorescence microscopy

Further transient transfections of SK-N-SH cells with ABAD-EGFP were carried out as above, in order to identify the organelle expressing ABAD. The cells were co-transfected with Clontech subcellular localisation plasmids, to express fluorescent subcellular proteins. A plasmid for cyan fluorescent protein tagged with an ER targeting sequence (ER-CFP) or a plasmid for red fluorescent protein tagged with an ER targeting sequence (ER-Red) were transfected to identify the ER with either cyan or red fluorescent protein, respectively. A plasmid for a red fluorescent protein tagged with a mitochondrial targeting sequence (pDsRed2-Mito) was transfected to identify the mitochondria with red fluorescent protein. Cells were fixed and mounted as before and imaged by fluorescence microscopy (Figures 3.4, 3.5 and 3.6).

Figure 3.4 shows ABAD-EGFP and pDs-Red-Mito both expressed in the mitochondria. Further imaging was done to identify the ER and mitochondria in SK-N-SH cells, to see if ABAD is expressed in both organelles.

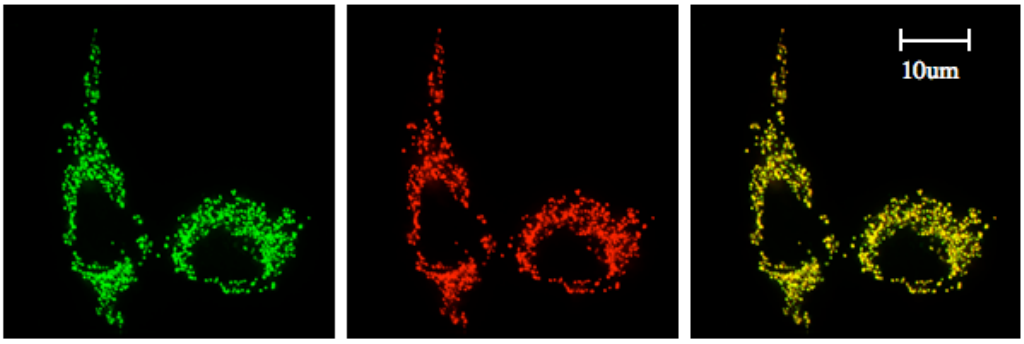

Fig. 3.4. Fluorescent microscope images of two SK-N-SH cells, co-transfected with ABAD-EGFP and pDsRed2-Mito. (a) Cells imaged with FITC filter (ex. 490nm. em. 528nm.) showing ABADEGFP. (b) Cells imaged with red filter (ex. 555nm. em. 617nm.) showing pDsRed2-Mito in mitochondria. (c) Converged image showing co-localisation of ABDGFP and pDsRed2-Mito. This shows ABADEGFP and pDs-Red-Mito both expressed in the mitochondria confirming localisation of ABAD in mitochondria in SK-N-SH cells.

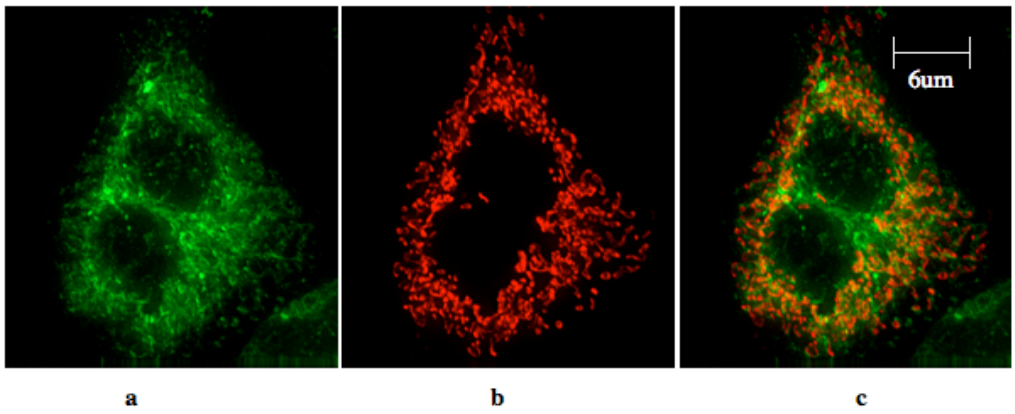

Fig. 3.5. Fluorescent microscope images of one SK-NS-H cell dividing, co-transfected with ERCFP and pDsRed2-Mito. (a) Cells imaged with cyan filter (ex. 436nM, em. 470nM) showing ERCFP in ER. (b) Cells imaged with red filter (ex. 555nm. em. 617nm.) showing pDsRed2-Mito in mitochondria. (c) Converged image showing the ERCFP and pDsRed-Mito. This shows the ERCFP expressed in the endoplasmic reticulum and the pDsRed2-Mito expressed in the mitochondria. The converged image shows the close association of the ER and mitochondria in SK-N-SH cells but no co-localisation of the ERCFP and pDsRed-Mito.

Figure 3.5 shows that the ER and mitochondria can be identified separately, suggesting that if ABAD was in the ER, it would show up clearly separate from the mitochondria in SK-N-SH cells. To confirm this, further imaging was done with co-transfection of ABAD-EGFP and ER-Red. Figure 3.6 shows a small amount of co-localisation of ABAD-EGFP with ER-Red, indicating that ABAD may be expressed or translocated into the ER of SK-N-SH cells. Again there appears to be some diffuse GFP staining seen in or around the nucleus and in the cytoplasm. This could be due either to mis-targeting or ABAD is secreted into the cytoplasm possibly due to cell stress. Otherwise the cells look healthy in morphology, with healthy nuclei.

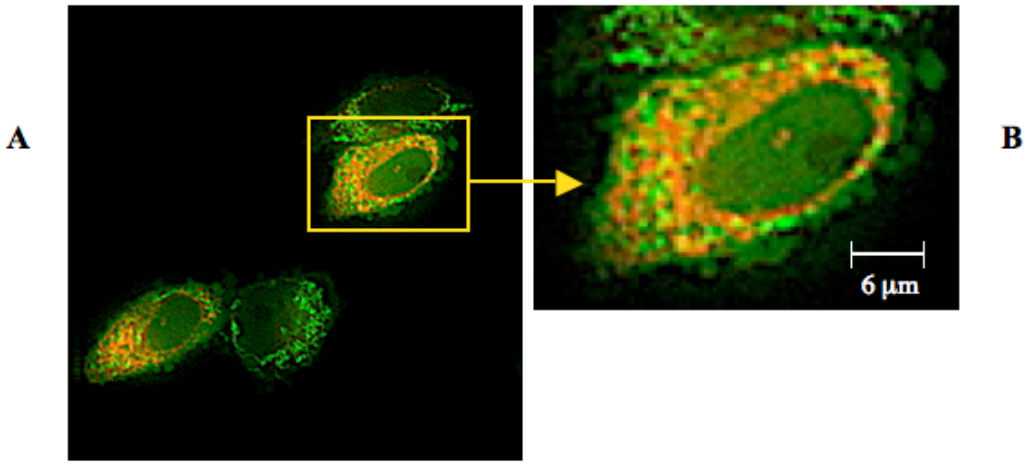

Fig. 3.6. A 0.1µm section through SK-N-SH cells co-transfected with ABAD-GFP and ER-Red (imaged on the Deltavision deconvolution microscope). (A) The converged image shows four cells expressing ABAD-GFP in the mitochondria with two of the cells co-expressing ER-Red in ER. (B) The cell with co-expression enlarged for detail. This possibly shows a little co-localisation of ABAD-EGFP with ER-Red .

These imaging studies concluded that ABAD is expressed in the mitochondria of SK-N-SH cells and may be translocated into the ER. More recent publications

have confirmed expression in the mitochondria and it is now accepted that ABAD is a mitochondrial enzyme. However there is evidence that lipids and membrane proteins can be exchanged directly between the ER and mitochondria via mitochondrial associated membranes (MAMS), membrane compartments that have close contact points with ER and mitochondria (Rusinol *et al.*, 1994). It is possible that ABAD is shuttled from one organelle to the other by this method (Stone *et al.*, 2009).

3.2.5 Stable expression of ABAD-EGFP in SK-N-SH cells

Expression of ABAD-EGFP was confirmed to be in the mitochondria with transient transfections of SK-N-SH cells. However there was also diffuse distribution of GFP within the cytosol of some of the cells (for example see Figures 3.3 and 3.6). As indicated above, one possibility for this was due to the overexpression of ABAD-EGFP causing the mis-targeting of the protein at the sub-cellular level. A similar effect had also been observed when using a different ABAD-GFP chimeric protein, where better targeting of GFP was found when it was expressed with a mitochondrial targeting sequence at the N terminal end (He *et al.*, 1999b). Therefore, two methods were employed to improve the targeting of ABAD-EGFP: 1) a stable expressing cell line was produced; 2) a second plasmid was developed where a mitochondrial targeting sequence (MTS) was ligated on to the N-terminus of the original ABAD-EGFP construct. The stable cell-line took several weeks to produce (see protocol in section 2.2.2 and 2.2.3) but as indicated in Figure 3.7, this new cell-line showed good stable expression of the ABAD-EGFP within the mitochondria and with improved targeting (Figure 3.7).

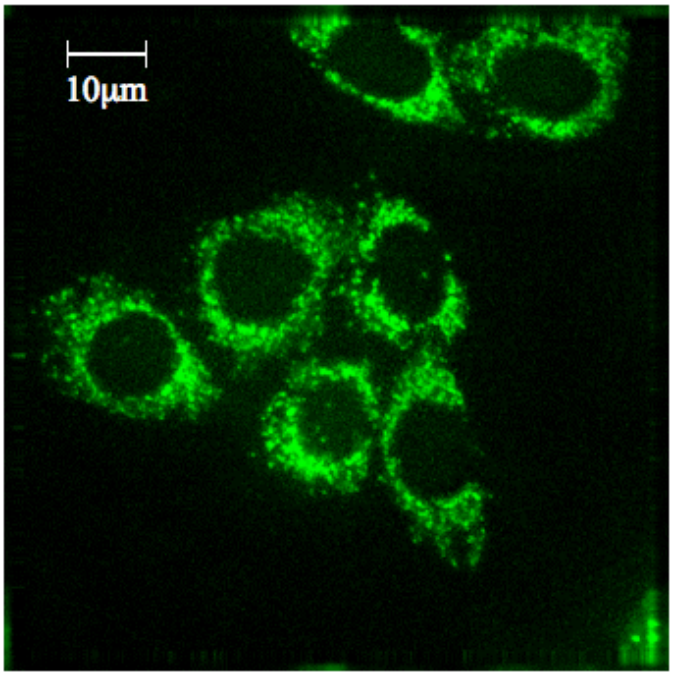

Fig. 3.7. Fluorescent microscope image of a group of SK-N-SH cells stably transfected and expressing ABAD-EGFP. Note there is no diffuse green staining in the cytosol.

3.2.6 Creation of new construct by cloning of a mitochondrial targeting sequence (MTS) into ABAD-EGFP plasmid.

In parallel with the work to establish a stable expression of ABAD-EGFP, an alternative transient method for targeted expression of ABAD was also explored. The production of a new plasmid construct of ABAD containing a mitochondrial targeting sequence was undertaken. This had been done previously with good results (He *et al.*, 2001).

3.2.6.1 Plasmid design

The construct was designed by inserting an N-terminal mitochondrial targeting sequence (MTS), at the N-terminus of the ABAD-EGFP plasmid (Figure 3.8). The ABAD-EGFP expressing plasmid had been designed previously from the Clontech pEGFP-N3 plasmid (Figure 3.2). The 'vector' encoding the ABAD-EGFP gene was made first by removing the nucleotide sequence between the Nde1 and EcoR1 restriction sites in the ABAD-EGFP plasmid between nucleotides 234 and 629 (Figure 3.8b) using restriction enzymes Nde1 and EcoR1 (New England Biolabs). The insert was made from the sequence of the N-terminal MTS from the Clontech pDsRed2mito (subunit VIII human cytochrome C oxidase) plasmid (hereafter called MTS) from a start codon ATG at nucleotide 597 to nucleotide 683, 86 base pairs (Figure 3.8c). The MTS insert was produced by PCR using the pDsRed2-Mito plasmid as a template with primers:

Primer 1 sequence, sense - (NdeI restriction site highlighted)

5'-AGTGTAT***CATATG***CCAAGTACG-3'

Primer 2 sequence, antisense – (EcoRI restriction site highlighted)

5'-G***GAATTC***GGCGACCGGTGGATCCCC-3'

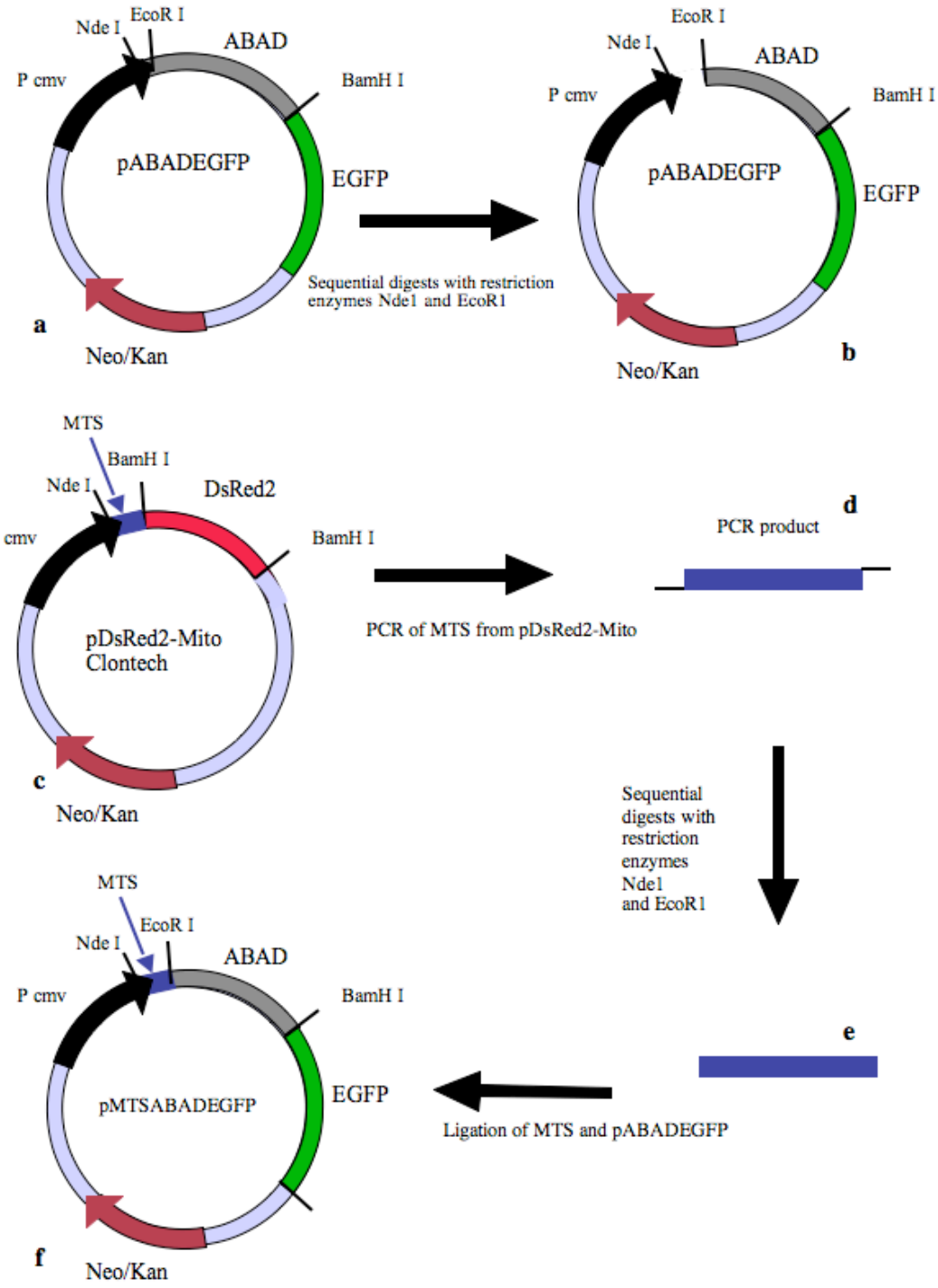

Fig. 3.8. Cloning strategy for pMTS-ABAD-EGFP. (a) The pABAD-EGFP plasmid was digested sequentially with NdeI and EcoRI to produce the vector (b) pABAD-EGFP. (c) The pDsRed2-Mito plasmid was used as the template for PCR of MTS to produce the PCR product (d). The PCR product containing the MTS was cleaned and digested (e). The digested PCR product was ligated into the vector pABAD-EGFP to give a final construct of pMTS-ABAD-EGFP (f).

The resulting PCR product was sequentially digested with NdeI and EcoRI restriction enzymes. This MTS insert and ABAD-EGFP vector were cleaned using a Promega Wizard DNA clean-up system. The MTS insert was then ligated into the ABAD-EGFP vector with T4 DNA ligase to produce MTS-ABAD-EGFP (Figure 3.8 e and f). DH5α competent cells were transformed with the MTS-ABAD-EGFP plasmid DNA and spread on agar plates containing 50μg ml^{-1} kanamycin. The plates were incubated overnight at 37^{o} C and four colonies were selected and cultured in LB for 18hr. The DNA was extracted using a Promega Mini-Prep kit. The new plasmid DNA was transfected into SK-N-SH cells. For comparison the new construct was also transfected into another neuronal cell line, PC12, which was also available in the laboratory. The cells were fixed, mounted and imaged under fluorescent microscopy (Figure 3.9).

Figure 3.9 shows good transient transfection and targeting of ABAD to the mitochondria in both neuronal cell lines. The PC12 cells are smaller than SK-N-SH cells with less cytosol (Figures 3.9, 3.10). They require slightly more complicated growth conditions and do not adhere well to plastic culture flasks unless treated with collagen IV. In general they are known to be more difficult to culture and transfect than SK-N-SH cells. However they are useful as a neuronal cell line as they cease proliferation when treated with NGF (nerve growth factor) and produce long neurites and show morphology consistent with neuronal differentiation (Foehr, 2000). They are useful as a model system for primary neuronal cells.

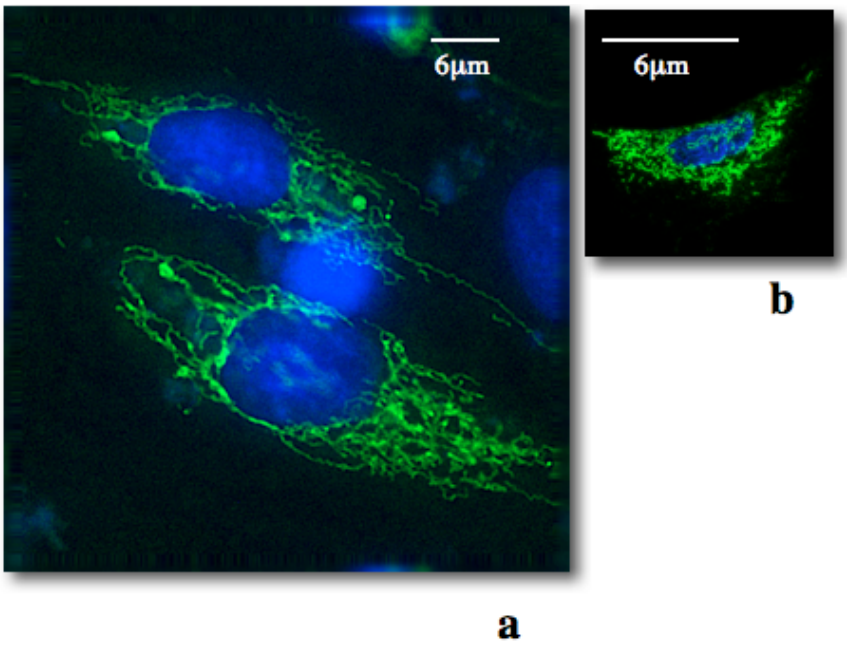

Fig. 3.9. Fluorescent microscope images of transient transfections of cells with MTS-ABAD-EGFP, with blue DAPI staining of nuclei. (a) SK-N-SH cells. (b) PC12 cell.

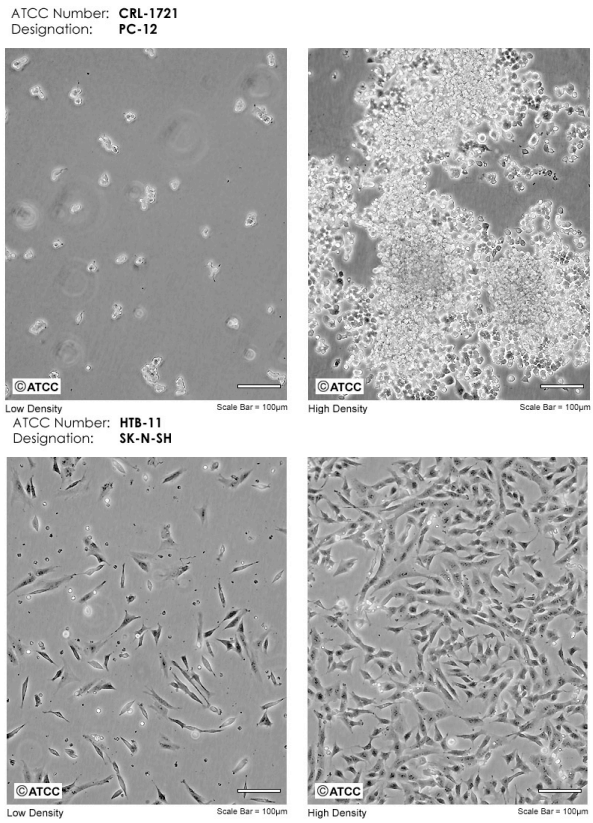

Fig 3.10 Microscope phase contrast images of the cultivation of PC12 cells (top) and SK-N-SH cells (bottom) for comparison (taken from ATCC product sheets).

Due to the ease of cultivation and transfection, it was decided to continue with the SK-N-SH cell line expressing ABAD to develop the AD model. However, the MTS-ABAD-EGFP construct and the PC12 cells were used subsequently in the laboratory to develop other constructs for use in another cellular model and developing FRET experiments.

3.3 Developing an *in vitro* model for AD

During development of the *in vitro* model, both the stable cell line SK-N-SH cells transfected with ABAD-EGFP and SK-N-SH cells transiently transfected with MTS-ABAD-EGFP were used in further studies to test the toxicity of the synthetic human Aβ42 peptide (Biosource International). The toxicity at different concentrations of the Aβ42 peptide was tested both in MTT viability assays and also in assessing its ability to induce the potential reported translocation of ABAD to the plasma membrane (Yan *et al.*, 1997a).

3.3.1 MTT cell viability assays with Aβ42

Prior to experiments studying the potential translocation of ABAD in SK-N-SH cells, it was first necessary to establish the toxic conditions required to initiate a cellular response. To assess the dose of Aβ42 required to show a toxic effect in cells over-expressing ABAD, a dose dependent, cell viability assay was performed using a MTT (3-(4,5-Dimethylthiazol-2-yl)-2,5-diphenyltetrazolium bromide) assay. This is a colorimetric assay to determine cell viability, by noting the change in colour of the tetrazole substrate from yellow to purple, when it is reduced by active reductase enzymes from living cells (Mosmann, 1983). Lyophilised Aβ42 peptide (FW 4514, Biosource International) was reconstituted

(as per the manufacturer's recommendations) in 100µl sterile nuclease free water to a concentration of 5mg ml^{-1}, and then further diluted in PBS to make a working stock concentration of 1mg ml^{-1}. 30-50µl aliquots of this stock were pre-incubated as required, at 37^0C for 24hr.

A 96 well micro tissue culture plate was seeded with SK-N-SH (ABAD-EGFP) cells, at a cell density of 1 x 10^4 cells per well (approx. 2 x 10^4 cm^{-2}). The SK-N-SH (ABAD-EGFP) stable cell line was used to enable a direct comparison between the different imaging studies. The cells were incubated in normal growth medium for 12hr at 37^0C with 5% CO_2. The synthetic Aβ42 peptide was then added to the cells in the 96 well plate at different concentrations, as shown in Figure 3.11, and the cells further incubated for 16-18 hr, after which an MTT assay was performed and the results of this are shown in Figure 3.12. The control cells were assumed to have 100% viability and the other readings were then compared to this to give a final % of viability.

	1	2	3	4	5	6	7	8	9	10	11	12
A												
B			No Aβ	No Aβ	0.1µM Aβ	0.1µM Aβ	1µM Aβ	1µM Aβ	2µM Aβ	2µM Aβ		
C			No Aβ	No Aβ	0.1µM Aβ	0.1µM Aβ	1µM Aβ	1µM Aβ	2µM Aβ	2µM Aβ		
D			No Aβ	No Aβ	0.1µM Aβ	0.1µM Aβ	1µM Aβ	1µM Aβ	2µM Aβ	2µM Aβ		
E			No Aβ	No Aβ	0.1µM Aβ	0.1µM Aβ	1µM Aβ	1µM Aβ	2µM Aβ	2µM Aβ		
F			No Aβ	No Aβ	0.1µM Aβ	0.1µM Aβ	1µM Aβ	1µM Aβ	2µM Aβ	2µM Aβ		
G			No Aβ	No Aβ	0.1µM Aβ	0.1µM Aβ	1µM Aβ	1µM Aβ	2µM Aβ	2µM Aβ		
H												

Fig. 3.11. The template of the 96 well plate showing different concentrations of Aβ42 peptide added. Columns 3 and 4, negative controls, no Aβ added. Columns 5 and 6, 0.1µM Aβ added. Columns 7 and 8, 1µM Aβ added. Columns 9 and 10, 2µM Aβ added. The outer wells were filled with growth medium only, as readings at the edges of the plate can be unreliable. Each condition had 12 individual readings.

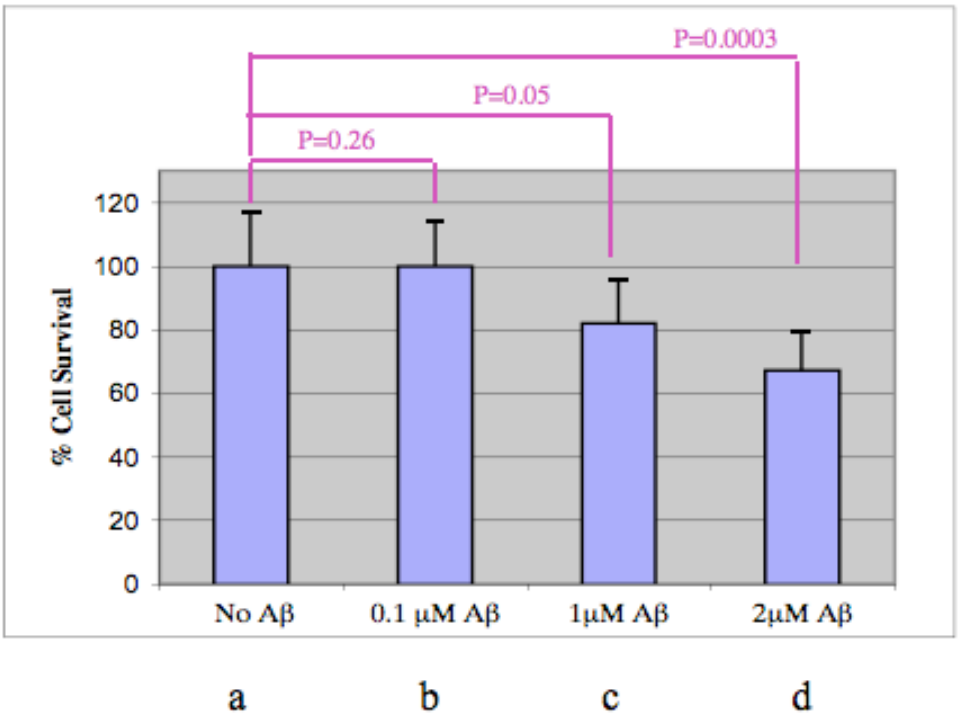

Fig. 3.12. Results from the MTT readings of SK-N-SH (ABAD-EGFP) cells incubated for 16hr with Aβ42 as shown. An average reading was taken from the 12 replicate samples. Error bars show one standard deviation. (a) Negative control. (b)-(d) Cells incubated with increasing concentrations of Aβ42; (b) 0.1μM, (c)1μM, (d) 2μM. From the student t test, the probability (p) values are shown.

Using the Student t-test, with a significance level of P=0.05. P values above this are not significant and below this are taken as significant, Table 3.1.

	No Aβ	0.1μM Aβ	1μM Aβ	2μM Aβ
readings @ 570nm	0.67	0.63	0.55	0.44
SD	0.19	0.12	0.17	0.13
t test P values		**P=0.26**	**P=0.05**	**P=0.0003**

Table 3.1 Student t test p values of the readings giving the results of the MTT assay in Figure 3.12. The average readings taken for the MTT assay and the standard deviation are also shown. The t test P values show that the readings for 1μM and 2μM Aβ compared to the reading with no Aβ are statistically significant.

The results from the MTT assay indicated that the addition of either 1μM and 2μM Aβ42 was statistically different to the other treated cells, therefore a minimum of 1μM Aβ42 was used in the following toxicity studies.

3.3.2 Fluorescence imaging studies of Aβ42 toxicity

Previous studies have shown that ABAD is released into the cytosol and is subsequently rapidly translocated to the plasma membrane; however, this was performed at a single time point, 24hr after the addition of Aβ. Therefore, it was unknown how early this event could occur.

Therefore experiments were designed to monitor by live imaging, the stable SK-N-SH (ABAD-EGFP) cell-line. SK-N-SH (ABAD-EGFP) cells were grown in glass-bottomed WillCo-dish® tissue culture dishes with lids and incubated to 80% confluence (16-18hr) in an incubator at 37^0C with 5% CO_2. The cells were then further incubated for 20hr in an enclosed Perspex hood on a rig attached to the Deltavision deconvolution microscope. The glass-bottomed dish was positioned on the microscope oil objective lens and focused onto a group of 3 or 4 cells. The conditions were regulated over the 20hr: the rig was heated at 37^0C and 5% CO_2 was continuously pumped into the WillCo-dish®, through a thin plastic tube introduced into a pre-drilled hole in the lid. Images of the cells were taken every 1-2hr (Figure 3.13). The live imaging showed that the cells grew and multiplied over a 17hr period with no shuttling of ABAD in and out of the mitochondria.

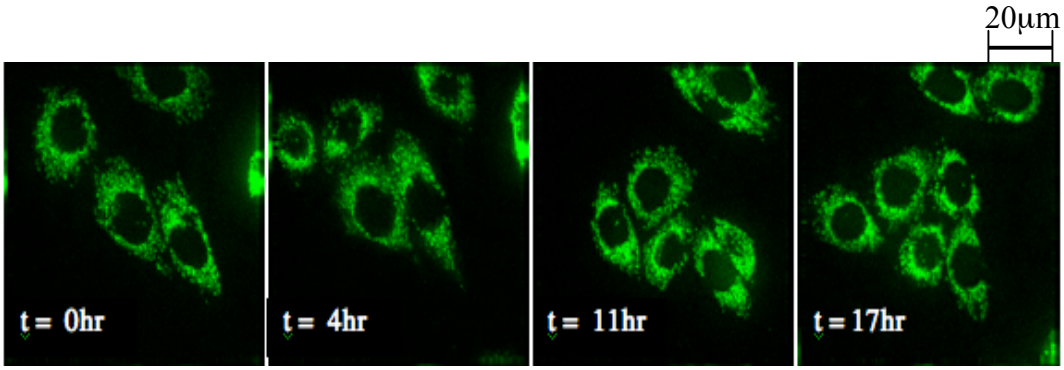

a b c d

Fig. 3.13. Live imaging of stably transfected SK-N-SH (ABAD-EGFP) cells. These images show a time-course to 17hr. (a) Four cells selected for imaging. (b) The same cells at 4 hr, with division of one cell, seen top left. (c) The same cells at 11 hr. More division seen. (d) At 17hr, cells alive with healthy morphology, showing that the cells survive and divide in these growth conditions, without requiring a change of growth medium. There is no evidence of ABAD-EGFP translocating to the plasma membrane.

This experiment was repeated under the same conditions but with the addition of 1μM Aβ42, to visualise the toxic effect on the cells, but also a mitochondrial marker pDsRed2-Mito (Clontech) was also transiently transfected into the cells (pDsRed2-Mito is a mammalian expression vector encoding a mitochondrial targeting sequence and the *Discosoma sp.* red fluorescent protein). The pDsRed2-Mito was included to compare the reaction of these two mitochondrial proteins when the cells are reacting to the addition of the Aβ peptide.

The SK-N-SH (ABAD-EGFP) cells were grown as before in glass-bottomed WillCo-dish tissue culture dishes and incubated to 50-60% confluence (12-16 hr) in an incubator at 37^0C with 5% CO_2. The cells were then transfected with 2μg pDsRed2-Mito DNA using lipofectamine (Invitrogen) and incubated to 80% confluence (12-16 hr). At this stage 50% growth medium was replaced with fresh

pre-warmed medium. The Aβ42 peptide (Biosource) was pre-incubated for 24hr at 37^0C as before, and added to the growth medium at a final concentration of 1μM. The cells were further incubated for 20hr in an enclosed Perspex hood on a rig attached to the microscope. The conditions were regulated: the rig was heated at 37^0C and 5% CO_2 was continuously pumped into the Willco dish. Images of the cells were taken every 1-2hr, using the Deltavision deconvolution microscope (Figure 3.14).

As indicated in Figure 3.14, these images indicate the cytotoxic effect of 1μM Aβ42 on SK-N-SH (ABAD-EGFP) cells. There appears to be a rapid toxic effect by 4hr post incubation with Aβ42. By 4hr (b) approximately 50% of the cells are dead or showing considerable change in morphology, with shrinking and collapse of the mitochondria and the plasma membrane. Significantly, in these cells there appears to be GFP, but not DsRed-Mito, expression in the cytosol and nucleus, indicating the selective export of ABAD. By 11hr (c) the cells affected continue to shrink and the mitochondria are reduced in volume and number. By 17hr incubation (d), 90% of cells had shrunk showing a change in morphology consistent with cell death. The nuclear membrane became indistinct and most cells were no longer attached to the tissue culture dish. This live imaging experiment with the Aβ peptide shows a more rapid toxic effect and less cell viability at 16hr than was shown with the MTT assay using the same cells. One possibility is that this may be due to changing the conditions slightly by co-transfecting with pDsRed Mito. However, it was significant to observe that the pDsRed-Mito protein does not appear to be released from the mitochondria in the

same manner as ABAD-EGFP. This may be reflected by the fact that ABAD is located to the matrix of the mitochondria whereas pDsRed mito is targeted to the mitochondrial inner membrane which could explain the differences in the reaction to Aβ toxic insult.

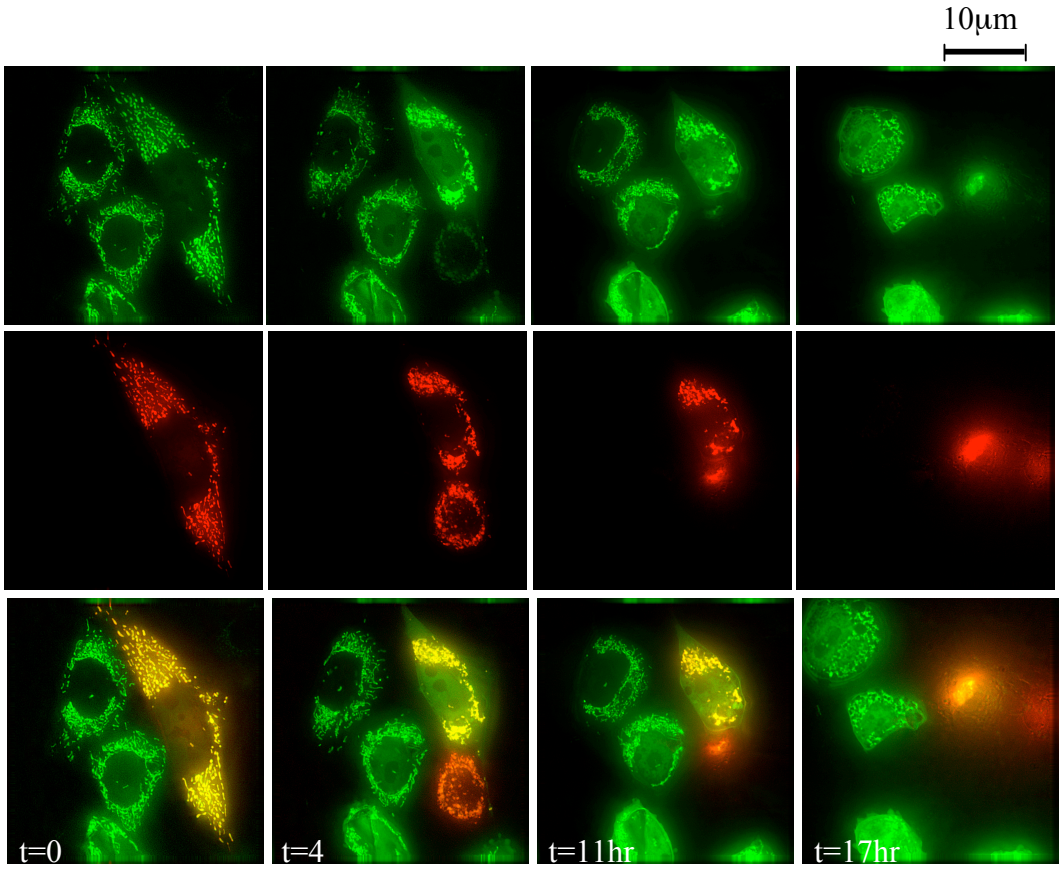

Fig. 3.14. Live imaging of stable SK-N-SH (ABAD-EGFP) cells, co transfected with pDsRed2-Mito and incubated with 1μM Aβ42 over 17hr. The images show a time-course to 17hr post incubation with Aβ. Top row, cells imaged with FITC filter (ex. 490nm. em. 528nm) Middle row: the same images with red filter (ex. 555nm. em. 617nm). Bottom row: converged images. (A) Before adding Aβ. (B) 4hr incubation with Aβ. (C) 11hr incubation with Aβ. (D) 17hr incubation with Aβ.

3.4 Assays to assess apoptosis

The live imaging showed that a 1μM dose of synthetic Aβ42 produced a toxic effect within 17hr, to cells overexpressing ABAD. Further studies were designed to assess if this toxicity *in vitro* was due to apoptosis. Apoptosis is characterised by an increase in cytosolic Ca^{2+} due to ion channel receptors being activated by a toxin. A major stage of the cascade of cellular events involved in apoptosis is the release of cytochrome C from the mitochondria into the cytosol, which has been reported to occur within about five minutes, however the mechanism by which it translocates to the cytosol during apoptosis is the subject of debate (Goldstein *et al.*, 2000; Martinou *et al.*, 2000). It is proposed that cytochrome C is released either by the swelling of the mitochondrial matrix causing rupture of the outer mitochondrial membrane or a pore is developed in the mitochondrial membrane large enough to allow the protein to pass through.

3.4.1 Toxic effects of actinomycin D, PBS and Aβ42 on SK-N-SH (ABAD-EGFP) cells

Prior to experiments to study apoptosis in SK-N-SH cells, it was necessary to establish the toxic conditions required to initiate a cellular response in these cells expressing the ABAD-EGFP, to confirm that the EGFP tag did not enhance/alter the cell's sensitivity. An experiment was therefore designed using the two toxins to compare results. MTT assays were carried out as before such that SK-N-SH (ABAD-EGFP) cells were incubated in 96 well tissue culture plates with either

100μM actinomycin D or 2μM Aβ42 for 24hr. 75% PBS was added as a positive control to kill the cells. PBS maintains a buffered environment at pH 7.4 but contains no growth factors such as provided by serum to maintain the cells and no glutamine to prevent degradation and ammonia build up. Therefore the cells cannot survive in PBS alone. The results are shown in Figure 3.15.

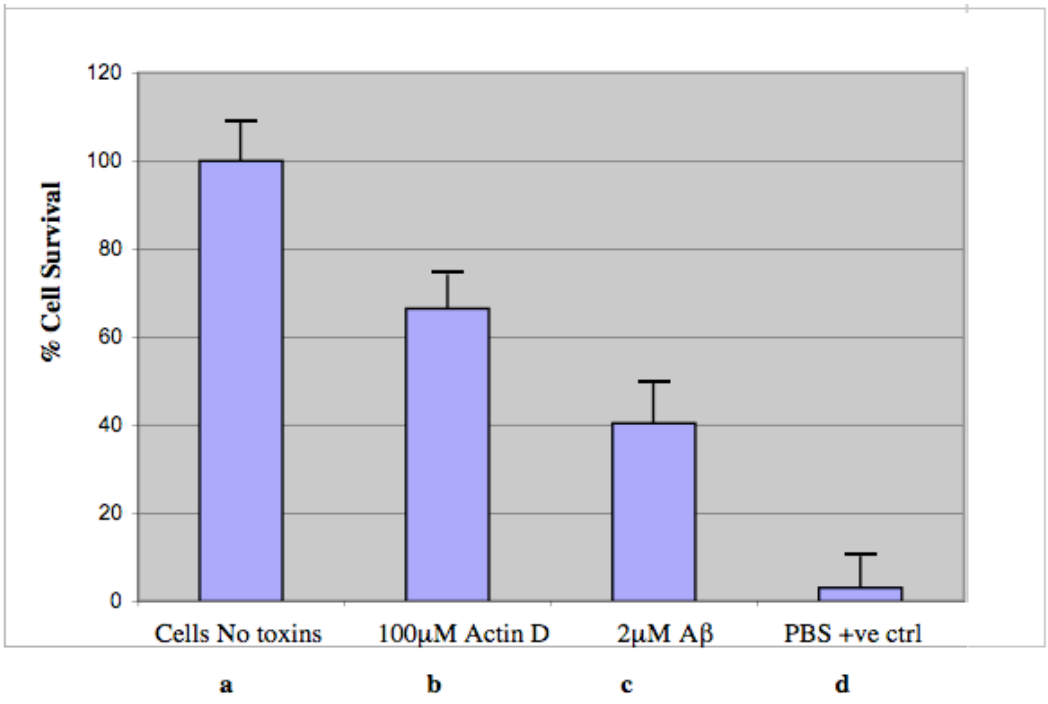

Fig. 3.15. Results of MTT assay with actinomycin D or Aβ42. SK-N-SH (ABAD-EGFP) cells were incubated for 24hr with toxins. Readings are averaged from replicates of 8 and error bars show ± SD. (a) Negative control. (b) Incubation with 100μM actinomycin D produces 65% survival. (c) Incubation with 2μM Aβ produces 40% survival. (d) Positive control with 75% PBS shows <5% survival. This shows at these doses, both Aβ and actinomycin D show evidence of toxicity but 2μM Aβ is more toxic than 100μM actinomycin D over a 24hr incubation period.

At these concentrations, 2μM Aβ is more toxic than 100μM actinomycin D over 24hr incubation. Further doses of actinomycin D were not tested at this stage and further assays for apoptosis were carried out at 100μM.

3.4.2 Subcellular fractionation and western blots

Initial experiments were designed to identify cytochrome C release from the mitochondria to the cytosol. In order to confirm that SK-N-SH (ABAD-EGFP) cells undergo apoptosis when incubated with Aβ42, subcellular fractionation was carried out on the cells after incubation for 24hr with 2μM Aβ42 peptide. For comparison and as a positive control, SK-N-SH (ABAD-EGFP) cells were also incubated with actinomycin D which is an antineoplastic antibiotic and inhibits cell proliferation by binding to double stranded DNA, inhibiting RNA synthesis and thus transcription (Sobell, 1985). It is a known inducer of apoptosis in tumour cells (Kleeff *et al.*, 2000).

The live imaging studies (section 3.3.2) appeared to show GFP release into the cytosol after a 4hr incubation with 2μM Aβ42 (Figure 3.14). Therefore it was proposed that ABAD-EGFP may be released rapidly from the mitochondria into the cytosol in a similar manner to cytochrome C and this could be another initial marker for apoptosis.

The experiment was designed to isolate the mitochondria from the cells by cellular fractionation after the addition of Aβ, and identify whether cytochrome C and/or ABAD were released into the cytosol by western immunoblotting. The SK-N-SH (ABAD-EGFP) cells were fractionated using a mitochondrial fractionation kit (Active Motif), which is designed to provide an optimized protocol to eliminate cross-contamination and produce high yields of properly

segregated mitochondrial and cytosolic fractions. The kit provides gentle lysis buffers and requires only a pestle homogeniser and the use of a benchtop centrifuge. The detailed protocol is found in section 2.4.2. The isolated fractions were analysed by western blot analysis using 0.5µg ml^{-1} anti-cytochrome C primary antibody (Santa Cruz mouse anti-cytochrome C) and 0.5µg ml^{-1} anti-mouse HRP (horseradish peroxidase) secondary antibody (Figure 3.16).

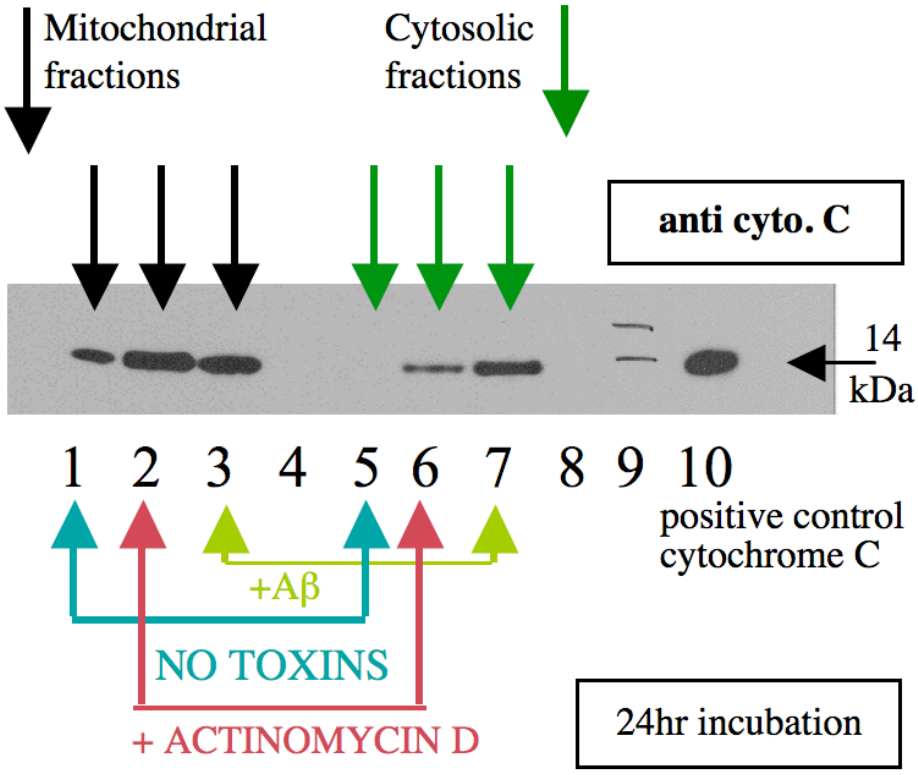

Fig. 3.16. Western blot of fractionated SK-N-SH (ABAD-EGFP) cells incubated for 24hr with 100µM actinomycin D or 2µM Aβ42, using anti-cytochrome C antibody. Lanes 1, 2, 3: mitochondrial fractions. Lanes 5, 6, 7: cytosolic fractions. Lanes 1&5: no toxins (negative control). Lanes 2&6: actinomycin D incubation. Lanes 3&7: Aβ incubation. Lane 4: empty lane. Lane 9: molecular weight markers. Lane 10: positive control for cytochrome C. This shows that cytochrome C is present in the mitochondria but only present in the cytosol after addition of the toxins, actinomycin D and Aβ (lanes 6&7), indicating that both toxins cause apoptosis after 24hr incubation with SK-N-SH (ABAD-EGFP) cells.

In order to identify if ABAD-EGFP is released from the mitochondria into the cytosol in a similar manner to cytochrome C, a repeat experiment was carried out. The SK-N-SH (ABAD-EGFP) cells were incubated with Aβ42 overnight for 16hr. The cells were fractionated as before. The isolated fractions were analysed by western blot using 0.5μg ml^{-1} anti-ABAD antibody (kindly donated by SD Yan, Columbia University NY, USA) (Figure 3.17).

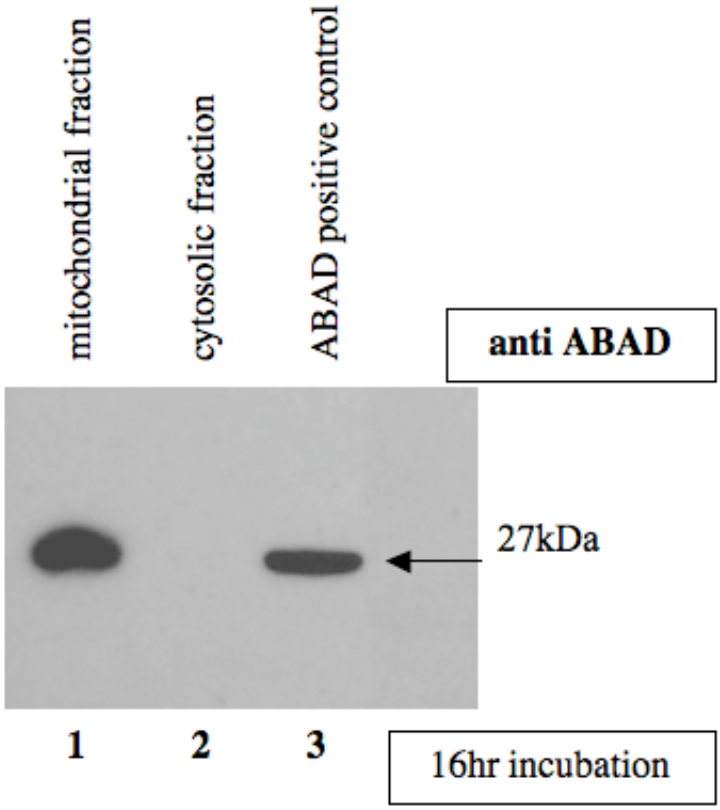

Fig. 3.17. Western blot of fractionated SK-N-SH (ABAD-EGFP) cells incubated for 16hr, using 0.5μg ml^{-1} anti-ABAD antibody. Lane 1, mitochondrial fraction, lane 2, cytosolic fraction and lane 3, positive control for ABAD. This shows that ABAD-EGFP is not released into the cytosol when SK-N-SH (ABAD-EGFP) cells are incubated with 2μM Aβ42 for 16hr.

These western blot analysis results did not appear to match the live imaging results. To verify if ABAD-EGFP release into the cytosol is time dependent, a further experiment was carried out where SK-N-SH (ABAD-EGFP) cells were incubated with 2μM Aβ42 for up to 48hr. Samples were taken and fractionated at 18hr, 26hr and 48hr after incubation with Aβ (Figure 3.18).

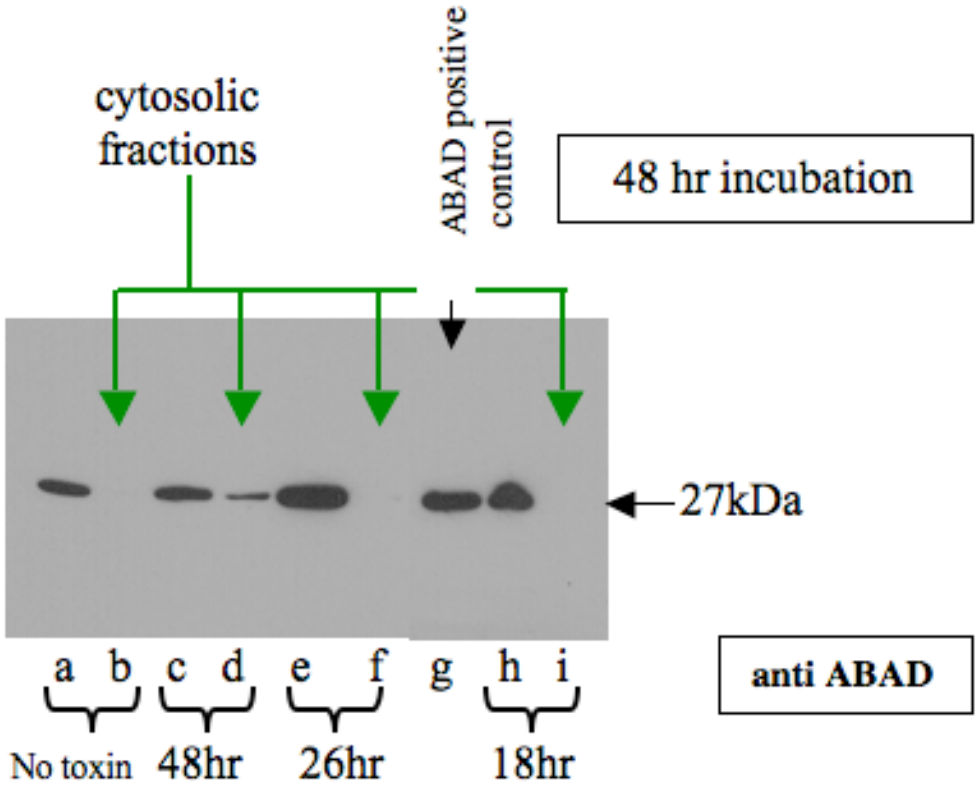

Fig. 3.18. Western blot of fractionated SK-N-SH (ABAD-EGFP) cells incubated for up to 48hr with 2μM Aβ42. Western blot analysis using anti-ABAD antibody. Lanes (a), (c), (e) and (h) mitochondrial fractions and lanes (b), (d), (f) and (i) cytosolic fractions (green arrows). Lanes (a) and (b) cells with no Aβ incubation. Lanes (c) and (d) cells after 48hr incubation with Aβ. Lanes (e) and (f) cells after 26hr incubation with Aβ. Lane (g) Positive control for ABAD. Lanes (h) and (i) cells after 18hr incubation with Aβ. This shows that when SK-N-SH (ABAD-EGFP) cells are incubated with 2μM Aβ42 for 48h, ABAD is released into cytosol. There is no evidence of ABAD being released before 48hr indicating that the release of ABAD into the cytosol is time dependent.

These results may indicate that ABAD is released from the mitochondria late in the death of a cell, or these results may be due to the poor sensitivity of the antibodies used that may only detect high concentrations of the proteins in the cellular lysate. The live imaging experiments performed previously appeared to show ABAD-EGFP beginning to be released into the cytosol after 4hr incubation with 2μM Aβ42. This may indicate that ABAD-EGFP is released slowly from the mitochondria over a period of hours. This is supported by the western blots after 24hr and 48hr incubation with the Aβ42 peptide. It is therefore difficult to make a direct comparison of the results here, using these different techniques. Similarly the MTT assays may not be sensitive enough and the results could be masked by the cells dividing.

However, all the western blots show that Aβ42 peptide induces apoptosis in SK-N-SH (ABAD-EGFP) cells, shown by cytochrome C release from the mitochondria into the cytosol within 16hr. ABAD is seen in the cytosol after 48hr incubation with the Aβ peptide. From these results in SK-N-SH cells, ABAD does not appear to be mimicking the rapid release of cytochrome C into the cytosol and it is therefore not an early marker for apoptosis.

3.4.3 Investigation of apoptotic pathways induced in SK-N-SH (ABAD-EGFP) cells

3.4.3.1 Investigation of caspase inhibition of apoptosis

Further MTT assays were carried out with a pan-caspase inhibitor Boc D-fmk (Kamiya Biomedical Co.), to identify if the apoptotic pathway was caspase

mediated. Cells were incubated for 24hr in a 96 well tissue culture dish with the toxins Aβ or actinomycin D or the pan-caspase inhibitor (Figure 3.19).

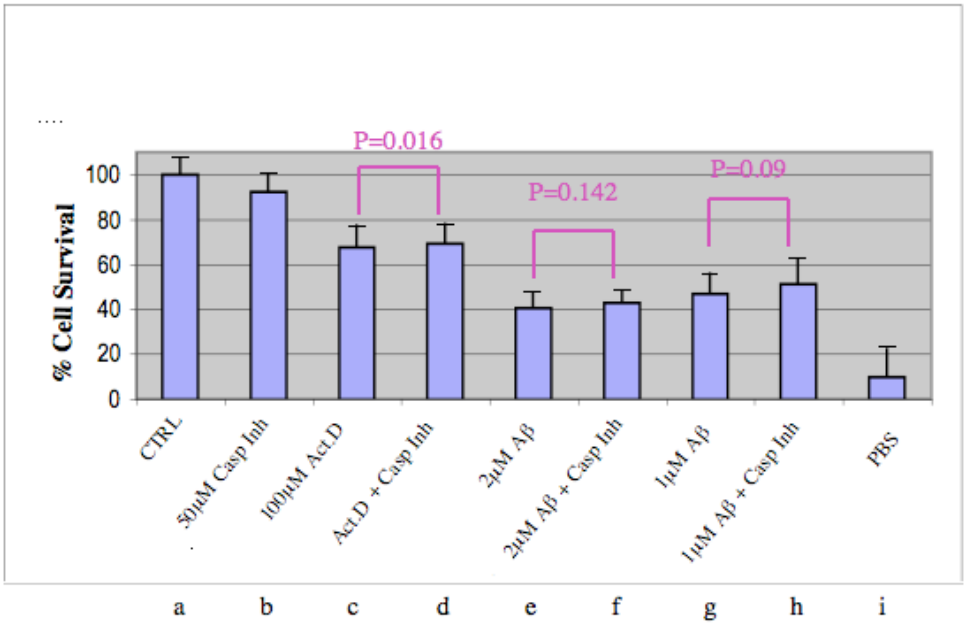

Fig. 3.19. Results of the MTT assay with actinomycin D or Aβ. SK-N-SH (ABAD-EGFP) cells were incubated for 24hr with toxins, without and with the pan caspase inhibitor Boc D-fmk. (a) Negative control (b) incubation with caspase inhibitor only (c) Incubation with 100μM actinomycin D shows reduced viability to 74%.(d) Incubation with 100μM actinomycin D and caspase inhibitor (e) Incubation with 2μM shows reduced viability to 62.5% (f) Incubation with 2μM Aβ and caspase inhibitor (g) Incubation with 1μM Aβ shows reduced viability to 71 % (h) Incubation with 1μM Aβ and caspase inhibitor (i) Positive control with 75% PBS. Readings are averaged from replicates of 7 and error bars show +1SD. The t test gave P values as shown.

These results show that the caspase inhibitor had a significant effect on toxicity caused by actinomycin D (p=0.016), but not on toxicity caused by the Aβ peptide (P=0.142 and P= 0.09). This would indicate that actinomycin D and Aβ induce

apoptosis by different pathways: actinomycin D activates the caspase pathway but Aβ does not.

3.4.3.2 Investigation of inhibition of apoptosis by the novel inhibitor TAT24

Further studies were carried out using the peptide inhibitor, TAT24. This was developed using the amino acid sequence 93-116 from ABAD fused to a TAT sequence from the HIV virus. The TAT sequence allows the peptide to enter the cell membrane (Lustbader *et al.*, 2004). Two MTT assays were carried out with this inhibitor peptide: 1) Cells were incubated for 24hr in a 96 well tissue culture dish with Aβ without or with TAT24; results are shown in Figure 3.20. and 2) Cells were incubated for 24hr in a 96 well tissue culture dish with actinomycin D without or with TAT24; results shown in Figure 3.21.

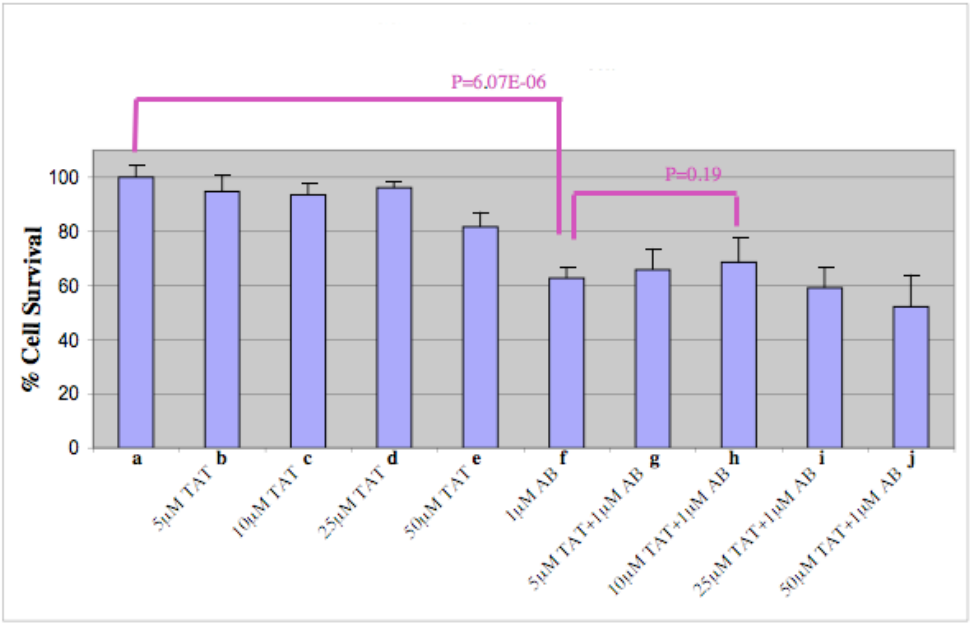

Fig. 3.20. Results of the MTT assay with 1μM Aβ. SK-N-SH (ABAD-EGFP) cells were incubated for 24hr with Aβ without or with the TAT24 peptide inhibitor. Lane (a) negative control. Lanes (b) to (e) show cells incubated with increasing concentrations of TAT24 peptide only. Lane (f) cells incubated with 1uM AB. Lanes (g) to (j) show cells

incubated with 1uM AB and with TAT24 inhibitor at increasing concentrations. Error bars show +1 SD. The t test gave P values as shown.

These results show that 1μM Aβ had a significant toxic effect on the SK-N-SH cells (lane f) but the TAT24 peptide inhibitor did not significantly inhibit the toxicity caused by the Aβ peptide (p=0.19). Figure 3.21 also shows that 50μM actinomycin D had a significant toxic effect on the SK-N-SH cells (lane f) but adding the TAT24 inhibitor had no significant change in the cell viability. Therefore from these initial experiments the TAT24 peptide inhibitor appears to be unable to inhibit Aβ toxicity on SK-N-SH (ABAD-EGFP) cells.

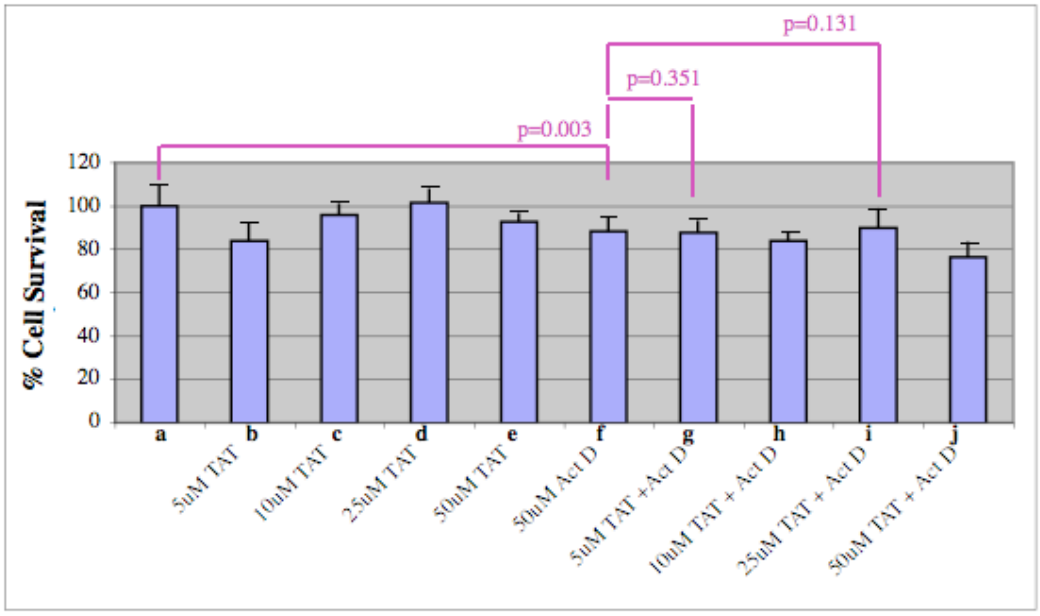

Fig. 3.21. Results of the MTT assay with 50μM actinomycin D. SK-N-SH (ABAD-EGFP) cells were incubated for 24hr with actinomycin D without or with the TAT24 peptide inhibitor. Lane (a) negative control. Lanes (b) to (e) show cells incubated with increasing concentrations of TAT24 peptide only. Lane (f) cells incubated with 50μM actinomycin D. Lanes (g) to (j) show cells incubated with 5050μM actinomycin D and with the TAT24 inhibitor at increasing concentrations. Error bars show +1 SD. The t test gave P values as shown.

3.5 Investigating the Aβ42 peptide

There were many problems duplicating many of these experiments, with inconsistent cell viability after toxic insult. The cause was unclear. It was possibly due to problems incubating with the Aβ peptide or a problem using the SK-N-SH cell line. To check growth conditions for the SK-N-SH cells, an experiment was performed changing the concentration of serum in the growth media, as it was proposed that the serum may be inhibiting the Aβ42 peptide toxicity. Comparison of cell viability was carried out using the MTT assay on the SK-N-SH (ABAD-EGFP) cells incubated with either Aβ42 or 500nM staurosporin or in concentrations from 1μM to 20μM, and lowering the serum concentration to 2% (from 5-10%) and lowering seeding cell density to $5x10^3$ cells per well (from $1x10^4$). Staurosporin was chosen as another inducer of apoptosis, as earlier results had indicated that Aβ and actinomycin D possibly induce apoptosis by different pathways. Staurosporin induces apoptosis by inhibiting protein kinases (Ruegg and Burgess, 1989). The results are shown in Figure 3.22 and indicate that the cell viability after incubation with Aβ42 peptide remained inconsistent and will require much more extensive investigation. Specifically, the results with staurosporin and serum free media were as expected with greatly reduced cell viability. From these results the change in growth conditions appeared to make little difference with the addition of the Aβ peptide. This was also shown by the inconsistency of the dose of Aβ required to causing cell death when compared to previous assays (Figures 3.12 and 3.14). Previously 2μM Aβ reduced viability to ~78%. Whilst in the current experiment 2μM Aβ reduced viability to ~ 81%. But >5μM Aβ was required to reduce cell viability to

~78% and 10μM reduced cell viability to 21%. 500nM staurosporin was adequate to show toxicity with cell viability below 15%. Cells incubated without serum showed viability reduced to ~20%.

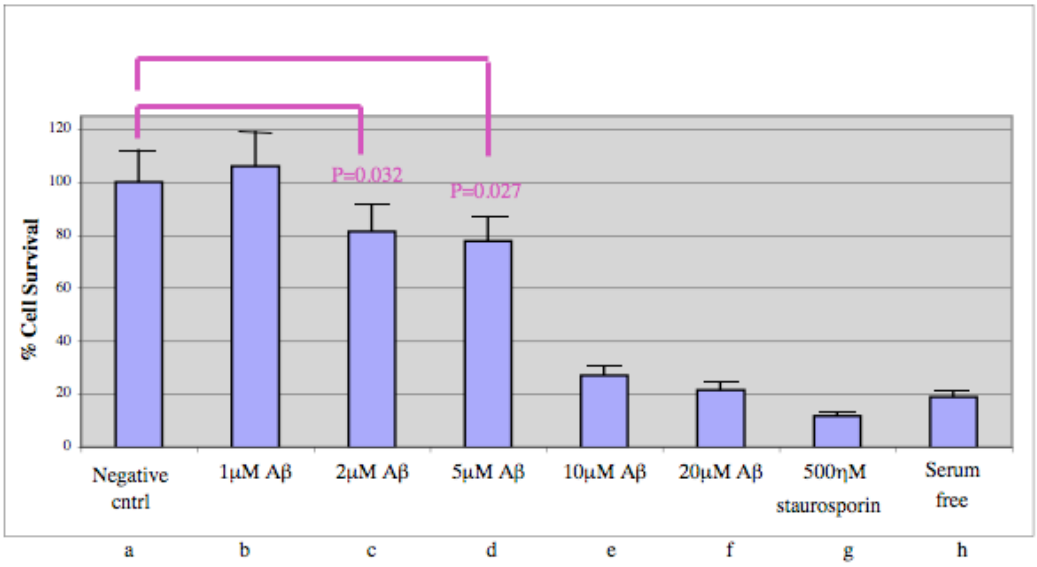

Fig. 3.22. Results of the MTT assay with staurosporin or Aβ. SK-N-SH (ABAD-EGFP) cells were cultured in reduced serum medium in a 96 well plate and the toxins added as shown. (a) Negative control, no toxins. (b) Incubation with 1μM Aβ. (c) Incubation with 2μM Aβ. (d) Incubation with 5μM Aβ. (e) Incubation with 10μM Aβ. (f) Incubation with 20μM Aβ. (g) Incubation with 500nM staurosporin. (h) incubation in serum free medium. Error bars show +1 SD. The t test gave p values as shown.

3.5.1 Investigating the oligomeric and fibrillar forms of the Aβ42 peptide

The experiments presented in this chapter aimed to assess the suitability of SK-N-SH cells and pre-incubated synthetic Aβ, as an *in vitro* model for AD. Reproducibility of results was difficult after extensive attempts to keep all conditions consistent. During this time, there had been some debate focussed on whether Aβ fibrils or soluble oligomers of Aβ were the toxic form causing neurodegeneration and dementia (Kayed *et al.*, 2003). Protocols have been

published for consistent production of stable oligomeric or fibrillar preparations of Aβ42 (Dahlgren *et al.*, 2002). In these protocols, it was reported that oligomeric Aβ peptide inhibited neuronal viability 10-fold more than fibrils and 40 fold more than non-aggregated peptide, with significant reduction in cell viability with 10nM Aβ42. A further publication reported that the formation of oligomers, fibrils, and fibrillar aggregates is determined by time, concentration, temperature, pH, ionic strength, and Aβ species. A complete study of Aβ, either *in vivo* or *in vitro*, requires an understanding of the conditions that drive peptide assembly toward one conformational state or another. Any change that affects the conformation of Aβ likely affects its biological activity (Stine *et al.*, 2003). Soluble oligomers of Aβ have been isolated from brain, plasma and cerebrospinal fluid of canines (Head *et al.*, 2010) and AD patients (Fukumoto *et al.*, 2010). Subsequently, it is now recognised that soluble intermediate oligomeric Aβ is a toxic form of the peptide before amyloid plaques are deposited in the brain.

3.5.2 Immunostaining of Aβ added topically to growth medium

Experiments were designed to further investigate the synthetic Aβ peptide used in the laboratory. The first experiment fixed SK-N-SH (ABAD-EGFP) cells after incubation with Aβ. Immunostaining of the Aβ peptide was carried out using 0.5μg ml^{-1} anti-Aβ monoclonal antibody (Upstate clone 4G8), which binds to the epitope between amino acid residues 18 and 22 followed by staining with Alexa 568 red fluorescent secondary antibody (Figure 3.23). This immunostaining of the Aβ peptide confirmed aggregation outside the cell after topical application to the growth media.

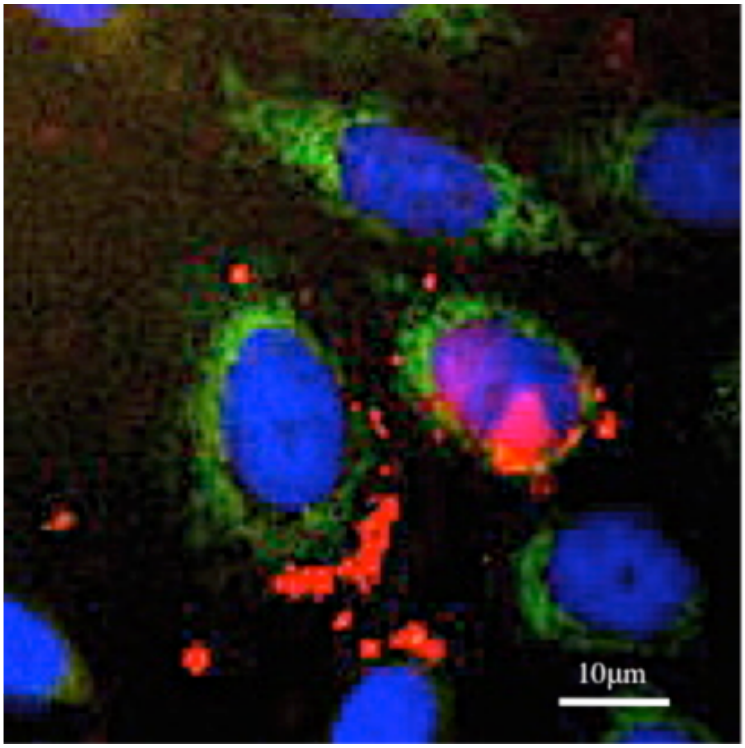

Fig. 3.23. SK-N-SH (ABAD-EGFP) cells incubated with Aβ peptide, fixed and stained. The Aβ peptide was immunostained with anti-Aβ primary antibody (Upstate clone 4G8), and Alexa 568 fluorescent secondary antibody. The nuclei are stained blue with DAPI. The red staining is consistent with aggregated peptide on the extracellular surface of the plasma membrane.

3.5.3 Electron microscopy of the Aβ peptide

Having identified the aggregated peptide by immunocytochemistry, some of the incubated peptide was examined by electron microscopy (Figure 3.24). A small sample of reconstituted Aβ peptide was examined by EM. The sample was pipetted onto a conductive screen and stained with uranyl acetate. The EM images confirmed the presence of multiple aggregated fibrils in the incubated peptide used in the experiments. Experimentally, it was impossible to control the amount of fibrillar Aβ produced during incubation of the peptide. It is possible that when there was more fibrillar peptide formed, the soluble and toxic monomeric form

was reduced. This then required an overall higher concentration of the Aβ peptide to attain the same level of toxicity in the cell viability assays

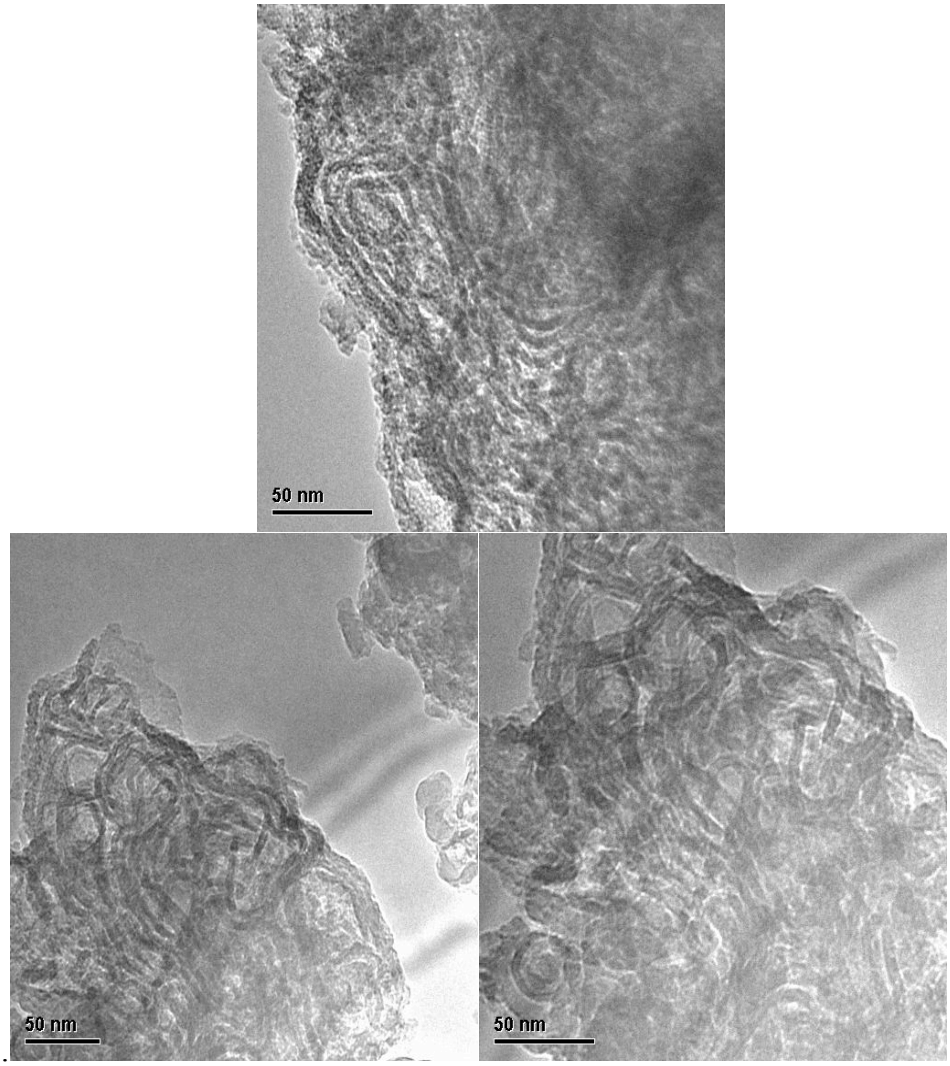

Fig. 3.24. Electron microscope images of synthetic Aβ. All the EM images show multiple tangled fibrillar structures. This suggested the Aβ peptide was mainly aggregated and fibrillar.

3.5.4 Introducing Aβ to cells using a carrier peptide - Chariot™(Actif Motif)

Because the direct addition of the synthetic peptide to the growth medium was

causing the peptide to aggregate outside the cell, another method of introducing the Aβ peptide to the inside of the cell was tried using a carrier peptide. The Active Motif Chariot™ system was used (section 2.2.8). This system uses a carrier peptide to bind to a peptide or protein and carry it through the cell membrane by permeabolisation and deposit it within the cytosol, where it is then released from the carrier peptide. The cells were incubated with the Aβ peptide together with the carrier peptide for up to 8hr (as per manufacturer's instructions), then fixed, immunostained and analysed under fluorescent microscopy (Figure 3.25).

The Chariot carrier peptide is able to introduce the Aβ peptide into the cells within four hours, which then show signs of severe toxicity. The Chariot carrier peptide is a good method to introduce the Aβ peptide into cells for toxicity studies.

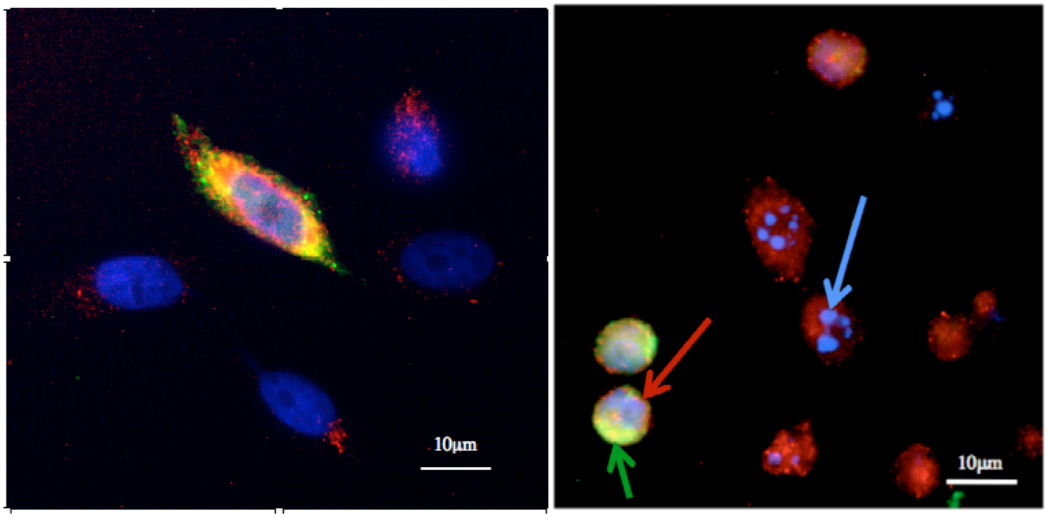

1 **2**

Fig. 3.25. SK-N-SH cells transiently transfected with MTS-ABAD-EGFP. After incubation for 16hr, the cells were then incubated further.

Image 1. As a negative control, cells were incubated for 4 hr with the chariot carrier peptide only. The nuclei stained blue with DAPI show a healthy morphology. The cell expressing ABAD-EGFP is also normal in shape. There is some red staining in all the cells which may be due to non- specific antibody binding or some endogenously expressed Aβ within the cells. However no significant toxicity was seen.

Image 2. Cells incubated for 4 hr with synthetic Aβ peptide using the Active Motif Chariot carrier peptide.

The cells were fixed and immunostained with 0.5µg ml^{-1} anti-Aβ monoclonal antibody (Upstate clone 4G8), and Alexa 568 red fluorescent secondary antibody, and the nuclei stained with DAPI. This clearly shows the toxic effect on the cells after 4 hr incubation with Aβ peptide. The cells are shrunken and have no clear outline. The Aβ is seen within the cell, stained red, surrounding the nucleus that is stained blue. The nuclei show DNA fragmentation consistent with the formation of apoptotic bodies (blue arrow). Only two of the cells, on the left in image 2, are expressing ABAD-EGFP. There are two or three small areas of yellow indicating co-localisation of ABAD with Aβ (green arrow). In these cells there are discrete red spots which look like a perinuclear red stained ring (red arrow).

3.5.5. Transfection with $mAPP_{swe}$ plasmid

Another method used to try and overcome the problem of the aggregated Aβ peptide, was to transfect SK-N-SH cells with a mutant APP plasmid ($mAPP_{swe}$). This plasmid comprises a mammalian Cre/Lox vector which expresses $mAPP_{swe}$, with a double mutation K670N/M671L, which after translation produces excess Aβ peptide within the cell (Thinakaran *et al.*, 1996). The cells were transfected with 1μg of plasmid DNA and incubated for 18 hr before being fixed and immunostained for Aβ peptide as before with anti-Aβ primary antibody (Upstate clone 4G8), and Alexa 568 fluorescent secondary antibody, and then imaged using fluorescent microscopy (Figure 3.26).

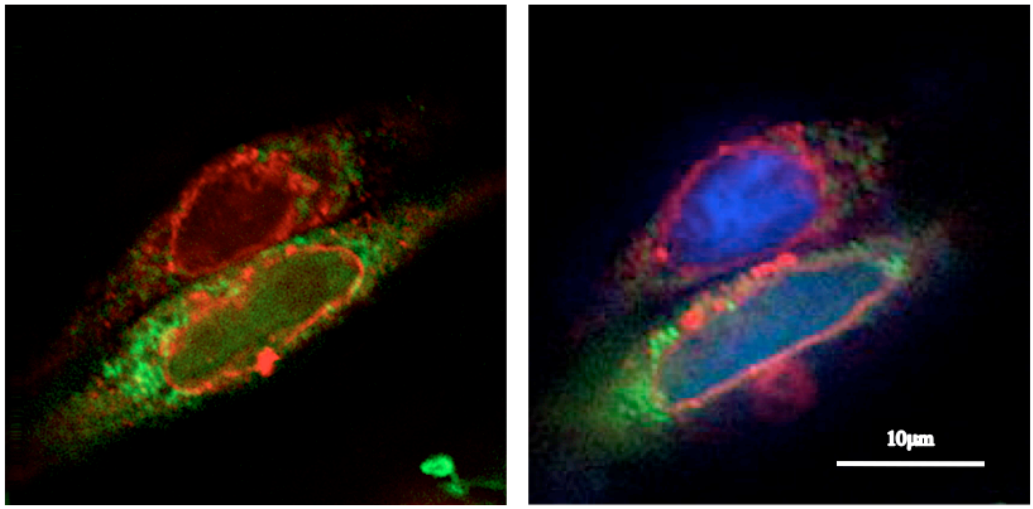

Fig. 3.26. Two example images of SK-N-SH (ABAD-EGFP) cells transfected with mutant APP and incubated for 18 hr before fixing and staining. The Aβ peptide was immunostained with anti-Aβ primary antibody (Upstate clone 4G8), and Alexa 568 fluorescent secondary antibody. The cells on the right have blue DAPI staining of nuclei. The ABAD-EGFP is seen expressed green in the mitochondria. There is a clear red perinuclear ring in all cells, indicating localisation of Aβ around the nucleus. There is no obvious co-localisation of ABAD with Aβ.

The cells transfected with mAPP and incubated for 18hr showed no sign of apoptosis with the nuclei clearly seen, indicating that these cells appear quite healthy. Further experiments were conducted, transfecting cells and incubating for 48hr before fixing, to see if a longer incubation was required for co-localisation of ABAD and Aβ and to induce apoptosis (Figure 3.27).

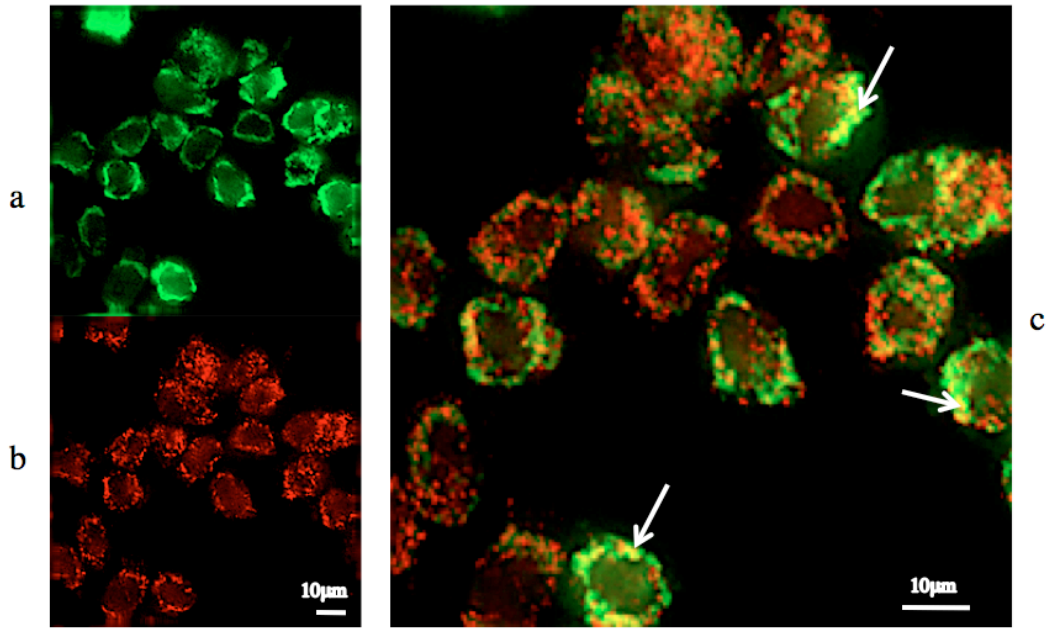

Fig. 3.27. SK-N-SH cells transfected with mutant APP and incubated for 48hr before fixing and staining. (a) cells imaged with FITC filter (ex. 490nm. em. 528nm.). (b) cells imaged with red filter (ex. 555nm. em. 617nm.). (c) converged image. This shows cellular toxicity with shrunken and misshapen cell outlines and little or no integrity of the mitochondria. The red stained Aβ peptide appears to be located as discrete spots within the cell and possibly still in a perinuclear ring. The Aβ is not completely colocalised with the mitochondria as there are clear green areas. However there is some evidence of localised colocalisation marked with arrows. The nuclei were not stained with DAPI in this experiment.

Transfection with mAPP for 48hrs shows a strong toxic effect on the cells but with only limited co-localisation seen of Aβ peptide with ABAD-EGFP. The

$mAPP_{swe}$ plasmid is also a good method to introduce Aβ into the cell by translation of the mAPP gene followed by cleavage to produce the peptide.

A perinuclear collection of Aβ has been reported before (Georgopoulou *et al.*, 2001). That study reported alteration in the glycosylation state of APP resulting in a decrease in the secretion of the neuroprotective, soluble form of the protein and a parallel increase in the deposition of the cellular protein within the perinuclear region of the cell. APP is also reported to be found in endosomes in a perinuclear pattern and introduction of copper compounds promotes trafficking of APP to the cell surface (Acevedo *et al.*, 2011). It is also reported that Aβ accumulates with SOD1 and aggregates in the perinuclear region (Yoon *et al.*, 2009). SOD1 is a key antioxidant enzyme, one of the major targets for oxidative damage in the brains of patients suffering from Alzheimers disease (AD). It is possible that these images are showing one or more of these conditions. Binding to SOD1 could be evidence that these experiments are simultaneously showing another intracellular interaction in this *in vitro* AD model.

3.5.6 MTT assays using soluble oligomeric Aβ

Some soluble oligomeric Aβ was obtained (by kind donation from Aynun Begum Dept Medicine UCLA) from the laboratory where the original oligomers were produced (Kayed and Glabe, 2006). There was only enough to try some limited MTT assay experiments, to verify toxicity with the soluble oligomeric Aβ peptide compared with the synthetic peptide previously used. Some inhibitory studies were also carried out using the inhibitory peptide TAT24 (amino acid residues

corresponding to residues 93-116 of the ABAD sequence), labelled as 'TAT' in Figure 3.28.

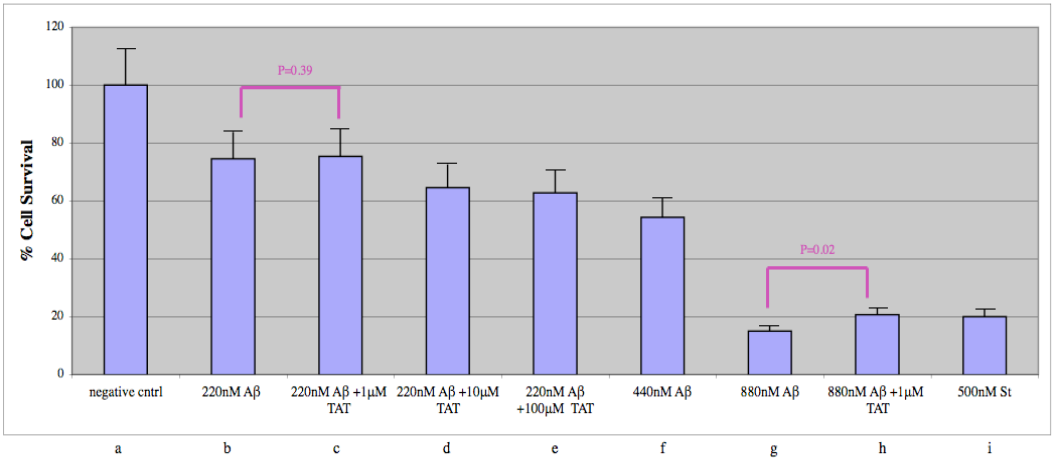

Fig. 3.28. Results of the MTT assay with oligomeric Aβ +/- inhibitor TAT24. SK-N-SH (ABAD-EGFP) cells were cultured as shown. (a): negative control. No toxins. (b) 220nM soluble Aβ. (c) 220nM soluble Aβ with 1uM inhibitor. (d) 220nM soluble Aβ with 10uM inhibitor. (e) 220nM soluble Aβ with 100uM inhibitor. (f) 440nM soluble Aβ. (g) 880nM soluble Aβ. (h) 880nM soluble Aβ with 1uM inhibitor. (i) 500nM staurosporin. The t test gave Pvalues as shown.

These results show that the soluble peptide proved to be much more toxic than the peptide used previously; 50% viability with 440nM (lane f). The concentration was 10x lower than the synthetic peptide used before and similar to physiological concentrations. Endogenous Aβ is <100nM where its production or breakdown is modified (Pearson and Peers 2006). Interestingly the TAT24 peptide inhibitor showed significant inhibition at 1μM with 880 nM oligomeric Aβ peptide (lanes g and h. P= 0.02). However 1uM showed no significant inhibition with 220nM Aβ (lanes b and c. P=0.39). Also the data showed that the addition of 10uM and 100uM of the TAT inhibitor with 220 nM Aβ increased the toxicity to the cells,

(lanes d and e). A very limited supply of the soluble oligomeric Aβ allowed only this one experiment and not all the variables of Aβ concentrations with TAT24 concentrations could be tested. The TAT24 inhibitor was tested with the lowest and highest Aβ concentrations, ie 220nM and 880nM Aβ.

3.6 Primary neurons from murine embryonic cells

Experiments with primary neurons was not possible due to problems with availability of mice. However in collaboration with Dr C. Connolly, university of Dundee, we provided the plasmids ABAD-EGFP and pDsRedmito2 to be transfected into their primary cell cultures. Once transfected the cells were incubated for 18hr then fixed. The cells showed ABAD-EGFP co-localised with pDsRedmito2 in discreet areas along the axons and around the nucleus in the cell body (Figure 3.29).

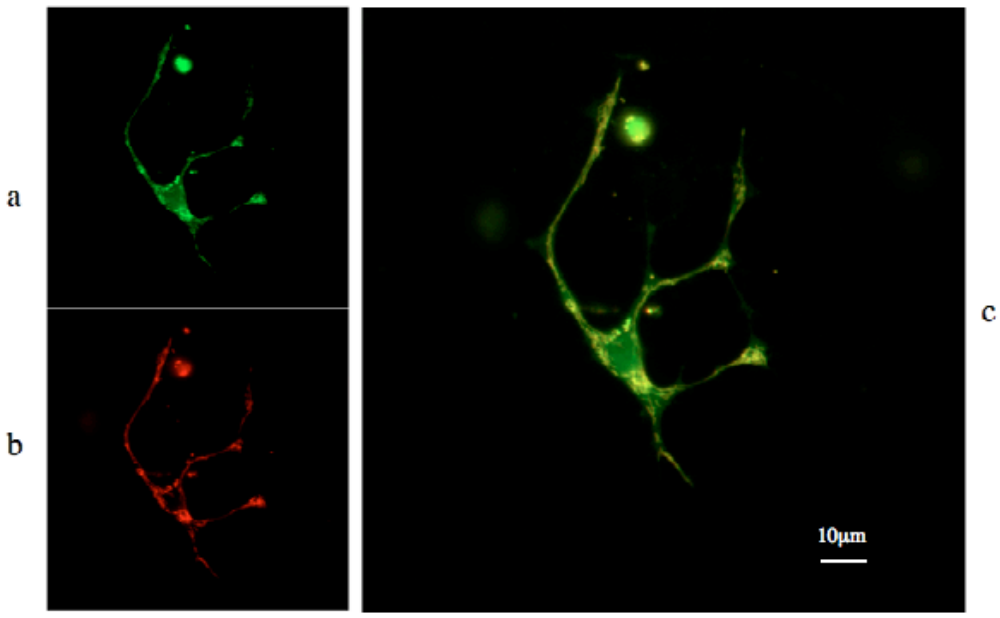

Fig. 3.29. Primary cortical cells co-transfected with ABAD-EGFP and with pDsRedmito2. (a) cells imaged with green FITC filter (ex. 490nm. em. 528nm.) (b) cells imaged with red filter (ex. 555nm. em. 617nm.). (c) converged image. These cells show ABAD-EGFP colocalised with pDsRedmito2 in discreet areas along the axons and around the nucleus in the cell body

3.7 Culture of multipotent neurospheres from murine neuronal stem cells

To obtain a primary cell system that would reduce the number of mice required and would provide cell cultures that could last for six to eight weeks, a system was established to grow neurospheres from murine neuronal stem cells (see section 2.2.3 for protocol). This work was carried out in the laboratory of Professor Alessandra D'Azzo, St Jude Children's Hospital, Memphis.

From two mouse pups (p3-p6), a supply of neurospheres was cultured for 6-8 weeks in serum free medium. When required, neurospheres were differentiated into the three primary phenotypes, astrocytes, oligodendrocytes and neurons, by removing epidermal growth factor (EGF) from the growth media and adding a low concentration of serum (Figure 3.30).

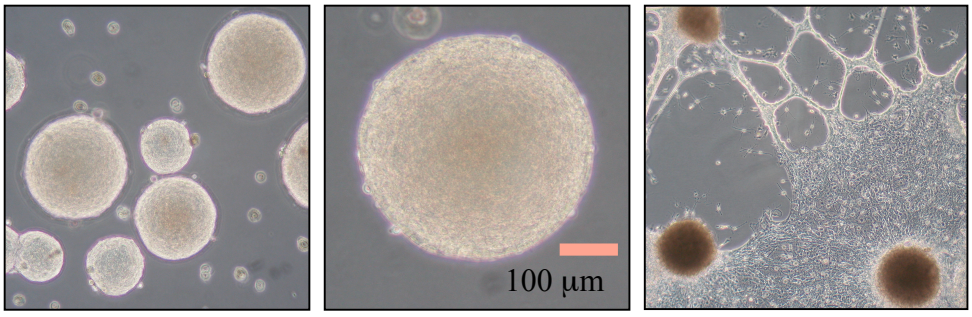

a b c

Fig. 3.30. Phase Contrast microscope images of neurospheres from murine neural stem cells. (a) Proliferating neurospheres in suspension, six days in culture. (b) Isolated neurosphere, containing approximately 10,000 cells. (c) Adherent cells differentiating 48hr after removal of EGF and addition of serum.

3.7.1 Immunostaining neurospheres

It is possible to stain neurospheres before differentiation. They can be fixed and stained with different neuronal markers and the different neuronal cells can be identified. Figure 3.31 shows an example of neurospheres that have been stained to identify glial cells and neurons.

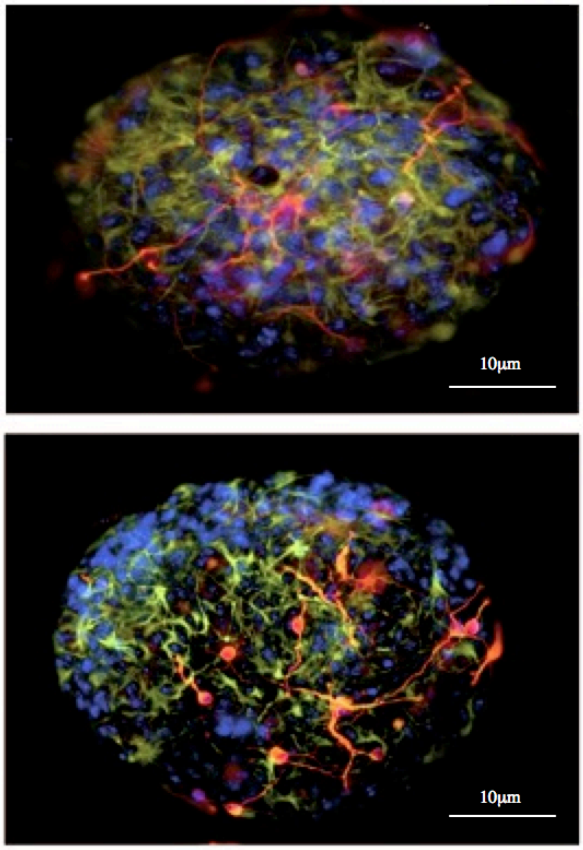

Fig 3.31. An example of stained neurospheres, taken from (Tessitore *et al.*, 2004). A. Neurosphere from a wild type mouse and B. Neurosphere from a transgenic mouse. mouse. The cells have been immunostained with antibody markers for astrocytes, anti-GFAP polyclonal antibody (Immunon) (Glial fibrillary acidic protein-GFAP) green, and neurons, anti-β III-tubulin monoclonal antibody (Covance) (β-III tubilin) red. Nuclei Hoechst stain blue.

For the purpose of establishing a reliable cytotoxic system to investigate ABAD and Aβ, by culturing neurospheres, some immunostaining experiments were performed with differentiated neurospheres cultured from wild type (WT) and mAPP mice. The neurospheres were cultured then processed into a single cell

suspension and differentiated for three days by withdrawal of EGF (section 2.2.3). The cells were then fixed and permeabilised and stained with 0.5µg anti-ABAD primary polyclonal antibody (Pierce) for endogenous expression of ABAD (Figure 3.32).

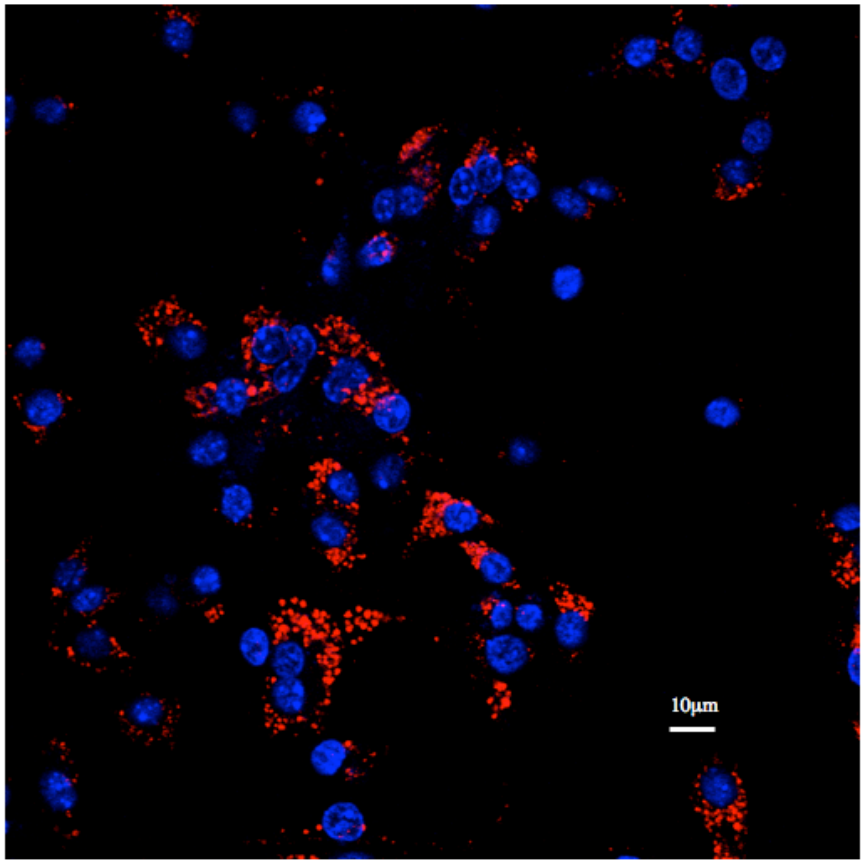

Fig. 3.32. Endogenous expressed ABAD in WT murine neurospheres, differentiated for three days then fixed and immunostained with anti-ABAD primary polyclonal antibody (Pierce) and Alexa 568 fluorescent secondary antibody (red).

Having identified ABAD endogenously expressed in the differentiated cells, the experiment was repeated, staining also for the mitochondrial translocase protein TOM40 using anti-TOM40 (Santa Cruz Biotech.). Figure 3.33 indicates that co-localisation of the two mitochondrial proteins was clearly seen.

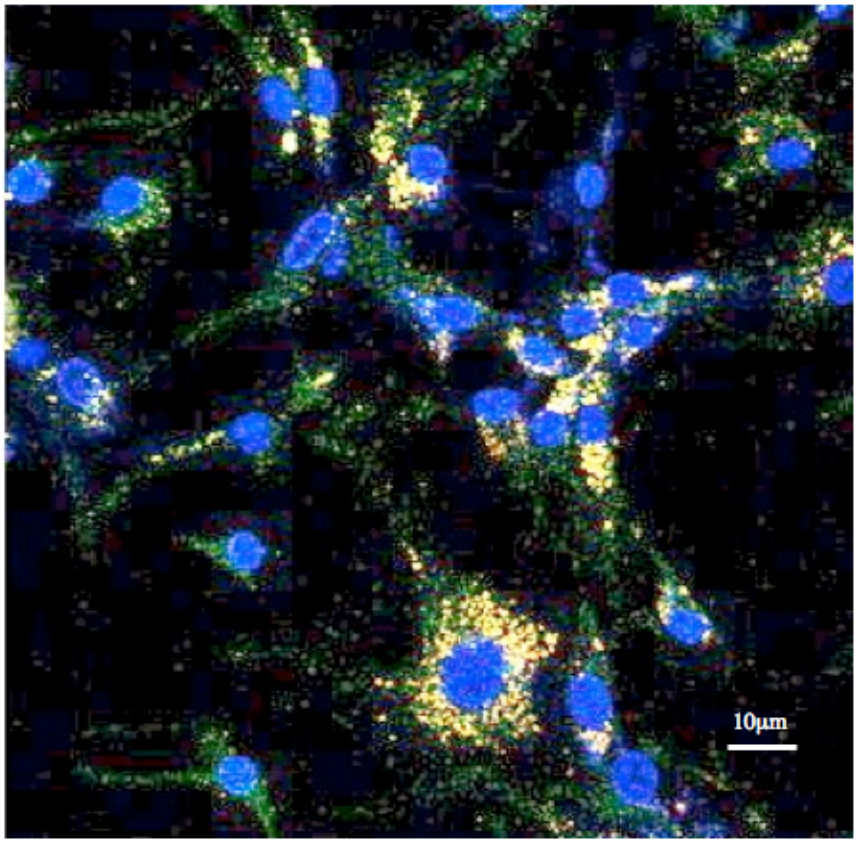

Fig. 3.33. Immunostaining showing co-localisation of endogenous expressed ABAD stained red and TOM40, stained green.

Double immunostaining was done with an anti APP polyclonal antibody specific for APP770 and an anti-ABAD polyclonal antibody, for another experiment with cells cultured from a Tg mAPP mouse. Figure 3.34 shows that these cells show APP stained green, spread throughout the cytosol and ABAD stained red, shown by co-localisation with the APP as discreet yellow spots in the cytosol (orange arrow).

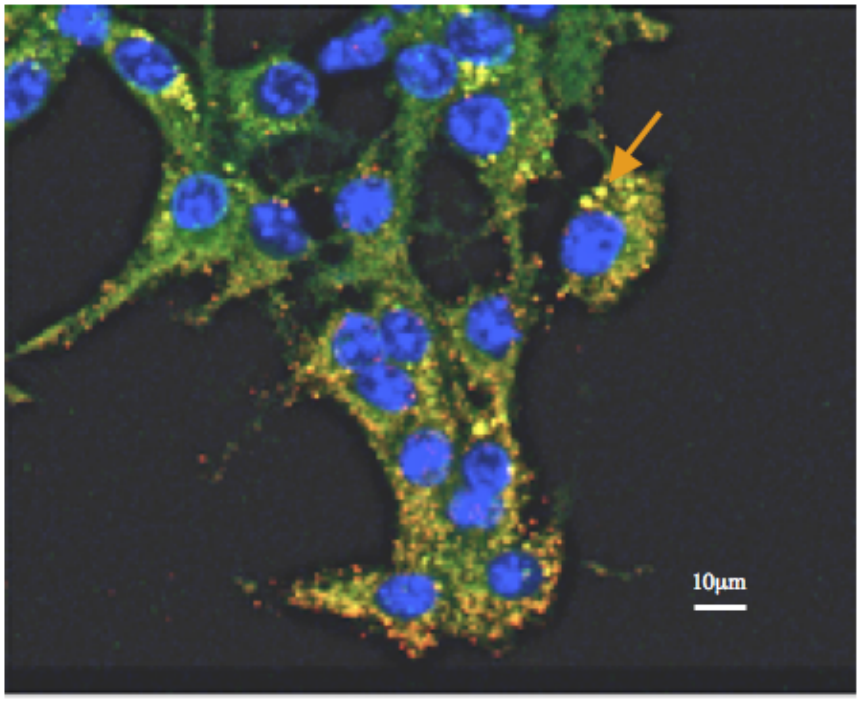

Fig. 3.34. Differentiated neurospheres from Tg mAPP mouse. DAPI stained nuclei. APP stained green. Some yellow co-localisation seen (orange arrow) with ABAD stained red.

These preliminary experiments indicated that this system appears to be robust and worth developing further. The neurospheres can be transfected and differentiated into different neuronal phenotypes and comparisons can be made between wild type and different transgenic mouse models.

3.8 Discussion

From these experiments it was possible to confirm that ABAD is expressed in the mitochondria of SK-N-SH cells but may be translocated to the ER. Figure 3.6 shows some co-localisation of ABAD-EGFP with ER-Red. Recent publications, now report ABAD interacting with Aβ in the mitochondria (Lustbader *et al.*, 2004; Yan and Stern, 2005; Yao *et al.*, 2011) supporting these *in vitro* studies.

For further *in vitro* studies, a cellular AD model was produced by transfecting a plasmid expressing ABAD-EGFP into SK-N-SH cells and developing a stably expressing cell line. Another construct was developed with a mitochondrial targeting sequence for transient transfections to express the fusion protein MTS-ABAD-EGFP. This provided the capability of allowing rapid transient transfections of cells and was subsequently used as a template for other cellular studies in the laboratory requiring ABAD expression, e.g. using FRET to analyse possible binding partners for ABAD within the cell.

SK-N-SH cells were chosen based on previous experiments where they had been used to study ABAD, to confirm cellular localisation and effects of toxicity when incubated with Aβ (Yan *et al.*, 1997a; Yan *et al.*, 1999). This cell line was also well characterised for neuronal cytotoxic studies. However, several studies identified this cell line as having a protective effect against some toxic insults, shown to be toxic to other cell types and some studies were not able to reproduce apoptosis with the addition of Aβ ((Ba *et al.*, 2003). This poses the question, is this the best cell line to use for investigating AD. During the period of this research, another group developed and published a system to provide a reliable cytotoxic and neuroprotective screen for AD using SK-N-SH cells (Ba *et al.*, 2003). They used four cytotoxic insults: the Aβ peptide, 1-methyl-4-phenyl-1.2.3.6-tetrahydropyridine (MPTP), high cell density culture and serum deprivation. SK-N-SH cells were incubated with the toxins for 96hr. The ability of all toxic insults to induce apoptosis was tested and all induced apoptosis except the Aβ peptide. However several protein kinase inhibitors were then trialled to provide information on the cell death pathways activated under these conditions.

The p38 MAP kinase inhibitor, SB203580 (1 μM), and the PKC inhibitor, chelerythrine (5 μM) successfully inhibited the loss in viability caused by Aβ and the high density culture, respectively but not the other toxins. This would indicate that the cell toxicity caused by Aβ was due to apoptosis. The results were confusing, indicating that the cytotoxic models used may each have its unique cytotoxic pathway. Ba et al incubated the cells for 96 hours whereas in the experiments for this thesis, possible toxic effects were seen as early as 4-11hr, using fluorescent microscopy. However MTT assays and western blots needed 24 – 48hr to show significant changes. These results indicate that it is important to identify the most sensitive assay, but also it is necessary to compare the effects on different neuronal cell lines to identify the cellular pathways involved in the cytotoxic events. It may be necessary for further in vitro experiments to incubate cells for much longer, up to 96hr (Ba *et al.*, 2003).

In these experiments, toxicity has been shown in the SK-N-SH (ABAD-EGFP) cell line using the synthetic Aβ42 peptide. However, doses required to produce a toxic effect were inconsistent and generally high concentrations were required. Generally 1- 2μM Aβ42 was needed to show a significant change in the cells, but in some experiments this needed to be increased to 5-10μM Aβ42, whilst it is interesting to note that physiological concentrations are in the region of 20nM (Yan *et al.*, 1997a). It was difficult to show consistent and reliable cytotoxic results, and this seem to stem from the fact that there was a problem with the consistency of the Aβ42 peptide used, despite extensive trials. EM studies did show that the Aβ42 peptide used in most of the experiments did develop into

fibrils. At the time that these experiments were being performed, it was being reported that it was probably the soluble prefibrillar Aβ that was toxic (Glabe, 2005). A limited supply of the soluble oligomeric form of Aβ was provided and this did give more consistent results at a much lower concentrations. In the future, a good consistent supply of the soluble oligomeric form would allow more reliable experiments and give more consistent results.

Fluorescent immunostaining was able to confirm Aβ aggregation on the exterior of the cell surface with no evidence of toxicity. Another two methods were used to introduce the same Aβ peptide within the cell. First using a carrier peptide to permeate the cell membrane and transfer the synthetic peptide from the growth medium into the cell. Second a plasmid expressing a mutant form of APP that produces excess Aβ peptide was transfected into the cells. Both of these methods showed greater toxicity than by topical application of Aβ alone. The experiments indicated that when the Aβ peptide is in closer proximity with intracellular ABAD a strong toxic effect is seen. These two methods were more reliable at introducing Aβ into the cell by two distinct and different methods, direct import and transcription, translation of the mAPP gene followed by proteolytic cleavage.

In summary, SK-N-SH proved a useful cell line to investigate some aspects of toxicity but it may not be the cell line of choice to show apoptosis. SK-N-SH cells are consistent with a neuronal phenotype (Ba *et al.*, 2003). However, SK-N-SH cells have few glutamate receptors, and there is evidence that SK-N-SH cells resist toxic insults due to lack of NMDA receptors (Pizzi *et al.*, 2002). This could

be overcome by differentiation of SK-N-SH cells by retinoic acid that may provide a better model as they produce functional NR1 and NR2B-type NMDA receptors. Other factors that affected cell growth and behaviour were cell density and growth medium conditions. Seeding cell density was critical to cell growth and survival. An average of 10-15 x 10^3 cells cm^{-2} was optimum. Different batches of serum in the growth medium also affected results. Sometimes a difference of 2% to 10% serum was required to obtain comparable results. It was possible, however, to monitor the location of ABAD in living cells and the toxic effect of Aβ over several hours.

Three techniques were used to compare the results of intracellular Aβ; fluorescent microscopy, MTT assays of whole cell tissue cultures followed by western blots of cellular fractionation to isolate the mitochondria. Fluorescent microscopy shows a toxic effect on cells transfected with ABAD within 11hrs. However, western blot analysis of ABAD released from the mitochondria to the cytosol occurs at a later stage of cell death (approximately 48hr), unlike cytochrome C that is released within 4-6hrs. This indicates that ABAD is probably not a useful early marker for apoptosis and responds differently to cytochrome C. The early release of cytochrome C indicates that Aβ induces apoptosis in this cell line. This disagrees with the results shown using SK-N-SH cell alone, where they could not show apoptosis (Ba *et al.*, 2003). This would indicate that ABAD has a crucial role in inducing apoptosis in SK-N-SH cells. Further investigation using the oligomeric Aβ peptide would provide a more reliable toxic Aβ source.

Producing a primary murine embryonic cell culture was possible but it was time

consuming and relied on good breeding of the laboratory mice. This proved to be a problem on several occasions. The transfections of the primary cells were improved by use of the Amaxa nucleofection system, but contamination of the cells and the necessity to complete an experiment within a week made this an unreliable system to use. Therefore, development of the murine neurosphere cell culture system could be a way forward as it can be easily set up in a tissue culture laboratory with minimal animal usage. It is also cost efficient, reliable and robust system and would be a useful system to adopt. The cells can be cultured in suspension for 6-8 weeks minimum and have little or no problems with contamination. For experiments they can be differentiated into the three main neuronal cell phenotypes and can be grown as monolayers for fixing and staining.

Chapter 4

Proteomic analysis of brain tissue from novel transgenic mouse models for Alzheimer's disease.

4.1 Background and aims

The original amyloid cascade hypothesis states that neurodegeneration begins with abnormal processing of APP and results in extracellular Aβ deposition (Hardy and Higgins, 1992). The original neuronal cytoskeleton degeneration hypothesis, led by tau expression, states that cytoskeletal changes lead to neurofibrillary tangle formation, leading to the neuronal changes seen in AD (Neve and Robakis, 1998). These two original hypotheses still cause debate about the cellular changes occurring before or at the time of onset of the disease. Knowledge of the changes in protein expression and post-translational modification *in vivo,* may lead to identifying biomarkers to aid in the diagnosis but also in following the progression of AD. The proteins that are identified may also provide good targets for drug development to aid the treatment of this disease.

Proteomics is now widely used to investigate proteins involved in neurodegenerative disorders (Korolainen *et al.*, 2010), and the application of proteomics to AD research was first published in 2001/2002 (Butterfield, 2002; Butterfield *et al.*, 2003; Schonberger *et al.*, 2001). Proteomics is the analysis of an organism's complete complement of proteins, often repeated under different conditions, e.g. a normal cell versus a disease affected cell, in order to identify

changes in protein expression in these different conditions. For analysis, proteins are usually identified by their separation by two-dimensional (2D) gel electrophoresis that separates on the basis of mass and charge differences. The proteins of interest are cut from the gel and digested by trypsin, followed by a choice of methods to identify the peptides and computer database analysis to identify the proteins. For the study reported here, the determination of the molecular mass of the resulting peptides was made by matrix-assisted laser desorption/ionization time-of-flight (MALDI-TOF) mass spectrometry and then database searching to identify the protein.

For this thesis, the aim was to investigate changes in protein expression *in vivo*, from the mouse brain of novel AD models. Proteomic analysis of brain tissue from novel transgenic mice, developed to increase neuronal expression of ABAD and/or mAPP (mutant amyloid precursor protein), was carried out in order to investigate the effect of this over-expression on other proteins in the central nervous system (CNS).

Preliminary proteomic studies had been carried out using mice aged between 8 and 12 months, as an age match for middle to late stage AD, by Dr Jim Aiton (Senior Lecturer in School of Medicine, University of St Andrews) while affiliated with Dr Gunn-Moore's research group. The protein expression in mouse brain was investigated by comparing protein profiles between control (wild type - WT) and transgenic (Tg) mice. 2D gel electrophoresis was used to separate the proteins and MALDI-TOF mass spectrometry was used to identify the proteins. Any novel proteins that were found to be up-regulated in the transgenic

models when compared to WT, were followed up by further western blot analysis on 4-8 month old mice. This was carried out to try and confirm these changes in expression and also identify how early the changes in protein expression could be detected. For the initial experiments, whole brain tissue samples were used.

The progression of AD pathology affects different areas of the brain (Braak and Braak, 1991). However some studies have shown that protein changes in human AD brain were not specific to regions of severe degeneration (Schonberger *et al.*, 2001). For this thesis further experiments analysed the proteins expressed in the hippocampus and the cortex of 4-8 month mice. Further detailed analysis was attempted by pre-fractionation of the samples to isolate just the mitochondria, where ABAD is expressed. This was performed to remove other cellular proteins, common to all samples, hoping to allow better identification of mitochondrial proteins, and so provide useful information on other expression changing mitochondrial proteins and potentially identify those involved with mitochondrial dysfunction.

4.2 Protein expression *in vivo* using novel AD transgenic mouse models

Mice have been used as animal models in research for over one hundred years due to the ease with which they can be kept in laboratory conditions. They can reproduce rapidly, are easy and inexpensive to handle, have short life-spans and can be genetically manipulated. Transgenic mice were developed in the 1980's by introducing specific genes into the oocytes of mice and then continued by

selective breeding. This allowed genetic animal models to be produced for research into specific diseases. Due to their rapid rate of reproduction, effects of specific diseases can be monitored over a life-time of the animal (Duyckaerts *et al.*, 2008). As discussed in section 1.10, human and mouse brains are very similar in gene expression and brain structure (Strand *et al.*, 2007).

Several genetically modified mice have been bred as models for AD, each suitable for examining different AD phenotypes. The following are five genes that have been associated with the disease: amyloid precursor protein (APP), presenilin 1 (PS1), presenilin 2 (PS2), apolipoprotein allele 4 (ApoE4), and the tau protein. Several double transgenic mice have also been bred to express a combination of two of these proteins. More recently, a triple transgenic model has been bred, PS1(M146V), APP(Swe), and tau(P301L) (Oddo *et al.*, 2003). This model exhibits Aβ plaques by 6 months of age as well as neurofibrillary tangles by 10-12 months of age, and therefore shows both AD phenotypes in one model.

For this study, three transgenic models were used: a transgenic mutant APP (Tg mAPP) where mice produce an excess of the Aβ peptide, and two novel transgenic mice that were developed as models for AD by our collaborators at Columbia university, New York, USA (Lustbader *et al.*, 2004; Takuma *et al.*, 2005b). These models either over-express ABAD (Tg ABAD), or over-express ABAD in an Aβ rich environment (2 x Tg mAPP/ABAD). The models expressing ABAD were produced with neuronal-targeted expression of ABAD generated under the control of the PDGF-B chain promoter (Lustbader *et al.*, 2004; Takuma *et al.*, 2005b). An existing transgenic mouse strain was provided

by Dr Mucke (University of California), expressing a mutant form of human amyloid precursor protein, a minigene encoding hAPP695, 751 and hAPP770 bearing V717/F, K670M, N671L mutations: Tg mAPP mice, J-20 line (Mucke *et al.*, 2000). Tg ABAD mice were also crossed with Tg mAPP mice to produce double transgenics (2xTg mAPP/ABAD). Transgenic mice in this study were on the C57BL/6 background (Lustbader *et al.*, 2004; Takuma *et al.*, 2005c; Yan *et al.*, 2000a; Yao *et al.*, 2007).

The double transgenic mice express high levels of ABAD and produce high concentrations of Aβ peptide (Lustbader *et al.*, 2004). Neurons from the double transgenic mice show evidence of free radical-induced stress. In the radial arm water maze test they demonstrate accelerated decline in spatial learning/memory (Bliss and Collingridge, 1993; Morgan *et al.*, 2000) compared to non-transgenic littermates. This was evident from 5 months of age (Lustbader *et al.*, 2004). Pathological changes include generation of super-oxide anion and hydrogen peroxide in response to leakage of reactive oxygen species from the mitochondria (Takuma *et al.*, 2005c; Yan and Stern, 2005). Using these novel transgenic animals, changes in protein expression in the mouse brain were analysed for these three transgenic models against controls (WT) non-transgenic littermates.

4.3 Mouse brain protein identification by 2D gel electrophoresis from mature (8-12 months) transgenic AD models.

Previous studies had already shown that ABAD and Aβ were over-expressed in these transgenic mice, and evidence of their co-localisation is shown in Figure 4.1 taken from (Lustbader *et al.*, 2004). In this chapter, preliminary proteomic studies

were carried out using transgenic mice aged between 8 and 12 months old, age matched as a useful model to examine the middle to late stages of dementia in Alzheimer's disease (Clancy *et al.*, 2001; Finlay and Darlington, 1995; Finlay *et al.*, 2001). More recent work has characterized gene expression and transcriptional changes in different tissues, as a function of age in mice (Zahn *et al.*, 2007) providing a more accurate time line for protein expression and indicating the importance of age matching when comparing protein expression in tissues.

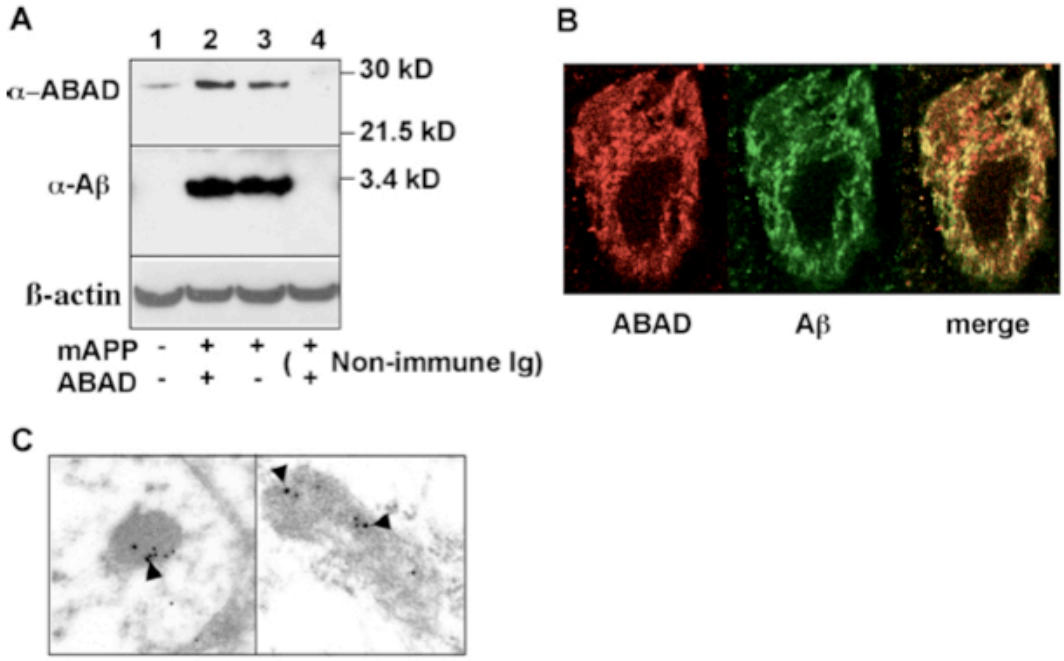

Fig. 4.1. Demonstration of ABAD-Aβ complex in brains of Tg mAPP/ABAD mice. (A) Western blot analysis of co-immunoprecipitation of ABAD and Aβ from mitochondria of transgenic mice. Mitchondrial fractions (500 mg) from cerebral cortex of (1) non Tg, (2) Tg mAPP and (3) Tg mAPP/ABAD mice were immunoprecipitated with mouse anti-Aβ IgG (6E10; 8 μg/ml), or (4) nonimmune IgG (8 μg/ml) at 4°C overnight followed by Western blotting with mouse anti-ABAD (1:10,000). The middle panel shows total input protein reprobed with anti-Aβ antibody (6E 10). Lower panel shows immunoblotting of

β-actin for crude extracts from mouse brains. (B) Co-localization of ABAD and Aβ in the brain of a Tg mAPP/ABAD mouse using confocal microscopy with antibodies to ABAD (red) and Aβ (green) (magnification 300-fold). (C) Co-localization of ABAD and Aβ in mitochondria of brains from Tg mAPP/ABAD mouse using electron microscopy. Double immunogold staining was performed with rabbit anti-Aβ IgG and mouse anti-ABAD IgG followed by goat anti-rabbit IgG conjugated to 12 nm gold particles (for Aβ1-42) and goat anti-mouse IgG conjugated to 18 nM gold particles (for ABAD). Arrowheads depict gold particles localizing ABAD antigen. The smaller gold particles represent sites of localization of Aβ. (Taken from (Lustbader *et al*., 2004))

For the initial experiments, 2D gel proteomic analysis (Section 2.6) was performed on whole mouse brain tissue from three mice of each genotype (Tg mAPP, Tg ABAD, 2 x Tg mAPP/ABAD and WT) matched for age and sex. Using the whole brain tissue gave a high total protein concentration, which provided multiple well-defined protein spots on the gels. This enabled good comparison of protein expression between all the transgenic and wild type mice (Figure 4.2).

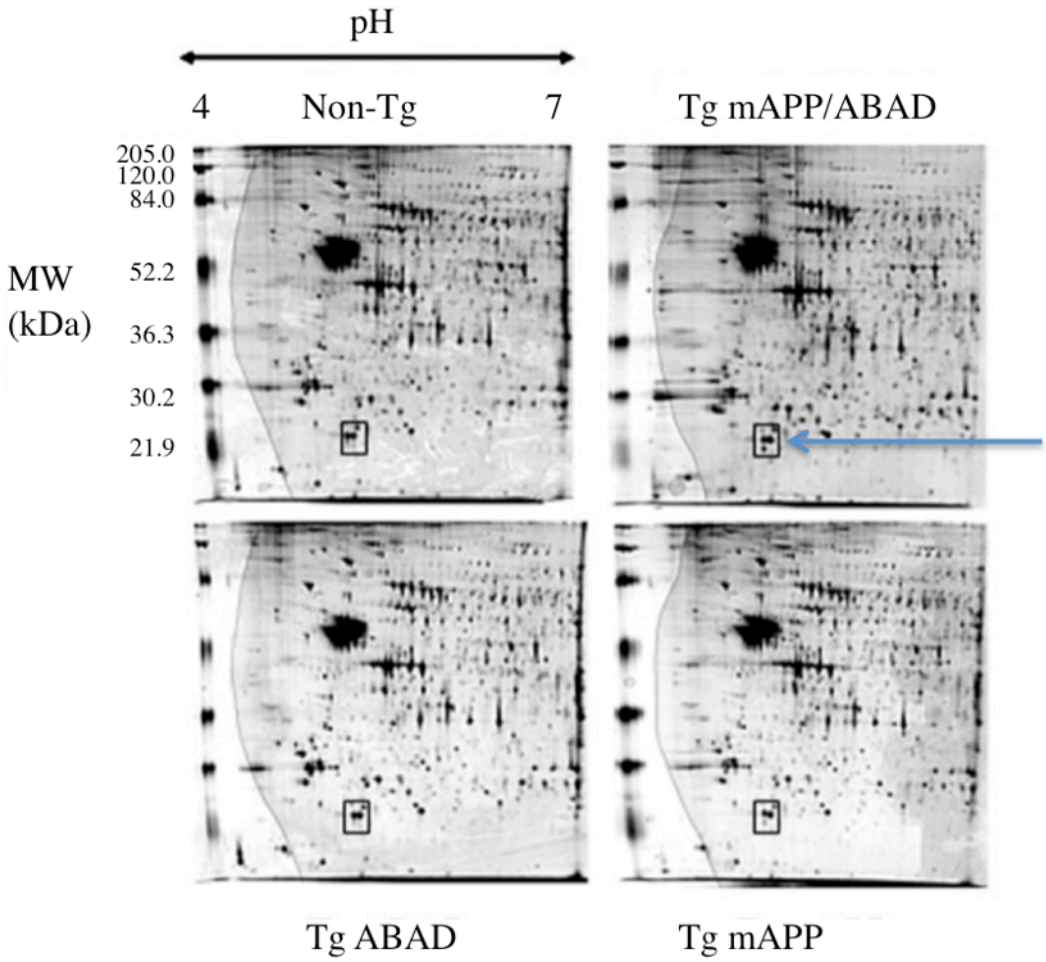

Fig. 4.2. 2D gels from tissue samples of each genotype. (Taken from (Yao *et al.*, 2007). The square (blue arrow) outlines the area on the gels identifying an example protein expressed only in the Tg mAPP/ABAD sample, subsequently identified as peroxiredoxin II (MW 22kDa).

Results from the 2D gels of whole brain tissue (Figure 4.2) showed several enhanced spots, equivalent to up-regulated proteins, in the transgenic or double transgenic phenotypes. Magnified sections from the 2D gels for four of these up-regulated proteins are shown in Figure 4.3. The double transgenic (2xTg mAPP/ABAD) showed proteins with increased expression (identified by blue ring) that are not expressed in the control samples.

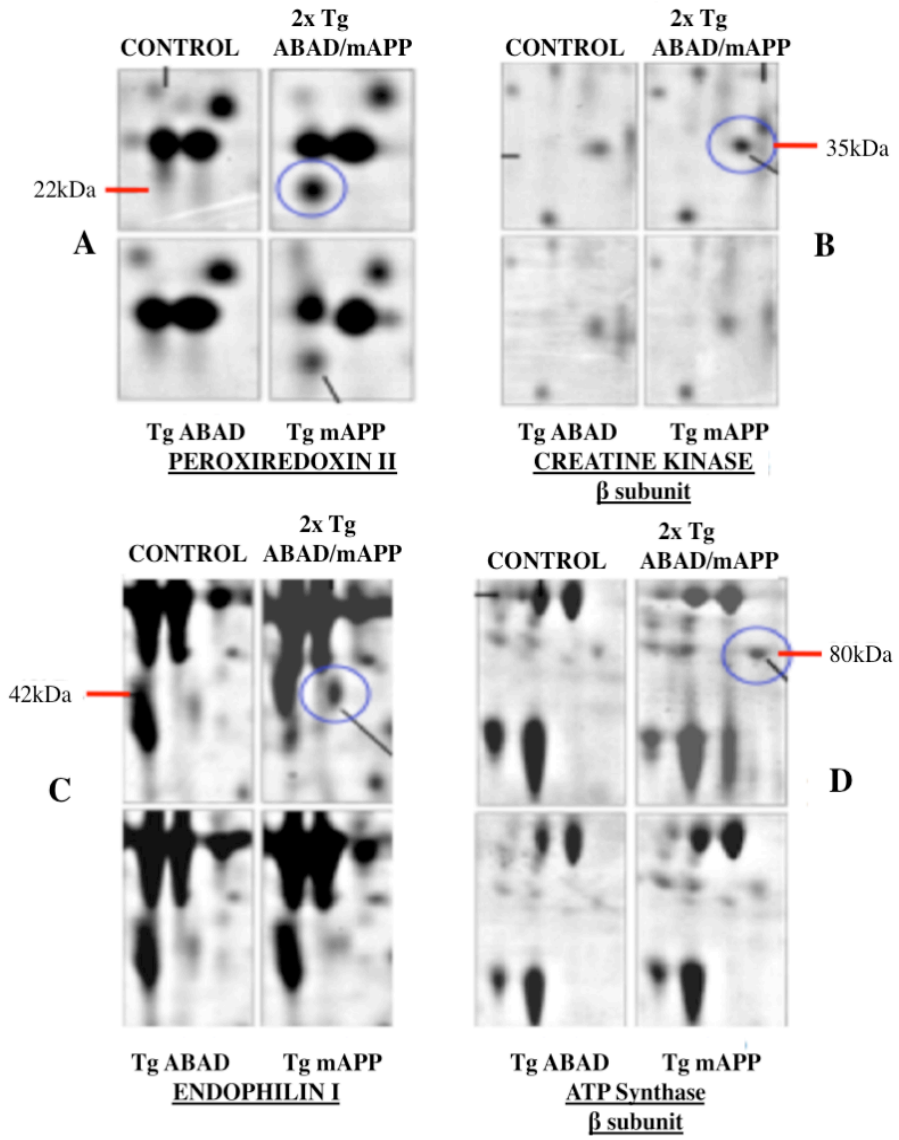

Fig. 4.3. Magnified detail from 2D gels with tissue samples from each genotype (as Figure 4.2) from whole brain tissue of eight month old mice. Four novel proteins were subsequently identified from the spots as upregulated in 2xTg ABAD/mAPP genotype (ringed in blue), A. peroxiredoxin II, B. creatinine Kinase β subunit, C. endophilin I, and D. ATP synthase β subunit. It was also noted that peroxiredoxin II was also expressed in the Tg mAPP model.

4.3.1 Choice of method for identification of proteins

In order to identify the proteins in these spots, the amino acid sequence needed to

be determined. There are two main methods of protein sequencing, by mass spectrometry or Edman degradation using N-terminal residue identification. Both methods require the protein to be identified by the smaller peptide chains within the protein. Further computer analysis of the peptide sequences reconstructs the overall sequence and identifies the protein. The Edman degradation method uses the chemicals 2,4-dinitrofluorobenzene (DFNB - Sanger's reagent), dansyl chloride, and phenylisothiocyanate (PITC, Edman's reagent) to label the free unprotonated amino groups to identify the N-terminal residues of the peptide sequences within the protein (Niall, 1973). The main disadvantage of the Edman degradation is that the size of the peptide chains identified is limited. The peptides need in reality to be a length of ≤ 30 residues or the degradation process is incomplete. This can be overcome by cleaving the larger peptides into smaller fragments but it is time consuming. However Mass Spectrometry is now available and easily automated and provides accurate data on the peptide sequences. The data is produced as a peak list of molecular weights of the peptides and when compared against numerous protein sequence databases such as UniprotKB or Genebank, the protein can be identified. Mass spectrometry was used to identify the protein spots in this study.

4.3.2 Mass Spectrometry analysis

The protein spots were cut from the gels. The gel was then destained with acetonitrile and subjected to reduction and alkylation before digestion with trypsin at 37^0C (Rosenfeld *et al.*, 1992). The peptides were extracted with 10% formic acid. The spots were cut from the gels and trypsinised. The trypsin digest cleaves the protein after all lysine (K) and arginine (R) amino acid residues, except when

followed by a proline (P) residue. The proteins were individually digested into a number of peptide chains. For analysis by MALDI-TOF mass spectrometry, 0.5µl of the digest solution was applied to the MALDI target with 0.5µl alpha-cyano-4- hydroxycinnamic acid matrix (0.5 mL, 10 mg/mL in 50:50 acetonitrile: 0.1% TFA) and allowed to dry. MALDI MS was acquired using a 4800 MALDI-TOF/TOF Analyser (Applied Biosystems, Foster City, CA) equipped with an Nd/YAG 355 nm laser and calibrated using a mixture of peptides. Mass spectrometry MALDI-TOF analysis obtained information related to the peptides' mass and charge. The masses of these peptides are very accurate and provide a 'peptide mass fingerprint'. The peptide sequences and masses were entered into the 'MASCOT' search engine, which uses mass spectrometry data to identify proteins from primary sequence databases. The proteins were identified from the data, which showed the peptides matched to the highest scoring protein match or alternative protein match if so indicated. The mass spectrometry results gave a combined score, based on the statistical chance that the group of peptides matching a particular protein could occur by chance. Scores above a certain 'identity' threshold were generally considered valid as the match has a less than 5% chance of occurring randomly (Lahm and Langen, 2000; Steen and Mann, 2004).

Using endophilin 1 as an example: there are three isoforms of endophilin I, II and III, and their protein sequences are different as shown in Figure 4.4, and the expected peptide sequences from the tryptic digest of endophilin I are shown in Figure 4.5.

Q62420 Endophilin I- mouse

```
10          20          30          40          50          60
MSVAGLKKQF HKATQKVSEK VGGAEGTKLD DDFKEMERKV DVTSRAVMEI MTKTIEYLQP
         70          80          90         100         110         120
NPASRAKLSM INTMSKIRGQ EKGPGYPQAE ALLAEAMLKF GRELGDDCNF GPALGEVGEA
        130         140         150         160         170         180
MRELSEVKDS LDMEVKQNFI DPLQNLHDKD LREIQHHLKK LEGRRLDFDY KKKRQGKIPD
        190         200         210         220         230         240
EELRQALEKF DESKEIAESS MFNLLEMDIE QVSQLSALVQ AQLEYHKQAV QILQQVTVRL
        250         260         270         280         290         300
EERIRQASSQ PRREYQPKPR MSLEFATGDS TQPNGGLSHT GTPKPPGVQM DQPCCRALYD
        310         320         330         340         350
FEPENEGELG FKEGDIITLT NQIDENWYEG MLHGQSGFFP INYVEILVAL PH
```

Q62419 Endophilin II- mouse

```
10          20          30          40          50          60
MSVAGLKKQF YKASQLVSEK VGGAEGTKLD DDFKDMEKKV DVTSKAVAEV LVRTIEYLQP
         70          80          90         100         110         120
NPASRAKLTM LNTVSKIRGQ VKNPGYPQSE GLLGECMVRH GKELGGESNF GDALLDAGES
        130         140         150         160         170         180
MKRLAEVKDS LDIEVKQNFI DPLQNLCDKD LKEIQHHLKK LEGRRLDFDY KKKRQGKIPD
        190         200         210         220         230         240
EELRQALEKF EESKEVAETS MHNLLETDIE QVSQLSALVD AQLDYHRQAV QILEELADKL
        250         260         270         280         290         300
KRRVREASSR PKREFKPRPR EPFELGELEQ PNGGFPCAPA PKITASSSFR SSDKPIRMPS
        310         320         330         340         350         360
KSMPPLDQPS CKALYDFEPE NDGELGFREG DLITLTNQID ENWYEGMLHG QSGFFPLSYV

QVLVPLPQ
```

Q62421 Endophilin III- mouse

```
10          20          30          40          50          60
MSVAGLKKQF HKASQLFSEK ISGAEGTKLD EEFLNMEKKI DITSKAVAEI LSKATEYLQP
         70          80          90         100         110         120
NPAYRAKLGM LNTVSKLRGQ VKATGYPQTE GLLGDCMLKY GKELGEDSAF GNSLVDVGEA
        130         140         150         160         170         180
LKLMAEVKDS LDINVKQTFI DPLQLLQDKD LKEIGHHLRK LEGRRLDYDY KKRRVGKIPE
        190         200         210         220         230         240
EEIRQAVEKF EESKELAERS MFNFLENDVE QVSQLAVFVE AALDYHRQST EILQELQSKL
        250         260         270         280         290         300
ELRISLASKV PKREFMPKPV NMSSTDANGV GPSSSSKTPG TDTPADQPCC RGLYDFEPEN
        310         320         330         340
EGELGFKEGD IITLTNQIDE NWYEGMLRGE SGFFPINYVE VIVPLPP
```

Fig. 4.4. Protein sequences of the three isoforms of mouse endophilin from the SwissProt database. The residues highlighted in red show the sequence specificity of the Zymed anti-endophilin I antibody used in the western blots (section 4.4.3 and 4.4.4). The residues highlighted in green identify some of the differences in the sequences in this central section.

Endophilin I mouse Trypsin: /K-\P /R-\P

fragment	residues	sequence
T30	173-173	(K)K(R)
T29	172-172	(K)K(K)
T25	160-160	(K)K(L)
T2	8-8	(K)K(Q)
T9	39-39	(R)K(V)
T31	174-174	(K)R(Q)
T27	165-165	(R)R(L)
T41	253-253	(R)R(E)
T13	66-67	(R)AK(L)
T15	77-78	(K)IR(G)
T39	244-245	(R)IR(Q)
T32	175-177	(R)QGK(I)
T18	100-102	(K)FGR(E)
T23	150-152	(K)DLR(E)
T4	13-16	(K)ATQK(V)
T16	79-82	(R)GQEK(G)
T5	17-20	(K)VSEK(V)
T26	161-164	(K)LEGR(R)
T38	240-243	(R)LEER(I)
T3	9-12	(K)QFHK(A)
T8	35-38	(K)EMER(K)
T34	185-189	(R)QALEK(F)
T35	190-194	(K)FDESK(E)
T10	40-45	(K)VDVTSR(A)
T20	123-128	(R)ELSEVK(D)
T1	1-7	(-)MSVAGLK(K)
T6	21-28	(K)VGGAEGTK(L)
T7	29-34	(K)LDDDFK(E)
T40	246-252	(R)QASSQPR(R)
T28	166-171	(R)LDFDYK(K)
T33	178-184	(K)IPDEELR(Q)
T24	153-159	(R)EIQHHLK(K)
T42	254-260	(R)EYQPKPR(M)
T11	46-53	(R)AVMEIMTK(T)
T21	129-136	(K)DSLDMEVK(Q)
T14	68-76	(K)LSMINTMSK(I)
T37	228-239	(K)QAVQILQQVTVR(L)
T12	54-65	(K)TIEYLQPNPASR(A)
T22	137-149	(K)QNFIDPLQNLHDK(D)
T17	83-99	(K)GPGYPQAEALLAEAMLK(F)
T44	297-312	(R)ALYDFEPENEGELGFK(E)
T19	103-122	(R)ELGDDCNFGPALGEVGEAMR(E)
T43	261-296	(R)MSLEFATGDSTQPNGGLSHTGTPKPPGVQMDQPCCR(A)
T36	195-227	(K)EIAESSMFNLLEMDIEQVSQLSALVQAQLEYHK(Q)
T45	313-352	(K)EGDIITLTNQIDENWYEGMLHGQSGFFPINYVEILVALPH(-)

Fig. 4.5. Peptide sequences expected from the tryptic digest of endophilin I, shown in order of residue length. The order of peptides in the protein sequence is shown in the left hand column, T1 being first.

From the sequences in Figure 4.4, it can be seen that the peptide sequences expected from the tryptic digests of the different isoforms will also be different. The expected tryptic digests of endophilin I is shown in figure 4.5 and the expected tryptic digests of endophilin II and III are shown in the Appendix. Database searching of the peptide sequences identified isoform endophilin I.

4.3.3 Results from mass spectrometry analysis

Table 4.1 shows the results from mass spectrometry analysis, identifying five upregulated proteins in the 2 x Tg mAPP/ABAD AD mouse model compared to WT. The proteins were identified as apolipoprotein E, peroxiredoxin II, creatine kinase β subunit, endophilin I, and the β-subunit of ATP synthase. Apolipoprotein E (ApoE) is well known to be associated with late onset AD. Having identified ApoE in these transgenic models provides evidence that these are good phenotypes for the AD model, but as the main aim was to identify novel biomarkers for AD, ApoE was not selected for further investigation at this stage. However, the other proteins could be potential novel biomarkers for AD whose expression correlate with over-expression of Aβ in Alzheimer's disease brains. These four proteins were therefore investigated further.

The columns in Table 4.1 indicate the peptide masses, molecular weight and PI that match with a database of known digests. The results give a predicted result and observed result. The masses matched are a probability that the peptide masses match a particular protein. A good match is between 5 and 20%. The predicted and observed molecular weights sometimes differ if there is only part of the protein or the protein is part of a complex, as with ATP synthase β subunit. However all the PI's match well.

Spot No.	Masses matched	Sequence cover %	Molecular Weight Predicted	Molecular Weight Observed	PI Predicted	PI Observed	SwissProt Acession No	Protein Identified
1	13 (16%)	48	33227	34000	5.8	5.7	P08226	Apolipoprotein E (precursor)
2	8 (10%)	39	21779	22000	5.2	5.0	Q61171	Peroxiredoxin II
3	4 (8%)	15	42714	35000	5.4	6.7	Q61171	Creatine Kinase, B chain
4	16(13%)	42	56667	80000	5.2	5.1	P56480	ATP synthase beta chain, mitochondrial (precursor)
5	12 (10%)	35	39877	42000	5.33	5.1	Q62420	SH3 domain protein 2A Endophilin 1

Table 4.1. Details of the five proteins identified from mass spectrometry.

4.3.4 Characterisation of the four proteins chosen for further study

It was interesting to note that all of these proteins are reported to be active in pathways involved with neuronal growth, lipid transport or cellular stress responses. The identification in a change in these proteins' expression in this AD model, suggests either a protective or toxic effect in the developing pathology of AD. Some of the proteins identified are involved with energy supplying pathways. Of the identified proteins, their potential significance is briefly described below, and for some they are discussed further in the discussion.

4.3.4.1 Peroxiredoxin II

Peroxiredoxin II (PrxII) is a cytosolic member of a family of peroxidases with high antioxidant efficiency and regulates H_2O_2 mediated signaling (Wood *et al.*, 2003). Mammalian peroxiredoxins have six distinct members located in subcellular compartments, mainly where oxidative stress occurs (Table 4.2).

Prx Subtype	PrxI	PrxII	PrxIII	PrxIV	PrxV	PrxVI
Cellular location	Cytosol, Nucleus	Cytosol, Membrane	Mitochondria	Cytosol, Golgi. Secreted	Mitochondria, Peroxisome, Cytosol	Cytosol

Table 4.2 Cellular locations of peroxiredoxin subgroups.

Induction of peroxiredoxins is observed as a response to increased production of reactive oxygen species (Kang *et al.*, 1998). The increased expression of PrxII is linked to oxidative stress that correlates well with the development of AD pathology. Increased protein levels of PrxII could provide protection against neuronal cell death induced by hydrogen peroxide (Kim *et al.*, 2001). PrxII has also been reported to have increased expression in the frontal cortex of patients with AD, Parkinson's disease, Pick's disease and Down's syndrome (Kim *et al.*, 2001; Krapfenbauer *et al.*, 2003), and so its identification as being up-regulated in these transgenic animals provided confidence in them being a relevant AD animal model.

4.3.2.2 Endophilin 1

Endophilin 1 is a presynaptic protein that binds to dynamin, a GTPase involved with endocytosis and recycling of synaptic vesicles (Schmidt *et al.*, 1999). Endophilins contain an SH3 domain at their C-terminus and are involved in membrane trafficking in the endocytic pathway. Endophilin 1 also acts as a substrate for the endosome-localised ubiquitin ligase, Itch and this interaction may be involved in ubiquitin-mediated sorting mechanisms operating at the level of endosomes (Angers *et al.*, 2004). Endophilin binds other endocytic proteins, synaptojanin and dynamin (Reutens and Begley, 2002) and is known to have a

role in vesicle formation. The binding of endophilin 1 with dynamin mediates synaptic vesicle invagination from the plasma membrane, to create channels in the membrane, as such this may be linked to abnormal transition of peptides or lipids through the plasma membrane in AD (Sundborger *et al.*, 2011). In addition, it is known that phospholipid metabolites can accumulate in cell membranes that contribute to Aβ deposition (Breteler, 2000) and potentially endophilin I may contribute to this as well.

4.3.4.3 ATP synthase β subunit

This is part of the intermembranous, five protein complex in the mitochondria which drives protons between the intermembrane space and the matrix. This complex catalyses ATP synthesis, and is essential for cell energy and survival. The identified β chain is the catalytic subunit (Ackrell, 2000). CNS tissue uses ATP rapidly and requires a constant energy reservoir for rapid regeneration of ATP. There is evidence that suggests expression of ATP synthase β subunit is tissue specific, the highest levels in the heart and the lowest in liver and kidney (Neckelmann *et al.*, 1989). ABAD and Aβ disrupt mitochondrial function in AD and so it is probable that this relationship alters the regulation of this protein during the progression of AD.

4.3.4.4 Creatine kinase β subunit

Creatine kinases (CK) are a family of enzymes that regulate ATP levels and as such are central in energy homeostasis in tissues with large fluctuating energy changes. This is particularly so in muscle and the brain (Monge *et al.*, 2008). CK

is elevated in serum after injury and is a significant marker for myocardial infarction (Alpert *et al.*, 2000). It is also known to be elevated in fatty acid and glycerol metabolism disorders: medium-chain acyl dehydrogenase deficiency (MCADD) and long-chain hydroxyacyl-CoA dehydrogenase deficiency (LCHADD) (Lund *et al.*, 2010). Therefore an abnormal increase in expression of this protein could be related to the over-expression of ABAD and its catabolism of fatty acids. Other studies have noted an increase in CK expression in early stages of AD with a significant decrease in CK in the late stages in human AD brain (Lynn *et al.*, 2010).

4.3.4.5 ApoE

The protein ApoE transports fat-soluble proteins, cholesterol and lipoproteins into the lymphatic system. ApoE generally aids proteolytic disruption of the Aβ peptide. However the ApoE4 isoform has been linked with AD as it is less efficient at this proteolysis (Deane *et al.*, 2008). Individuals with the ApoE4 isoform gene are more susceptible to late stage AD. Cerebrospinal fluid (CSF) contains only high-density lipoproteins composed of ApoE and ApoJ secreted from astrocytes and of ApoA-I and ApoA-II transported via the blood brain barrier (Suzuki *et al.*, 2002). These apolipoproteins can bind to Aβ and possibly relate to its clearance. In this study, the 2D gel analysis on 8-12 month mice showed increase expression of ApoE in 2 x Tg mAPP/ABAD, and therefore indicates that ABAD and APP expression levels may affect ApoE expression, but due to commitments, further study was not pursued in this thesis.

4.4 Protein identification in immature (4-8 months) mouse model by western immunoblotting

Having identified novel proteins over-expressing in these AD transgenic models, further studies on four proteins were carried out to investigate how early the changes in expression could be identified. The 2 x Tg mAPP/ABAD AD mice had previously shown some cognitive behavioural changes at 5 months (Bliss and Collingridge, 1993; Caspersen *et al.*, 2005; Lustbader *et al.*, 2004; Morgan *et al.*, 2000; Yan and Stern, 2005). Therefore samples of brain tissue were extracted from freshly sacrificed 4- and 8-month old mice of wild type, and the 2 x Tg mAPP/ABAD phenotypes. To analyse the hippocampus, this was isolated from the cortex before the preparation of the samples (carried out during a visit to Professor SD Yan, Columbia University). Four or five samples each of hippocampal and remaining cortex tissue were obtained from each transgenic model and non-transgenic littermates. The tissue samples were homogenized immediately, flash frozen and stored at -80^0C until required. For the western blot analysis, total protein concentration was first assessed by Bradford assay (section 2.3.1). Each of the tissue samples was divided into 4, for western blot analysis with antibodies against peroxiredoxin II, creatine kinase β subunit, endophilin I, and the β-subunit of ATP synthase. The samples were prepared for SDS-PAGE by adding protein denaturing buffer containing bromophenol blue dye, and run on mini 10 or 12% SDS-PAGE gels. The proteins were transferred to nitrocellulose membranes for western immunoblotting. The western blotting antibodies against the proteins of interest were rabbit endophilin I, anti-peroxiredoxin II, anti ATP synthase and anti creatine kinase, β-Actin was used as a control. In the following Figures 4.4 to 4.11 are shown the results of these western blot analyses.

4.4.1 Peroxiredoxin (PrxII) – hippocampal samples

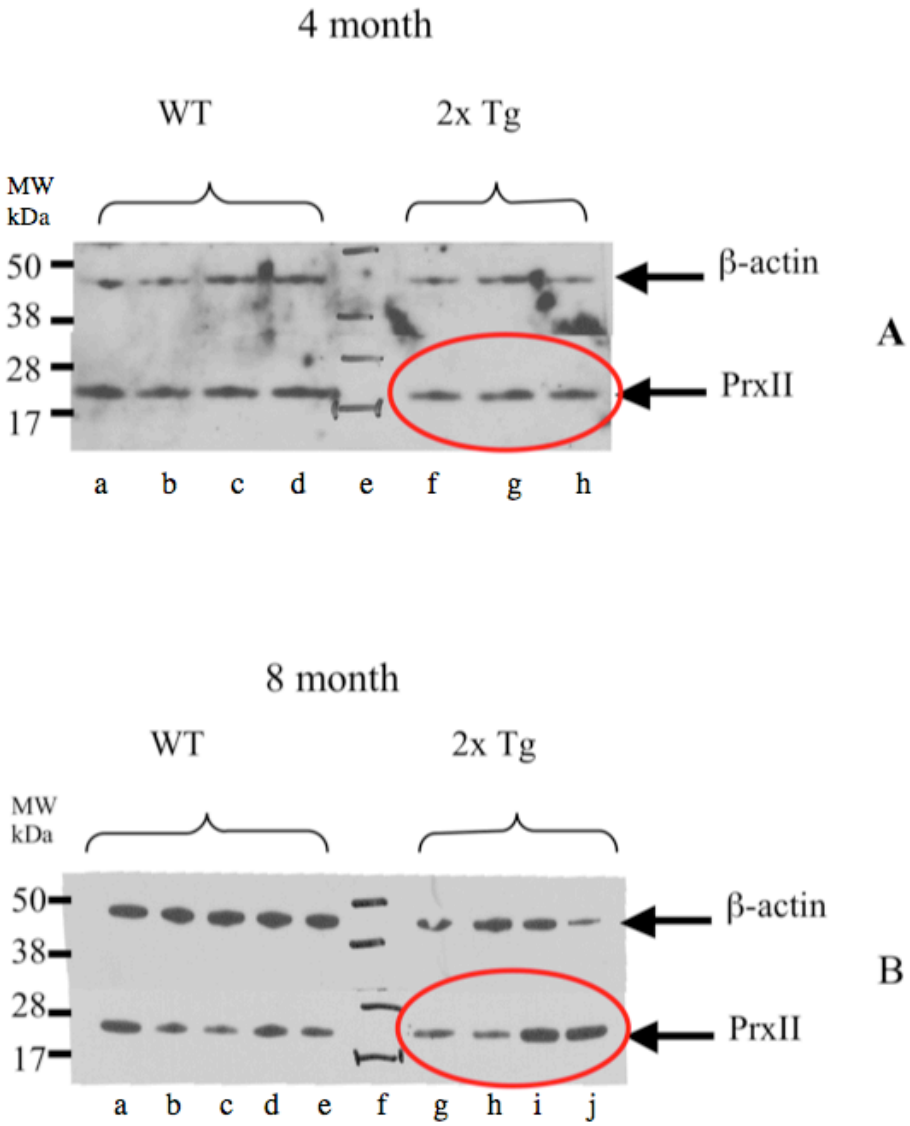

Fig. 4.4. Western blots using 0.5µg/ml rabbit anti-PrxII antibody (Alexis CA) on hippocampus tissue samples. 12µg protein was loaded in each lane. Blot A (top) shows tissue samples from 4-month old mice, comparing four WT samples (lanes a-d) with three 2 x Tg mAPP/ABAD samples (lanes f-h). Blot B (bottom) shows tissue samples from 8-month old mice, comparing five WT samples (lanes a-e) with four double transgenic samples, 2 x Tg mAPP/ABAD (lanes g-i). PrxII expression in 2 x Tg mAPP/ABAD mice is shown circled. Blot A shows little or no difference in the PrxII expression in WT and 2 x Tg mAPP/ABAD mice at 4-months age. Blot B shows increase in expression of PrxII in two of the 2 x Tg mAPP/ABAD samples (lanes i and j) at 8-months age.

4.4.2 Peroxiredoxin (PrxII) – cortex sample

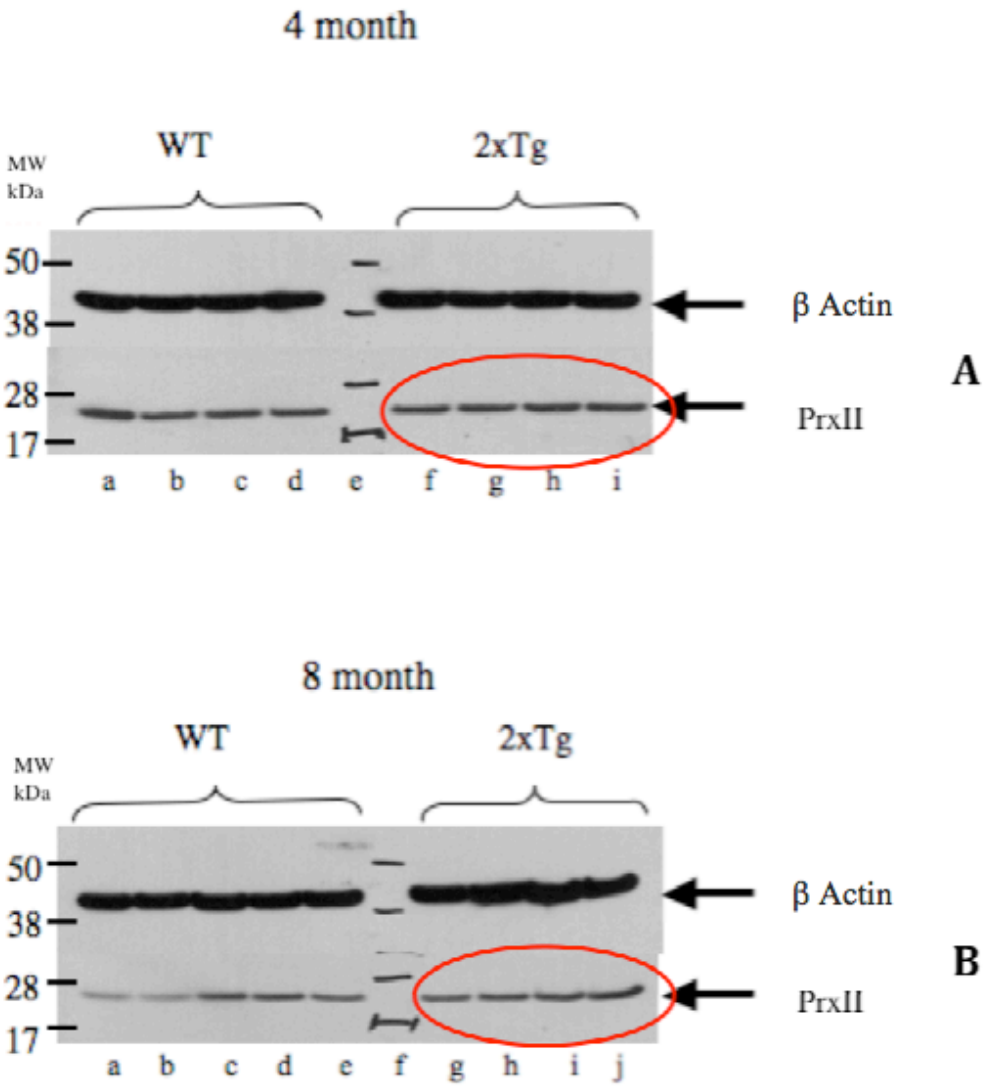

Fig. 4.5. Western blots using 0.5µg/ml rabbit anti-PrxII antibody (Alexis CA) on cortex tissue samples. 50µg protein was loaded in each lane. Blot A (top) shows tissue samples from 4-month old mice, comparing four WT samples (lanes a-d) with four 2 x Tg mAPP/ABAD samples (lanes f-i). Blot B (bottom) shows tissue samples from 8-month old mice, comparing five WT samples (lanes a-e) with four double transgenic samples, 2 x Tg mAPP/ABAD. (lanes g-j). PrxII expression in 2 x Tg mAPP/ABAD mice is shown circled. Blot A shows a little increase in the PrxII expression in 2 x Tg mAPP/ABAD mice at 4-months age. Blot B shows a slight increase in expression of PrxII in all 2 x Tg mAPP/ABAD samples (lanes g,h,i and j) at 8-months age.

4.4.3 Endophilin – hippocampal samples

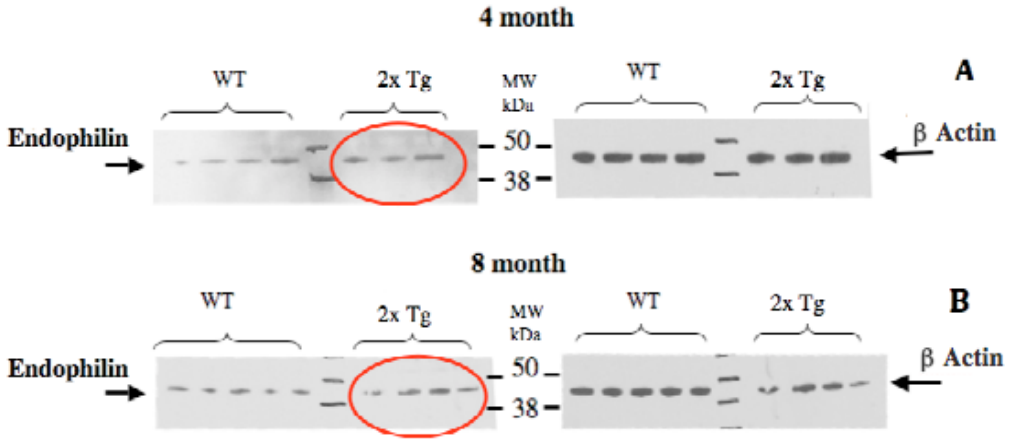

Fig. 4.6. Western blots using 0.5µg/ml anti-endophilin I antibody (Zymed laboratories) on hippocampus tissue samples. 12µg protein was loaded in each lane. Blot A (top left) shows tissue samples from 4-month old mice, comparing four WT samples with three 2 x Tg mAPP/ABAD samples. The membrane was stripped and reprobed to identify β-actin separately as the molecular weights were very similar (top right). Blot B (bottom left) shows tissue samples from 8-month old mice, comparing five WT samples with four 2 x Tg mAPP/ABAD samples. Again the membrane was stripped and reprobed to identify β-actin (bottom right). Endophilin expression in 2 x Tg mAPP/ABAD mice is shown circled. The 8-month blots show little or no difference in the endophilin expression in WT and 2 x Tg mAPP/ABAD mice. At 4-months there is increased expression in 2 x Tg mAPP/ABAD compared to WT.

4.4.4. Endophilin – cortex samples

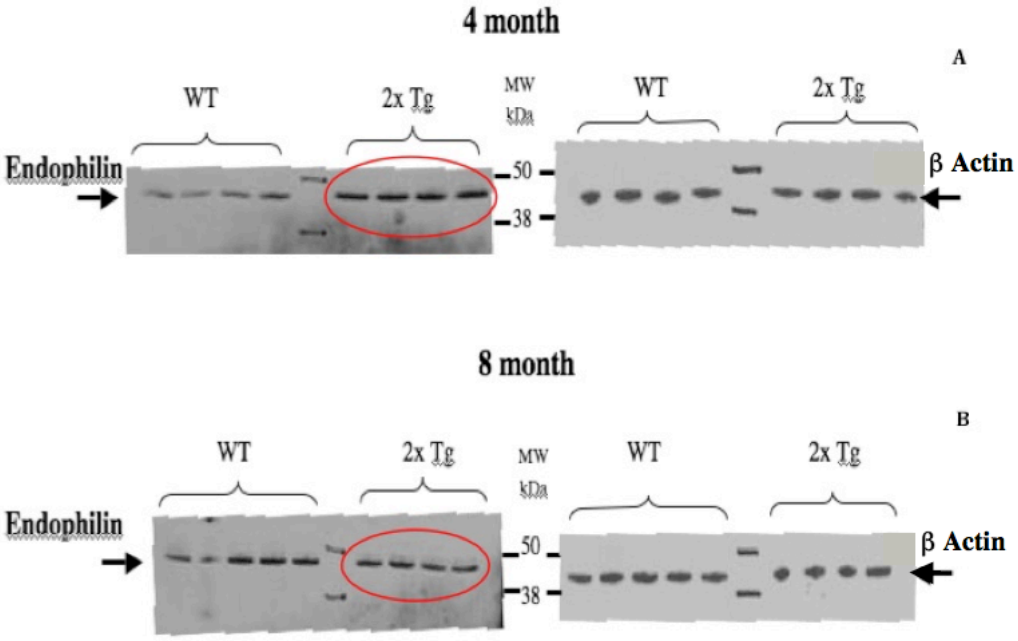

Fig. 4.7. Western blots using 0.5μg/ml anti-endophilin I antibody (Zymed laboratories) on cortex tissue samples. 12μg protein was loaded in each lane. Blot A (top left) shows tissue samples from 4-month old mice, comparing four WT samples with four 2 x Tg mAPP/ABAD (labelled 2xTg in the figure) samples. The membrane was stripped and reprobed to identify β-actin separately, as the molecular weights were very similar (top right). Blot B (bottom left) shows tissue samples from 8-month old mice, comparing five WT samples with four 2 x Tg mAPP/ABAD samples. Endophilin expression in 2 x Tg mAPP/ABAD mice is shown circled. Again the membrane was stripped and reprobed to identify β-actin (bottom right). Blot B shows little or no difference in the endophilin expression in WT and 2 x Tg mAPP/ABAD mice at 8-months age. However blot A shows a definite increase in expression of endophilin in all the 2 x Tg mAPP/ABAD samples at 4-months age.

4.4.5 ATP synthase β subunit- hippocampus samples

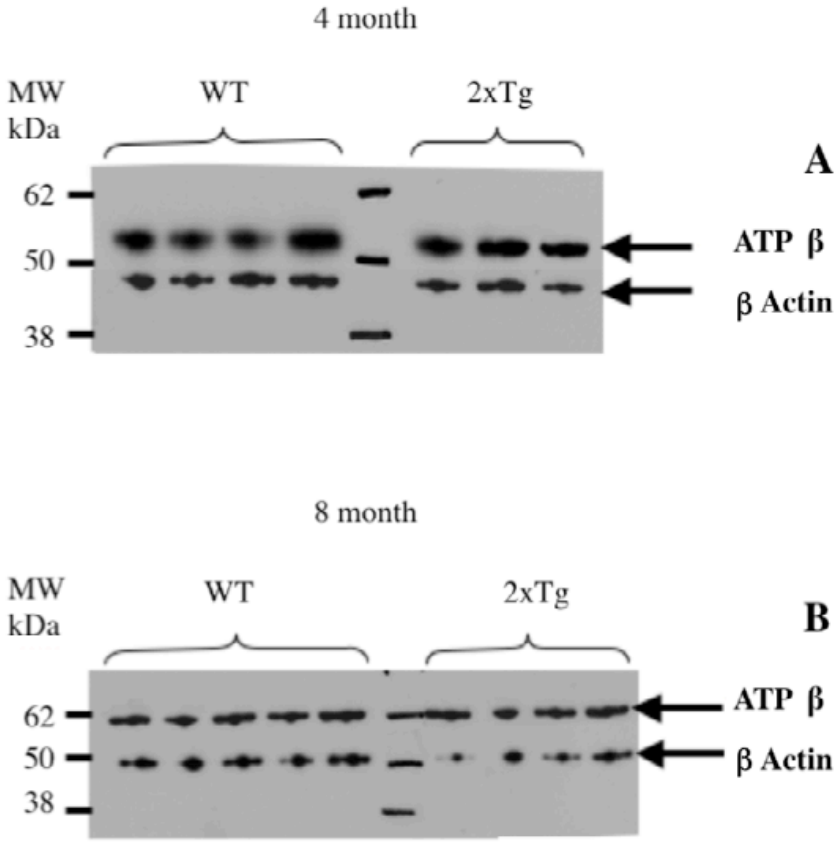

Fig. 4.8. Western blots using 1.0μg/ml anti-ATP synthase antibody (Pierce) on hippocampus tissue samples. 12μg protein was loaded in each lane for the 4-month samples. 5μg protein was loaded in each lane for the 8-month samples. Blot A (top) shows tissue samples from 4-month old mice, comparing four WT samples with three 2 x Tg mAPP/ABAD samples. Blot B (bottom) shows tissue samples from 8-month old mice, comparing five WT samples with four double transgenic samples, 2 xT g mAPP/ABAD. Both blots show little or no difference in the ATP synthase expression in WT and 2 x Tg mAPP/ABAD mice at 4 and 8 months of age. However because less sample (5μg) was needed to obtain optimal staining of the 8-month samples, this may indicate that the ATP synthase expression is generally higher in the 8-month old mice.

4.4.6 ATP synthase β subunit – cortex samples

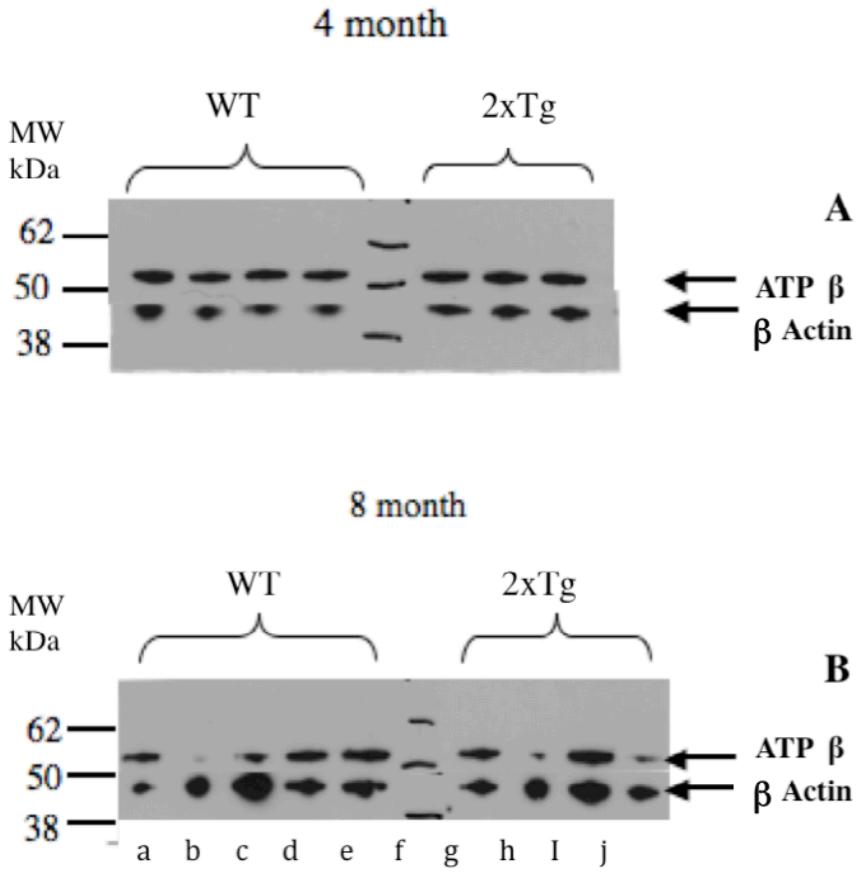

Fig. 4.9. Western blots using 1.0μg/ml anti-ATP synthase antibody (Pierce) on cortex tissue samples. 5μg protein was loaded in each lane for all samples. Blot A (top) shows tissue samples from 4-month old mice, comparing four WT samples with three 2 x Tg mAPP/ABAD samples. Blot B (bottom) shows tissue samples from 8-month old mice, comparing five WT samples with four double transgenic samples, 2 x Tg mAPP/ABAD. Blot A (4 months) shows little or no difference in the ATP synthase expression in WT and 2 x Tg mAPP/ABAD mice. Blot B (8 months) shows reduced expression in two of the WT (lanes b and c) and also in two of the 2 x Tg mAPP/ABAD (lanes h and j), compared with the β-actin control.

4.4.7 Creatine kinase β subunit - hippocampus samples

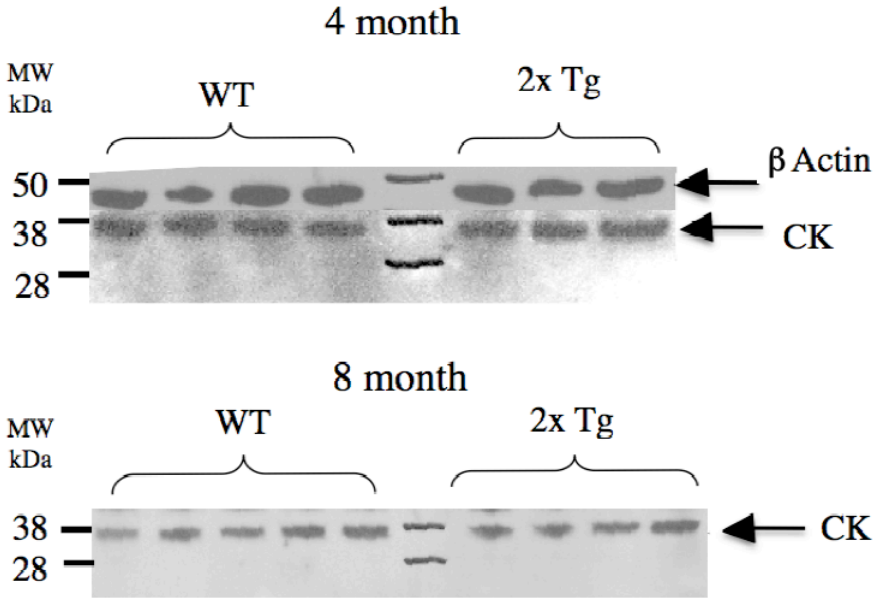

Fig. 4.10. Western blots using 0.5μg/ml anti-CKβ antibody (Santa Cruz) on hippocampus tissue samples. 12μg protein was loaded in each lane for the 4-month and the 8-month samples. Blot A (top) shows tissue samples from 4-month old mice, comparing four WT samples with three 2 x Tg mAPP/ABAD samples. Blot B (bottom) shows tissue samples from 8-month old mice, comparing five WT samples with four double transgenic samples, 2 x Tg mAPP/ABAD. Both blots show little or no difference in CKβ expression in WT and 2 x Tg mAPP/ABAD mice at 4 and 8 months of age.

4.4.8 Creatine kinase β subunit - cortex samples

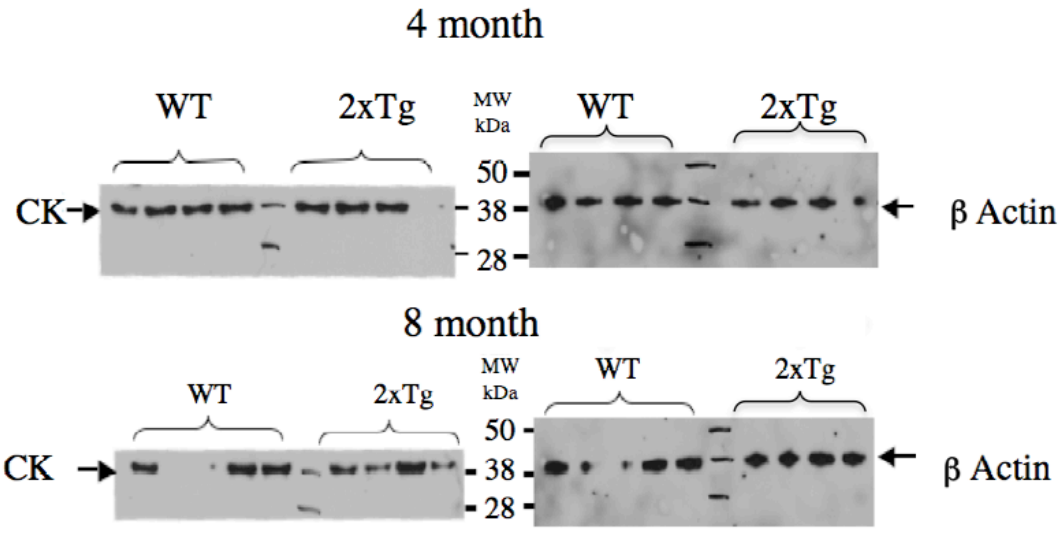

Fig. 4.11. Western blots using 0.5μg/ml anti-CKβ antibody (Santa Cruz) on cortex tissue samples. 12μg protein was loaded in each lane for the 4-month and the 8-month samples. Blot A (top) shows tissue samples from 4-month old mice, comparing four WT samples with four 2 x Tg mAPP/ABAD samples. Blot B (bottom) shows tissue samples from 8-month old mice, comparing four WT samples with four double transgenic samples, 2 x Tg mAPP/ABAD. Both blots show little or no difference in CKβ expression in WT and 2 x Tg mAPP/ABAD mice at 4 and 8 months of age.

A summary of the results from Figures 4.4 to 4.11 is shown in Table 4.3, where the protein expression in 2 x Tg mAPP/ABAD is compared to WT. This Table shows that PrxII and endophilin I are both up-regulated in the 4-month AD model. PrxII appeared to remain to be up-regulated at 8 months and the other proteins remained constant in expression.

	4 MONTHS			8 MONTHS	
	WT	2X Tg		WT	2x Tg
PrxII hippo.	=	=			+
PrxII cortex		+			+
Endo I hippo.		+		=	=
Endo I cortex		+		=	=
ATP synthase hippo.	=	=		=	=
ATP synthase cortex	=	=		=	=
CKB hippo.	=	=		=	=
CKB cortex	=	=		=	=
SDH					-
GPDH					-

Table 4.3 Protein expression in samples as shown by the western blots, between WT and 2 x Tg mAPP/ABAD mice at 4 and 8 months of age.

+ up-regulated expression. **–** down-regulated expression. **=** no difference.

4.5 Protein identification in isolated mitochondria

Because ABAD expression is predominantly in the mitochondria in neurons, proteomic analysis of isolated brain mitochondria was also carried out, as it was hoped that this could provide more detailed protein markers specifically for mitochondrial function. Therefore the mitochondria were isolated from whole brain tissue. Three wild type and three double transgenic (2 x Tg mAPP/ABAD) mice were sacrificed, to provide six samples for this study. The brains were extracted from 8-month old mice and the mitochondria isolated by centrifugal fractionation (section 2.4.2). The mitochondrial fractions were prepared for 2D

gel analysis to a final volume of 150µl (section 2.6.2 and 2.6.3). The protein expression from these isolated mitochondria was again analysed using 2D gel analysis and MALDI-TOF mass spectrometry. Unfortunately there was only a very small quantity of mitochondrial protein from each individual sample for adequate resolution on a 2D gel. Therefore two or three samples were pooled together for further analysis. This only allowed two gels for comparison of each different paradigm and unfortunately the protein separation was slightly different each time. An example of a comparison of samples from WT and 2 x Tg mAPP/ABAD mice on 2D gels is shown in Figures 4.12, 4.13 and 4.14.

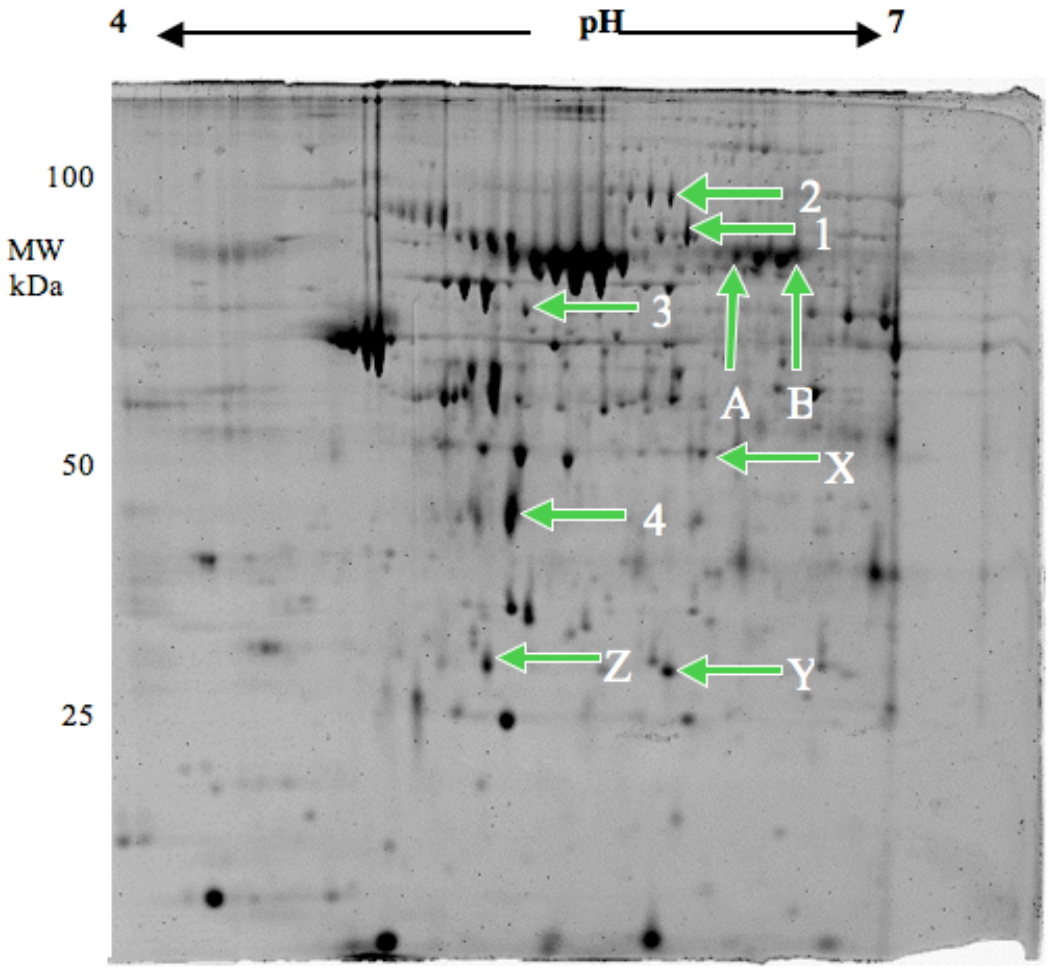

Fig. 4.12. A 2D gel of mitochondrial tissue from WT mouse 8 months of age. The green arrows show protein spots identified which were not seen in 2 x Tg mAPP/ABAD mice. Identified proteins are labelled and described below.

The proteins as indicated in Figure 4.12 were selected for identification by MALDI-TOF mass spectrometry and were subsequently identified as: A and B: succinate dehydrogenase (SDH), 72.5kDa, 1: glycerol phosphate dehydrogenase (GPDH), 81kDa, 2, 3 and 4: hypothetical proteins, and X, Y and Z: keratin probably as a result of contamination.

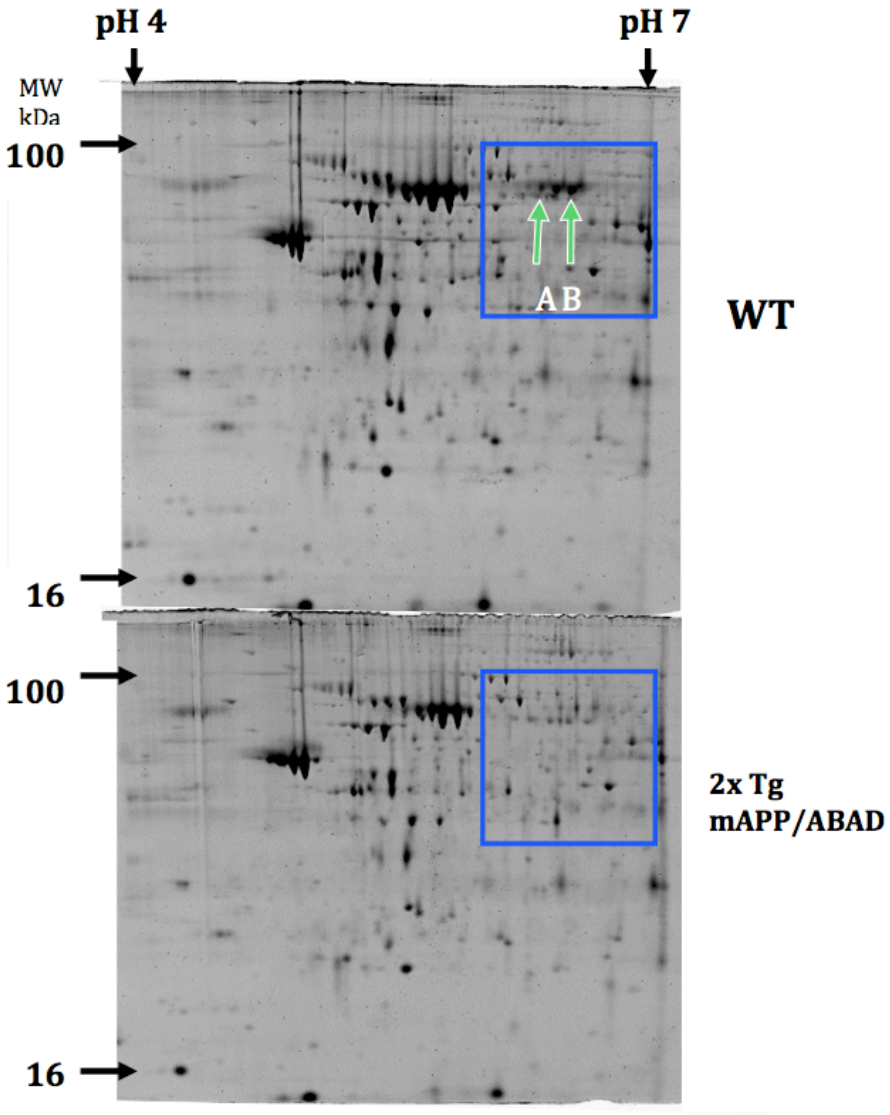

Fig. 4.13. Two 2D gels of mitochondrial samples comparing WT with 2 xTg mAPP/ABAD samples. The top gel is from WT mice, the bottom gel is from the 2 x Tg mAPP/ABAD mice. The green arrows point to protein spots A and B, two proteins that expressed in WT mice but not in the 2 x Tg mAPP/ABAD. Areas in blue squares are shown in more detail in Figure 4.14.

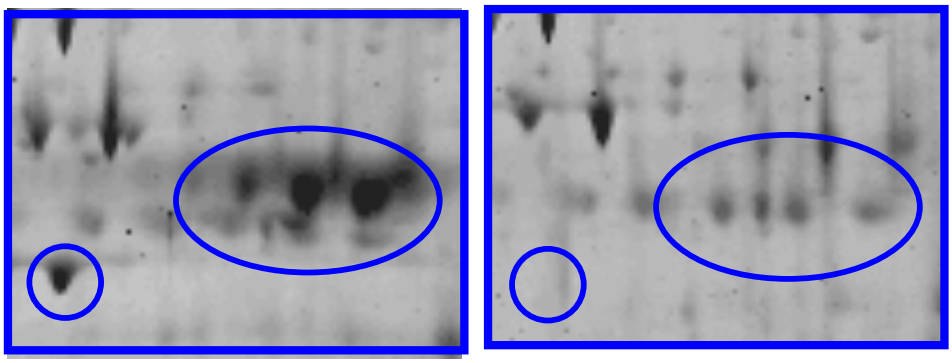

Fig. 4.14. Magnified detail from 2D gels shown in Figure 4.12. This shows proteins expressed in WT mice but not in 2 x Tg mAPP/ABAD mice. Mass spectrometry identified the three spots as succinate dehydrogenase. The isolated protein (ringed in blue, bottom left) was identified as a hypothetical protein (a protein without any known function or family). The three spots show succinate dehydrogenase as different isomers probably with different post-translational modifications, producing changes in the pI with little or no change in the mass.

SDH is part of the intermembranous 4-protein complex, complex II, bound to the inner mitochondrial membrane where it participates in the citric acid cycle and the electron transfer chain. GPDH lies on the cytosolic side of the outer mitochondrial membrane and contributes to the electron transport chain in the mitochondria. Both these proteins are down regulated in the 2 x Tg mAPP/ABAD model (Figures 4.12 and 4.13). This is possibly as a response to cellular stress and a sign of mitochondrial dysfunction, and as such provides more evidence that ABAD and Aβ are implicated in mitochondrial dysfunction. The 2D gel analysis of mitochondrial samples from 8-month mice showed significantly down-regulation of SDH and GPDH in the 2 xTg ABAD/mAPP model indicating that the energy production is compromised in these cells.

4.6 Protein changes seen in transgenic mice and Alzheimer's patients

To confirm and extend the results of the proteomic analysis, PrxII and endophilin I were analysed by immunostaining the temporal cortex from brains of 2 x Tg mAPP/ABAD mice and post mortem tissue from Alzheimer's patients, by our collaborators (Professor Yan's laboratory, Columbia University, New York (Figures 4.15 and 4.16).

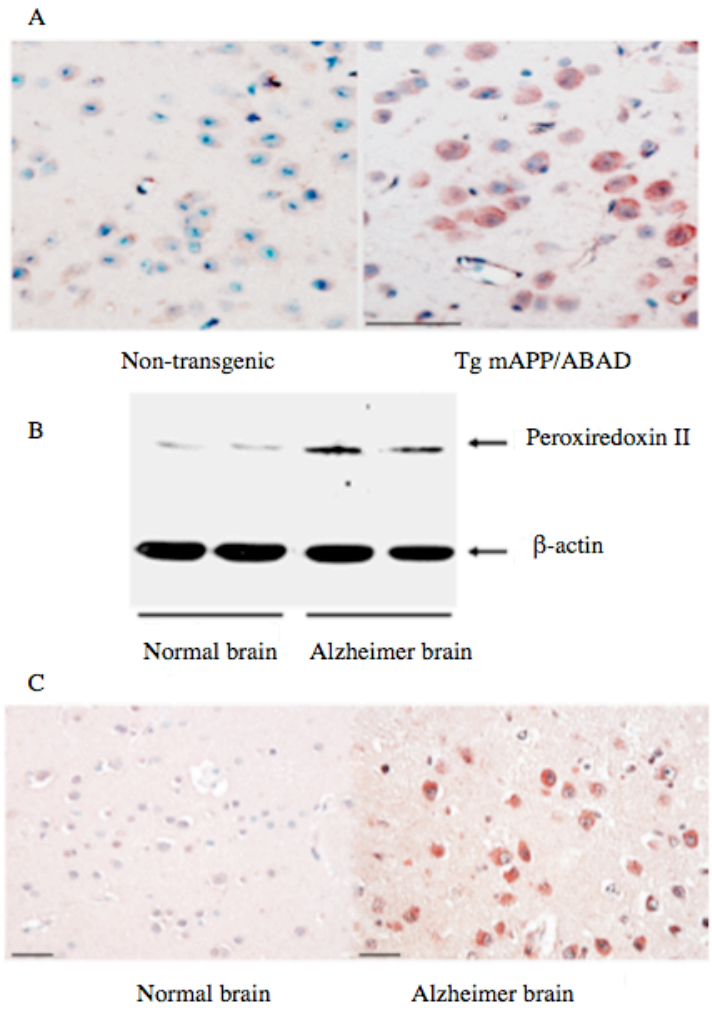

Fig. 4.15. Staining of excess PrxII in the 2 x Tg mAPP/ABAD tissue in mice and in human AD brain tissue. This confirms increased expression of PrxII in 2 x Tg mAPP/ABAD mice. (A) Immunocytochemistry of mouse brain tissue. (B) Western blot of PrxII and β-actin in AD brain tissue. (C) Immunocytochemistry of AD brain (temporal cortex). Scale bar 5μm. (Figure taken from (Yao *et al.*, 2007)).

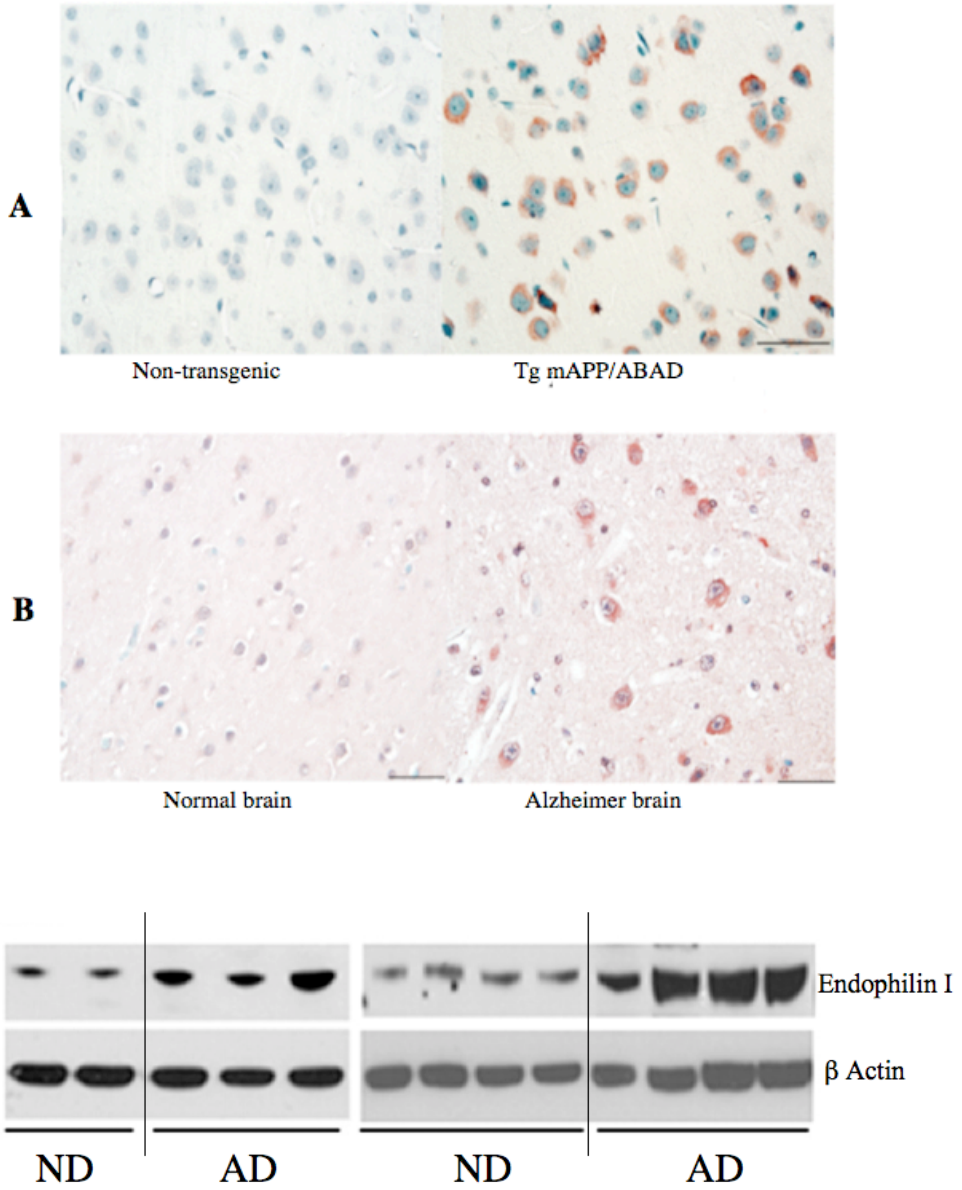

Fig. 4.16. Staining of excess endophilin I in the 2 x Tg mAPP/ABAD tissue in mice and in human AD brain tissue. This confirms the increased expression of endophilin I in 2 x Tg mAPP/ABAD mice. (A) Immunocytochemistry of mouse brain tissue. (B) Immunocytochemistry of AD brain, temporal cortex. Scale bar 5μm. Western blot analysis of endophilin I and β-actin from temporal cortex of Alzheimer patients (AD, n = 7) and non-demented age matched controls (ND, n = 6) showing a significant increase in endophilin I expression in the AD compared to age matched non demented (ND) brain. (Taken from (Ren *et al.*, 2008)

The first study (Figure 4.15 from (Yao *et al.*, 2007)) concluded that increased expression of PrxII was able to protect cortical neurons in the presence of excess Aβ. This implies that the increased expression of PrxII was a cellular response to diseased brains attempting to protect from further oxidative damage. Significantly, the expression of PrxII in living mice could be returned to normal when treated with a novel peptide inhibitor, TAT-mito-ABAD (Section 3.4.3.2).

The second study (Figure 4.16 from (Ren *et al.*, 2008)) concluded that the increased expression of endophilin was partly responsible for activating JNK and contributed to a decrease in cell viability. Endophilin I expression could also be reversed to normal in mice treated with the novel peptide inhibitor, TAT-mito-ABAD.

These combined data confirm that the interaction of ABAD and Aβ increases the expression of PrxII and endophilin I and the novel TAT-mito-ABAD peptide can disrupt the interaction.

4.7 Discussion

As AD is a neurodegenerative disease, it would be expected that there would be protein abnormalities in the brain, and so a proteomic analysis is an ideal methodology for identifying these changes. However, it is important to note that the use of 2-D gels has its limitations in the range of proteins that can be detected. The two-dimensional gel method is generally incompatible with proteins of extreme size, pI, and/or hydrophobicity, and it is difficult and time consuming to

determine the identity of hundreds of protein spots displayed on a two-dimensional gel (Liao *et al.*, 2004). Only the soluble and most abundant proteins will be visualised, excluding many membrane proteins. Very low and very high molecular weight proteins, outside the limits of the gel, or those outside the pI limits of the IEF strips will be excluded. However, the technique does provide valuable information, adequate for studying disease processes involving the CNS. One interesting finding was that several spots appeared grouped in lines, having a similar mass but different pI. This phenomenon has been noted before (Kim *et al*., 2001; Schonberger *et al*., 2001) and has been assumed to be due to either proteolysis or different isoforms of the protein. The different isoforms are most likely due to post-translational modifications of the proteins, for example phosphorylation or more likely oxidation. This was particularly seen in the mitochondrial 2D gel with the three spots identified as succinate dehydrogenase (Figure 4.14).

The proteomic experiments described here have successfully identified proteins that were up-regulated in mature mice (8-12 months) in novel transgenic mouse models for AD, where ABAD is over expressed in the presence of excess Aβ. The proteins identified were ApoE, endophilin I, peroxiredoxin II, the ATP synthase β subunit and the creatinine kinase β subunit. All, apart from ApoE, were investigated further in younger mice (4-8 months) to discover how early the changes in protein expression could be detected. In addition, two mitochondrial proteins were also found to be down regulated in the 2 x Tg mAPP/ABAD AD model: SDH and GPDH. For two of these proteins identified, peroxiredoxin II and endophilin I, subsequent work has now shown the significance of these findings.

Peroxiredoxin II (PrxII)

In this study PrxII was identified as being up-regulated in the cortex and hippocampus of the double transgenic AD model over-expressing ABAD and mAPP (figures 4.4 and 4.5). These results are supported by other studies, where PrxII has now been identified and confirmed as a protein elevated early and late in the AD mouse model and it can also be identified in AD brain tissue at post mortem (Figure 4.15) (Yao *et al.*, 2007). It is now thought that the increase in expression probably acts as a protective antioxidant that can protect neurons from Aβ induced toxicity, as it has been shown that cortical neurons expressing elevated levels of PrxII are protected against toxic levels of Aβ (Yao *et al.*, 2007). In addition, it is has been subsequently shown that PrxII expression can also be used as a means of assessing the progression of the disease. Specifically it has been shown that 2 x Tg mAPP/ABAD mice injected peritoneally for 2 weeks with a synthetic peptide (residues 93-116 of ABAD linked to TAT and a mitochondrial targeting sequence) show a decreased expression of PrxII (Yao *et al.*, 2007). This indicates that this synthetic peptide disrupts the ABAD-Aβ interaction *in vivo,* but also that PrxII expression can be used as a means of assessing this interaction. It is interesting to note that previous studies have shown that the expression of PrxII is induced following the production of reactive oxygen species in damaged neurons (Han *et al.*, 2005; Simzar *et al.*, 2000).

Endophilin I

In this study endophilin 1 was identified as being elevated in expression in both 4-month samples from the cortex and hippocampus, suggesting its involvement in cell destruction at an early stage in AD pathology. By 8 months it did not appear

to be up-regulated with respect to the WT mouse brains. However, studies from our collaborators did confirm that endophilin I expression is indeed elevated in the AD brain (Figures 4.6, 4.7 and 4.16 (Ren *et al.*, 2008)). This is significant as this was the first recorded increased expression of this protein in the AD brain. Unlike the other proteins isolated, endophilin I does not appear to be connected with energy supplying pathways, but further studies have shown that the increase of endophilin I in neurons is linked to an increase in activation of the stress kinase JNK with subsequent death of neurons (Ren *et al.*, 2008). It has also been shown to be an indicator of the interaction between ABAD and Aβ, as endophilin I expression levels return to normal if the interaction of ABAD and Aβ is perturbed in the same manner as was shown in PrxII (Ren *et al.*, 2008). Other proteomic studies have identified increased expression of synaptojanin in human AD (Schonberger *et al.*, 2001) responsible for neuronal growth and synaptic transmission.

The CKβ subunit expression and the ATP synthase β subunit were not seen in the 4 month AD mouse model, indicating that they are probably only activated late in AD pathology, as detected in the 2D gel analysis. Both proteins are actively involved in energy production in cells. CKβ is known to regenerate ATP and is induced by cellular stress and it has been reported as being up regulated in other AD proteomic studies (Aksenov *et al.*, 2001; Shiozaki and Iseki, 2004). Subsequently, increased expression of the ATP synthase β subunit has been reported in other AD proteomic studies (Korolainen *et al.*, 2006; Pamplona *et al.*, 2005).

Two proteins were identified as being down-regulated in the 2x Tg mAPP/ABAD model: SDH and GPDH. This is probably as a response to cellular stress and a sign of mitochondrial dysfunction consistent with LOAD. Both proteins are involved in normal mitochondrial function. SDH is active within mitochondria, involved in both the citric acid cycle and the electron transport chain, and it has been reported that Aβ targets SDH, suppressing its activity (Kaneko *et al*., 1995). Recently there was evidence that Complex I is down regulated in a triple transgenic model expressing tau and in the same model Complex IV is down regulated, but Aβ dependent (Eckert *et al.*, 2010). GPDH is a major contributor of electrons to the electron transport chain in mitochondria and is a major link between lipid metabolism and carbohydrate metabolism (Ackrell, 2000).

GPDH along with ATP synthase and CK, have all been reported to be oxidatively modified and dysfunctional in AD brain, indicating a damaged energy metabolic pathway reducing the overall levels of ATP (Castegna *et al*., 2002). Changes in cell potential, Ca^{2+} withdrawal, and opening of voltage gated Ca^{2+} channels would all be altered by decreased levels of ATP secondary to energy metabolism changes in the brain. Changes in ATP levels could also allow phosphatidylserine to activate the outer membrane, a signal for apoptosis (Castegna *et al*., 2004). ATP levels are very important at nerve terminals for normal neuronal function and decreased ATP levels may lead to loss of synapses and synaptic function which leads to memory loss, eventually leading to cell death and consequently to cognitive decline in AD patients.

If the anomalous concentrations of any of these proteins could be detected in CSF or plasma, these proteins could be useful as biomarkers for the early stages of the disease. For one of the identified proteins this now appears to be the case as subsequent studies identified that hydroxyoctadecadienoic acid (HODE) and oxidatively modified peroxiredoxins (oxPrx-2 and oxPrx-6) levels in plasma and/or erythrocytes in AD patients were significantly higher than those in the healthy controls (Yoshida *et al.*, 2009). The HODE levels correlated with clinical dementia scores. Plasma and erythrocyte levels of HODE, or erythrocyte levels of both HODE and oxPrx, correlated with vascular dementia and was able to distinguish it from AD, indicating that measures of oxPrx in erythrocytes is a potential biomarker for AD diagnosis.

From these studies it appears that in AD, when Aβ inhibits ABAD activity, there is a consequence that specific genes are activated. It is interesting to note that for two of these proteins, their functions appear to be in direct opposition to one another at an early stage of AD. For example Prx-II expression promotes cell survival while endophilin I expression promotes neuronal death until the equilibrium in AD eventually shifts to cell death. This indicates that throughout the development of AD pathology there is a continuous battle between proteins expressed to protect the neurons and proteins expressed as a part of the cascade towards cell death. This study has identified proteins that are involved in this battle. However it is still unknown whether these proteins can act as specific biomarkers in AD diagnosis. As yet there is no evidence of them showing up in CSF analyses. However the results add to the continuing search for an early diagnosis and subsequent treatment for AD.

Chapter 5

Identifying small molecule inhibitors to the ABAD/Aβ complex using fragment based screening.

5.1 Background and aims

The ABAD/Aβ complex has been shown to be involved in the early stages of AD, mediating Aβ toxicity. Finding an inhibitor to the formation of this complex may help in identifying a useful drug towards the treatment for AD. High throughput screening of the ABAD/Aβ complex, using the identification of low molecular weight compounds that bind to ABAD, (fragment based screening, FBS), might provide lead compounds for further chemical synthesis aimed at producing a therapeutic compound.

5.2 Fragment-based screening for drug discovery and design

Drug development is long and expensive, taking approximately 15 years to bring a drug to market. Therefore the aim of FBS is to attempt to shorten the process by producing high quality lead, drug-like compounds.

5.2.1 Conventional high-throughput screening (HTS)

HTS has been widely used in drug discovery. During the 1990's pharmaceutical companies developed large libraries of drug-like compounds, comprising typically over 200,000 compounds with diverse chemical properties. The compounds in a HTS library were required to be chemically diverse and show good absorption and

permeability properties, demonstrating good 'ADME' (Absorption, Distribution, Metabolism and Excretion) profiles.

The pharmaceutical company Pfizer developed a smaller library using the clinical phase II selection process as a filter (Lipinski *et al*., 2001). This used the hypothesis that most poor compounds would fail at pre-clinical and stage I Phases. All compounds entering Phase II trials are registered internationally as an International Non-proprietary Name (INN) and in the United States as United States Adopted Names (USAN). Pfizer selected a subset of compounds by filtering out drugs from The World Drug Index (WDI). WDI is a large computerised database of approximately 50,000 drugs, and the final library contained 2245 compounds (Lipinski *et al*., 2001). Pfizer then analysed the physico-chemical properties of these compounds, identifying four important parameters that are described below:

1. Molecular weight (MW). A high MW is related to poor intestinal and blood-brain barrier permeability (Pardridge *et al*., 1995).
2. Lipophilicity (clogP). Lipophilicity is related to absorption. Almost all studies analyse the physico-chemical properties of compounds using the ratio of solubility in octanol compared to the solubility in water. This ratio is measured as the calculated LogP (clogP) (Abraham, 2010).
3. Hydrogen bond donor groups. An excessive number of hydrogen bond donor groups impairs permeability across membrane bilayers (Abraham, 2010). A quick and simple calculation of hydrogen bond donors can be made by adding the number of NH bonds and OH bonds.

4. Hydrogen bond acceptor groups. Similarly too many hydrogen bond acceptor groups also hinder permeability across a membrane bilayer. The sum of Ns and Os are a rough guide to the H bond accepting properties.

Having analysed this library of compounds, using the four parameters mentioned, Christopher Lipinski drew up the following rules for suitable lead compounds for HTS, (the so-called 'Lipinski's rule of 5' (Lipinski *et al*., 2001) because the cut-offs for each parameter were all close to 5 or a multiple of 5.

5.2.2 Lipinski's 'rule of 5'

The compounds should have:

- Molecular Weight < 500 Da
- CLogP < 5
- H-bond donors ≤ 5 (in aromatic rings)
- H-bond acceptors ≤ 10

'The rule of 5' became the framework for the development of orally bioavailable drug candidates. It was based on the distribution of calculated properties of several thousand drugs. There are therefore always some drugs that lie outside the parameter cut-offs. Noticeable exceptions to the rules are vitamins, cardiac glycosides, antibiotics and antifungals (Lipinski *et al*., 2001). It was suggested that these break the rules by acting as substrates to naturally occurring transporters. However most compounds fulfil 'The rule of 5' requirements.

Previously, conventional HTS of biological compounds of clinical interest was carried out using biochemical and cell based assays. The instrumentation required expensive robotic liquid handling equipment that could pipette μl volumes into 384 well microplates. However, the results from the primary screens failed to produce many hits with up to 70% of the compounds failing to progress to further drug development.

5.2.3 Fragment based screening

Fragment based screening (FBS) was developed as a tool for drug discovery, using a target-based approach (Ciulli and Abell, 2007; Hajduk and Greer, 2007; Jhoti, 2005). The last decade has produced much structural information on soluble proteins and structure-based methods are now being used increasingly in the role of drug discovery. Many drug discovery projects on protein targets now use FBS involving biophysical verification of protein-ligand interactions using NMR, surface plasmon resonance (SPR), X-ray crystallography and mass spectrometry at some stage during development. Several drugs are now entering clinical usage, particularly in oncology and these methods are being used more in drug discovery for CNS diseases and conditions such as Alzheimer's Disease (Hubbard, 2011). An example of a drug currently in use, developed in 2003 using this method is Imatinib/Gleevec (Novartis) – which blocks ATP binding sites on specific mutant tyrosine kinases, inhibiting proliferation pathways in chronic myeloid leukaemia, and gastrointestinal stromal tumours (cytokine independent) (Fabbro *et al*., 2002).

FBS has now become the predominant initial screening in most pharmaceutical research today. It is a method of rapid high throughput screening of low

molecular weight compounds (<300Da), or fragments, binding to a biological target. When fragments are identified that bind to the protein, they can be chemically elaborated to form a combined larger compound, with a higher binding affinity, with the aim of producing a pharmaceutical product.

The first stage in FBS was to develop libraries of fragments (Teague *et al*., 1999). It was found to be more efficient to screen collections of small molecules/fragments (<=300Da) and then expand, merge or link them (Erlanson *et al*., 2004b). This approach had been described earlier in 1981 (Jencks, 1981), but linking several weak-binding ligands to produce one high affinity binding compound was and still remains a challenge. The ability to show 'Structure-Activity Relationships' by nuclear magnetic resonance, 'SAR by NMR' (Shuker *et al*., 1996), demonstrated how compounds with nanomolar affinities for a protein were rapidly discovered by linking together two ligands with micromolar affinities. This method reduced the amount of chemical synthesis and time required for the discovery of high-affinity ligands and was particularly useful in target-directed drug research. This 'fragment-based' approach was further developed and fragments were combined and used as initial lead compounds in drug discovery, with the aim of identifying novel compounds with improved affinity, selectivity and pharmaceutical properties (Hann *et al*., 2001).

For a fragment based screening library, the 'Rule of 5' was further developed to a 'Rule of 3' and included two other parameters; the number of rotatable bonds and the polar surface area (Congreve *et al*., 2003):

- Molecular weight ≤ 300 Da
- Octanol/water partition coefficient, CLogP < 3
- H-bond donors ≤ 3
- H-bond acceptors ≤ 3
- Flexible bonds ≤ 3
- Polar surface area ≤ 60Å

Several commercial small molecule compound libraries are available now. For this study the 'Maybridge Ro3 Fragment Library' was used. This library is composed of ~1000 compounds ≤300Da. The compounds all demonstrate good ADME (Absorption, Distribution, Metabolism and Excretion) profiles. This makes them ideal candidates for development beyond the initial screening assay, showing a good probability for an oral drug surviving the development stages. The compounds are stored at 200mM in 100% DMSO in ten polypropylene 96-well deep-well plates. Plate 1 holds compounds 1- 96, Plate 2 compounds 97-192, etc..

5.2.4 FBS improvements over conventional HTS

A conventional HTS uses typically > 1 x 10^6 compounds with molecular weight ~500Da, 'drug-sized' molecules. They are more potent but less efficient binders. They have a high binding affinity (K_d ~1μM - 20μM) but with low ligand efficiency (Figure 5.1 (A)). In contrast FBS compounds exhibit low binding affinity, (K_d ~1-20 mM), but a high ligand efficiency (Figure 5.1 (B)).

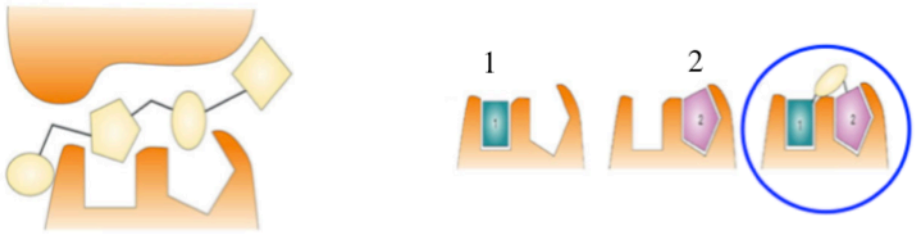

A low quality HTS hit
(A)

Two good fragment hits 'linked'
(B)

Fig. 5.1. Comparison of HTS with FBS. This shows an example of a large HTS compound in (A) and two separate small fragment compounds in (B) binding to the same biological target. The HTS hit binds strongly but is inefficient. The small fragments (1) and (2) are very efficient but have weak binding affinities. The binding is improved when the two fragments are merged or linked (shown circled). (Taken from (Hajduk and Greer, 2007).

On average the compounds with a MW ~ 200Da require a half maximal inhibitory concentration (IC_{50}), from 100μM to 1mM. FBS has developed an increased quality of lead compounds, with less false positives. Compared to HTS compounds, most FBS compounds are more soluble. Because of the low molecular weight of FBS compounds, they exhibit a lower complexity providing a higher probability of matching a protein-binding site. They contain discrete functional groups, e.g. carboxylates and amines, and the atoms in the fragments are directly involved in the desired protein binding interaction, creating efficient binders. In reality, fewer compounds are used but have a higher success rate.

5.3 Overall rationale of FBS

The overall rationale of FBS is as follows:

1. Select the biological target protein
2. Screen with FBS compounds, using a suitable quick assay e.g. thermal shift assay.
3. Validate the 'hits' by NMR, SPR, X-Ray crystallography or mass spectrometry.
4. Optimise the selection of fragments by chemical structure in collaboration with combinatorial chemists.
5. Combinatorial chemistry links or merges the fragments together to produce a high binding affinity 'drug' compound for *in vitro* and *in vivo* trials.

5.3.1 Benefits of the thermal shift assay

In this study, the thermal shift assay was used to screen the compounds. This assay is easy to set up in a routine research laboratory and the equipment required is comparatively low cost. Equipment required for this assay is a high temperature fluorescence microplate reader. This study used the Stratagene Mx3005P system. This system has a rapid temperature ramping and allows very accurate temperature control from 25°C up to 95°C, in 0.5°C increments, heating for 60s at each increment. Fluorescence readings are taken at each temperature increment. The software available allows the data to be shown in a graphic format, either as melting (dissociation) curves or showing the peak dissociation temperatures.

The assay can identify ligand binding without prior structural information of the protein. Molecules that bind to unfolded proteins which tend to be destabilisers can be identified by a reduction in dissociation temperature and can be excluded as lead compounds early in the screening, reducing time and cost. Only small volumes (<100µl) of protein and compounds are used in the microplates. Each 96 well plate assay is completed within 2 – $2^{1}/_{2}$ hr, allowing for a screen of a fragment library of 1000 compounds in 1-2 days.

5.3.2 Principle of the thermal shift assay

The thermal shift assay uses the principle that a protein unfolds when heat energy is applied to the protein until there is enough energy to exert a conformational entropy change (Murphy *et al*., 1990). A positive thermal shift is seen when the protein is made more energetically stable and unfolds at a higher temperature. A ligand binding to a target protein can alter the protein's native state, normally making it more stable. This can be shown by an increase in the protein's dissociation temperature. The midpoint of the melting curve for the protein will increase when a ligand binds more tightly to the native state than in the unfolded state. The assay follows the fluorescent signal from the protein dye Sypro Orange (Invitrogen), when a temperature gradient is applied to the samples (Figure 5.2).

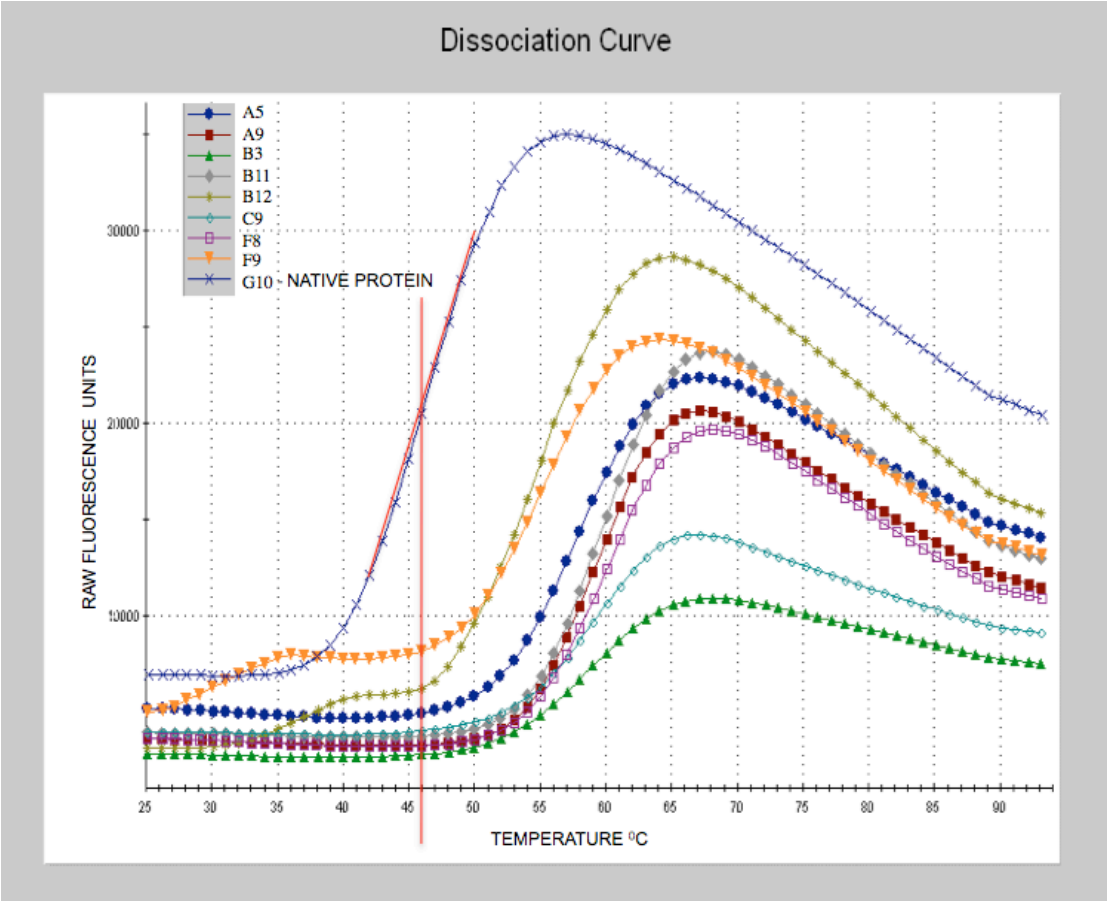

Fig 5.2. Examples of dissociation curves from a 96 well microplate thermal shift assay, heating the protein and compounds from 25°C to 90°C. This shows a native protein (in well G10) and thermal shifts (positive 'hits') with the same protein binding to eight different low molecular weight fragments (in wells A5, A9, B3, B11, B12, C9, F8 and F9). The red lines show the centre of the dissociation curve for the native protein, showing a dissociation temperature of 46°C. The other dissociation curves show an increase in the dissociation temperatures, between 55°C and 60°C, when the compounds bind to the protein.

Figure 5.2 shows the data as a graph comparing temperature vs. fluorescence signal. This same data can also be shown as dissociation temperature peaks (Figure 5.3).

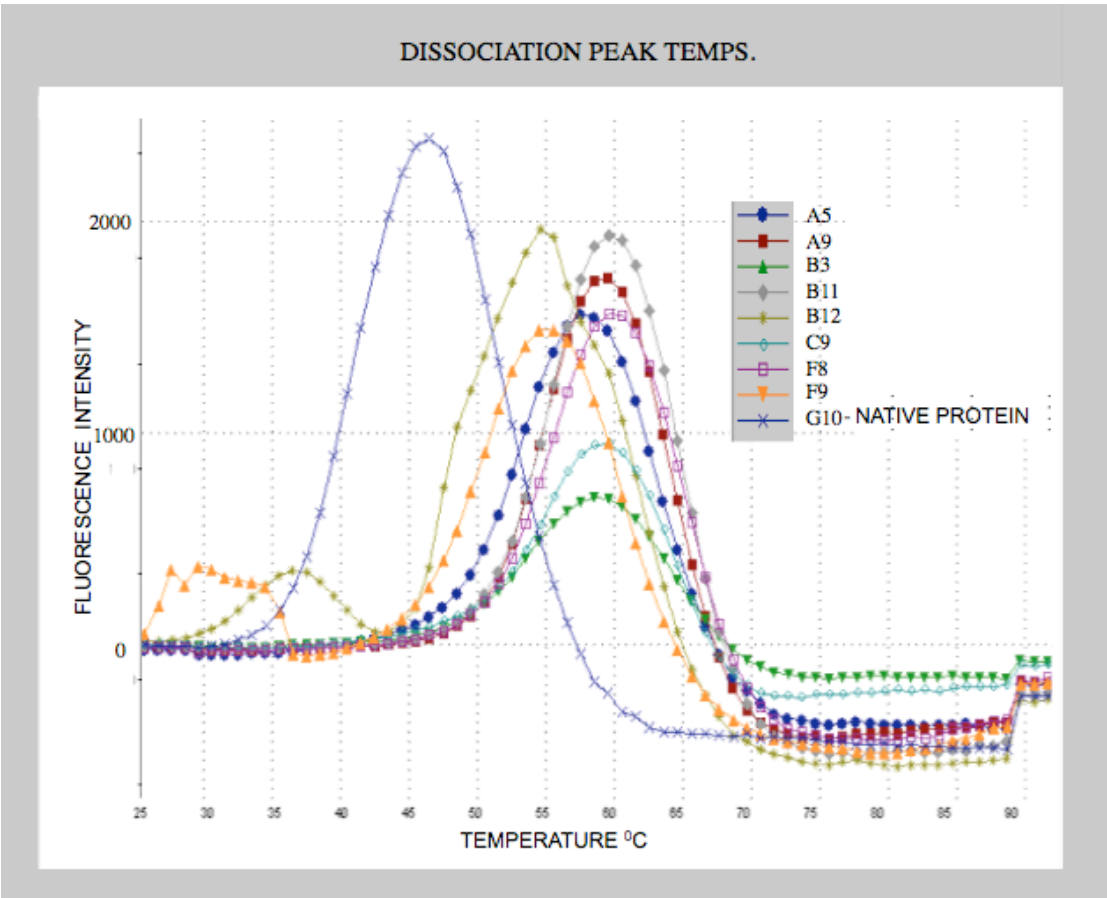

Fig. 5.3. Data shown as dissociation temperature peaks of native protein (in well G10), at 46°C, with a corresponding increase in dissociation temperatures of ligand-protein complexes (in wells A5, A9, B3, B11, B12, C9, F8 and F9). Assay as Figure 5.2.

The assay uses the protein-binding fluorescent dye, Sypro Orange. This dye is excited by UV light or light filtered with a wavelength peak of 470nm and emits at a wavelength of 570nm. The fluorescent signal of Sypro Orange changes as the protein undergoes structural change. The fluorescence is measured at discreet time points as the temperature of the protein is gradually increased over time, from 25°C and the protein unfolds. When Sypro Orange is initially added to a folded protein in solution, it is exposed to an aqueous environment and the fluorescent signal is quenched. As the temperature rises and the protein unfolds, the dye

preferentially binds to the protein's hydrophobic core. The dye becomes unquenched and so there is an increase in the fluorescent signal.

5.4. Determination of the dissociation temperature for ABAD

The fluorescent signal and dissociation temperature is protein specific. It is necessary first to optimise the concentration of protein required to give an optimal fluorescent reading on dissociation. Most buffers are suitable for the assay.

5.4.1 Initial optimisation of ABAD concentration with Sypro Orange

The concentration of ABAD required for the thermal shift assays was optimised using one negative control and seven different protein concentrations repeated in triplicates. A sample of 50μM ABAD was prepared with PBS buffer. This was diluted in the wells of a 96 well microplate to give final concentrations between 1μM and 20μM. Sypro Orange (Invitrogen) is supplied as a 5000X concentrated solution in dimethylsulfoxide (DMSO). Aliquots of purified human ABAD (hABAD) were mixed in PBS buffer with Sypro Orange at a final concentration of 5x, in a total volume of 100μl for each well in a 96 well microplate as shown in Table 5.1.

The Sypro Orange was prepared first and diluted 1:1000 with PBS buffer to 5x concentration from a stock of 5000x. This mixture was pipetted into 24 wells in a 96 well microplate, A1, A2, A3 to H1, H2, H3 as shown in Table 5.2, using volumes as shown in Table 5.1.

Per well	A1-3	B1-3	C1-3	D1-3	E1-3	F1-3	G1-3	H1-3
Final µM Protein	**0**	**1**	**2**	**3**	**4**	**5**	**8**	**10**
Vol Protein (50µM)	0	2	4	6	8	10	16	20
buffer/SyproO(5x) mix µl	100	98	96	94	92	90	84	80
Total Vol µl	100	100	100	100	100	100	100	100

Table 5.1. Experimental setup for optimisation of Sypro Orange concentration.

	1	2	3
A	A1	A2	A3
B	B1	B2	B3
C	C1	C2	C3
D	D1	D2	D3
E	E1	E2	E3
F	F1	F2	F3
G	G1	G2	G3
H	H1	H2	H3

Table 5.2. Wells charged with Sypro Orange optimisation as described in the text.

The ABAD was next added from a 50µM stock to produce final concentrations of 1, 2, 3, 4, 5, 8, 10 µM, as shown in Table 5.1. The microplate was sealed with optically clear, heatproof tape, placed in the fluorescence microplate reader and heated from 25°C to 80°C in 0.5°C increments for 60s at each temperature increment. Readings were taken at each temperature increment. The dissociation peak temperatures are shown in Figure 5.4.

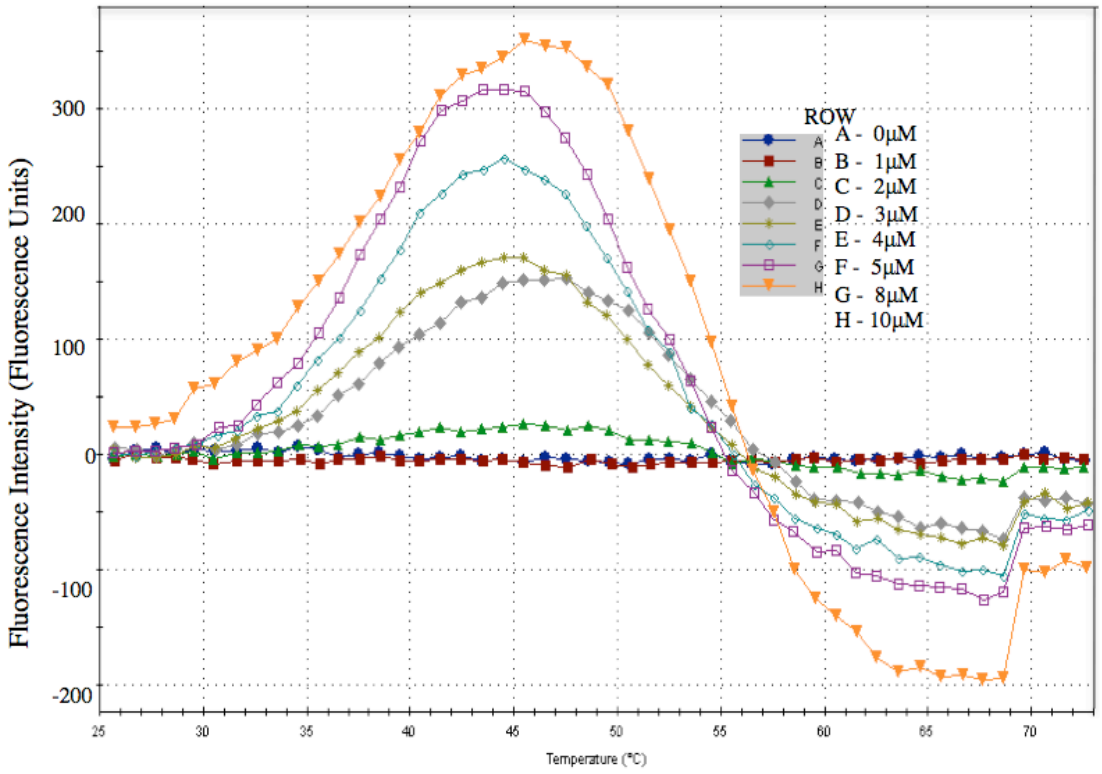

Fig. 5.4. The thermal dissociation assay for native ABAD at concentrations between 1–10μM, heated from 25°C to 70°C, showing the dissociation peak temperatures. The readings for each concentration are averaged from the three sets of readings (eg A = A1-A3) giving one final trace. Peaks are seen clearly for concentrations of ABAD above 3μM (D-H).

From this optimisation, it can be seen that changes in protein concentration can alter the dissociation temperature by up to 3°C. Because of the possibility of pipetting errors when preparing protein samples at different times, it was therefore important to use the same prepared sample of protein for each assay.

A concentration of 5μM ABAD was chosen for the initial screening with the chemical fragment compounds. This concentration used the least volume of stock protein and gave stable readings over the temperature range.

5.5 FBS of ABAD with Maybridge compounds 1-96

The chemical fragment compounds are stored long term in deep well (1ml) polypropylene 96 well plates, at a concentration of 200mM in 100%DMSO at 4°C, covered with aluminium sealing strips and further light protected by covering the entire plate with aluminium foil.

For the assay, DMSO should be no more than 5% in the final samples. On the day of the assay, 96 well, deep microplates (1ml wells) were prepared by further dilution of the compounds with PBS, equivalent to 4000x concentration of the protein (5µM) as selected from the optimisation assay. The compounds were prepared at room temperature, diluting 1:10 with PBS buffer to 20mM in 10% DMSO (Table 5.3a). The protein stock was diluted to a 2x concentration of the protein, as selected from the optimisation assay. In the 96 well plate assay, this gave a final protein concentration of 5µM and a final compound concentration of 10mM in 5% DMSO.

	1	2	3	4	5	6	7	8	9	10	11	12
A	A1	A2	A3	A4	A5	A6	A7	A8	A9	A10	A11	A12
B	B1	B2	B3	B4	B5	B6	B7	B8	B9	B10	B11	B12
C	C1	C2	C3	C4	C5	C6	C7	C8	C9	C10	C11	C12
D	D1	D2	D3	D4	D5	D6	D7	D8	D9	D10	D11	D12
E	E1	E2	E3	E4	E5	E6	E7	E8	E9	E10	E11	E12
F	F1	F2	F3	F4	F5	F6	F7	F8	F9	F10	F11	F12
G	G1	G2	G3	G4	G5	G6	G7	G8	G9	G10	G11	G12
H	H1	H2	H3	H4	H5	H6	H7	H8	H9	H10	H11	H12

Table 5.3a. A 96-well microplate template showing wells containing chemical fragment compounds – 1 ml of 20mM chemical fragment compounds in 10% DMSO + PBS buffer. The chemical fragment compounds are shown numerically in Table 5.3b.

WELL NUMBERS	CHEMICAL FRAGMENT COMPOUNDS
A1 – A12	1 - 12
B1 – B12	13 - 24
C1 – C12	25 – 36
D1 – D12	37 – 48
E1 – E12	49 – 60
F1 – F12	61 – 72
G1 – G12	73 - 84
H1 – H12	85 - 96

Table 5.3b. Distribution of fragments among the 96 wells for Plate 1. Some compounds were unavailable at the time of this study. Therefore wells A1, B2, B9, B10, D5, E6, E11 and G5 contained no compounds and were used as controls.

ABAD was mixed at a concentration of 10 μM with Sypro Orange in PBS and 50μl aliquots were pipetted into a 96 well non-skirted microplate (0.2ml wells), suitable for a thermal cycler. 50μl aliquots of the 20mM fragments were then added to the plate, in the same 96 well format shown in Fig 5.5. This gave a final protein concentration of 5μM and a final compound concentration of 10mM in 5% DMSO. The eight blank wells were used as controls, containing 5μM ABAD with Sypro Orange and PBS but no compounds. A thermal shift assay was carried out as before with increments of temperature to 75°C. Some of the dissociation curves are shown in Figures 5.5 and 5.6.

From compounds 1-96, in Plate 1, 23 compounds gave a positive thermal shifts ≥ 3°C, indicating that they could bind to ABAD. The 23 compounds are shown in Table 5.4.

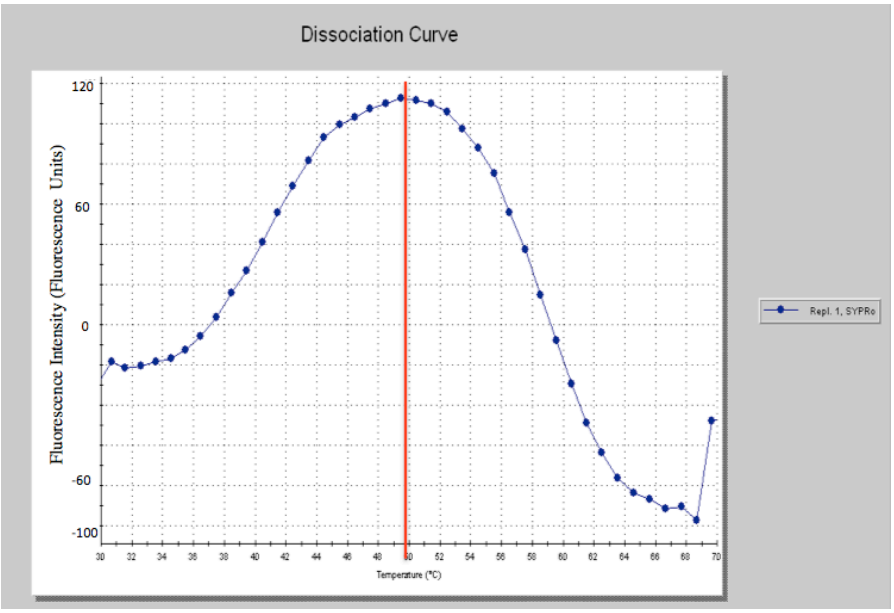

Fig. 5.5. Dissociation peak of ABAD. This shows an averaged trace from the eight control samples of ABAD, showing a dissociation temperature of 50°C.

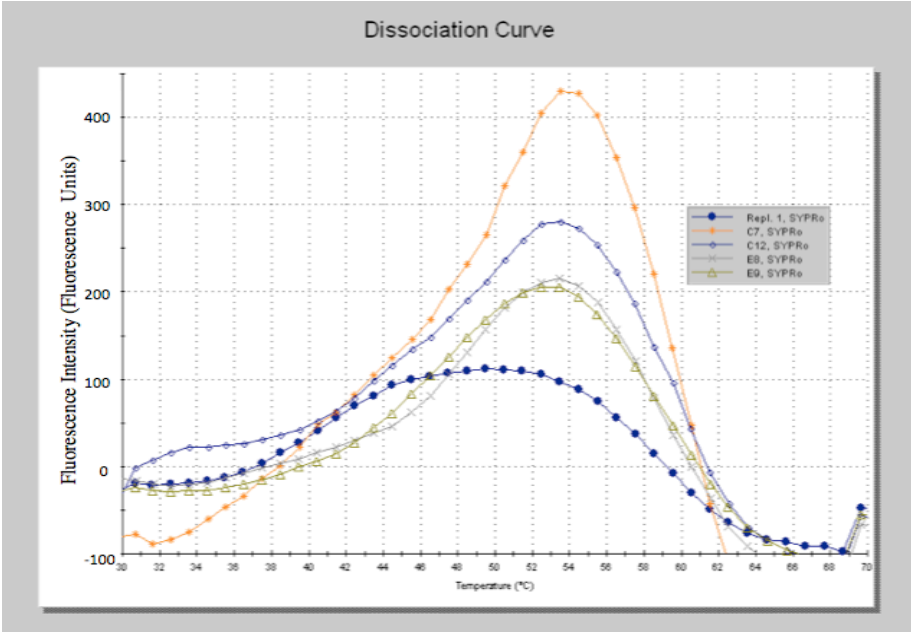

Fig. 5.6. Dissociation curves of ABAD control and four examples of compounds binding that indicate a positive thermal shift. The ABAD control is shown as a single blue trace, showing a dissociation temperature of 50°C. The other four traces show four ligand-protein complexes in wells C7, C12, E8 and E9, all showing a positive thermal shift >3°C

due to increased stability. The largest shift, the ligand-protein complex in well C7, shown in orange, was ~54°C (+4°C).

Well No.	Compound No.	Compound name	Formula	MW	Compound structure
A4	4	3,5-dimethylisoxazole	$C_5 H_7 N O$	97.1	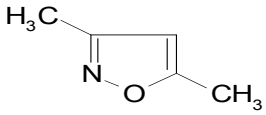
A5	5	3-furylmethylamine	$C_5 H_7 N O$	97.1	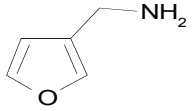
A6	6	3-methyl-1H-pyrazol-5-amine	$C_4 H_7 N_3$	97.1	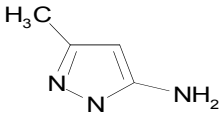
A7	7	1-methyl-1H-pyrazol-5-ylamine	$C_4 H_7 N_3$	97.1	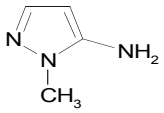
A8	8	1-methyl-1H-pyrazol-3-amine	$C_4 H_7 N_3$	97.1	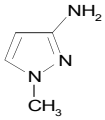
A12	12	tetrahydro-4H-pyran-4-one	$C_5 H_8 O_2$	100.1	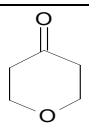
B1	13	1,4-diazepane	$C_5 H_{12} N_2$	100.2	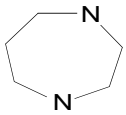
B3	15	1-methyl-1H-imidazole-5-carbonitrile	$C_5 H_5 N_3$	107.1	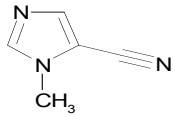
B4	16	5-methylpyridin-2-amine	$C_6 H_8 N_2$	108.1	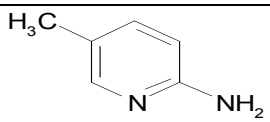
B7	19	6-methylpyridin-2-ol	$C_6 H_7 N O$	109.1	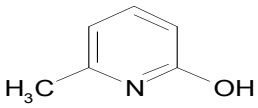
B8	20	1-(1H-pyrrol-3-yl)ethan-1-one	$C_6 H_7 N O$	109.1	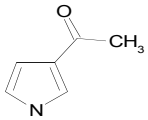
B9	21	pyridine-2,3-diamine	$C_5 H_7 N_3$	109.1	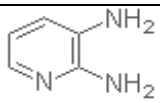

B12	24	1,3,5-trimethyl-1H-pyrazole	$C_6H_{10}N_2$	110.2	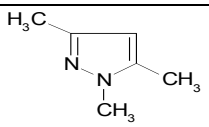
C7	31	6-methyl-2,3,4,5-tetrahydropyridazin-3-one	$C_5H_8N_2O$	112.1	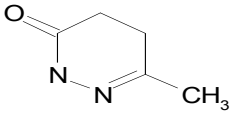
C12	36	2,5-dimethylpiperazine	$C_6H_{14}N_2$	114.2	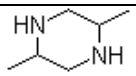
E8	56	N-methyl-N-(4-pyridinylmethyl)amine	$C_7H_{10}N_2$	122.2	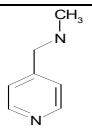
E9	57	N-methyl-N-(3-pyridylmethyl)amine	$C_7H_{10}N_2$	122.2	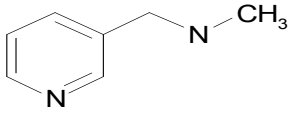
G4	76	(1,5-dimethyl-1H-pyrazol-3-yl)methanol	$C_6H_{10}N_2O$	126.2	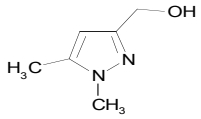
H3	87	azepan-2-one oxime	$C_6H_{12}N_2O$	128.2	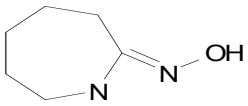
H5	89	3,5-difluoroaniline	$C_6H_5F_2N$	129.1	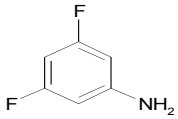
H6	90	piperidine-4-carboxylic acid	$C_6H_{11}NO_2$	129.2	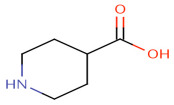
H7	91	3-piperidinecarboxylic acid	$C_6H_{11}NO_2$	129.2	
H12	96	1-eth-1-ynyl-4-methoxybenzene	C_9H_8O	132.2	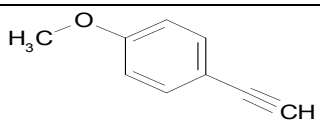

Table 5.4. Chemical details of the fragments giving ≥ 3°C thermal shift.

5.6 FBS of ABAD with NAD^+ cofactor

As ABAD binds nicotinamide adenine dinucleotide (NAD^+) during its enzymatic activity, a repeat optimisation of concentrations was carried out for ABAD in the presence of NAD^+. Six aliquots of purified ABAD from 5 -12 µM were mixed with aliquots of NAD^+ at concentrations 50 - 200 µM, in a total volume of 100µl in an 8 well strip. A control was included without NAD^+. The samples were sealed with optically clear and heat-proof tape and heated from 25°C to 80°C, in 0.5°C steps. The results of the thermal shift are shown in Figure 5.7.

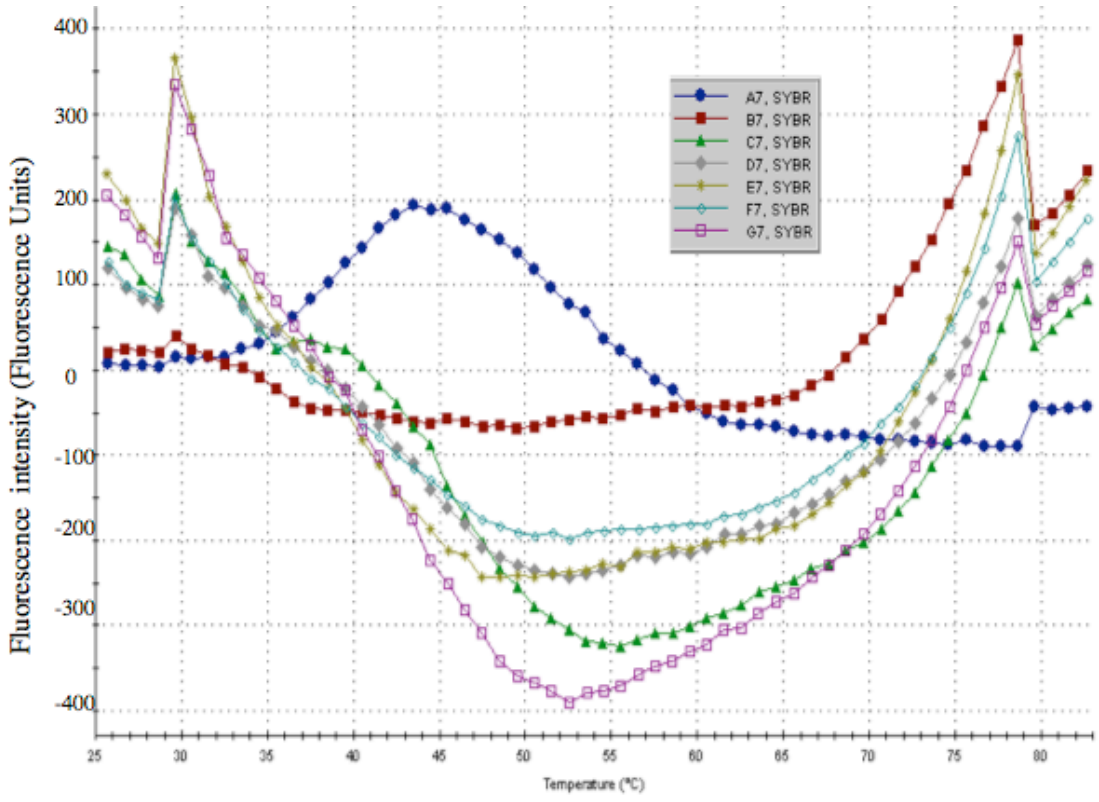

Fig. 5.7. Dissociation peak temperatures of ABAD and mixes of ABAD in the presence of NAD^+. ABAD without NAD^+ (blue trace) shows a dissociation peak temperature ~ 44-45°C. The samples with NAD^+ began showing dissociation peak temperatures at the end of the assay, at ≥80°C. The peaks at ~80°°C would indicate ABAD is very stable

with the addition of the NAD^+ cofactor . The optimal mixture, shown by the red trace (B7) was 10 μM ABAD with 100 μM NAD^+.

5.6.1 FBS of ABAD with NAD^+ against compounds 289-300 and 337-348

Approximately 5% of the chemical fragment compounds are expected to bind to a protein in any one assay. ABAD bound to 23 compounds in Plate 1, equivalent to 26% of the compounds in that plate. Plate 1 contained the compounds with the lowest molecular weights (MW 94-132Da). Therefore, it was decided to use compounds with a higher MW for the thermal shift assay of ABAD in the presence of NAD^+. The compounds were taken from Plate 4 (MW 162- 170Da). This was chosen to try to limit the positive hits to ~ 5%. Due to a limited amount of the stock of ABAD protein, an initial thermal shift assay was performed with a reduced number of compounds. 24 chemical fragment compounds were used for this assay (Table 5.5). The dissociation peak temperatures for compounds 337-348 are shown in Figure 5.8.

WELL NUMBERS	CHEMICAL FRAGMENT COMPOUNDS
A1 – A12	289-300
E1 – E12	337-348

Table 5.5. Compounds selected from plate 4.

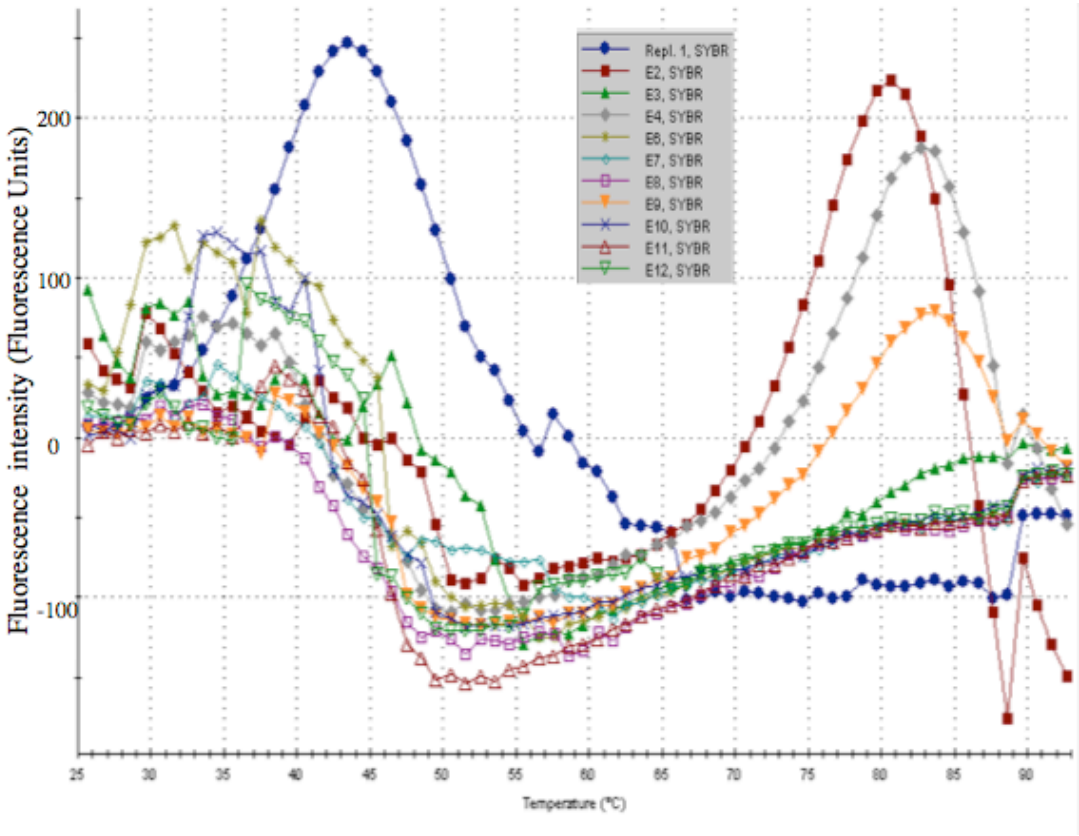

Fig. 5.8. Thermal shift assay from 25°C to 90°C for ABAD with NAD^+ cofactor and compounds 337 – 348 in wells E1-E12. Wells E1 and E5 are controls with only ABAD showing a peak dissociation temperature of 44^0C. The compounds in E2, E4, and E9 show a range of high dissociation temperatures from 80°C - 84°C. Although a control for ABAD with NAD^+ was not included in this assay, the optimisation assay had shown a peak dissociation temperature of ~80°C. The compounds in wells E4 and E9 show positive thermal shifts of around 3°C.

From this limited assay compounds 340 and 345 produce positive thermal shifts Table 5.6.

Well No.	Compound No.	Compound name	Formula	MW	Compound structure
E4	340	2-(1H-pyrazol-1-yl)benzonitrile	$C_{10}H_7N_3$	169.2	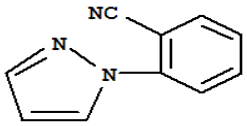
E9	345	2-hydroxybicyclo[3.2.1]octane-6-carboxylic acid	$C_9H_{14}O_3$	170.2	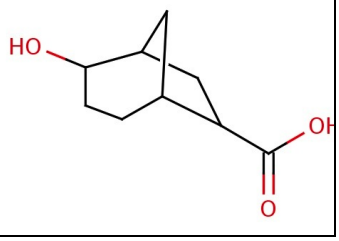

Table 5.6. Chemical details of compounds 340 and 345

5.7 Discussion

The extracellular accumulation of Aβ peptide plaques in the brain has been associated with the development of AD (Masters and Beyreuther, 1987). However there is now increasing evidence that soluble Aβ within cells and its interaction with the mitochondria plays a significant role in the progression of the disease (Muirhead *et al*., 2010). Therefore modulating mitochondrial interactions therapeutically could prevent neuronal cell death in AD. Aβ binding to mitochondrial proteins interferes with the normal function of the proteins, resulting in mitochondrial dysfunction, disruption of cell homeostasis and ultimately cell death. Recent electron microscopy of Aβ in mouse neuroblastoma cells has shown fragmentation of the mitochondria (Manczak *et al*., 2010). ABAD is an example of a mitochondrial protein that has been shown to bind Aβ within the mitochondrial matrix. This complex has been shown to have a toxic response in cells in AD mouse models and human brain post mortem tissue (Lustbader *et al*., 2004).

Methods to prevent cell death due to mitochondrial dysfunction are being currently investigated, including the development of cell-permeable mitochondrial-penetrating peptides (Horton *et al*., 2008). These peptides are synthesised using repeats of synthetic cyclohexylanine residue attached to a D-arginine. These mitochondrial-penetrating peptides are limited by their size and hydrophobicity, as only repeats of 3 or 4 (of a synthetic cyclohexylanine residue attached to a D-arginine) allow them to accumulate in the mitochondrial matrix without interfering with cellular activity. Larger peptides disrupt the mitochondrial function. However this has been shown to be useful for transporting chemotherapy agents for the purpose of disrupting cellular function in tumour cells (Horton *et al*., 2008).

Previous studies that have identified compounds that inhibit ABAD or the ABAD/Aβ interaction, and include a compound that Pfizer designated 'AG18501' (1-azepan-1-yl-2-phenyl-2-(4-thioxo-1,4-dihydro-pyrazolo[3,4-d]pyrimidin-5-yl)-ethanone) that was observed bound in the crystal structure of rat ABAD (Kissinger *et al*., 2004). Fig 5.11

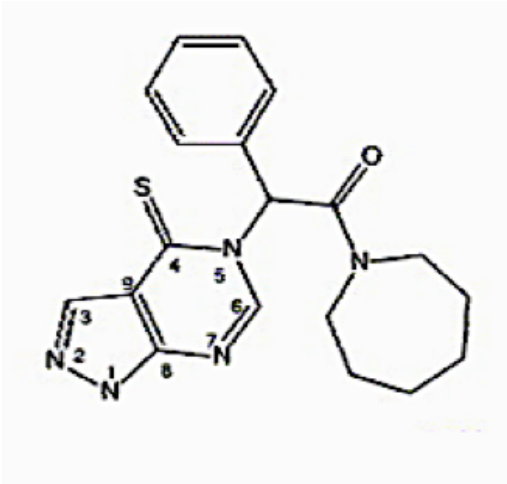

Fig. 5.11. Chemical structure of Pfizer compound AG18501.

AG18501 inhibited ABAD activity with an IC_{50} = 92nM. The crystallographic studies showed AG18501 bound to the substrate-binding cavity of ABAD simultaneously also binding to the cofactor NAD^+. Isothermal titration calorimetry (ITC) confirmed the necessity of NAD^+ to be present for AG18501 to be active (Kissinger *et al*., 2004). Further studies with AG18051 showed no detectable inhibition of two closely related members of the SDR family, at concentrations as high as 100 μM, showing AG18501 to be a novel small molecule specific inhibitor for ABAD. A very recent study has now indicated that AG18501 also prevents the ABAD/Aβ interaction (Lim *et al*., 2011). As such AG18501 shows a neuroprotective effect in vitro, promoting cell survival in part by preventing the generation of ROS and stabilizing estradiol levels. This is significant as one of ABAD's functions is to convert estrone to estradiol, and this is disrupted in the ABAD/Aβ interaction (Yang *et al*., 2007).

In another study, (Xie *et al*., 2006) frentizole (1-(6-Methoxybenzothiazol-2-yl)-3-phenylurea, Figure 5.12) was found to also act as an inhibitor of the Aβ binding to ABAD.

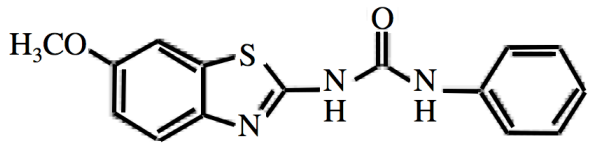

Fig. 5.12. Chemical structure of frentizole.

Frentizole is a benzothiazole urea, an analogue of thioflavine T, which was initially identified as the inhibitor of the ABAD/Aβ interaction. Frentizole is a Food and Drug Administration (FDA) approved immunosuppressive drug and is a non-toxic antiviral agent used clinically in rheumatoid arthritis and systemic lupus erythematosus (Xie *et al*., 2006). Analogues of frentizole were developed with variations at the aromatic rings and their linking group. Two analogues where identified as the most potent inhibitors with IC50s of <10uM. These were low molecular weight compounds with logP values of 1.34 and 1.15 show a good possibility of crossing the blood brain barrier, and so are being further tested for their CNS penetration capability and will be tested on animal models if successful.

However, finding suitable therapeutics for AD is complicated by the need to find drugs that are suitable for the target patients, i.e. the elderly. Frentizole has already been used clinically as an immunosuppressive drug and as an antiviral in the USA, but as with many drugs, it has notable side-effects that would not be recommended for treatment of the elderly e.g. hepatic toxicity (Kay *et al*., 1980).

In addition, though Kissinger and Lim have produced specific inhibitor of a mitochondrial dysfunction, inhibiting the ABAD/Aβ interaction *in vitro*, it remains whether these compounds will work *in vivo*.

In the last decade FBS has become the chosen method for initial screening for small molecule therapeutic compounds against a biological target of interest (Erlanson *et al*., 2004a). In this initial study, ABAD was screened with the first 88 compounds of the Maybridge Ro3 library and 23 of these were shown to bind producing a thermal shift ≥3°C. In addition, limited initial screening of ABAD with its cofactor NAD^+ also showed another two compounds that bound, producing a thermal shift >2°C.

These screens need repeating for verification and expanded to include the whole library for a complete analysis of possible combinations of ligand binding with ABAD/Aβ complex. Also further screens should include conditions when the ABAD protein is in an ABAD/Aβ complex with the FBS compounds, but also in the presence of NAD^+ and a substrate such as acetoacyl CoA. It is important to examine ABAD as an active enzyme with its substrates and products, as the binding of any of these molecules could affect the binding with the Aβ peptide and the FBS compounds. Screening the Aβ peptide alone will also give useful information on ligand binding to the peptide without ABAD. With optimised conditions for protein, cofactor, substrate, peptide and compounds, FBS will provide information on good ligand binding to ABAD/Aβ complex. Screening using the 1000 Maybridge compounds aims to provide approximately 50 lead

compounds (5% of total). The ligand binding of these compounds could next be verified further using the NMR technique of Saturation Transfer Difference (STD) (Haselhorst *et al*., 2009). This is a robust technique suitable for proteins approximately 30kDa or larger, which can detect weak binding ligands with a K_d ~10mM. The compounds finally verified by NMR, can then act as chemical building blocks for further manipulation and synthesis in collaboration with combinatorial chemists. This information will complement other kinetic, SPR, NMR (Yan *et al*., 2007b) and crystallographic information known for ABAD (Lustbader *et al*., 2004; Powell *et al*., 2000).

In summary the availability of potent, specific inhibitors of ABAD should help elucidate the role of this enzyme in AD pathogenesis. FBS is a very useful technique for finding lead compounds for possible drug development by identifying small molecule compounds that bind to ABAD and the ABAD/Aβ complex. These starting compounds can then be manipulated to synthesise larger compounds with a higher binding efficiency. The study presented here has identified 25 lead compounds that bind to ABAD. These are presented for consideration as the starting point of future therapeutic strategies that will hopefully provide new compounds for the treatment of AD.

Chapter 6

Thesis summary and discussion

Alzheimer's disease remains a non-discriminating disease, mainly affecting the elderly, for which there is no curative treatment or a diagnostic biomarker to monitor progression of the disease. It is characterised by accumulation of extracellular amyloid plaques and intracellular neurofibrillary tangles in the brain (Selkoe and Abraham, 1986). Treatments at present have not developed from using acetyl-cholinesterase inhibitors to alleviate the symptoms, and/or the introduction of an NMDA receptor inhibitor that also alleviates symptoms. None of these treatments halt or cure the disease (Herrmann *et al.*, 2011a). Current research into possible treatments concentrates on reducing the expression or activity of the toxic Aβ peptide or preventing the production of hyperphosphorylated tau. This includes development of β-secretase inhibitors and inhibitors of tau aggregation (Herrmann *et al.*, 2011a).

Mitochondrial dysfunction has been shown to play a major role in neurodegenerative diseases including AD (Brown *et al.*, 2001). Therefore, the causes and consequences of mitochondrial dysfunction in AD might impact on future therapeutic approaches to this disease. Mitochondrial dysfunction in AD was first recognized by analysis of two mitochondrial proteins, pyruvate dehydrogenase and α ketoglutarate dehydrogenase, the rate-limiting steps of the Krebs cycle, that showed defects in energy metabolism (Gibson *et al.*, 1998). Neuropsychological deficits similar to those in AD are seen in other situations e.g.

hypoglycemia in diabetics, hypoxic hypoxia, urinary tract infections in the elderly and vitamin deficiencies (Gibson and Duffy, 1981; Gibson *et al*., 1981) but these are temporary and reversible. In AD, the neuropsychological deficits become irreversible.

ABAD is a mitochondrial protein that was first identified by a yeast 2 hybrid screen as an intracellular binding partner to the Aβ peptide (Yan *et al.*, 1997a). ABAD is an enzyme whose primary function is catalysing the third stage of the β-oxidation of fatty acids.

This thesis began by establishing a reliable *in vitro* cytotoxic system. This system used SK-N-SH neuroblastoma cell culture to confirm expression and/or translocation of ABAD within the cell. Further toxicity experiments used this cell line with the addition of a synthetic Aβ42 peptide. At first a stably transfected SK-N-SH cell line was developed, expressing ABAD fused with EGFP. Transient transfections of ABAD-EGFP produced inconsistent ABAD expression, often with apparent non-targeted expression of the EGFP tagged protein within the cell. This had been previously reported (He *et al.*, 2001), and so expression was improved by two approaches. First, a stable expressing cell-line was produced that indicated that when the ABAD-EGFP fusion protein was expressed this resulted in exclusive expression within the mitochondria. Second, a mitochondrial targeting sequence (MTS) was added to the N-terminus of the fusion protein, which produced well-targeted expression in mitochondria. This construct enabled the design of further experiments using transient transfection of cells.

Further studies investigated the toxic effect of the ABAD/Aβ interaction. Using the stable cell line, live fluorescent imaging over a 24hr period showed the toxic effects of incubating the cells with a synthetic Aβ peptide in real-time. Cells died within 11hr of incubation with the peptide. To verify this result, the experiments were repeated in 96-well tissue culture dishes and analysed for cell viability using an MTT assay. The experiments were also repeated in T75 tissue culture flasks, but here the cells were harvested and fractionated to isolate the mitochondria. These fractionated samples were analysed by western blot analysis for expression of ABAD and cytochrome C, and for evidence of apoptosis by release of the proteins from the mitochondria into the cytosol. Using these three techniques, the results were not consistent. Of note was the observation that the seeding density was kept consistent but the final area for cell growth in the flasks and dishes varied greatly. The 96-well plate wells have a growth area of ~0.2 cm^2, the growth area in the Willco dish for live fluorescent imaging was ~9.5 cm^2 and the T75 flask is 75cm^2. It is possible that the difference in final cell numbers influenced the result in each case. The fluorescent imaging is the most sensitive technique, however the western blot analysis should be sensitive although we have found that antibodies vary in their sensitivity and efficiency of detection. The MTT assays were performed on the smallest number of cells and growth area. It is possible that the results were masked by the dividing cells, as SK-N-SH cells are known to clump when over confluent (Biedler *et al.*, 1973).

It was unclear for some time how ABAD and the Aβ peptide interacted within the cell. ABAD is expressed in the mitochondrial matrix. The Aβ peptide is the result of proteolytic cleavage of the APP protein and was originally thought to be

cleaved outside the cell, aggregated and formed the recognisable plaques identified in AD. However Aβ exists in several forms ranging from soluble monomers, to intermediate soluble oligomers, to insoluble fibrils and has been shown to enter the cell and the mitochondria *in vitro* by two pathways, direct import and localised synthesis. The soluble Aβ has been shown to enter the cell and has been identified in the mitochondria with ABAD (Lustbader *et al.*, 2004). Translocation of APP and Aβ has been shown to be dependent on the mitochondrial translocase, via the mitochondrial receptors TOM20, TOM70 and the general mitochondrial import pore of the outer membrane TOM40 and also the translocase of the inner membrane TIM23 (Hansson Petersen *et al.*, 2008). The translocase system imports Aβ40 directly into the mitochondria of neuroblastoma cells, SH-SY5Y. Both Aβ40 and Aβ42 were imported into isolated rat liver mitochondria by the same mechanism. The translocation of Aβ into mitochondria is independent of the mitochondrial membrane potential. Aβ40 was clearly associated with the mitochondrial inner membrane and not the matrix. Gold labelling of Aβ42 showed 75% of the peptide in mitochondrial cristae, 18% in matrix and 7% outer membrane (Hansson Petersen *et al.*, 2008). These results provide evidence for the ABAD/Aβ42 interaction in the mitochondria.

Many of the cellular experiments performed in this thesis exhibited problems with the synthetic Aβ42 peptide used, which gave inconsistent results. The synthetic peptide was provided in a non-toxic lyophilised form, reconstituted in dH_2O to a concentration of 5 mg ml^{-1} and then further dilution with buffer to 1 mg ml^{-1}, then aliquoted and frozen at -20^0C until required. The manufacturers recommended

pre-incubation at 37^0C for 24–36 hr before use, however trials incubating at different concentrations and for different times, indicated that an optimum concentration of 20μM incubated for 12hrs produced the most toxic sample. Immunostaining cells after incubation with this Aβ peptide, showed that the peptide aggregated outside of the cells (Figure 3.23). Other studies at that time had identified that it was the soluble monomeric and oligomeric form of Aβ that was most toxic (Kayed and Glabe, 2006). Electron microscopy of the pre-incubated peptide, showed that the Aβ peptide formed mainly fibrils (Figure 3.24). This most likely explained the problems of inconsistent toxicity using this product. It was also thought that fibrillar Aβ may be protective by sequestering the Aβ into deposits (Tomiyama, 2010). Two other methods were therefore used to introduce Aβ into the cell to investigate the ABAD/Aβ interaction. First, transient transfection with a mutated full-length form of the APP molecule (mAPP) into the ABAD-EGFP stably expressing SK-N-SH cells produced an excess of the Aβ peptide within the cells and cell death was observed within 48hrs. Another method used a carrier peptide (Chariot® Active Motif) to permeabolise the cell membrane and carry the Aβ peptide inside the cell and cell death was noted within 4hrs. Toxic effects were seen with both these methods by fluorescent microscopy, indicating that when Aβ and ABAD are in close proximity a strong toxic effect occurs. When soluble oligomeric peptide was obtained, a lower concentration of the peptide (nM) showed strong toxic effects, compared to the μM concentration with the synthetic peptide. There are now more reliable recombinant Aβ peptides, which prove to be more soluble, due to the purification techniques used, e.g. expressed as a fusion protein, with ubiquitin,

preventing aggregation (Lee *et al*., 2005). Evidence also suggests they are more toxic *in vitro* and *in vivo* (Finder *et al*., 2009).

The results from this thesis indicate that the SK-N-SH cell line may not be the best neuronal cell line to investigate Aβ toxicity, as there are studies that indicate that the cell line promotes a protective mechanism on the cells particularly when seeded at high density (Ba *et al.*, 2003). Experiments in this thesis could not conclusively show that Aβ induced apoptosis in the SK-N-SH cells. Another study also had evidence that Aβ was not able to induce apoptosis in this cell line (Ba *et al.*, 2003). To establish a more reliable system, murine neurospheres were cultured and some preliminary fluorescent microscopy experiments showed it to be a robust and useful system to use in the future.

The *in vitro* cytotoxic system used for this thesis was problematic but was able to show toxic effects in the cells when ABAD and Aβ interacted. This *in vitro* system could be improved for the future by the use of soluble monomeric Aβ and culturing murine neurospheres.

Further information on downstream effects of the ABAD/Aβ complex was investigated by proteomic studies using 2D gel electrophoresis and mass spectrometry analysis. Methodological limitations in 2D gel electrophoresis proteomics have been reviewed previously (Garbis *et al.*, 2005). Proteins at the extremes of the pI or MW range are generally not included due to the physical limitations of the equipment used. And although tissue samples are prepared in a

denaturing buffer containing 8M urea, some very insoluble proteins will not be mobilised, which may include many membrane proteins. 2D gel electrophoresis cannot identify all proteins but it does contribute to the wider knowledge of AD when used with other cell and animal studies. The studies for this thesis were carried out using samples from two novel transgenic mouse models for AD, developed by Prof. Shi Du Yan (Columbia University, NY, USA). The mouse models expressed ABAD (Tg ABAD) or ABAD with mutant APP (2 x Tg mAPP/ABAD). Proteomic analysis of mouse brains by 2D gel electrophoresis was carried out using these transgenic mice. Seven proteins of interest linked with AD were identified: ApoE, PrxII, ATP synthase β subunit, creatine kinase β subunit, SDH, GPDH and endophilin I. The first six were involved with maintaining energy metabolism in the cell, only endophilin I was involved in activating JNK and promoting cell death. Three of the proteins were mitochondrial (ATP synthase, SDH and GPDH), promoting mitochondrial function and ATP synthesis. Five proteins were up regulated (ApoE, PrxII, ATP synthase β subunit, creatine kinase β subunit, and endophilin I) and two of the mitochondrial proteins were down regulated (SDH and GPDH) in the transgenic model compared to the WT. Further experiments identified that PrxII and endophilin I were over expressed in a 4-month, early AD mouse model (Table 4.3). These results indicate that the ABAD/Aβ complex activates protein expression, of which several are involved in mitochondrial function. The proteins expressed as a result of this complex mainly try to promote and sustain cellular health with only endophilin I involved in the destruction of the cells. This has since been confirmed and several studies on the ABAD/Aβ complex now show it to be involved in mitochondrial dysfunction (Ren *et al.*, 2008; Yao *et al.*, 2007).

The proteomic studies for this thesis have contributed to the wider knowledge of AD.

Because of its involvement with mitochondrial dysfunction in AD, the ABAD/Aβ complex could be a useful target for therapy in AD. However as ABAD is essential for fatty acid metabolism it is important not to alter its normal catalytic activity. *Conversely* the ABAD/Aβ complex requires ABAD catalytic activity to mediate the Aβ toxicity. A compound that could inhibit the complex forming without affecting normal ABAD function may add to the therapeutic strategies to alleviate AD.

Fragment based screening is a very efficient method for drug discovery (Erlanson *et al.*, 2004a). It provides multiple small lead compounds that are then linked or expanded to produce a larger therapeutic end product. An in-house library of 1000 compounds has been developed, based on the commercially available Maybridge fragment library. Some initial screens were carried out with ABAD and ABAD with NAD^+, its cofactor. Several compounds were identified that bound to ABAD or ABAD with NAD^+ making it more stable. This screen used approximately 100 compounds and has led the way for further screening including ABAD in the presence of the Aβ peptide. The complete library has now been screened (data unpublished). It is important that any hits from the thermal shift screening are confirmed by other biophysical methods such as NMR and SPR, as these preliminary screening methods can produce false positive hits. Ultimately, X-ray crystallography will allow a definitive view of the binding of any of these fragments to confirm that they are structurally relevant for chemical elaboration.

These future studies will require close collaboration with synthetic chemists to develop a novel compound suitable to prevent the toxic effects of the ABAD/Aβ complex.

This thesis has studied a novel protein-Aβ complex that has subsequently been shown to be involved in mitochondrial dysfunction in AD. Expansion of the techniques and methods used may contribute towards a better understanding of the pathogenesis and therapeutic treatment of AD.

Bibliography

Abraham, M.H. (2010). The permeation of neutral molecules, ions, and ionic species through membranes: Brain permeation as an example. J Pharm Sci. *100*, 1690-1701.

Acevedo, K.M., Hung, Y.H., Dalziel, A.H., Li, Q.X., Laughton, K., Wikhe, K., Rembach, A., Roberts, B., Masters, C.L., Bush, A.I., and Camakaris, J. (2011). Copper promotes the trafficking of the amyloid precursor protein. J Biol Chem *286*, 8252-8262.

Ackrell, B.A. (2000). Progress in understanding structure-function relationships in respiratory chain complex II. FEBS Lett *466*, 1-5.

Aisen, P.S. (2002). Anti-inflammatory agents in Alzheimer's disease. Curr Neurol Neurosci Rep *2*, 405-409.

Aisen, P.S., Gauthier, S., Vellas, B., Briand, R., Saumier, D., Laurin, J., and Garceau, D. (2007). Alzhemed: a potential treatment for Alzheimer's disease. Curr Alzheimer Res *4*, 473-478.

Aksenov, M.Y., Aksenova, M.V., Butterfield, D.A., Geddes, J.W., and Markesbery, W.R. (2001). Protein oxidation in the brain in Alzheimer's disease. Neuroscience *103*, 373-383.

Alpert, J.S., Thygesen, K., Antman, E., and Bassand, J.P. (2000). Myocardial infarction redefined--a consensus document of The Joint European Society of Cardiology/American College of Cardiology Committee for the redefinition of myocardial infarction. J Am Coll Cardiol *36*, 959-969.

Amtul, Z., Uhrig, M., Rozmahel, R.F., and Beyreuther, K. (2011). Structural insight into the differential effects of omega-3 and omega-6 fatty acids on the production of Abeta peptides and amyloid plaques. J Biol Chem *286*, 6100-6107.

Anandatheerthavarada, H.K., Biswas, G., Robin, M.A., and Avadhani, N.G. (2003). Mitochondrial targeting and a novel transmembrane arrest of Alzheimer's amyloid precursor protein impairs mitochondrial function in neuronal cells. J Cell Biol *161*, 41-54.

Angers, A., Ramjaun, A.R., and McPherson, P.S. (2004). The HECT domain ligase itch ubiquitinates endophilin and localizes to the trans-Golgi network and endosomal system. J Biol Chem *279*, 11471-11479.

Ba, F., Pang, P.K., and Benishin, C.G. (2003). The establishment of a reliable cytotoxic system with SK-N-SH neuroblastoma cell culture. J Neurosci Methods *123*, 11-22.

Baker, L.D., Frank, L.L., Foster-Schubert, K., Green, P.S., Wilkinson, C.W., McTiernan, A., Plymate, S.R., Fishel, M.A., Watson, G.S., Cholerton, B.A., Duncan, G.E., Mehta, P.D., and Craft, S. (2010). Effects of aerobic exercise on mild cognitive impairment: a controlled trial. Arch Neurol *67*, 71-79.

Barberger-Gateau, P., Raffaitin, C., Letenneur, L., Berr, C., Tzourio, C., Dartigues, J.F., and Alperovitch, A. (2007). Dietary patterns and risk of dementia: the Three-City cohort study. Neurology *69*, 1921-1930.

Barger, S.W., DeWall, K.M., Liu, L., Mrak, R.E., and Griffin, W.S. (2008). Relationships between expression of apolipoprotein E and beta-amyloid precursor protein are altered in proximity to Alzheimer beta-amyloid plaques: potential explanations from cell culture studies. J Neuropathol Exp Neurol *67*, 773-783.

Barrett, P.J., Sanders, C.R., Kaufman, S.A., Michelsen, K., and Jordan, J.B. (2011). NSAID-based gamma-secretase modulators do not bind to the amyloid-beta polypeptide. Biochemistry *50*, 10328-10342.

Barycki, J.J., O'Brien, L.K., Strauss, A.W., and Banaszak, L.J. (2000). Sequestration of the active site by interdomain shifting. Crystallographic and spectroscopic

evidence for distinct conformations of L-3-hydroxyacyl-CoA dehydrogenase. J Biol Chem *275*, 27186-27196.

Baumeister, R., Leimer, U., Zweckbronner, I., Jakubek, C., Grunberg, J., and Haass, C. (1997). Human presenilin-1, but not familial Alzheimer's disease (FAD) mutants, facilitate Caenorhabditis elegans Notch signalling independently of proteolytic processing. Genes Funct *1*, 149-159.

Behl, C., Davis, J.B., Klier, F.G., and Schubert, D. (1994). Amyloid beta peptide induces necrosis rather than apoptosis. Brain Res *645*, 253-264.

Bentahir, M., Nyabi, O., Verhamme, J., Tolia, A., Horre, K., Wiltfang, J., Esselmann, H., and De Strooper, B. (2006). Presenilin clinical mutations can affect gamma-secretase activity by different mechanisms. J Neurochem *96*, 732-742.

Biedler, J.L., Helson, L., and Spengler, B.A. (1973). Morphology and growth, tumorigenicity, and cytogenetics of human neuroblastoma cells in continuous culture. Cancer Res *33*, 2643-2652.

Birktoft, J.J., Holden, H.M., Hamlin, R., Xuong, N.H., and Banaszak, L.J. (1987). Structure of L-3-hydroxyacyl-coenzyme A dehydrogenase: preliminary chain tracing at 2.8-A resolution. Proc Natl Acad Sci U S A *84*, 8262-8266.

Bliss, T.V., and Collingridge, G.L. (1993). A synaptic model of memory: long-term potentiation in the hippocampus. Nature *361*, 31-39.

Braak, H., and Braak, E. (1991). Neuropathological stageing of Alzheimer-related changes. Acta Neuropathol *82*, 239-259.

Braak, H., and Braak, E. (1996). Development of Alzheimer-related neurofibrillary changes in the neocortex inversely recapitulates cortical myelogenesis. Acta Neuropathol *92*, 197-201.

Breteler, M.M. (2000). Vascular risk factors for Alzheimer's disease: an epidemiologic perspective. Neurobiol Aging *21*, 153-160.

Brown, A.M., Sheu, R.K., Mohs, R., Haroutunian, V., and Blass, J.P. (2001). Correlation of the clinical severity of Alzheimer's disease with an aberration in mitochondrial DNA (mtDNA). J Mol Neurosci *16*, 41-48.

Butterfield, D.A. (2002). Amyloid beta-peptide (1-42)-induced oxidative stress and neurotoxicity: implications for neurodegeneration in Alzheimer's disease brain. A review. Free Radic Res *36*, 1307-1313.

Butterfield, D.A., Abdul, H.M., Opii, W., Newman, S.F., Joshi, G., Ansari, M.A., and Sultana, R. (2006). Pin1 in Alzheimer's disease. J Neurochem *98*, 1697-1706.

Butterfield, D.A., Boyd-Kimball, D., and Castegna, A. (2003). Proteomics in Alzheimer's disease: insights into potential mechanisms of neurodegeneration. J Neurochem *86*, 1313-1327.

Campion, D., Dumanchin, C., Hannequin, D., Dubois, B., Belliard, S., Puel, M., Thomas-Anterion, C., Michon, A., Martin, C., Charbonnier, F., Raux, G., Camuzat, A., Penet, C., Mesnage, V., Martinez, M., Clerget-Darpoux, F., Brice, A., and Frebourg, T. (1999). Early-onset autosomal dominant Alzheimer disease: prevalence, genetic heterogeneity, and mutation spectrum. Am J Hum Genet *65*, 664-670.

Carlson, C., Estergard, W., Oh, J., Suhy, J., Jack, C.R., Jr., Siemers, E., and Barakos, J. (2011). Prevalence of asymptomatic vasogenic edema in pretreatment Alzheimer's disease study cohorts from phase 3 trials of semagacestat and solanezumab. Alzheimers Dement *7*, 396-401.

Carpenter, M.K., Crutcher, K.A., and Kater, S.B. (1993). An analysis of the effects of Alzheimer's plaques on living neurons. Neurobiol Aging *14*, 207-215.

Carver, E.A., and Stubbs, L. (1997). Zooming in on the human-mouse comparative map: genome conservation re-examined on a high-resolution scale. Genome Res *7*, 1123-1137.

Caspersen, C., Wang, N., Yao, J., Sosunov, A., Chen, X., Lustbader, J.W., Xu, H.W., Stern, D., McKhann, G., and Yan, S.D. (2005). Mitochondrial Abeta: a potential focal point for neuronal metabolic dysfunction in Alzheimer's disease. FASEB J *19*, 2040-2041.

Castegna, A., Aksenov, M., Thongboonkerd, V., Klein, J.B., Pierce, W.M., Booze, R., Markesbery, W.R., and Butterfield, D.A. (2002). Proteomic identification of oxidatively modified proteins in Alzheimer's disease brain. Part II: dihydropyrimidinase-related protein 2, alpha-enolase and heat shock cognate 71. J Neurochem *82*, 1524-1532.

Castegna, A., Lauderback, C.M., Mohmmad-Abdul, H., and Butterfield, D.A. (2004). Modulation of phospholipid asymmetry in synaptosomal membranes by the lipid peroxidation products, 4-hydroxynonenal and acrolein: implications for Alzheimer's disease. Brain Res *1004*, 193-197.

Chen, X., Walker, D.G., Schmidt, A.M., Arancio, O., Lue, L.F., and Yan, S.D. (2007). RAGE: a potential target for Abeta-mediated cellular perturbation in Alzheimer's disease. Curr Mol Med *7*, 735-742.

Christensen, D.Z., Bayer, T.A., and Wirths, O. (2008a). Intracellular Abeta triggers neuron loss in the cholinergic system of the APP/PS1KI mouse model of Alzheimer's disease. Neurobiol Aging *31*, 1153-1163.

Christensen, D.Z., Kraus, S.L., Flohr, A., Cotel, M.C., Wirths, O., and Bayer, T.A. (2008b). Transient intraneuronal A beta rather than extracellular plaque pathology correlates with neuron loss in the frontal cortex of APP/PS1KI mice. Acta Neuropathol *116*, 647-655.

Citron, M., Westaway, D., Xia, W., Carlson, G., Diehl, T., Levesque, G., Johnson-Wood, K., Lee, M., Seubert, P., Davis, A., Kholodenko, D., Motter, R., Sherrington, R., Perry, B., Yao, H., Strome, R., Lieberburg, I., Rommens, J., Kim, S., Schenk, D., Fraser, P., St George Hyslop, P., and Selkoe, D.J. (1997). Mutant presenilins of Alzheimer's disease increase production of 42-residue amyloid beta-protein in both transfected cells and transgenic mice. Nat Med *3*, 67-72.

Ciulli, A., and Abell, C. (2007). Fragment-based approaches to enzyme inhibition. Curr Opin Biotechnol *18*, 489-496.

Clancy, B., Darlington, R.B., and Finlay, B.L. (2001). Translating developmental time across mammalian species. Neuroscience *105*, 7-17.

Cole, G.M., Morihara, T., Lim, G.P., Yang, F., Begum, A., and Frautschy, S.A. (2004). NSAID and antioxidant prevention of Alzheimer's disease: lessons from in vitro and animal models. Ann N Y Acad Sci *1035*, 68-84.

Collin, R.W., and Martens, G.J. (2006). The coding sequence of amyloid-beta precursor protein APP contains a neural-specific promoter element. Brain Res *1087*, 41-51.

Comas-Herrera, A., Wittenberg, R., Pickard, L., and Knapp, M. (2003). Cognitive Impairment in Older People: Its Implications for Future Demand for Services and Costs - Report to the Alzheimer's Research Trust (London School of Economics).

Congreve, M., Carr, R., Murray, C., and Jhoti, H. (2003). A 'rule of three' for fragment-based lead discovery? Drug Discov Today *8*, 876-877.

Corder, E.H., Robertson, K., Lannfelt, L., Bogdanovic, N., Eggertsen, G., Wilkins, J., and Hall, C. (1998). HIV-infected subjects with the E4 allele for APOE have excess dementia and peripheral neuropathy. Nat Med *4*, 1182-1184.

Cotman, C.W., and Su, J.H. (1996). Mechanisms of neuronal death in Alzheimer's disease. Brain Pathol *6*, 493-506.

Crook, R., Ellis, R., Shanks, M., Thal, L.J., Perez-Tur, J., Baker, M., Hutton, M., Haltia, T., Hardy, J., and Galasko, D. (1997). Early-onset Alzheimer's disease with a presenilin-1 mutation at the site corresponding to the Volga German presenilin-2 mutation. Ann Neurol *42*, 124-128.

Dahlgren, K.N., Manelli, A.M., Stine, W.B., Jr., Baker, L.K., Krafft, G.A., and LaDu, M.J. (2002). Oligomeric and fibrillar species of amyloid-beta peptides differentially affect neuronal viability. J Biol Chem *277*, 32046-32053.

Dangour, A.D., Whitehouse, P.J., Rafferty, K., Mitchell, S.A., Smith, L., Hawkesworth, S., and Vellas, B. (2010). B-vitamins and fatty acids in the prevention and treatment of Alzheimer's disease and dementia: a systematic review. J Alzheimers Dis *22*, 205-224.

De Meyer, G., Shapiro, F., Vanderstichele, H., Vanmechelen, E., Engelborghs, S., De Deyn, P.P., Coart, E., Hansson, O., Minthon, L., Zetterberg, H., Blennow, K., Shaw, L., and Trojanowski, J.Q. (2010). Diagnosis-independent Alzheimer disease biomarker signature in cognitively normal elderly people. Arch Neurol *67*, 949-956.

De Strooper, B., and Annaert, W. (2000). Proteolytic processing and cell biological functions of the amyloid precursor protein. J Cell Sci *113 (Pt 11)*, 1857-1870.

De Strooper, B., Annaert, W., Cupers, P., Saftig, P., Craessaerts, K., Mumm, J.S., Schroeter, E.H., Schrijvers, V., Wolfe, M.S., Ray, W.J., Goate, A., and Kopan, R. (1999). A presenilin-1-dependent gamma-secretase-like protease mediates release of Notch intracellular domain. Nature *398*, 518-522.

Deane, R., Du Yan, S., Submamaryan, R.K., LaRue, B., Jovanovic, S., Hogg, E., Welch, D., Manness, L., Lin, C., Yu, J., Zhu, H., Ghiso, J., Frangione, B., Stern, A., Schmidt, A.M., Armstrong, D.L., Arnold, B., Liliensiek, B., Nawroth, P., Hofman, F., Kindy, M., Stern, D., and Zlokovic, B. (2003). RAGE mediates

amyloid-beta peptide transport across the blood-brain barrier and accumulation in brain. Nat Med *9*, 907-913.

Deane, R., Sagare, A., Hamm, K., Parisi, M., Lane, S., Finn, M.B., Holtzman, D.M., and Zlokovic, B.V. (2008). apoE isoform-specific disruption of amyloid beta peptide clearance from mouse brain. J Clin Invest *118*, 4002-4013.

Deiana, S., Harrington, C.R., Wischik, C.M., and Riedel, G. (2009). Methylthioninium chloride reverses cognitive deficits induced by scopolamine: comparison with rivastigmine. Psychopharmacology (Berl) *202*, 53-65.

Delibas, N., Ozcankaya, R., and Altuntas, I. (2002). Clinical importance of erythrocyte malondialdehyde levels as a marker for cognitive deterioration in patients with dementia of Alzheimer type: a repeated study in 5-year interval. Clin Biochem *35*, 137-141.

Devi, L., and Anandatheerthavarada, H.K. (2010). Mitochondrial trafficking of APP and alpha synuclein: Relevance to mitochondrial dysfunction in Alzheimer's and Parkinson's diseases. Biochim Biophys Acta *1802*, 11-19.

Devi, L., Prabhu, B.M., Galati, D.F., Avadhani, N.G., and Anandatheerthavarada, H.K. (2006). Accumulation of amyloid precursor protein in the mitochondrial import channels of human Alzheimer's disease brain is associated with mitochondrial dysfunction. J Neurosci *26*, 9057-9068.

Driver, J.A., and Lu, K.P. (2010). Pin1: a new genetic link between Alzheimer's disease, cancer and aging. Curr Aging Sci *3*, 158-165.

Du, H., Guo, L., Fang, F., Chen, D., Sosunov, A.A., McKhann, G.M., Yan, Y., Wang, C., Zhang, H., Molkentin, J.D., Gunn-Moore, F.J., Vonsattel, J.P., Arancio, O., Chen, J.X., and Yan, S.D. (2008). Cyclophilin D deficiency attenuates mitochondrial and neuronal perturbation and ameliorates learning and memory in Alzheimer's disease. Nat Med *14*, 1097-1105.

Duyckaerts, C., Potier, M.C., and Delatour, B. (2008). Alzheimer disease models and human neuropathology: similarities and differences. Acta Neuropathol *115*, 5-38.

Eckert, A., Schulz, K.L., Rhein, V., and Gotz, J. (2010). Convergence of amyloid-beta and tau pathologies on mitochondria in vivo. Mol Neurobiol *41*, 107-114.

Engel, C.K., Mathieu, M., Zeelen, J.P., Hiltunen, J.K., and Wierenga, R.K. (1996). Crystal structure of enoyl-coenzyme A (CoA) hydratase at 2.5 angstroms resolution: a spiral fold defines the CoA-binding pocket. EMBO J *15*, 5135-5145.

Erlanson, D.A., McDowell, R.S., and O'Brien, T. (2004a). Fragment-based drug discovery. J Med Chem *47*, 3463-3482.

Erlanson, D.A., Wells, J.A., and Braisted, A.C. (2004b). Tethering: fragment-based drug discovery. Annu Rev Biophys Biomol Struct *33*, 199-223.

Esler, W.P., Marshall, J.R., Stimson, E.R., Ghilardi, J.R., Vinters, H.V., Mantyh, P.W., and Maggio, J.E. (2002). Apolipoprotein E affects amyloid formation but not amyloid growth in vitro: mechanistic implications for apoE4 enhanced amyloid burden and risk for Alzheimer's disease. Amyloid *9*, 1-12.

Fabbro, D., Parkinson, D., and Matter, A. (2002). Protein tyrosine kinase inhibitors: new treatment modalities? Curr Opin Pharmacol *2*, 374-381.

Filling, C., Keller, B., Hirschberg, D., Marschall, H.U., Jornvall, H., Bennett, M.J., and Oppermann, U. (2008). Role of short-chain hydroxyacyl CoA dehydrogenases in SCHAD deficiency. Biochem Biophys Res Commun *368*, 6-11.

Filling, C., Wu, X., Shafqat, N., Hult, M., Martensson, E., Shafqat, J., and Oppermann, U.C. (2001). Subcellular targeting analysis of SDR-type hydroxysteroid dehydrogenases. Mol Cell Endocrinol *171*, 99-101.

Finder, V.H., Vodopivec, I., Nitsch, R.M., and Glockshuber, R. (2009). The recombinant amyloid-beta peptide Abeta1-42 aggregates faster and is more neurotoxic than synthetic Abeta1-42. J Mol Biol *396*, 9-18.

Finlay, B.L., and Darlington, R.B. (1995). Linked regularities in the development and evolution of mammalian brains. Science *268*, 1578-1584.

Finlay, B.L., Darlington, R.B., and Nicastro, N. (2001). Developmental structure in brain evolution. Behav Brain Sci *24*, 263-278; discussion 278-308.

Fodero-Tavoletti, M.T., Rowe, C.C., McLean, C.A., Leone, L., Li, Q.X., Masters, C.L., Cappai, R., and Villemagne, V.L. (2009). Characterization of PiB binding to white matter in Alzheimer disease and other dementias. J Nucl Med *50*, 198-204.

Foehr (2000). The NF-B-inducing Kinase Induces PC12 Cell Differentiation and Prevents Apoptosis*. JBC *275*, 34021-34024.

Folstein, M.F., Folstein, S.E., and McHugh, P.R. (1975). "Mini-mental state". A practical method for grading the cognitive state of patients for the clinician. J Psychiatr Res *12*, 189-198.

Frackowiak, J., Mazur-Kolecka, B., Kaczmarski, W., and Dickson, D. (2001). Deposition of Alzheimer's vascular amyloid-beta is associated with decreased expression of brain L-3-hydroxyacyl-coenzyme A dehydrogenase (ERAB). Brain Res *907*, 44-53.

Fraser, P.E., Nguyen, J.T., Inouye, H., Surewicz, W.K., Selkoe, D.J., Podlisny, M.B., and Kirschner, D.A. (1992). Fibril formation by primate, rodent, and Dutch-hemorrhagic analogues of Alzheimer amyloid beta-protein. Biochemistry *31*, 10716-10723.

Fukumoto, H., Tokuda, T., Kasai, T., Ishigami, N., Hidaka, H., Kondo, M., Allsop, D., and Nakagawa, M. (2010). High-molecular-weight beta-amyloid oligomers are elevated in cerebrospinal fluid of Alzheimer patients. FASEB J *24*, 2716-2726.

Garbis, S., Lubec, G., and Fountoulakis, M. (2005). Limitations of current proteomics technologies. J Chromatogr A *1077*, 1-18.

Gasparini, L., Ongini, E., and Wenk, G. (2004). Non-steroidal anti-inflammatory drugs (NSAIDs) in Alzheimer's disease: old and new mechanisms of action. J Neurochem *91*, 521-536.

Gelissen, I.C., Hochgrebe, T., Wilson, M.R., Easterbrook-Smith, S.B., Jessup, W., Dean, R.T., and Brown, A.J. (1998). Apolipoprotein J (clusterin) induces cholesterol export from macrophage-foam cells: a potential anti-atherogenic function? Biochem J *331 (Pt 1)*, 231-237.

Georgopoulou, N., McLaughlin, M., McFarlane, I., and Breen, K.C. (2001). The role of post-translational modification in beta-amyloid precursor protein processing. Biochem Soc Symp, 23-36.

Gibson, G.E., and Duffy, T.E. (1981). Impaired synthesis of acetylcholine by mild hypoxic hypoxia or nitrous oxide. J Neurochem *36*, 28-33.

Gibson, G.E., Pulsinelli, W., Blass, J.P., and Duffy, T.E. (1981). Brain dysfunction in mild to moderate hypoxia. Am J Med *70*, 1247-1254.

Gibson, G.E., Sheu, K.F., and Blass, J.P. (1998). Abnormalities of mitochondrial enzymes in Alzheimer disease. J Neural Transm *105*, 855-870.

Glabe, C.C. (2005). Amyloid accumulation and pathogensis of Alzheimer's disease: significance of monomeric, oligomeric and fibrillar Abeta. Subcell Biochem *38*, 167-177.

Glenner, G.G., and Wong, C.W. (1984). Alzheimer's disease and Down's syndrome: sharing of a unique cerebrovascular amyloid fibril protein. Biochem Biophys Res Commun *122*, 1131-1135.

Glicksman, M.A., Cuny, G.D., Liu, M., Dobson, B., Auerbach, K., Stein, R.L., and Kosik, K.S. (2007). New approaches to the discovery of cdk5 inhibitors. Curr Alzheimer Res *4*, 547-549.

Goate, A., Chartier-Harlin, M.C., Mullan, M., Brown, J., Crawford, F., Fidani, L., Giuffra, L., Haynes, A., Irving, N., James, L., and et al. (1991). Segregation of a missense mutation in the amyloid precursor protein gene with familial Alzheimer's disease. Nature *349*, 704-706.

Golabek, A.A., Soto, C., Vogel, T., and Wisniewski, T. (1996). The interaction between apolipoprotein E and Alzheimer's amyloid beta-peptide is dependent on beta-peptide conformation. J Biol Chem *271*, 10602-10606.

Goldstein, J.C., Waterhouse, N.J., Juin, P., Evan, G.I., and Green, D.R. (2000). The coordinate release of cytochrome c during apoptosis is rapid, complete and kinetically invariant. Nat Cell Biol *2*, 156-162.

Gomez-Isla, T., Hollister, R., West, H., Mui, S., Growdon, J.H., Petersen, R.C., Parisi, J.E., and Hyman, B.T. (1997). Neuronal loss correlates with but exceeds neurofibrillary tangles in Alzheimer's disease. Ann Neurol *41*, 17-24.

Gong, C.X., Liu, F., Grundke-Iqbal, I., and Iqbal, K. (2005). Post-translational modifications of tau protein in Alzheimer's disease. J Neural Transm *112*, 813-838.

Gonzalez-Gross, M., Marcos, A., and Pietrzik, K. (2001). Nutrition and cognitive impairment in the elderly. Br J Nutr *86*, 313-321.

Gotz, J., Lim, Y.A., Ke, Y.D., Eckert, A., and Ittner, L.M. (2010). Dissecting toxicity of tau and beta-amyloid. Neurodegener Dis *7*, 10-12.

Graves, A.B., Larson, E.B., Edland, S.D., Bowen, J.D., McCormick, W.C., McCurry, S.M., Rice, M.M., Wenzlow, A., and Uomoto, J.M. (1996). Prevalence of dementia and its subtypes in the Japanese American population of King County, Washington state. The Kame Project. Am J Epidemiol *144*, 760-771.

Green, R.C., Schneider, L.S., Amato, D.A., Beelen, A.P., Wilcock, G., Swabb, E.A., and Zavitz, K.H. (2009). Effect of tarenflurbil on cognitive decline and activities of daily living in patients with mild Alzheimer disease: a randomized controlled trial. JAMA *302*, 2557-2564.

Gschwind, M., and Huber, G. (1995). Apoptotic cell death induced by beta-amyloid 1-42 peptide is cell type dependent. J Neurochem *65*, 292-300.

Haass, C., and De Strooper, B. (1999). The presenilins in Alzheimer's disease--proteolysis holds the key. Science *286*, 916-919.

Haass, C., and Selkoe, D.J. (2007). Soluble protein oligomers in neurodegeneration: lessons from the Alzheimer's amyloid beta-peptide. Nat Rev Mol Cell Biol *8*, 101-112.

Hajduk, P.J., and Greer, J. (2007). A decade of fragment-based drug design: strategic advances and lessons learned. Nat Rev Drug Discov *6*, 211-219.

Han, Y.H., Kim, H.S., Kim, J.M., Kim, S.K., Yu, D.Y., and Moon, E.Y. (2005). Inhibitory role of peroxiredoxin II (Prx II) on cellular senescence. FEBS Lett *579*, 4897-4902.

Hann, M.M., Leach, A.R., and Harper, G. (2001). Molecular complexity and its impact on the probability of finding leads for drug discovery. J Chem Inf Comput Sci *41*, 856-864.

Hansson Petersen, C.A., Alikhani, N., Behbahani, H., Wiehager, B., Pavlov, P.F., Alafuzoff, I., Leinonen, V., Ito, A., Winblad, B., Glaser, E., and Ankarcrona, M. (2008). The amyloid beta-peptide is imported into mitochondria via the TOM import machinery and localized to mitochondrial cristae. Proc Natl Acad Sci U S A *105*, 13145-13150.

Hardy, J. (2009). The amyloid hypothesis for Alzheimer's disease: a critical reappraisal. J Neurochem *110*, 1129-1134.

Hardy, J.A., and Higgins, G.A. (1992). Alzheimer's disease: the amyloid cascade hypothesis. Science *256*, 184-185.

Harold, D., Abraham, R., Hollingworth, P., Sims, R., Gerrish, A., Hamshere, M.L., Pahwa, J.S., Moskvina, V., Dowzell, K., Williams, A., Jones, N., Thomas, C., Stretton, A., Morgan, A.R., Lovestone, S., Powell, J., Proitsi, P., Lupton, M.K., Brayne, C., Rubinsztein, D.C., Gill, M., Lawlor, B., Lynch, A., Morgan, K., Brown, K.S., Passmore, P.A., Craig, D., McGuinness, B., Todd, S., Holmes, C., Mann, D., Smith, A.D., Love, S., Kehoe, P.G., Hardy, J., Mead, S., Fox, N., Rossor, M., Collinge, J., Maier, W., Jessen, F., Schurmann, B., van den Bussche, H., Heuser, I., Kornhuber, J., Wiltfang, J., Dichgans, M., Frolich, L., Hampel, H., Hull, M., Rujescu, D., Goate, A.M., Kauwe, J.S., Cruchaga, C., Nowotny, P., Morris, J.C., Mayo, K., Sleegers, K., Bettens, K., Engelborghs, S., De Deyn, P.P., Van Broeckhoven, C., Livingston, G., Bass, N.J., Gurling, H., McQuillin, A., Gwilliam, R., Deloukas, P., Al-Chalabi, A., Shaw, C.E., Tsolaki, M., Singleton, A.B., Guerreiro, R., Muhleisen, T.W., Nothen, M.M., Moebus, S., Jockel, K.H., Klopp, N., Wichmann, H.E., Carrasquillo, M.M., Pankratz, V.S., Younkin, S.G., Holmans, P.A., O'Donovan, M., Owen, M.J., and Williams, J. (2009). Genome-wide association study identifies variants at CLU and PICALM associated with Alzheimer's disease. Nat Genet *41*, 1088-1093.

Haselhorst, T., Lamerz, A.C., and Itzstein, M. (2009). Saturation transfer difference NMR spectroscopy as a technique to investigate protein-carbohydrate interactions in solution. Methods Mol Biol *534*, 375-386.

He, X.Y., Merz, G., Mehta, P., Schulz, H., and Yang, S.Y. (1999a). Human brain short chain L-3-hydroxyacyl coenzyme A dehydrogenase is a single-domain multifunctional enzyme. Characterization of a novel 17beta-hydroxysteroid dehydrogenase. J Biol Chem *274*, 15014-15019.

He, X.Y., Merz, G., Yang, Y.Z., Mehta, P., Schulz, H., and Yang, S.Y. (2001). Characterization and localization of human type10 17beta-hydroxysteroid dehydrogenase. Eur J Biochem *268*, 4899-4907.

He, X.Y., Schulz, H., and Yang, S.Y. (1998). A human brain L-3-hydroxyacyl-coenzyme A dehydrogenase is identical to an amyloid beta-peptide-binding protein involved in Alzheimer's disease. J Biol Chem *273*, 10741-10746.

He, X.Y., Wen, G.Y., Merz, G., Lin, D., Yang, Y.Z., Mehta, P., Schulz, H., and Yang, S.Y. (2002). Abundant type 10 17 beta-hydroxysteroid dehydrogenase in the hippocampus of mouse Alzheimer's disease model. Brain Res Mol Brain Res *99*, 46-53.

He, X.Y., Zhang, G., Blecha, F., and Yang, S.Y. (1999b). Identity of heart and liver L-3-hydroxyacyl coenzyme A dehydrogenase. Biochim Biophys Acta *1437*, 119-123.

Head, E., Pop, V., Sarsoza, F., Kayed, R., Beckett, T.L., Studzinski, C.M., Tomic, J.L., Glabe, C.G., and Murphy, M.P. (2010). Amyloid-beta peptide and oligomers in the brain and cerebrospinal fluid of aged canines. J Alzheimers Dis *20*, 637-646.

Henderson, A.S., and Jorm, A.F. (1997). Some contributions to the epidemiology of dementia and depression. Int J Geriatr Psychiatry *12*, 145-154.

Hendrie, H.C., Hall, K.S., Pillay, N., Rodgers, D., Prince, C., Norton, J., Brittain, H., Nath, A., Blue, A. and Kaufert, J. (1993). Alzheimer's disease is rare in Cree. Int Psychogeriatr *5*, 5-14.

Herrmann, N., Chau, S.A., Kircanski, I., and Lanctot, K.L. (2011a). Current and emerging drug treatment options for Alzheimer's disease: a systematic review. Drugs *71*, 2031-2065.

Herrmann, N., Li, A., and Lanctot, K. (2011b). Memantine in dementia: a review of the current evidence. Expert Opin Pharmacother *12*, 787-800.

Hoe, H.S., and Rebeck, G.W. (2008). Regulated proteolysis of APP and ApoE receptors. Mol Neurobiol *37*, 64-72.

Hoepfner, D., Schildknegt, D., Braakman, I., Philippsen, P., and Tabak, H.F. (2005). Contribution of the endoplasmic reticulum to peroxisome formation. Cell *122*, 85-95.

Horton, K.L., Stewart, K.M., Fonseca, S.B., Guo, Q., and Kelley, S.O. (2008). Mitochondria-penetrating peptides. Chem Biol *15*, 375-382.

Hubbard, R.E. (2011). Structure-based drug discovery and protein targets in the CNS. Neuropharmacology *60*, 7-23.

Hutton, M., Perez-Tur, J., and Hardy, J. (1998). Genetics of Alzheimer's disease. Essays Biochem *33*, 117-131.

Irvine, G.B., El-Agnaf, O.M., Shankar, G.M., and Walsh, D.M. (2008). Protein aggregation in the brain: the molecular basis for Alzheimer's and Parkinson's diseases. Mol Med *14*, 451-464.

Jencks, W.P. (1981). On the attribution and additivity of binding energies. Proc Natl Acad Sci U S A *78*, 4046-4050.

Jhamandas, J.H., and MacTavish, D. (2004). Antagonist of the amylin receptor blocks beta-amyloid toxicity in rat cholinergic basal forebrain neurons. J Neurosci *24*, 5579-5584.

Jhoti, H. (2005). A new school for screening. Nat Biotechnol *23*, 184-186.

Kadowaki, H., Nishitoh, H., Urano, F., Sadamitsu, C., Matsuzawa, A., Takeda, K., Masutani, H., Yodoi, J., Urano, Y., Nagano, T., and Ichijo, H. (2005). Amyloid beta induces neuronal cell death through ROS-mediated ASK1 activation. Cell Death Differ *12*, 19-24.

Kaneko, I., Yamada, N., Sakuraba, Y., Kamenosono, M., and Tutumi, S. (1995). Suppression of mitochondrial succinate dehydrogenase, a primary target of beta-amyloid, and its derivative racemized at Ser residue. J Neurochem *65*, 2585-2593.

Kang, J., Lemaire, H.G., Unterbeck, A., Salbaum, J.M., Masters, C.L., Grzeschik, K.H., Multhaup, G., Beyreuther, K., and Muller-Hill, B. (1987). The precursor of Alzheimer's disease amyloid A4 protein resembles a cell-surface receptor. Nature *325*, 733-736.

Kang, S.W., Chae, H.Z., Seo, M.S., Kim, K., Baines, I.C., and Rhee, S.G. (1998). Mammalian peroxiredoxin isoforms can reduce hydrogen peroxide generated in response to growth factors and tumor necrosis factor-alpha. J Biol Chem *273*, 6297-6302.

Kay, D.R., Valentine, T.V., Walker, S.E., Valentine, M.H., and Bole, G.G. (1980). Frentizole therapy of active systemic lupus erythematosus. Arthritis Rheum *23*, 1381-1387.

Kayed, R., and Glabe, C.G. (2006). Conformation-dependent anti-amyloid oligomer antibodies. Methods Enzymol *413*, 326-344.

Kayed, R., Head, E., Thompson, J.L., McIntire, T.M., Milton, S.C., Cotman, C.W., and Glabe, C.G. (2003). Common structure of soluble amyloid oligomers implies common mechanism of pathogenesis. Science *300*, 486-489.

Kessler, J., Herholz, K., Grond, M., and Heiss, W.D. (1991). Impaired metabolic activation in Alzheimer's disease: a PET study during continuous visual recognition. Neuropsychologia *29*, 229-243.

Kim, J., Lee, H.J., and Lee, K.W. (2010). Naturally occurring phytochemicals for the prevention of Alzheimer's disease. J Neurochem *112*, 1415-1430.

Kim, S.H., Fountoulakis, M., Cairns, N., and Lubec, G. (2001). Protein levels of human peroxiredoxin subtypes in brains of patients with Alzheimer's disease and Down syndrome. J Neural Transm Suppl, 223-235.

Kim, W., and Hecht, M.H. (2005). Sequence determinants of enhanced amyloidogenicity of Alzheimer Aβ42 peptide relative to Aβ40. J Biol Chem *280*, 35069-35076.

Kissinger, C.R., Rejto, P.A., Pelletier, L.A., Thomson, J.A., Showalter, R.E., Abreo, M.A., Agree, C.S., Margosiak, S., Meng, J.J., Aust, R.M., Vanderpool, D., Li, B., Tempczyk-Russell, A., and Villafranca, J.E. (2004). Crystal structure of human ABAD/HSD10 with a bound inhibitor: implications for design of Alzheimer's disease therapeutics. J Mol Biol *342*, 943-952.

Kleeff, J., Kornmann, M., Sawhney, H., and Korc, M. (2000). Actinomycin D induces apoptosis and inhibits growth of pancreatic cancer cells. Int J Cancer *86*, 399-407.

Kojro, E., Gimpl, G., Lammich, S., Marz, W., and Fahrenholz, F. (2001). Low cholesterol stimulates the nonamyloidogenic pathway by its effect on the alpha -secretase ADAM 10. Proc Natl Acad Sci U S A *98*, 5815-5820.

Korolainen, M.A., Goldsteins, G., Nyman, T.A., Alafuzoff, I., Koistinaho, J., and Pirttila, T. (2006). Oxidative modification of proteins in the frontal cortex of Alzheimer's disease brain. Neurobiol Aging *27*, 42-53.

Korolainen, M.A., Nyman, T.A., Aittokallio, T., and Pirttila, T. (2010). An update on clinical proteomics in Alzheimer's research. J Neurochem *112*, 1386-1414.

Krapfenbauer, K., Engidawork, E., Cairns, N., Fountoulakis, M., and Lubec, G. (2003). Aberrant expression of peroxiredoxin subtypes in neurodegenerative disorders. Brain Res *967*, 152-160.

Kremer, J.J., and Murphy, R.M. (2003). Kinetics of adsorption of beta-amyloid peptide Abeta(1-40) to lipid bilayers. J Biochem Biophys Methods *57*, 159-169.

Kuhn, P.H., Wang, H., Dislich, B., Colombo, A., Zeitschel, U., Ellwart, J.W., Kremmer, E., Rossner, S., and Lichtenthaler, S.F. (2010). ADAM10 is the physiologically relevant, constitutive alpha-secretase of the amyloid precursor protein in primary neurons. EMBO J *29*, 3020-3032.

LaFerla, F.M., Green, K.N., and Oddo, S. (2007). Intracellular amyloid-beta in Alzheimer's disease. Nat Rev Neurosci *8*, 499-509.

Lahm, H.W., and Langen, H. (2000). Mass spectrometry: a tool for the identification of proteins separated by gels. Electrophoresis *21*, 2105-2114.

Lambert, M.P., Barlow, A.K., Chromy, B.A., Edwards, C., Freed, R., Liosatos, M., Morgan, T.E., Rozovsky, I., Trommer, B., Viola, K.L., Wals, P., Zhang, C., Finch, C.E., Krafft, G.A., and Klein, W.L. (1998). Diffusible, nonfibrillar ligands derived from Abeta1-42 are potent central nervous system neurotoxins. Proc Natl Acad Sci U S A *95*, 6448-6453.

Lee, E.K., Hwang, J.H., Shin, D.Y., Kim, D.I., and Yoo, Y.J. (2005). Production of recombinant amyloid-beta peptide 42 as an ubiquitin extension. Protein Expr Purif *40*, 183-189.

Lee, J.H., Barral, S., and Reitz, C. (2008). The neuronal sortilin-related receptor gene SORL1 and late-onset Alzheimer's disease. Curr Neurol Neurosci Rep *8*, 384-391.

Lemere, C.A., and Masliah, E. (2010). Can Alzheimer disease be prevented by amyloid-beta immunotherapy? Nat Rev Neurol *6*, 108-119.

Levitan, D., Doyle, T.G., Brousseau, D., Lee, M.K., Thinakaran, G., Slunt, H.H., Sisodia, S.S., and Greenwald, I. (1996). Assessment of normal and mutant human presenilin function in Caenorhabditis elegans. Proc Natl Acad Sci U S A *93*, 14940-14944.

Levy, E., Carman, M.D., Fernandez-Madrid, I.J., Power, M.D., Lieberburg, I., van Duinen, S.G., Bots, G.T., Luyendijk, W., and Frangione, B. (1990). Mutation of the Alzheimer's disease amyloid gene in hereditary cerebral hemorrhage, Dutch type. Science *248*, 1124-1126.

Lewis, J.M. (1993). Jonathan Swift and Alzheimer's disease. Lancet *342*, 504.

Liao, L., Cheng, D., Wang, J., Duong, D.M., Losik, T.G., Gearing, M., Rees, H.D., Lah, J.J., Levey, A.I., and Peng, J. (2004). Proteomic characterization of postmortem amyloid plaques isolated by laser capture microdissection. J Biol Chem *279*, 37061-37068.

Lim, Y.A., Grimm, A., Giese, M., Mensah-Nyagan, A.G., Villafranca, J.E., Ittner, L.M., Eckert, A., and Gotz, J. (2011). Inhibition of the mitochondrial enzyme ABAD restores the amyloid-beta-mediated deregulation of estradiol. PLoS One *6*, e28887.

Lipinski, C.A., Lombardo, F., Dominy, B.W., and Feeney, P.J. (2001). Experimental and computational approaches to estimate solubility and permeability in drug discovery and development settings. Adv Drug Deliv Rev *46*, 3-26.

Liu, R.Q., Zhou, Q.H., Ji, S.R., Zhou, Q., Feng, D., Wu, Y., and Sui, S.F. (2010). Membrane localization of beta-amyloid 1-42 in lysosomes: a possible mechanism for lysosome labilization. J Biol Chem *285*, 19986-19996.

Luengo-Fernandez, R., J., L., and A., G. (2010). Dementia 2010 (Alzheimer's Research Trust and University of Oxford).

Luhrs, T., Ritter, C., Adrian, M., Riek-Loher, D., Bohrmann, B., Dobeli, H., Schubert, D., and Riek, R. (2005). 3D structure of Alzheimer's amyloid-beta(1-42) fibrils. Proc Natl Acad Sci U S A *102*, 17342-17347.

Luna-Medina, R., Cortes-Canteli, M., Sanchez-Galiano, S., Morales-Garcia, J.A., Martinez, A., Santos, A., and Perez-Castillo, A. (2007). NP031112, a thiadiazolidinone compound, prevents inflammation and neurodegeneration under excitotoxic conditions: potential therapeutic role in brain disorders. J Neurosci *27*, 5766-5776.

Lund, A.M., Skovby, F., Vestergaard, H., Christensen, M., and Christensen, E. (2010). Clinical and biochemical monitoring of patients with fatty acid oxidation disorders. J Inherit Metab Dis *33*, 495-500.

Lustbader, J.W., Cirilli, M., Lin, C., Xu, H.W., Takuma, K., Wang, N., Caspersen, C., Chen, X., Pollak, S., Chaney, M., Trinchese, F., Liu, S., Gunn-Moore, F., Lue, L.F., Walker, D.G., Kuppusamy, P., Zewier, Z.L., Arancio, O., Stern, D., Yan, S.S., and Wu, H. (2004). ABAD directly links Abeta to mitochondrial toxicity in Alzheimer's disease. Science *304*, 448-452.

Lynn, B.C., Wang, J., Markesbery, W.R., and Lovell, M.A. (2010). Quantitative changes in the mitochondrial proteome from subjects with mild cognitive impairment, early stage, and late stage Alzheimer's disease. J Alzheimers Dis *19*, 325-339.

Mackic, J.B., Bading, J., Ghiso, J., Walker, L., Wisniewski, T., Frangione, B., and Zlokovic, B.V. (2002). Circulating amyloid-beta peptide crosses the blood-brain barrier in aged monkeys and contributes to Alzheimer's disease lesions. Vascul Pharmacol *38*, 303-313.

Manczak, M., Mao, P., Calkins, M.J., Cornea, A., Reddy, A.P., Murphy, M.P., Szeto, H.H., Park, B., and Reddy, P.H. (2010). Mitochondria-targeted antioxidants protect against amyloid-beta toxicity in Alzheimer's disease neurons. J Alzheimers Dis *20 Suppl 2*, S609-631.

Mandel, R.J. (2010). CERE-110, an adeno-associated virus-based gene delivery vector expressing human nerve growth factor for the treatment of Alzheimer's disease. Curr Opin Mol Ther *12*, 240-247.

Marques, A.T., Fernandes, P.A., and Ramos, M.J. (2008). Molecular dynamics simulations of the amyloid-beta binding alcohol dehydrogenase (ABAD) enzyme. Bioorg Med Chem *16*, 9511-9518.

Martinou, J.C., Desagher, S., and Antonsson, B. (2000). Cytochrome c release from mitochondria: all or nothing. Nat Cell Biol *2*, E41-43.

Masters, C.L., and Beyreuther, K. (1987). Neuronal origin of cerebral amyloidogenic proteins: their role in Alzheimer's disease and unconventional virus diseases of the nervous system. Ciba Found Symp *126*, 49-64.

Masters, C.L., Simms, G., Weinman, N.A., Multhaup, G., McDonald, B.L., and Beyreuther, K. (1985). Amyloid plaque core protein in Alzheimer disease and Down syndrome. Proc Natl Acad Sci U S A *82*, 4245-4249.

McDaniel, M.A., Maier, S.F., and Einstein, G.O. (2003). "Brain-specific" nutrients: a memory cure? Nutrition *19*, 957-975.

McGuinness, B., Craig, D., Bullock, R., and Passmore, P. (2009). Statins for the prevention of dementia. Cochrane Database Syst Rev, CD003160.

McKhann, G., Drachman, D., Folstein, M., Katzman, R., Price, D., and Stadlan, E.M. (1984). Clinical diagnosis of Alzheimer's disease: report of the NINCDS-ADRDA Work Group under the auspices of Department of Health and Human Services Task Force on Alzheimer's Disease. Neurology *34*, 939-944.

McLaughlin, L., Zhu, G., Mistry, M., Ley-Ebert, C., Stuart, W.D., Florio, C.J., Groen, P.A., Witt, S.A., Kimball, T.R., Witte, D.P., Harmony, J.A., and Aronow, B.J.

(2000). Apolipoprotein J/clusterin limits the severity of murine autoimmune myocarditis. J Clin Invest *106*, 1105-1113.

Miners, J.S., Baig, S., Palmer, J., Palmer, L.E., Kehoe, P.G., and Love, S. (2008). Abeta-degrading enzymes in Alzheimer's disease. Brain Pathol *18*, 240-252.

Miners, J.S., Baig, S., Tayler, H., Kehoe, P.G., and Love, S. (2009a). Neprilysin and insulin-degrading enzyme levels are increased in Alzheimer disease in relation to disease severity. J Neuropathol Exp Neurol *68*, 902-914.

Miners, S., Ashby, E., Baig, S., Harrison, R., Tayler, H., Speedy, E., Prince, J.A., Love, S., and Kehoe, P.G. (2009b). Angiotensin-converting enzyme levels and activity in Alzheimer's disease: differences in brain and CSF ACE and association with ACE1 genotypes. Am J Transl Res *1*, 163-177.

Monge, C., Beraud, N., Kuznetsov, A.V., Rostovtseva, T., Sackett, D., Schlattner, U., Vendelin, M., and Saks, V.A. (2008). Regulation of respiration in brain mitochondria and synaptosomes: restrictions of ADP diffusion in situ, roles of tubulin, and mitochondrial creatine kinase. Mol Cell Biochem *318*, 147-165.

Morgan, D., Diamond, D.M., Gottschall, P.E., Ugen, K.E., Dickey, C., Hardy, J., Duff, K., Jantzen, P., DiCarlo, G., Wilcock, D., Connor, K., Hatcher, J., Hope, C., Gordon, M., and Arendash, G.W. (2000). A beta peptide vaccination prevents memory loss in an animal model of Alzheimer's disease. Nature *408*, 982-985.

Mosconi, L., Berti, V., Glodzik, L., Pupi, A., De Santi, S., and de Leon, M.J. (2010). Pre-clinical detection of Alzheimer's disease using FDG-PET, with or without amyloid imaging. J Alzheimers Dis *20*, 843-854.

Mosmann, T. (1983). Rapid colorimetric assay for cellular growth and survival: application to proliferation and cytotoxicity assays. J Immunol Methods *65*, 55-63.

Mucke, L., Masliah, E., Yu, G.Q., Mallory, M., Rockenstein, E.M., Tatsuno, G., Hu, K., Kholodenko, D., Johnson-Wood, K., and McConlogue, L. (2000). High-level neuronal expression of abeta 1-42 in wild-type human amyloid protein precursor transgenic mice: synaptotoxicity without plaque formation. J Neurosci *20*, 4050-4058.

Muirhead, K.E., Borger, E., Aitken, L., Conway, S.J., and Gunn-Moore, F.J. (2010). The consequences of mitochondrial amyloid beta-peptide in Alzheimer's disease. Biochem J *426*, 255-270.

Murakami, Y., Ohsawa, I., Kasahara, T., and Ohta, S. (2009). Cytoprotective role of mitochondrial amyloid beta peptide-binding alcohol dehydrogenase against a cytotoxic aldehyde. Neurobiol Aging *30*, 325-329.

Murphy, K.P., Privalov, P.L., and Gill, S.J. (1990). Common features of protein unfolding and dissolution of hydrophobic compounds. Science *247*, 559-561.

Neckelmann, N., Warner, C.K., Chung, A., Kudoh, J., Minoshima, S., Fukuyama, R., Maekawa, M., Shimizu, Y., Shimizu, N., Liu, J.D., and et al. (1989). The human ATP synthase beta subunit gene: sequence analysis, chromosome assignment, and differential expression. Genomics *5*, 829-843.

Neve, R.L., and Robakis, N.K. (1998). Alzheimer's disease: a re-examination of the amyloid hypothesis. Trends Neurosci *21*, 15-19.

Niall, H.D. (1973). Automated Edman degradation: the protein sequenator. Methods Enzymol *27*, 942-1010.

Nixon, R.A., and Yang, D.S. (2011). Autophagy failure in Alzheimer's disease-locating the primary defect. Neurobiol Dis *43*, 38-45.

Oddo, S., Caccamo, A., Shepherd, J.D., Murphy, M.P., Golde, T.E., Kayed, R., Metherate, R., Mattson, M.P., Akbari, Y., and LaFerla, F.M. (2003). Triple-

transgenic model of Alzheimer's disease with plaques and tangles: intracellular Abeta and synaptic dysfunction. Neuron *39*, 409-421.

Ofman, R., Ruiter, J.P., Feenstra, M., Duran, M., Poll-The, B.T., Zschocke, J., Ensenauer, R., Lehnert, W., Sass, J.O., Sperl, W., and Wanders, R.J. (2003). 2-Methyl-3-hydroxybutyryl-CoA dehydrogenase deficiency is caused by mutations in the HADH2 gene. Am J Hum Genet *72*, 1300-1307.

Oppermann, U.C., Salim, S., Tjernberg, L.O., Terenius, L., and Jornvall, H. (1999). Binding of amyloid beta-peptide to mitochondrial hydroxyacyl-CoA dehydrogenase (ERAB): regulation of an SDR enzyme activity with implications for apoptosis in Alzheimer's disease. FEBS Lett *451*, 238-242.

Oster, T., and Pillot, T. (2010). Docosahexaenoic acid and synaptic protection in Alzheimer's disease mice. Biochim Biophys Acta *1801*, 791-798.

Ostrowski, S.M., Wilkinson, B.L., Golde, T.E., and Landreth, G. (2007). Statins reduce amyloid-beta production through inhibition of protein isoprenylation. J Biol Chem *282*, 26832-26844.

Ouimet, C.C., Katona, I., Allen, P., Freund, T.F., and Greengard, P. (2004). Cellular and subcellular distribution of spinophilin, a PP1 regulatory protein that bundles F-actin in dendritic spines. J Comp Neurol *479*, 374-388.

Pamplona, R., Dalfo, E., Ayala, V., Bellmunt, M.J., Prat, J., Ferrer, I., and Portero-Otin, M. (2005). Proteins in human brain cortex are modified by oxidation, glycoxidation, and lipoxidation. Effects of Alzheimer disease and identification of lipoxidation targets. J Biol Chem *280*, 21522-21530.

Panza, F., Solfrizzi, V., Frisardi, V., Imbimbo, B.P., Capurso, C., D'Introno, A., Colacicco, A.M., Seripa, D., Vendemiale, G., Capurso, A., and Pilotto, A. (2009). Beyond the neurotransmitter-focused approach in treating Alzheimer's disease: drugs targeting beta-amyloid and tau protein. Aging Clin Exp Res *21*, 386-406.

Pardridge, W.M., Boado, R.J., and Kang, Y.S. (1995). Vector-mediated delivery of a polyamide ("peptide") nucleic acid analogue through the blood-brain barrier in vivo. Proc Natl Acad Sci U S A *92*, 5592-5596.

Parri, H.R., Hernandez, C.M., and Dineley, K.T. (2011). Research update: Alpha7 nicotinic acetylcholine receptor mechanisms in Alzheimer's disease. Biochem Pharmacol *82*, 931-942.

Patel, A.N., and Jhamandas, J.H. (2012). Neuronal receptors as targets for the action of amyloid-beta protein (Abeta) in the brain. Expert Rev Mol Med *14*, e2.

Perez-Tur, J., Croxton, R., Wright, K., Phillips, H., Zehr, C., Crook, R., Hutton, M., Hardy, J., Karran, E., Roberts, G.W., Lancaster, S., and Haltia, T. (1996). A further presenilin 1 mutation in the exon 8 cluster in familial Alzheimer's disease. Neurodegeneration *5*, 207-212.

Perl, D.P. (2000). Neuropathology of Alzheimer's disease and related disorders. Neurol Clin *18*, 847-864.

Perl, D.P. (2010). Neuropathology of Alzheimer's disease. Mt Sinai J Med *77*, 32-42.

Phinney, A.L., Deller, T., Stalder, M., Calhoun, M.E., Frotscher, M., Sommer, B., Staufenbiel, M., and Jucker, M. (1999). Cerebral amyloid induces aberrant axonal sprouting and ectopic terminal formation in amyloid precursor protein transgenic mice. J Neurosci *19*, 8552-8559.

Pizzi, M., Boroni, F., Bianchetti, A., Moraitis, C., Sarnico, I., Benarese, M., Goffi, F., Valerio, A., and Spano, P. (2002). Expression of functional NR1/NR2B-type NMDA receptors in neuronally differentiated SK-N-SH human cell line. Eur J Neurosci *16*, 2342-2350.

Polidori, M.C., Griffiths, H.R., Mariani, E., and Mecocci, P. (2007). Hallmarks of protein oxidative damage in neurodegenerative diseases: focus on Alzheimer's disease. Amino Acids *32*, 553-559.

Postina, R. (2008). A closer look at alpha-secretase. Curr Alzheimer Res *5*, 179-186.

Poulin, S.P., Dautoff, R., Morris, J.C., Barrett, L.F., and Dickerson, B.C. (2011). Amygdala atrophy is prominent in early Alzheimer's disease and relates to symptom severity. Psychiatry Res *194*, 7-13.

Powell, A.J., Read, J.A., Banfield, M.J., Gunn-Moore, F., Yan, S.D., Lustbader, J., Stern, A.R., Stern, D.M., and Brady, R.L. (2000). Recognition of structurally diverse substrates by type II 3-hydroxyacyl-CoA dehydrogenase (HADH II)/amyloid-beta binding alcohol dehydrogenase (ABAD). J Mol Biol *303*, 311-327.

Preis, P.N., Saya, H., Nadasdi, L., Hochhaus, G., Levin, V., and Sadee, W. (1988). Neuronal cell differentiation of human neuroblastoma cells by retinoic acid plus herbimycin A. Cancer Res *48*, 6530-6534.

Priller, C., Bauer, T., Mitteregger, G., Krebs, B., Kretzschmar, H.A., and Herms, J. (2006). Synapse formation and function is modulated by the amyloid precursor protein. J Neurosci *26*, 7212-7221.

Qin, L., Liu, Y., Cooper, C., Liu, B., Wilson, B., and Hong, J.S. (2002). Microglia enhance beta-amyloid peptide-induced toxicity in cortical and mesencephalic neurons by producing reactive oxygen species. J Neurochem *83*, 973-983.

Rabinovici, G.D., Furst, A.J., Alkalay, A., Racine, C.A., O'Neil, J.P., Janabi, M., Baker, S.L., Agarwal, N., Bonasera, S.J., Mormino, E.C., Weiner, M.W., Gorno-Tempini, M.L., Rosen, H.J., Miller, B.L., and Jagust, W.J. (2010). Increased metabolic vulnerability in early-onset Alzheimer's disease is not related to amyloid burden. Brain *133*, 512-528.

Raina, S.K., Pandita, K.K., and Razdan, S. (2009). Incidence of dementia in a Kashmiri migrant population. Ann Indian Acad Neurol *12*, 154-156.

Ramirez-Lorca, R., Boada, M., Saez, M.E., Hernandez, I., Mauleon, A., Rosende-Roca, M., Martinez-Lage, P., Gutierrez, M., Real, L.M., Lopez-Arrieta, J., Gayan, J., Antunez, C., Gonzalez-Perez, A., Tarraga, L., and Ruiz, A. (2009). GAB2 gene does not modify the risk of Alzheimer's disease in Spanish APOE 4 carriers. J Nutr Health Aging *13*, 214-219.

Razdan, S., Kaul, R.L., Motta, A., Kaul, S., and Bhatt, R.K. (1994). Prevalence and pattern of major neurological disorders in rural Kashmir (India) in 1986. Neuroepidemiology *13*, 113-119.

Reddy, P.H. (2009a). Amyloid beta, mitochondrial structural and functional dynamics in Alzheimer's disease. Exp Neurol *218*, 286-292.

Reddy, P.H. (2009b). Role of mitochondria in neurodegenerative diseases: mitochondria as a therapeutic target in Alzheimer's disease. CNS Spectr *14*, 8-13; discussion 16-18.

Ren, Y., Xu, H.W., Davey, F., Taylor, M., Aiton, J., Coote, P., Fang, F., Yao, J., Chen, D., Chen, J.X., Yan, S.D., and Gunn-Moore, F.J. (2008). Endophilin I expression is increased in the brains of Alzheimer disease patients. J Biol Chem *283*, 5685-5691.

Reutens, A.T., and Begley, C.G. (2002). Endophilin-1: a multifunctional protein. Int J Biochem Cell Biol *34*, 1173-1177.

Roberson, E.D., Scearce-Levie, K., Palop, J.J., Yan, F., Cheng, I.H., Wu, T., Gerstein, H., Yu, G.Q., and Mucke, L. (2007). Reducing endogenous tau ameliorates amyloid beta-induced deficits in an Alzheimer's disease mouse model. Science *316*, 750-754.

Rosenfeld, J., Capdevielle, J., Guillemot, J.C., and Ferrara, P. (1992). In-gel digestion of proteins for internal sequence analysis after one- or two-dimensional gel electrophoresis. Anal Biochem *203*, 173-179.

Ruegg, U.T., and Burgess, G.M. (1989). Staurosporine, K-252 and UCN-01: potent but nonspecific inhibitors of protein kinases. Trends Pharmacol Sci *10*, 218-220.

Ruiz, J., Kouiavskaia, D., Migliorini, M., Robinson, S., Saenko, E.L., Gorlatova, N., Li, D., Lawrence, D., Hyman, B.T., Weisgraber, K.H., and Strickland, D.K. (2005). The apoE isoform binding properties of the VLDL receptor reveal marked differences from LRP and the LDL receptor. J Lipid Res *46*, 1721-1731.

Rusinol, A.E., Cui, Z., Chen, M.H., and Vance, J.E. (1994). A unique mitochondria-associated membrane fraction from rat liver has a high capacity for lipid synthesis and contains pre-Golgi secretory proteins including nascent lipoproteins. J Biol Chem *269*, 27494-27502.

Sambamurti, K., and Lahiri, D.K. (1998). ERAB contains a putative noncleavable signal peptide. Biochem Biophys Res Commun *249*, 546-549.

Sayre, L.M., Zelasko, D.A., Harris, P.L., Perry, G., Salomon, R.G., and Smith, M.A. (1997). 4-Hydroxynonenal-derived advanced lipid peroxidation end products are increased in Alzheimer's disease. J Neurochem *68*, 2092-2097.

Scheltens, P. (2009). Imaging in Alzheimer's disease. Dialogues Clin Neurosci *11*, 191-199.

Schenk, D. (2002). Amyloid-beta immunotherapy for Alzheimer's disease: the end of the beginning. Nat Rev Neurosci *3*, 824-828.

Scheuner, D., Eckman, C., Jensen, M., Song, X., Citron, M., Suzuki, N., Bird, T.D., Hardy, J., Hutton, M., Kukull, W., Larson, E., Levy-Lahad, E., Viitanen, M., Peskind, E., Poorkaj, P., Schellenberg, G., Tanzi, R., Wasco, W., Lannfelt, L.,

Selkoe, D., and Younkin, S. (1996). Secreted amyloid beta-protein similar to that in the senile plaques of Alzheimer's disease is increased in vivo by the presenilin 1 and 2 and APP mutations linked to familial Alzheimer's disease. Nat Med *2*, 864-870.

Schmidt, A., Wolde, M., Thiele, C., Fest, W., Kratzin, H., Podtelejnikov, A.V., Witke, W., Huttner, W.B., and Soling, H.D. (1999). Endophilin I mediates synaptic vesicle formation by transfer of arachidonate to lysophosphatidic acid. Nature *401*, 133-141.

Schneider, A., Biernat, J., von Bergen, M., Mandelkow, E., and Mandelkow, E.M. (1999). Phosphorylation that detaches tau protein from microtubules (Ser262, Ser214) also protects it against aggregation into Alzheimer paired helical filaments. Biochemistry *38*, 3549-3558.

Schneider, A., and Mandelkow, E. (2008). Tau-based treatment strategies in neurodegenerative diseases. Neurotherapeutics *5*, 443-457.

Schonberger, S.J., Edgar, P.F., Kydd, R., Faull, R.L., and Cooper, G.J. (2001). Proteomic analysis of the brain in Alzheimer's disease: molecular phenotype of a complex disease process. Proteomics *1*, 1519-1528.

Scott, W.K., Grubber, J.M., Conneally, P.M., Small, G.W., Hulette, C.M., Rosenberg, C.K., Saunders, A.M., Roses, A.D., Haines, J.L., and Pericak-Vance, M.A. (2000). Fine mapping of the chromosome 12 late-onset Alzheimer disease locus: potential genetic and phenotypic heterogeneity. Am J Hum Genet *66*, 922-932.

Selkoe, D.J., and Abraham, C.R. (1986). Isolation of paired helical filaments and amyloid fibers from human brain. Methods Enzymol *134*, 388-404.

Shimmyo, Y., Kihara, T., Akaike, A., Niidome, T., and Sugimoto, H. (2008). Epigallocatechin-3-gallate and curcumin suppress amyloid beta-induced beta-site APP cleaving enzyme-1 upregulation. Neuroreport *19*, 1329-1333.

Shiozaki, K., and Iseki, E. (2004). Decrease in GTP-sensitive high affinity agonist binding of muscarinic acetylcholine receptors in autopsied brains of dementia with Lewy bodies and Alzheimer's disease. J Neurol Sci *223*, 145-148.

Shuker, S.B., Hajduk, P.J., Meadows, R.P., and Fesik, S.W. (1996). Discovering high-affinity ligands for proteins: SAR by NMR. Science *274*, 1531-1534.

Simzar, S., Ellyin, R., Shau, H., and Sarafian, T.A. (2000). Contrasting antioxidant and cytotoxic effects of peroxiredoxin I and II in PC12 and NIH3T3 cells. Neurochem Res *25*, 1613-1621.

Sobell, H.M. (1985). Actinomycin and DNA transcription. Proc Natl Acad Sci U S A *82*, 5328-5331.

Spillantini, M.G., and Goedert, M. (2000). Tau mutations in familial frontotemporal dementia. Brain *123 (Pt 5)*, 857-859.

Steen, H., and Mann, M. (2004). The ABC's (and XYZ's) of peptide sequencing. Nat Rev Mol Cell Biol *5*, 699-711.

Stine, W.B., Jr., Dahlgren, K.N., Krafft, G.A., and LaDu, M.J. (2003). In vitro characterization of conditions for amyloid-beta peptide oligomerization and fibrillogenesis. J Biol Chem *278*, 11612-11622.

Stone, S.J., Levin, M.C., Zhou, P., Han, J., Walther, T.C., and Farese, R.V., Jr. (2009). The endoplasmic reticulum enzyme DGAT2 is found in mitochondria-associated membranes and has a mitochondrial targeting signal that promotes its association with mitochondria. J Biol Chem *284*, 5352-5361.

Strand, A.D., Aragaki, A.K., Baquet, Z.C., Hodges, A., Cunningham, P., Holmans, P., Jones, K.R., Jones, L., Kooperberg, C., and Olson, J.M. (2007). Conservation of regional gene expression in mouse and human brain. PLoS Genet *3*, e59.

Sundborger, A., Soderblom, C., Vorontsova, O., Evergren, E., Hinshaw, J.E., and Shupliakov, O. (2011). An endophilin-dynamin complex promotes budding of clathrin-coated vesicles during synaptic vesicle recycling. J Cell Sci *124*, 133-143.

Suzuki, T., Tozuka, M., Kazuyoshi, Y., Sugano, M., Nakabayashi, T., Okumura, N., Hidaka, H., Katsuyama, T., and Higuchi, K. (2002). Predominant apolipoprotein J exists as lipid-poor mixtures in cerebrospinal fluid. Ann Clin Lab Sci *32*, 369-376.

Tabira, T. (2010). [Development of new drugs for Alzheimer's disease]. Brain Nerve *62*, 787-796.

Takuma, K., Yan, S.S., Stern, D.M., and Yamada, K. (2005a). Mitochondrial dysfunction, endoplasmic reticulum stress, and apoptosis in Alzheimer's disease. J Pharmacol Sci *97*, 312-316.

Takuma, K., Yao, J., Huang, J., Xu, H., Chen, X., Luddy, J., Trillat, A.C., Stern, D.M., Arancio, O., and Yan, S.S. (2005b). ABAD enhances Abeta-induced cell stress via mitochondrial dysfunction. FASEB J *19*, 597-598.

Takuma, Y., Nouso, K., Makino, Y., Saito, S., and Shiratori, Y. (2005c). Prophylactic balloon-occluded retrograde transvenous obliteration for gastric varices in compensated cirrhosis. Clin Gastroenterol Hepatol *3*, 1245-1252.

Tanzi, R.E., Gusella, J.F., Watkins, P.C., Bruns, G.A., St George-Hyslop, P., Van Keuren, M.L., Patterson, D., Pagan, S., Kurnit, D.M., and Neve, R.L. (1987). Amyloid beta protein gene: cDNA, mRNA distribution, and genetic linkage near the Alzheimer locus. Science *235*, 880-884.

Teague, S.J., Davis, A.M., Leeson, P.D., and Oprea, T. (1999). The Design of Leadlike Combinatorial Libraries. Angew Chem Int Ed Engl *38*, 3743-3748.

Tekirian, T.L., Cole, G.M., Russell, M.J., Yang, F., Wekstein, D.R., Patel, E., Snowdon, D.A., Markesbery, W.R., and Geddes, J.W. (1996). Carboxy terminal of beta-

amyloid deposits in aged human, canine, and polar bear brains. Neurobiol Aging *17*, 249-257.

Tessitore, A., del, P.M.M., Sano, R., Ma, Y., Mann, L., Ingrassia, A., Laywell, E.D., Steindler, D.A., Hendershot, L.M., and d'Azzo, A. (2004). GM1-ganglioside-mediated activation of the unfolded protein response causes neuronal death in a neurodegenerative gangliosidosis. Mol Cell *15*, 753-766.

Thakur, M.K., and Mani, S.T. (2005). Estradiol regulates APP mRNA alternative splicing in the mice brain cortex. Neurosci Lett *381*, 154-157.

Thinakaran, G., Teplow, D.B., Siman, R., Greenberg, B., and Sisodia, S.S. (1996). Metabolism of the "Swedish" amyloid precursor protein variant in neuro2a (N2a) cells. Evidence that cleavage at the "beta-secretase" site occurs in the golgi apparatus. J Biol Chem *271*, 9390-9397.

Tieu, K., Perier, C., Vila, M., Caspersen, C., Zhang, H.P., Teismann, P., Jackson-Lewis, V., Stern, D.M., Yan, S.D., and Przedborski, S. (2004). L-3-hydroxyacyl-CoA dehydrogenase II protects in a model of Parkinson's disease. Ann Neurol *56*, 51-60.

Tobinick, E. (2009). Tumour necrosis factor modulation for treatment of Alzheimer's disease: rationale and current evidence. CNS Drugs *23*, 713-725.

Tomiyama, T. (2010). [Involvement of beta-amyloid in the etiology of Alzheimer's disease]. Brain Nerve *62*, 691-699.

Torroja, L., Ortuno-Sahagun, D., Ferrus, A., Hammerle, B., and Barbas, J.A. (1998). scully, an essential gene of Drosophila, is homologous to mammalian mitochondrial type II L-3-hydroxyacyl-CoA dehydrogenase/amyloid-beta peptide-binding protein. J Cell Biol *141*, 1009-1017.

Treacy, E.P., Lambert, D.M., Barnes, R., Boriack, R.L., Vockley, J., O'Brien L, K., Jones, P.M., and Bennett, M.J. (2000). Short-chain hydroxyacyl-coenzyme A dehydrogenase deficiency presenting as unexpected infant death: A family study. J Pediatr *137*, 257-259.

Vehmas, A.K., Borchelt, D.R., Price, D.L., McCarthy, D., Wills-Karp, M., Peper, M.J., Rudow, G., Luyinbazi, J., Siew, L.T., and Troncoso, J.C. (2001). beta-Amyloid peptide vaccination results in marked changes in serum and brain Abeta levels in APPswe/PS1DeltaE9 mice, as detected by SELDI-TOF-based ProteinChip technology. DNA Cell Biol *20*, 713-721.

White, L., Petrovitch, H., Ross, G.W., Masaki, K.H., Abbott, R.D., Teng, E.L., Rodriguez, B.L., Blanchette, P.L., Havlik, R.J., Wergowske, G., Chiu, D., Foley, D.J., Murdaugh, C., and Curb, J.D. (1996). Prevalence of dementia in older Japanese-American men in Hawaii: The Honolulu-Asia Aging Study. JAMA *276*, 955-960.

Williams, T.L., and Serpell, L.C. (2011). Membrane and surface interactions of Alzheimer's Abeta peptide--insights into the mechanism of cytotoxicity. FEBS J *278*, 3905-3917.

Williamson, J., Goldman, J., and Marder, K.S. (2009). Genetic aspects of Alzheimer disease. Neurologist *15*, 80-86.

Wirths, O., Multhaup, G., and Bayer, T.A. (2004). A modified beta-amyloid hypothesis: intraneuronal accumulation of the beta-amyloid peptide--the first step of a fatal cascade. J Neurochem *91*, 513-520.

Wood, Z.A., Poole, L.B., and Karplus, P.A. (2003). Peroxiredoxin evolution and the regulation of hydrogen peroxide signaling. Science *300*, 650-653.

Xie, L., Helmerhorst, E., Taddei, K., Plewright, B., Van Bronswijk, W., and Martins, R. (2002). Alzheimer's beta-amyloid peptides compete for insulin binding to the insulin receptor. J Neurosci *22*, RC221.

Xie, Y., Deng, S., Chen, Z., Yan, S., and Landry, D.W. (2006). Identification of small-molecule inhibitors of the Abeta-ABAD interaction. Bioorg Med Chem Lett *16*, 4657-4660.

Yamazaki, T., Koo, E.H., and Selkoe, D.J. (1996). Trafficking of cell-surface amyloid beta-protein precursor. II. Endocytosis, recycling and lysosomal targeting detected by immunolocalization. J Cell Sci *109 (Pt 5)*, 999-1008.

Yan, S.D., Fu, J., Soto, C., Chen, X., Zhu, H., Al-Mohanna, F., Collison, K., Zhu, A., Stern, E., Saido, T., Tohyama, M., Ogawa, S., Roher, A., and Stern, D. (1997a). An intracellular protein that binds amyloid-beta peptide and mediates neurotoxicity in Alzheimer's disease. Nature *389*, 689-695.

Yan, S.D., Roher, A., Chaney, M., Zlokovic, B., Schmidt, A.M., and Stern, D. (2000a). Cellular cofactors potentiating induction of stress and cytotoxicity by amyloid beta-peptide. Biochim Biophys Acta *1502*, 145-157.

Yan, S.D., Shi, Y., Zhu, A., Fu, J., Zhu, H., Zhu, Y., Gibson, L., Stern, E., Collison, K., Al-Mohanna, F., Ogawa, S., Roher, A., Clarke, S.G., and Stern, D.M. (1999). Role of ERAB/L-3-hydroxyacyl-coenzyme A dehydrogenase type II activity in Abeta-induced cytotoxicity. J Biol Chem *274*, 2145-2156.

Yan, S.D., Stern, D., and Schmidt, A.M. (1997b). What's the RAGE? The receptor for advanced glycation end products (RAGE) and the dark side of glucose. Eur J Clin Invest *27*, 179-181.

Yan, S.D., and Stern, D.M. (2005). Mitochondrial dysfunction and Alzheimer's disease: role of amyloid-beta peptide alcohol dehydrogenase (ABAD). Int J Exp Pathol *86*, 161-171.

Yan, S.D., Zhu, H., Zhu, A., Golabek, A., Du, H., Roher, A., Yu, J., Soto, C., Schmidt, A.M., Stern, D., and Kindy, M. (2000b). Receptor-dependent cell stress and amyloid accumulation in systemic amyloidosis. Nat Med *6*, 643-651.

Yan, Y., Liu, J., McCallum, S.A., Yang, D., and Wang, C. (2007a). Methyl dynamics of the amyloid-beta peptides Abeta40 and Abeta42. Biochem Biophys Res Commun *362*, 410-414.

Yan, Y., Liu, Y., Sorci, M., Belfort, G., Lustbader, J.W., Yan, S.S., and Wang, C. (2007b). Surface plasmon resonance and nuclear magnetic resonance studies of ABAD-Abeta interaction. Biochemistry *46*, 1724-1731.

Yang, S.Y., He, X.Y., and Miller, D. (2007). HSD17B10: a gene involved in cognitive function through metabolism of isoleucine and neuroactive steroids. Mol Genet Metab *92*, 36-42.

Yang, S.Y., He, X.Y., Olpin, S.E., Sutton, V.R., McMenamin, J., Philipp, M., Denman, R.B., and Malik, M. (2009). Mental retardation linked to mutations in the HSD17B10 gene interfering with neurosteroid and isoleucine metabolism. Proc Natl Acad Sci U S A *106*, 14820-14824.

Yankner, B.A. (1996). Mechanisms of neuronal degeneration in Alzheimer's disease. Neuron *16*, 921-932.

Yao, J., Du, H., Yan, S., Fang, F., Wang, C., Lue, L.F., Guo, L., Chen, D., Stern, D.M., Gunn Moore, F.J., Xi Chen, J., Arancio, O., and Yan, S.S. (2011). Inhibition of amyloid-beta (Abeta) peptide-binding alcohol dehydrogenase-Abeta interaction reduces Abeta accumulation and improves mitochondrial function in a mouse model of Alzheimer's disease. J Neurosci *31*, 2313-2320.

Yao, J., Taylor, M., Davey, F., Ren, Y., Aiton, J., Coote, P., Fang, F., Chen, J.X., Yan, S.D., and Gunn-Moore, F.J. (2007). Interaction of amyloid binding alcohol dehydrogenase/Abeta mediates up-regulation of peroxiredoxin II in the brains of

Alzheimer's disease patients and a transgenic Alzheimer's disease mouse model. Mol Cell Neurosci *35*, 377-382.

Yao, J.K., Wengenack, T.M., Curran, G.L., and Poduslo, J.F. (2009). Reduced membrane lipids in the cortex of Alzheimer's disease transgenic mice. Neurochem Res *34*, 102-108.

Yesavage, J.A., O'Hara, R., Kraemer, H., Noda, A., Taylor, J.L., Ferris, S., Gely-Nargeot, M.C., Rosen, A., Friedman, L., Sheikh, J., and Derouesne, C. (2002). Modeling the prevalence and incidence of Alzheimer's disease and mild cognitive impairment. J Psychiatr Res *36*, 281-286.

Yoon, E.J., Park, H.J., Kim, G.Y., Cho, H.M., Choi, J.H., Park, H.Y., Jang, J.Y., Rhim, H.S., and Kang, S.M. (2009). Intracellular amyloid beta interacts with SOD1 and impairs the enzymatic activity of SOD1: implications for the pathogenesis of amyotrophic lateral sclerosis. Exp Mol Med *41*, 611-617.

Yoshida, Y., Yoshikawa, A., Kinumi, T., Ogawa, Y., Saito, Y., Ohara, K., Yamamoto, H., Imai, Y., and Niki, E. (2009). Hydroxyoctadecadienoic acid and oxidatively modified peroxiredoxins in the blood of Alzheimer's disease patients and their potential as biomarkers. Neurobiol Aging *30*, 174-185.

Zahn, J.M., Poosala, S., Owen, A.B., Ingram, D.K., Lustig, A., Carter, A., Weeraratna, A.T., Taub, D.D., Gorospe, M., Mazan-Mamczarz, K., Lakatta, E.G., Boheler, K.R., Xu, X., Mattson, M.P., Falco, G., Ko, M.S., Schlessinger, D., Firman, J., Kummerfeld, S.K., Wood, W.H., 3rd, Zonderman, A.B., Kim, S.K., and Becker, K.G. (2007). AGEMAP: a gene expression database for aging in mice. PLoS Genet *3*, e201.

Zanetti, O., Solerte, S.B., and Cantoni, F. (2009). Life expectancy in Alzheimer's disease (AD). Arch Gerontol Geriatr *49 Suppl 1*, 237-243.

Zhang, M., Haapasalo, A., Kim, D.Y., Ingano, L.A., Pettingell, W.H., and Kovacs, D.M. (2006). Presenilin/gamma-secretase activity regulates protein clearance from the endocytic recycling compartment. FASEB J *20*, 1176-1178.

Appendix

endophilin 2 mouse
Trypsin:/K-\P /R-\P

Frag#	Res#	Sequence
T29	172-172	(K)K(K)
T2	8-8	(K)K(Q)
T8	39-39	(K)K(V)
T30	173-173	(K)K(R)
T25	160-160	(K)K(L)
T43	253-253	(K)R(E)
T39	242-242	(K)R(R)
T19	123-123	(K)R(L)
T31	174-174	(K)R(Q)
T27	165-165	(R)R(L)
T40	243-243	(R)R(V)
T12	66-67	(R)AK(L)
T38	240-241	(K)LK(R)
T41	244-245	(R)VR(E)
T14	77-78	(K)IR(G)
T32	175-177	(R)QGK(I)
T17	100-102	(R)HGK(E)
T23	150-152	(K)DLK(E)
T15	79-82	(R)GQVK(N)
T48	298-301	(R)MPSK(S)
T26	161-164	(K)LEGR(R)
T7	35-38	(K)DMEK(K)
T20	124-128	(R)LAEVK(D)
T3	9-12	(K)QFYK(A)
T34	185-189	(R)QALEK(F)
T35	190-194	(K)FEESK(E)
T9	40-45	(K)VDVTSK(A)
*T1	1-7	(-)MSVAGLK(K)
T5	21-28	(K)VGGAEGTK(L)
T6	29-34	(K)LDDDFK(D)
T42	246-252	(R)EASSRPK(R)
T28	166-171	(R)LDFDYK(K)
T47	291-297	(R)SSDKPIR(M)
T10	46-53	(K)AVAEVLVR(T)
T4	13-20	(K)ASQLVSEK(V)
T46	283-290	(K)ITASSSFR(S)
T33	178-184	(K)IPDEELR(Q)
T24	153-159	(K)EIQHHLK(K)
T21	129-136	(K)DSLDIEVK(Q)
T44	254-260	(R)EFKPRPR(E)
T13	68-76	(K)LTMLNTVSK(I)
T49	302-312	(K)SMPPLDQPSCK(A)
T37	228-239	(R)QAVQILEELADK(L)
T11	54-65	(R)TIEYLQPNPASR(A)
T22	137-149	(K)QNFIDPLQNLCDK(D)
T16	83-99	(K)NPGYPQSEGLLGECMVR (H)
T50	313-328	(K)ALYDFEPENDGELGFR(E)
T18	103-122	(K)ELGGESNFGDALLDAGE SNK(R)
T45	261-282	(R)EPFELGELEQPNGGFPC APAPK(I)
T36	195-227	(K)EVAETSMHNLLETDIEQ VSQLSALVDAQLDYHR(Q)
T51	329-368	(R)EGDLITLTNQIDENWYE GNLHGQSGFFPLSYVQVLVP LPQ(-)

endophilin 3 mouse
Trypsin:/K-\P /R-\P

Frag#	Res#	Sequence
T7	39-39	(K)K(I)
T2	8-8	(K)K(Q)
T27	172-172	(K)K(R)
T23	160-160	(R)K(L)
T40	253-253	(K)R(E)
T28	173-173	(K)R(R)
T29	174-174	(R)R(V)
T25	165-165	(R)R(L)
T11	66-67	(R)AK(L)
T13	77-78	(K)LR(G)
T30	175-177	(R)VGK(I)
T39	250-252	(K)VPK(R)
T16	100-102	(K)YGK(E)
T21	150-152	(K)DLK(E)
T14	79-82	(R)GQVK(A)
T24	161-164	(K)LEGR(R)
T37	240-243	(K)LELR(I)
T3	9-12	(K)QFHK(A)
T32	185-189	(R)QAVEK(F)
T34	195-199	(K)ELAER(S)
T38	244-249	(R)ISLASK(V)
T33	190-194	(K)FEESK(E)
T8	40-45	(K)IDITSK(A)
T18	123-128	(K)LMGEVK(D)
▪T1	1-7	(-)MSVAGLK(K)
T5	21-28	(K)ISGAEGTK(L)
T26	166-171	(R)LDYDYK(K)
T9	46-53	(K)AVAEILSK(A)
T22	153-159	(K)EIGHQLR(K)
T31	178-184	(K)IPEEEIR(Q)
T19	129-136	(K)DSLDINVK(Q)
T4	13-20	(K)ASQLFSEK(I)
T12	68-76	(K)LGMLNTVSK(L)
T6	29-38	(K)LDEEFLNMEK(K)
T36	228-239	(R)QSTEILQELQSK(L)
T10	54-65	(K)ATEYLQPNPAYR(A)
T42	278-291	(K)TPGTDTPADQPCCR(G)
T20	137-149	(K)QTFIDPLQLLQDK(D)
T15	83-99	(K)ATGYPQTEGLLGDCMLK (Y)
T43	292-307	(R)GLYDFEPENEGELGFK(E)
T17	103-122	(K)ELGEDSAFGNSLVDVGE ALK(L)
T45	329-347	(R)GESGFFPINYVEVIVPL PP(-)
T41	254-277	(R)EFMPKPVNMSSTDANGV GPSSSSK(T)
T44	308-328	(K)EGDIITLTNQIDENWYE GMLR(G)
T35	200-227	(R)SMFNFLENDVEQVSQLA VFVEAALDYHR(Q)

Publications

*Yao, J., *Taylor, **M.,** Davey, F., Ren, Y., Aiton, J., Coote, P., Fang, F., Chen, J.X., Yan, S.D., and Gunn-Moore, F.J. (2007). Interaction of amyloid binding alcohol dehydrogenase/Abeta mediates up-regulation of peroxiredoxin II in the brains of Alzheimer's disease patients and a transgenic Alzheimer's disease mouse model. Mol Cell Neurosci *35,* 377-382.

*Joint first authors

Cole, A.R., Noble, W., van Aalten, L., Plattner, F., Meimaridou, R., Hogan, D., **Taylor, M.,** LaFrancois, J., Gunn-Moore, F., Verkhratsky, A., Oddo, S., LaFerla, F., Giese, K. P., Dineley, K. T., Duff, K., Richardson, J. C., Yan, S. D., Hanger, D. P., Allan, S. M., Sutherland, C. (2007). Collapsin response mediator protein-2 hyperphosphorylation is an early event in Alzheimer's disease progression. J Neurochem *103,* 1132-1144.

Ren, Y., Xu, H.W., Davey, F., **Taylor, M.,** Aiton, J., Coote, P., Fang, F., Yao, J., Chen, D., Chen, J.X., Yan, S.D., and Gunn-Moore, F.J. (2008). Endophilin I expression is increased in the brains of Alzheimer disease patients. J Biol Chem *283,* 5685-5691.